AD-A200 289

AFWAL-TR-88-3041

FINITE ELEMENT ANALYSIS OF
F-16 BALLISTIC TESTS

DTIC FILE COPY

Gordon R. Negaard

ANAMET LABORATORIES, INC.
3400 Investment Boulevard
Hayward, CA 94545-3811

July 1988

Interim Report for Period August 1986 - August 1987

Approved for public release; distribution is unlimited.

DTIC
ELECTE
OCT 0 4 1988
S
D
H

FLIGHT DYNAMICS LABORATORY
AIR FORCE WRIGHT AERONAUTICAL LABORATORIES
AIR FORCE SYSTEMS COMMAND
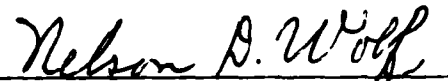WRIGHT-PATTERSON AIR FORCE BASE, OHIO 45433-6553

88 10 4 039

NOTICE

When Government drawings, specifications, or other data are used for any purpose other than in connection with a definitely Government-related procurement, the United States Government incurs no responsibility or any obligation whatsoever. The fact that the Government may have formulated or in any way supplied the said drawings, specifications, or other data, is not to be regarded by implication, or otherwise in any manner construed, as licensing the holder, or any other person or corporation; or as conveying any rights or permission to manufacture, use, or sell any patented invention that may in any way be related thereto.

This report has been reviewed by the Office of Public Affairs (ASD/PA) and is releasable to the National Technical Information Service (NTIS). At NTIS, it will be available to the general public, including foreign nations.

This technical report has been reviewed and is approved for publication.

DUANE E. VELEY, Project Engineer
Design & Analysis Methods Group

NELSON D. WOLF, Chief
Analysis & Optimization Branch

FOR THE COMMANDER

FREDERICK L. DIETRICH, Colonel, USAF
Chief, Structures Division

If your address has changed, if you wish to be removed from our mailing list, or if the addressee is no longer employed by your organization please notify AFWAL/FIBRA, W-PAFB, OH 45433-6553 to help us maintain a current mailing list.

Copies of this report should not be returned unless is required by security considerations, contractual obligations, or notice on a specific document.

REPORT DOCUMENTATION PAGE

Form Approved
OMB No. 0704-0188

1a. REPORT SECURITY CLASSIFICATION		1b. RESTRICTIVE MARKINGS
UNCLASSIFIED		NONE

2a. SECURITY CLASSIFICATION AUTHORITY	3. DISTRIBUTION/AVAILABILITY OF REPORT
N/A	Approved for public release; distribution is unlimited.
2b. DECLASSIFICATION/DOWNGRADING SCHEDULE	
N/A	

4. PERFORMING ORGANIZATION REPORT NUMBER(S)	5. MONITORING ORGANIZATION REPORT NUMBER(S)
887.1C	AFWAL-TR-88-3041

6a. NAME OF PERFORMING ORGANIZATION	6b. OFFICE SYMBOL (If applicable)	7a. NAME OF MONITORING ORGANIZATION
Anamet Laboratories, Inc.		Flight Dynamics Laboratory (AFWAL/FIBRA) Air Force Wright Aeronautical Laboratories

6c. ADDRESS (City, State, and ZIP Code)	7b. ADDRESS (City, State, and ZIP Code)
3400 Investment Blvd. Hayward, CA 94545-3811	Wright-Patterson AFB OH 45433-6553

8a. NAME OF FUNDING/SPONSORING ORGANIZATION	8b. OFFICE SYMBOL (If applicable)	9. PROCUREMENT INSTRUMENT IDENTIFICATION NUMBER
Flight Dynamics Laboratory	AFWAL/FIBRA	F33615-84-C-3216

8c. ADDRESS (City, State, and ZIP Code)	10. SOURCE OF FUNDING NUMBERS			
AFWAL/FIBRA Wright-Patterson AFB OH 45433-6553	PROGRAM ELEMENT NO.	PROJECT NO.	TASK NO	WORK UNIT ACCESSION NO.
	62201F	2401	02	65

11. TITLE (Include Security Classification)

Finite Element Analysis of F-16 Ballistic Tests

12. PERSONAL AUTHOR(S)

Gordon R. Negaard

13a. TYPE OF REPORT	13b. TIME COVERED	14. DATE OF REPORT (Year, Month, Day)	15. PAGE COUNT
Interim	FROM Aug 86 TO Aug 87	1988 July	231

16. SUPPLEMENTARY NOTATION

17.	COSATI CODES		18. SUBJECT TERMS (Continue on reverse if necessary and identify by block number)
FIELD	GROUP	SUB-GROUP	FINITE ELEMENT BALLISTIC TESTS
01	03	03	STRUCTURES
20	11		F-16

19. ABSTRACT (Continue on reverse if necessary and identify by block number)

The results of Finite Element analyses of an F-16 wing is presented. The analysis includes modeling of damage cases based on test results, modeling of patches to repair the damage, and NASTRAN static and dynamic analyses from which stresses, displacements, and natural frequencies were obtained.

20. DISTRIBUTION/AVAILABILITY OF ABSTRACT			21. ABSTRACT SECURITY CLASSIFICATION
☒ UNCLASSIFIED/UNLIMITED ☐ SAME AS RPT. ☐ DTIC USERS			UNCLASSIFIED

22a. NAME OF RESPONSIBLE INDIVIDUAL	22b. TELEPHONE (Include Area Code)	22c. OFFICE SYMBOL
Duane E. Veley	513-255-7191	AFWAL/FIBRA

DD Form 1473, JUN 86   *Previous editions are obsolete.*   SECURITY CLASSIFICATION OF THIS PAGE

FOREWORD

This technical report was prepared by Mr. Gordon R. Negaard
for Anamet Laboratories, Inc. under Purchase Order No 5963. the
technical effort reported herein was performed as a part of
Problem No. 4.2-26 of Air Force Contract No. F33615-84-C-3216
under which Anamet Laboratories, Inc. operates the Aerospace
Structures Information and Analysis Center (ASIAC), for the
Flight Dynamics Laboratory at Wright-Patterson Air Force Base in
Ohio.

The objective of this investigation was a finite element
analysis of F-16 ballistic tests. The investigation involved
modeling of damage cases based on test results, modeling of
patches to repair the damage, and a NASTRAN static and dynamic
analysis. Stresses and displacements were obtained from a static
analysis, and the natural frequencies of the models were obtained
from a dynamic analysis.

TABLE OF CONTENTS

LIST OF FIGURES

LIST OF TABLES

LIST OF FIGURES FOR
APPENDIX A - DYNAMIC ANALYSIS OF F-16 WING MODELS

LIST OF FIGURES FOR
APPENDIX B - STATIC ANALYSIS OF UNDAMAGED WING MODELS

LIST OF FIGURES FOR
APPENDIX C - ANALYSIS OF DAMAGE CASE #1

LIST OF FIGURES FOR
APPENDIX D - ANALYSIS OF DAMAGE CASE #2

LIST OF FIGURES FOR
APPENDIX E - ANALYSIS OF DAMAGE CASE #3

LIST OF FIGURES FOR
APPENDIX F - ANALYSIS OF DAMAGE CASE #4

LIST OF FIGURES FOR
APPENDIX G - ANALYSIS OF DAMAGE CASE #7

LIST OF FIGURES FOR
APPENDIX H - ANALYSIS OF DAMAGE CASE #9

LIST OF FIGURES FOR
APPENDIX I - ANALYSIS OF DAMAGE CASE #12

LIST OF FIGURES FOR
APPENDIX J - ANALYSIS OF DAMAGE CASE #15

LIST OF FIGURES FOR
APPENDIX K - ANALYSIS OF DAMAGE CASE #16

LIST OF FIGURES FOR
APPENDIX L - ANALYSIS OF DAMAGE CASE #17

1.0 INTRODUCTION

Analytical vulnerability techniques are intended to postulate and study damage to aircraft structures and attempt to predict the operational effects of such damage. For this study, a finite element analysis was used to quantify and evaluate the effects of real damage observed from live firings on an F-16 wing. The results are published in this report for comparison with test data from the live firings.

Each damage case was modeled by modifying the model by removing finite elements corresponding to the hole and by weakening damaged elements to approximate the damage from test data. A static analysis was then performed to calculate the residual strength degradation caused by the observed damage. A dynamic analysis was then used to calculate the changes in fundamental frequencies of the model. Combining these two effects, one can predict a reduction in the safe maneuver envelope in terms of maneuver load factor and airspeed. This technique can also be used to assess damage from various weapons in order to extend the study of experimental damage to simulation studies.

It must be cautioned that considerable experience and engineering judgment are required to model the damage and evaluate the effects. Benchmark studies are useful in order to establish confidence in the ability to predict damage effects using analytical techniques, and in providing procedures and guidelines in the use of such techniques. A large amount of detail has been included in this report in the hope that it will serve as such a benchmark.

2.0 DISCUSSION OF THE FINITE ELEMENT MODEL

It should be remembered that a finite element model is merely a mathematical model of a structure. It is an approach which allows one to solve complex problems, beyond the reach of classical analysis. The model is only an approximation of the actual structure, created by breaking the structure down into

1

smaller pieces such as plates, shells, rods, and bars, each of
which can be analyzed by classical means. It is generally
accepted that finite element results should be accurate within
five per cent for static analysis for a complex structure.

Finite element models should really be divided into two
groups, internal loads models and dynamic models. An internal
loads model looks much like the actual structure and is usually
the type model meant when referring to a "finite element model."
Displacements and forces are obtained at nodal or grid points.
Stresses within the idealized structures representing wing skin,
spar caps, and spar webs are also obtained. To get results
around cutouts, cracks in bolts or fittings, etc., an analyst
usually takes the internal forces that have been obtained for the
total structure and uses traditional hand analysis to obtain
stresses. In the case of complicated parts, one may go to a much
more detailed model. As an example, one may use solid elements
to subdivide the structure into much smaller pieces to obtain
stresses in areas of stress concentration. A dynamic model, on
the other hand, may not look much like the actual structure. A
wing, for example, may be modeled as a single beam, with bending
and torsional stiffnesses of the finite elements representing
those of the cross-section of the wing. Such a model obtains
quite accurate frequencies and mode shapes for dynamic analysis.
It can also be used to obtain wing root bending moments and
shears, for example, but it is not useful for internal stresses.
A dynamic model has the advantage that a small dynamic model
gives quite accurate results for its purposes in comparison to
the size of the model needed to obtain internal loads and
stresses.

2.1 The F-16 Wing Model

A finite element model of the F-16 wing obtained from
General Dynamics was used for this study. The model represents a
fully configured wing which includes the wingtip missile launcher,

pylons, and some nonstructural weight. The internal primary
structure of the wing is shown in Figure 1. As this drawing
illustrates, the F-16 wing is of multispar construction with very
little in the way of ribs except where hard points are necessary
for attachment points. The wing skin thickness varies from 0.5
inches inboard to 0.2 inches outboard. This thickness allows the
wing to carry a major portion of the the wing bending moment and
torsion. In addition, the wing skin and multiple spar construc-
tion provide multiple load paths, allowing considerable load
redistribution in the event of damage to the skin and one or more
spars. For the tests, the wing was supported in a cantilever
fashion at Butt Line (BL) 41.5. Test loads were applied along BL
120.0 where a series of hard points for a pylon are located.

The NASTRAN finite element model used is a conventional
membrane, shear panel, and rod representation with a few bar
elements added where necessary. The complete model has a total
of 1043 elements and 384 grid points. The model is rigidly
constrained at BL 41.5 to simulate the cantilever condition.
These constraints are located at Fuselage Stations (FS) 308.5,
324.5, 340.5, and 356.5 and represent bolt attach points. These
locations vary slightly from that shown in the test plan (Ref. 1)
where these points are listed as FS 309.8, 325.8, 341.8, and
357.8. This difference is probably due to the construction of
the finite element model. The modelers placed the constraints at
the end of the ribs rather than adding extra grid points and
elements to locate the constraints more precisely. The effect
should be unimportant, especially at any distance from the
constraints. Even at the area of the constraints, a detailed
stress analysis would probably find little error.

2.2 Validation of the Model

In order to use a finite element model with confidence, it
is necessary to be able to compare it against some known data.
In this case, although the finite element model appeared to be a

3
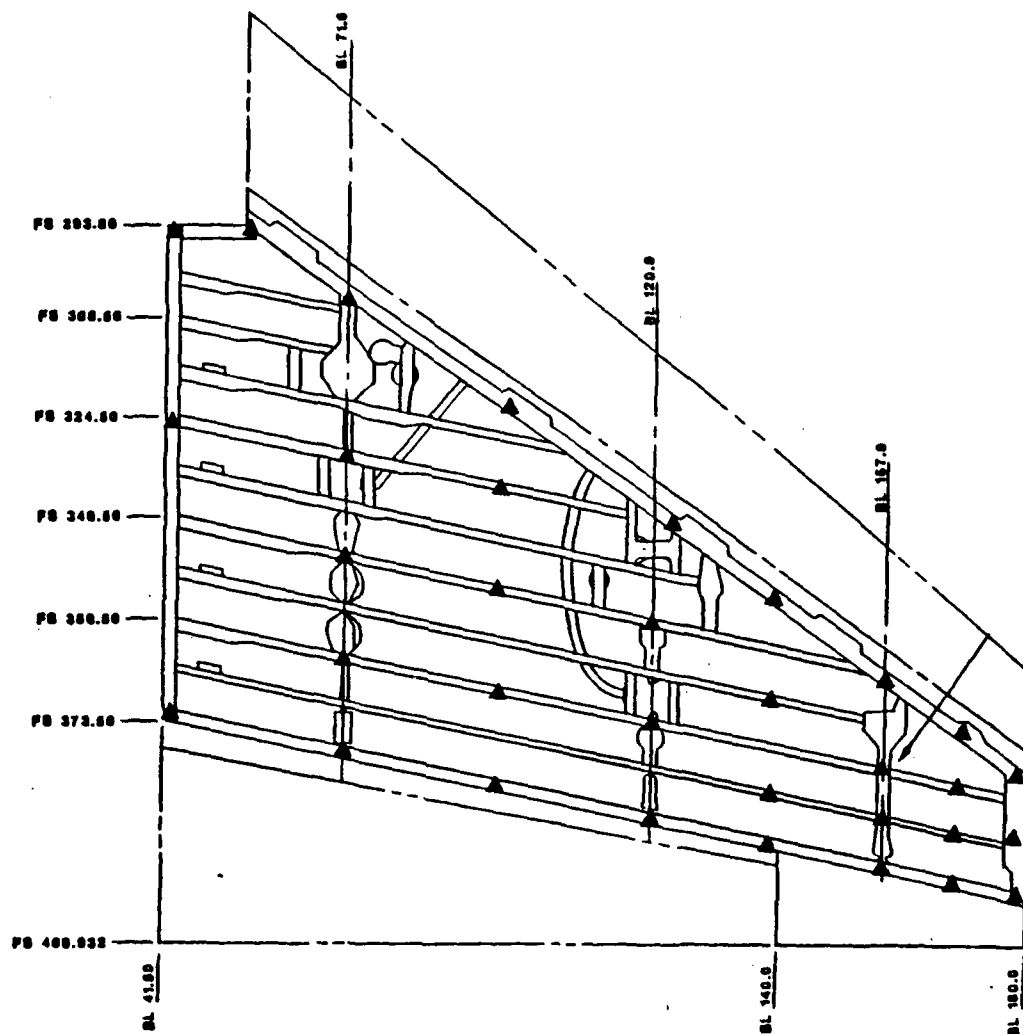
Figure 1.   Structural Layout of the F-16 Wing

good representation of an F-16 wing, it was first necessary to
convert it from MSC/NASTRAN into a COSMIC/NASTRAN version in
order to run it on the WPAFB version of NASTRAN. These changes,
although minor, needed to be checked out. It was also necessary
to make further modifications to this model so that it would
represent the actual structures under test. The three test
articles, referred to as Wing #1, Wing #2, and Wing #3, had been
stripped of all external structure including the leading and
trailing edge flaps. These wings were considerably lighter than
the fully configured wing. It was necessary to create four ver-
sions of the F-16 wing finite element model. The first two
models were used to validate the finite element analysis and
insure that the finite element model adequately represented the
real structure under test. The other two models were used to
represent the test articles. These finite element models are
referred to as Models D-1, D-2, D-3, and D-4. The D designation
is used to indicate that they were used primarily for dynamic
analysis.

A model would normally be validated using a known set of
loads and measuring experimental deflections against those calcu-
lated by the model. This was attempted first using a 30,000
pound or 6g load. The NASTRAN analysis indicated a displacement
of about 2.7 inches at BL 120.0 while experimental data showed
about 5.0 inches. This is at least partly because, while a
mathematic model can be rigidly constrained, the real structure
has small but finite rotations and displacements at the canti-
levered support. An attempt was made to measure these displace-
ments, but an analysis shows that the measured rotations of 0.15
degrees should cause only about 0.15 inches in vertical displace-
ment at BL 120.0 (See Figure 2). Measurement of small rotations
of this magnitude is a very difficult task, even under laboratory
conditions. It was decided that a comparison of dynamic effects
would be easier to make.

BL 41.5   BL 120.0

Tan θ = Y/X

θ = .15 degrees

tan(.15) = .0026

Y = X(.0026)

Y = (120.0 - 41.5)x(.0026)

Y = 0.2 inches
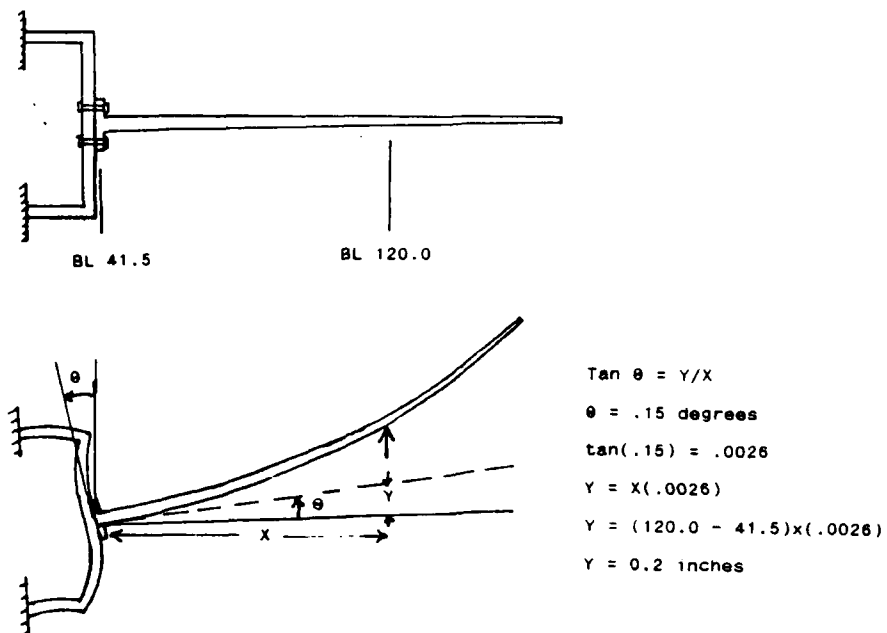
Figure 2.   Rotation of Test Fixture Under Load

2.3 Dynamic Analysis of the Model

After being converted from MSC NASTRAN, the original model, referred to as Model D-1, was checked out and compared to a ground vibration test documented in AFWAL FIBG-TM-83-187 (Ref. 2) where the wing was of a similar configuration. The missile launcher and pylons were then removed to make a further comparison with a clean F-16 wing documented in a General Dynamics memorandum (Ref. 3). This model is referred to as Model D-2. Two additional models were then made to simulate the test wings. In addition to removing attached structures such as flaps and ailerons, some nonstructural weight was also removed in order to match the weights of the actual test articles for the F-16 wing ballistic test. These two models are referred to as Models D-3 and D-4 and refer to Wing #1 and Wing #2, respectively, in the test plan.

The following summary of these models may help clarify their characteristics and their use:

Model D-1: This is a complete model of an F-16 wing including the Wingtip Missile Launcher. The model weight is 1753 pounds.

Model D-2: The structure is the same as Model D-1 except that the missile launcher and pylon are removed. This model is approximately the same as the one described in Reference 3. Some nonstructural weight had to removed to get the model down to the stripped wing weight which was determined to be approximately 1038 pounds.

Model D-3: This is Model D-2 except that both front and rear flaps are removed. This model is essentially a stripped torque box and weighs 840 pounds. This model represents the wing used for tests 1 through 7 and referred to in the test plan as Wing #1.

Model D-4:   Model D-3 except that the remaining outboard section
             of the rear flap was removed and weighs 830 pounds.
             This model represents the wing used in tests 8
             through 17 and referred to in the test plan as Wing
             #2.

        Plots of the finite element models of these four wing models
are shown in Figures A-1 through A-4. Dynamic runs were made to
determine the lowest four natural frequencies of each model.
Table 1 contains a list of the lowest four calculated modes for
the dynamic runs of the finite element models D-1 and D-2 with a
comparison with the results given in References 2 and 3. The
first four modes for models D-3 and D-4 are also included in this
table.
        Plots of the mode shapes for all four models are included as
Figures A-5 through A-20 in Appendix A. It can be noticed that
first and second wing bending are the two lowest modes, with the
first torsional mode only slightly higher than the second bending
mode. It would be possible for these two modes to cross and even
interact if the torsional stiffness was degraded significantly.
This could strongly affect flutter speed. The agreement between
model D-1 and the FIBG analysis can be seen to be fairly close.
So is the agreement between model D-2 and the General Dynamics
analysis of the stripped wing. Based on these results, Models
D-3 and D-4 should simulate the behavior of the two test wings
fairly accurately.

2.4 Static Analysis of the Model

        For the static analysis, a 30,000 pound load was applied to
the finite element model at BL 120.0. This load was matched to
the test load as closely as possible in magnitude and location.
The values of the applied load for the model were arrived at by
averaging the measured values at the three load cells over several
experimental tests. These loads are compared as follows:

8

TABLE 1

COMPARISON OF FIRST FOUR SYMMETRIC MODES (HERTZ)

FOR MODELS D-1 THROUGH D-4

Case	WT(lbs)	First	Second	Third	Fourth
Model D-1	1753	4.66	7.80	15.66	21.16
Ref. 2		5.08	7.57		
Model D-2	1038	10.03	26.97	32.99	41.44
Ref. 3		11.39	34.76	36.51	56.16
Model D-3	840	10.52	35.29	45.59	70.47
Model D-4	830	10.94	37.28	48.15	77.16

| | Load Cell No. | | |
	1	2	3
Load Cell Location (FS)	340.0	361.0	380.0
Model Load Location (FS)	341.9	362.6	378.6
Load (pounds)	17000	10000	3000

This table shows that the location of the model loads dupli-
cated the test loads within an inch or two. The bending moment,
torsion, and shear for the NASTRAN analysis should therefore
match the test conditions very closely. For each model, the
bending moment, torsion, and shear at the wing root were calcu-
lated by summing the constraint forces from NASTRAN. These
constraint forces varied slightly depending on the load paths in
each damage case; however the total bending moment, torsion, and
shear stayed almost constant, as would be expected. The summa-
tion of the forces for the undamaged wing D-3 is compared with
the test plan as follows:

	NASTRAN	Test Plan
Bending Moment	2,398,642 in.lbs	1,500,000 in.lbs
Torsion	9,564,664 in.lbs	700,000 in.lbs
Shear	30,000 lbs	30,000 lbs

Comparing these data, it would appear that the bending moment for
the model loads is somewhat too high, but the torsion is an order
of magnitude too high. In order to reduce the torsion, the
applied load at BL 120.0 would have to be moved considerably
forward, bringing it off of the actual wing. This is the result
of trying to replace a distributed load with a few concentrated
loads. A compromise usually has to be made in a case like this.

Plots of the displacements at BL 120.0 are included in all the damage cases for comparison with measured displacements. The calculated displacements of undamaged Wing #1 (Model D-3) can be seen in Appendix C, while the displacements for undamaged Wing #2 (Model D-4) can be seen in Appendix H. They are almost identical and range from about 2.40 inches at the leading edge to 2.74 inches at the trailing edge, a total of about one-third of an inch. Two interesting observations can be made from the plots in Appendices C and H. First, the wing warps under the applied load, creating a "washout condition." Second, the leading edge of the model deflects more than expected. This may be because the leading edge of the model is modeled too soft, but more likely, it is because the major load (17,000 pounds) is applied here. This amount of wing warping is probably due only to the test loads and would not occur under distributed air loads.

Contour plots of the stresses in the upper and lower skin surfaces were created to help illustrate the change in load path and stress pattern for each damage case and for comparison with strain data on the tests. The NASTRAN results matched this strain data quite well. Plots of the upper and lower wing surfaces and contour plots of the stresses on both surfaces are contained in Appendix B for both Models D-3 and D-4, although the differences between them are very small.

3.0 ANALYSIS OF THE DAMAGE

The damage cases are referred to as DC-1, etc., where the numbers correspond to the number of each test shot. DC-1R refers to the damage case model after modeling the repair to the wing. DC-1R therefore becomes the baseline or "before damage" case for DC-2 just as Model D-1 was the "before damage" case for DC-1. Some of the planned test shots were eliminated or consolidated, and some were not modeled, so although the damage cases run from DC-1 to DC-17, there are some gaps in the numbering of the cases.

11

DC-1, DC-2, DC-3, DC-4, and DC-7 represent the test shots on Wing #1. DC-9 and DC-12 represent the test shots on Wing #2, while DC-15, DC-16, and DC-17 are the test shots on Wing #3. The wings were not repaired after shots #7 and #17 so there are no repaired cases for those two shots. A separate appendix was prepared for each damage case (Appendices C through L) because of the large amount of material included. A short summary of the results of each case will be given here but the reader is referred to the appendices for plots, tables and details. For an in-depth understanding of each case, one needs to look at the locations, size, and pattern of the damaged areas, study the contour plots for the load paths and stress patterns, and compare the displacement plots and first torsional modes of the damage case to the before and after cases.

3.1 Analysis Procedure

The damage cases were modeled by removing upper and lower skin surface to represent the missing or cracked areas of the skin. The spars and ribs were either weakened or removed to represent internal damage. Both static and dynamic runs were made of each damage case to obtain stresses, displacements, and natural frequencies. The damaged model was then repaired to match the actual patch applied to the test article. Subsequently, static and dynamic analyses were performed on the repaired structure. The next damage case was then modeled using the previously repaired wing model to simulate the actual test item.

Plots illustrating the modeling of the damage to the upper and lower wing surfaces are included in each appendix. Contour plots of the stresses on both surfaces and plots of the first four mode shapes are also included. A summary of the results for each damage case compares the displacements under the applied load before test, after test, and after repair. A comparison is then made of the change in residual strength and the change in torsional frequency. For elastic analysis, wing strength can be

12

calculated as being inversely proportional to its deflection under load. Residual strength degradation can be calculated as a percentage of the original strength by dividing the change in displacement by the original displacement. Calculation of flutter effects is much more difficult since flutter is a very complex topic. One generalization that can be made is that flutter is generally directly proportional to the first torsional frequency. One can therefore make the assumption that a reduction in flutter speed will be directly proportional to the change in first torsional frequency divided by the original frequency. This summary is also included in each damage case.

3.2 Results of Damage Case 1

This shot was near the rear spar. Damage effects were minor. Very little wing skin was removed from the top or bottom surface. There was also very little spar damage. The change in residual strength and torsional strength was less than one per cent.

3.3 Results of Damage Case 2

This shot was slightly forward and a little inboard of damage case 1. There was slightly more surface removed and a little more spar damage but the damage effects were still minor. The change in both residual strength and torsion was approximately two per cent.

3.4 Results of Damage Case 3

This shot damaged a large amount of skin on the top surface as well some spars. Its location near the front spar apparently wiped out other load paths and caused the front spars to carry additional load as evidenced by the spike in the deflection pattern. Even after modeling the repair, this was still evident.

The change in residual strength was about 23 per cent while the change in torsional strength was about 35 per cent. This change in torsional strength can be seen in the plot of deflections in Figure E-1 where the amount of "washout" has decreased. The damage was obviously in front of the torsional axis of the wing to produce this effect. The effect of the change in stress contour pattern is also obvious in Figure E-4.

3.5 Results of Damage Case 4

This shot appeared to do considerable damage to the inboard section of the front spar; however the analysis did not indicate the damage to be very severe. The damage is apparently not in a heavy load-carrying area, which is confirmed by the stress contours. The residual strength change was about six per cent while the torsional effect was less than two per cent.

3.6 Results of Damage Case 7

There was considerable skin damage here, particularly on the upper surface; however the damage runs parallel to the spars so the effect on load-carrying capability was less than first suspected. The residual strength change was about five per cent while the the torsional effect was only about two per cent.

3.7 Results of Damage Case 9

This damage was in the inboard area near the rear edge. This is in area of high stress concentration and also quite far behind the torsional axis. Thus the damage, although not very severe, had a pronounced effect, especially on torsion. The residual strength change was only six per cent, but the torsional change was about 27 per cent.

14

3.8 Results of Damage Case 12

This shot appears to be near the torsional axis. The damage was quite severe, causing about a 20 per cent reduction in residual strength. The torsional change was less than four percent, however. Considerable skin was damaged on both top and bottom surfaces, but the damage to the bottom surface ran parallel to the spars, so the effect was minimized.

3.9 Results of Damage Case 15

The effects of this shot could be rated as minor to moderate. The residual strength change was about three per cent while the torsional change was about four per cent. The displacement plot in Figure J-1 shows the torsional effect very clearly even if it is small.

3.10 Results of Damage Case 16

The major damage was to the lower surface. The damage was not too severe and was also near the torsional axis. The residual strength reduction was about eight per cent while the torsional reduction was only about four per cent.

3.11 Results of Damage Case 17

This case was the most severe of those evaluated. It had the largest amount of damage to both wing surfaces. Two spars were completely severed and two more badly damaged. The loss in residual strength was almost 45 per cent, yet the torsional loss was only four per cent.

4.0 SUMMARY

A finite element analysis was conducted on ten damage cases modeled on test results from live firings on an F-16 wing. Stress and displacement results were obtained from static analysis and the natural frequencies of the models were obtained from a dynamic analysis. A comparison was made of residual strength degradation and changes in the natural modes of the damaged and undamaged models. Detailed results are contained in the appendices of this report. For convenience, a summary of the displacements for all the damage cases is contained in Table 2 and a summary of the first four symmetric modes of all the models is contained in Table 3.

TABLE 2

VERTICAL DISPLACEMENTS AT BL 120

FOR THE DAMAGE CASES

FS	387.9	378.6	370.6	362.6	354.6	349.7	346.6	341.9
D-3	2.74	2.71	2.63	2.66	2.49	2.43	2.40	2.55
DC-1	2.76	2.72	2.65	2.67	2.49	2.44	2.40	2.56
DC-1R	2.74	2.71	2.63	2.66	2.48	2.43	2.39	2.55
DC-2	2.82	2.79	2.71	2.74	2.55	2.49	2.45	2.60
DC-2R	2.76	2.73	2.65	2.68	2.50	2.44	2.41	2.56
DC-3	3.24	3.18	3.16	3.16	3.12	3.10	3.37	3.11
DC-3R	2.66	2.59	2.56	2.56	2.50	2.48	2.74	2.48
DC-4	2.79	2.74	2.71	2.71	2.67	2.65	2.91	2.68
DC-4R	2.70	2.64	2.61	2.61	2.56	2.54	2.80	2.54
DC-7	2.83	2.78	2.75	2.75	2.70	2.68	2.95	2.71
D-4	2.74	2.71	2.63	2.66	2.55	2.40	2.43	2.49
DC-9	3.02	2.95	2.83	2.83	2.67	2.52	2.56	2.63
DC-9R	2.77	2.73	2.65	2.67	2.55	2.40	2.43	2.49
DC-12	3.30	3.25	3.16	3.17	2.99	2.92	2.88	3.04
DC-12R	2.66	2.63	2.55	2.57	2.40	2.34	2.31	2.46
DC-15	2.87	2.83	2.74	2.75	2.55	2.49	2.45	2.60
DC-15R	2.75	2.71	2.64	2.66	2.49	2.43	2.40	2.55
DC-16	2.92	2.90	2.83	2.87	2.70	2.65	2.62	2.79
DC-16R	2.78	2.74	2.67	2.70	2.53	2.47	2.44	2.59
DC-17	3.97	3.88	3.76	3.73	3.49	3.39	3.32	3.51

TABLE 3

COMPARISON OF FIRST FOUR SYMMETRIC MODES (HERTZ)

FOR THE DAMAGE CASES

Case	WT(lbs)	First	Second	Third	Fourth
Model D-3	840	10.52	35.29	45.59	70.47
Model DC-1	832	10.49	35.26	45.15	70.21
Model DC-1R	835	10.54	35.28	45.62	70.48
Model DC-2	834	10.45	34.94	44.75	66.75
Model DC-2R	837	10.55	35.05	45.56	70.38
Model DC-3	830	9.54	29.64	38.11	47.23
Model DC-3R	838	10.54	35.23	47.02	70.67
Model DC-4	835	10.33	34.64	46.22	68.04
Model DC-4R	838	10.47	35.06	46.93	70.42
Model DC-7	831	10.24	34.61	46.04	67.33
Model DC-9	827	10.42	31.60	35.02	48.06
Model DC-9R	831	10.76	35.06	45.67	65.79
Model DC-12	827	9.88	34.14	43.87	66.29
Model DC-12R	832	10.86	34.87	45.54	65.37
Model DC-15	829	10.82	36.69	46.10	73.39
Model DC-15R	832	10.93	37.28	48.12	77.50
Model DC-16	828	10.89	36.10	46.13	76.37
Model DC-16R	831	10.93	37.50	48.13	78.37
Model DC-17	822	8.96	36.21	46.64	75.70

REFERENCES

1. Ritter, S. B., "Detailed Test Plan for Aircraft Joint Live Fire (JLF) Test," JLF-TP-16-S-1, September 1986.

2. Wright, R. L., "Ground Vibration Test of the AFWAL GF-16," AFWAL-TM-83-187-FIBE, April 1985.

3. LeBlanc, D. J., "F-16 Wing Frequency Data for Joint Live Fire Program," General Dynamics Memorandum, 28 May 1987.

APPENDIX A

DYNAMIC ANALYSIS OF F-16 WING MODELS
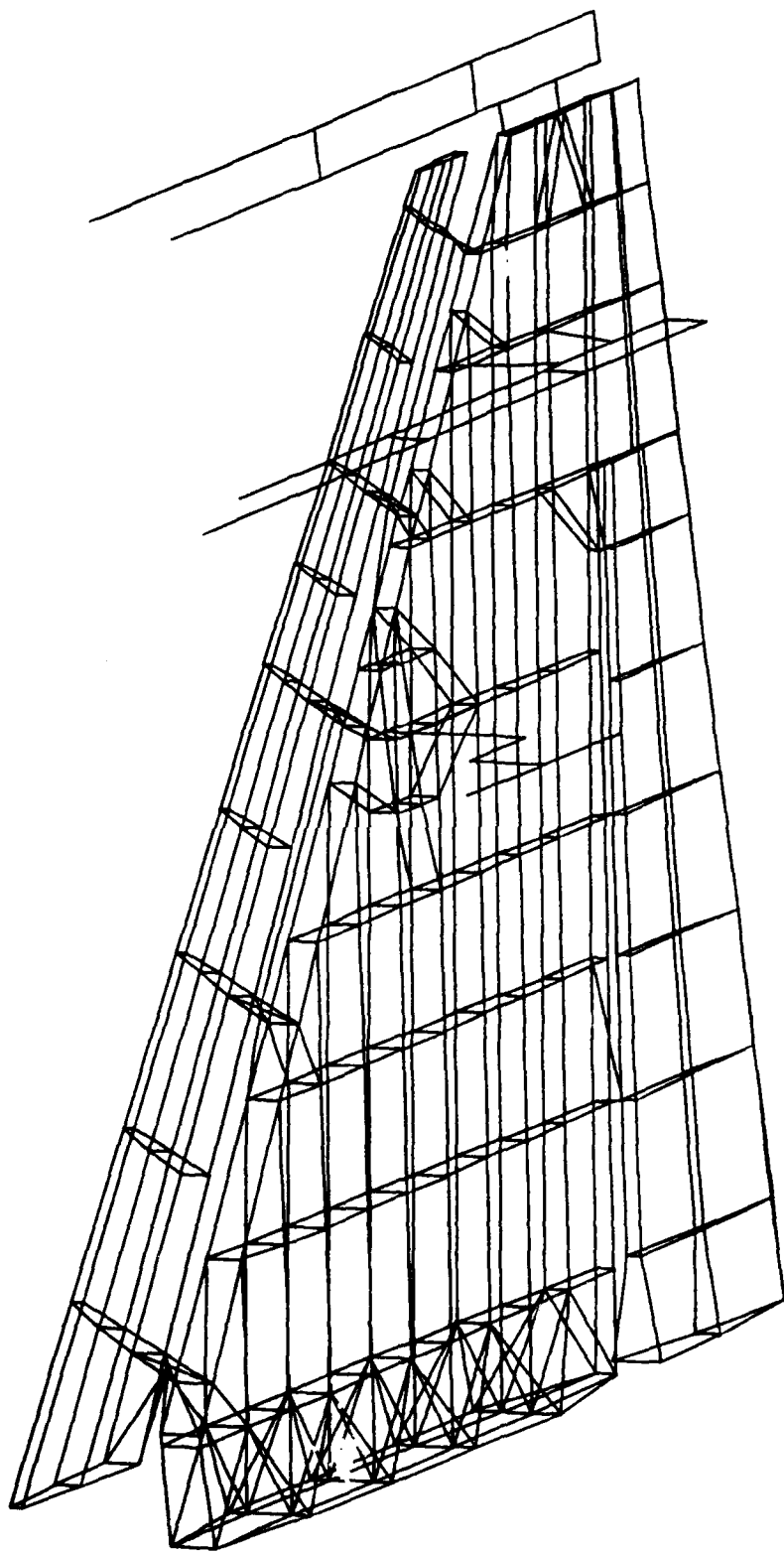
Figure A-1. Finite Element Model D-1
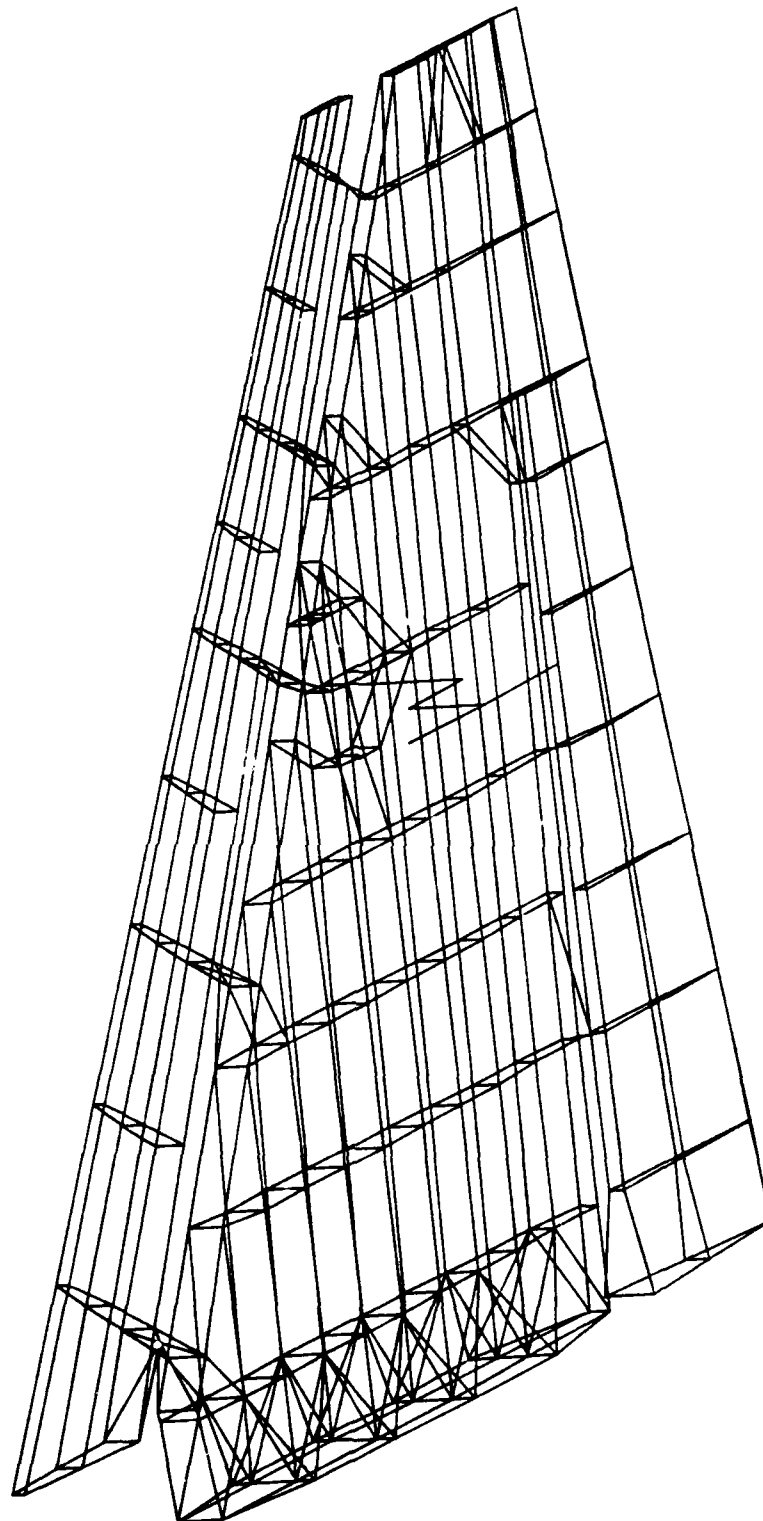
Figure A-2. Finite Element Model D-2

A-3
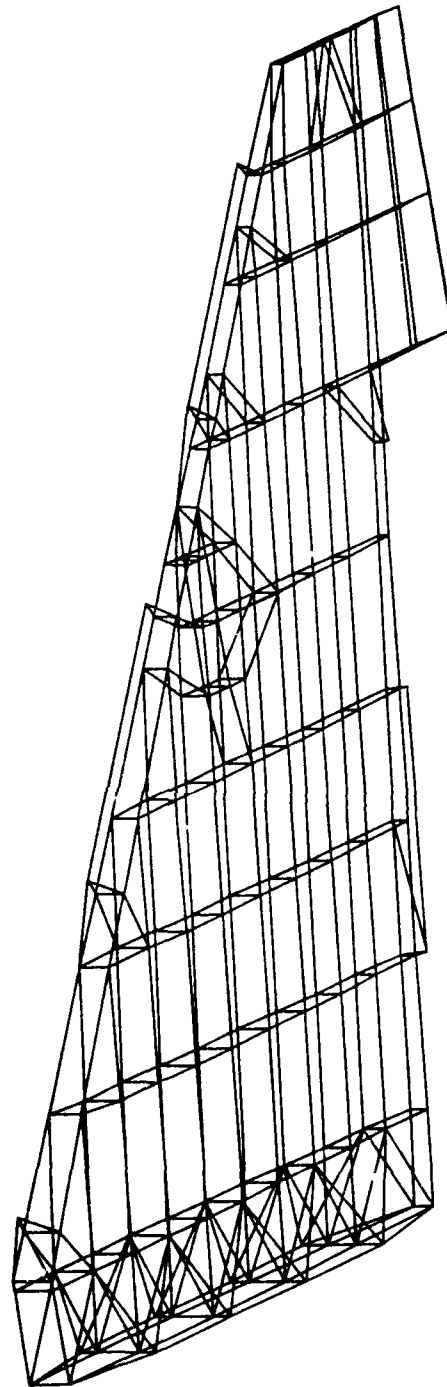
Figure A-3.   Finite Element Model D-3

A-4
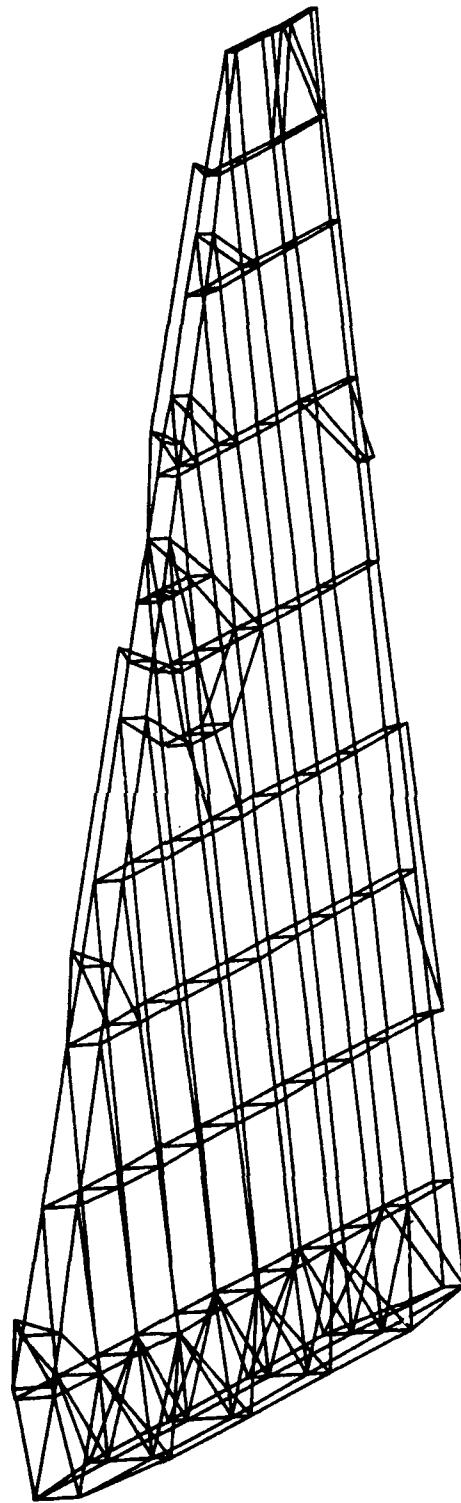
Figure A-4. Finite Element Model D-4

Symmetric Normal Modes for F-16 Wing Model D-1

Givens Method   Mode 1   Frequency =   4.66 Hertz
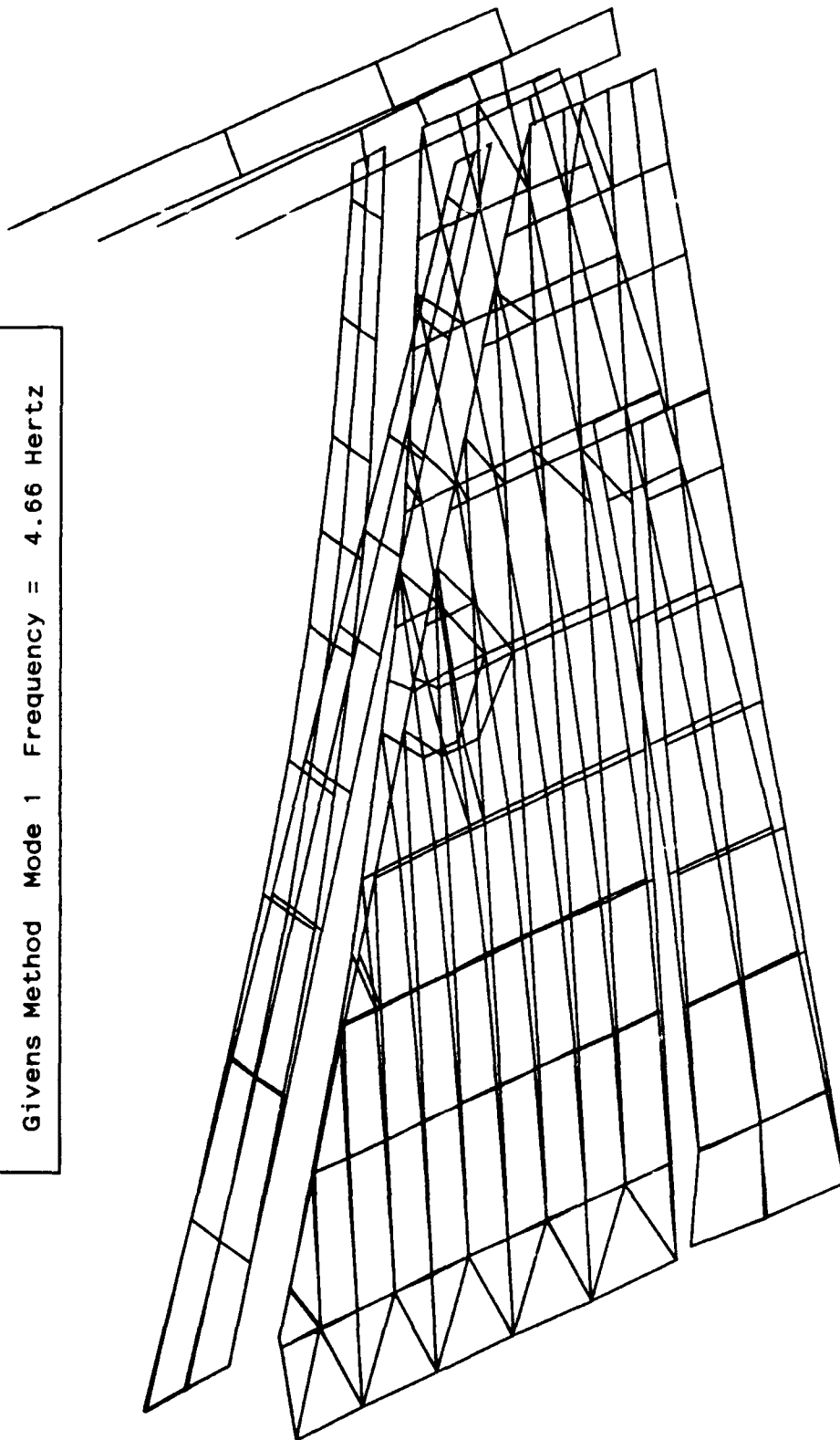
Figure A-5.   1st Wing Bending Mode (Model D-1)

Symmetric Normal Modes for F-16 Wing Model D-1

Givens Method   Mode 2   Frequency =   7.80 Hertz
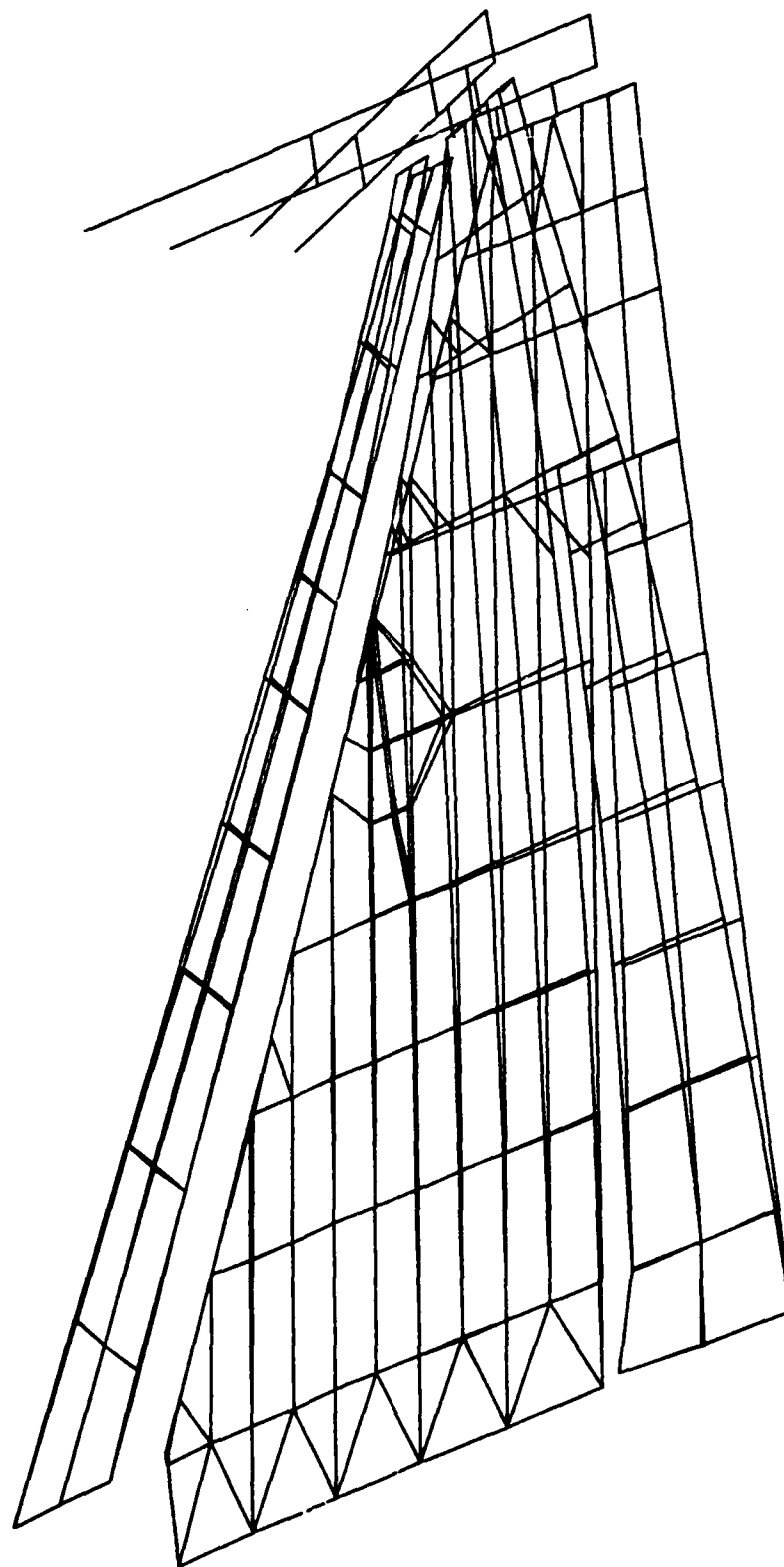
Figure A-6.   Missile Pitch Mode (Model D-1)

Symmetric Normal Modes for F-16 Wing Model D-1

Givens Method   Mode 3   Frequency = 15.66 Hertz
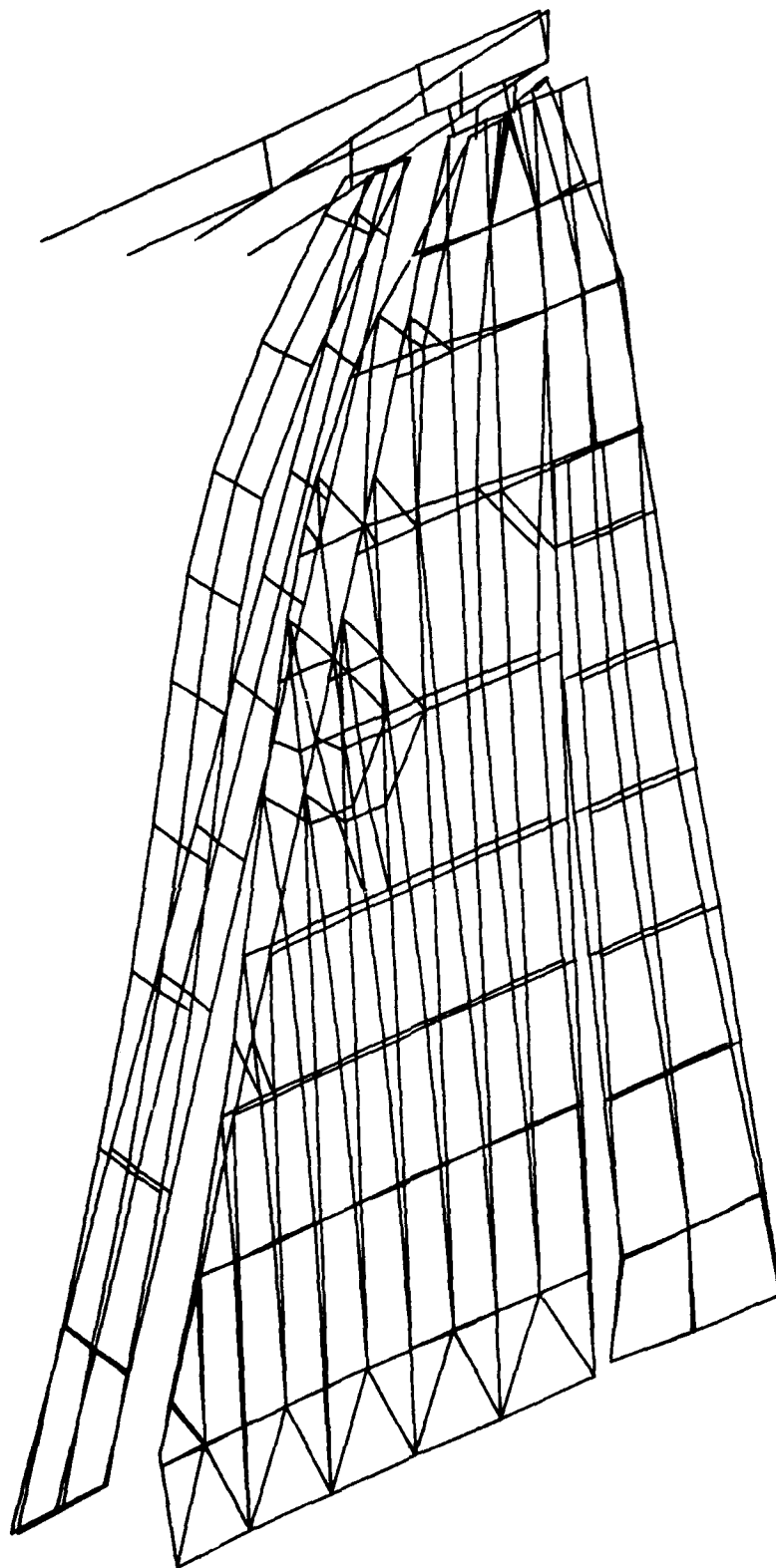
Figure A-7.   1st Torsional Mode (Model D-1)

Symmetric Normal Modes for F-16 Wing Model D-1

Givens Method   Mode 4   Frequency = 21.16 Hertz
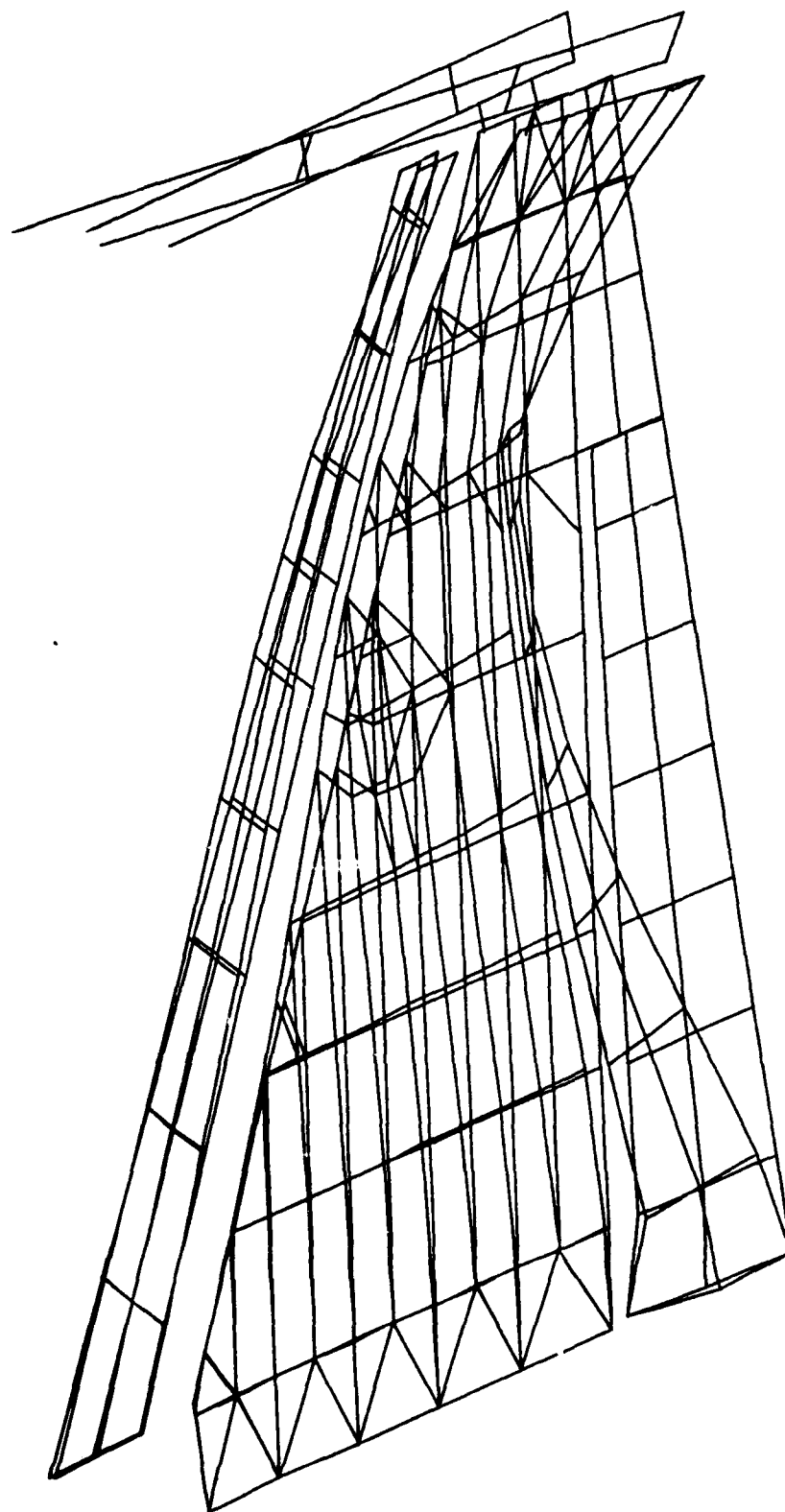
Figure A-8. 2nd Wing Bending Mode (Model D-1)

Symmetric Normal Modes for F-16 Wing Model D-2

Givens Method   Mode 1   Frequency = 10.03 Hertz
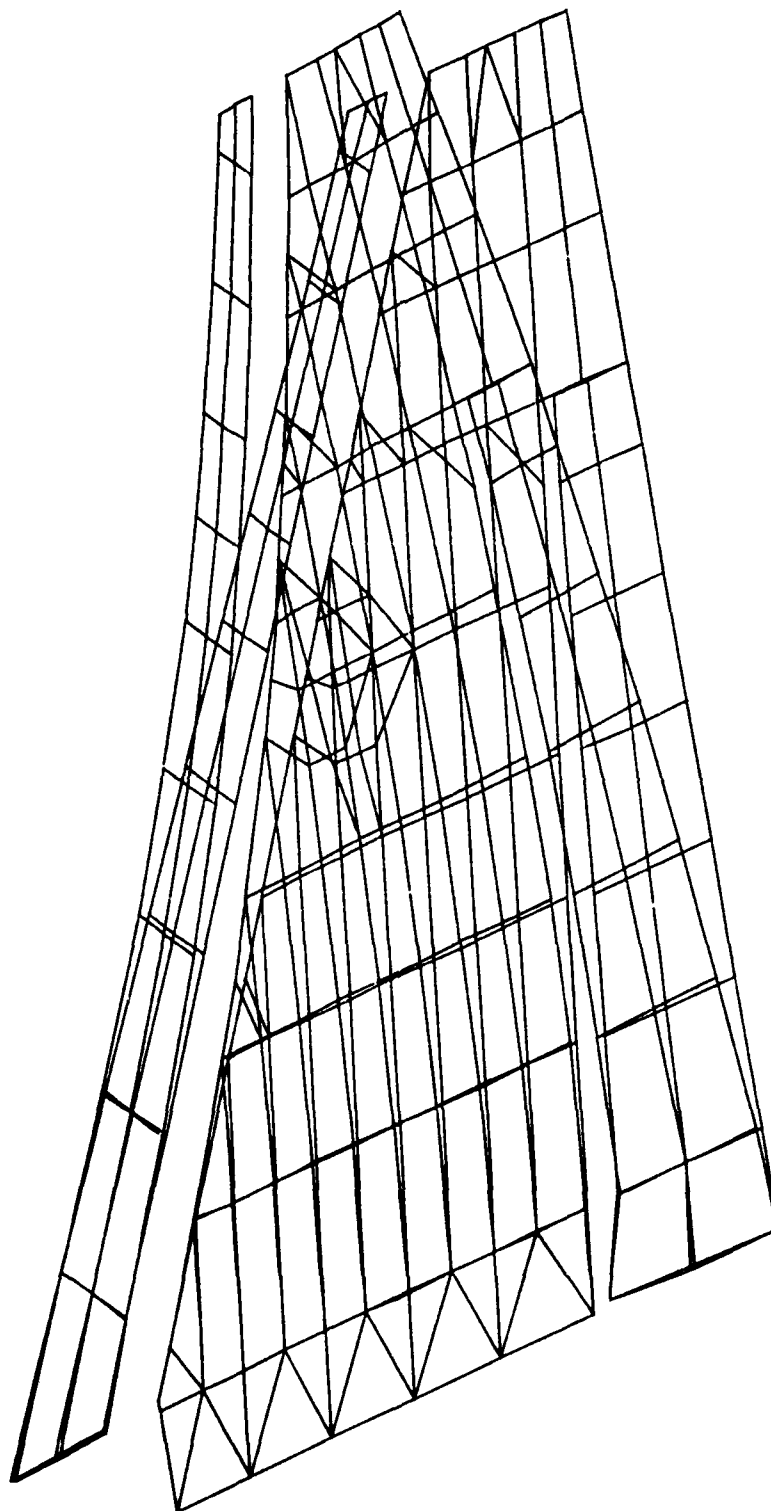
Figure A-9.   1st Wing Bending Mode (Model D-2)

Symmetric Normal Modes for F-16 Wing Model D-2

Givens Method   Mode 2   Frequency = 26.97 Hertz
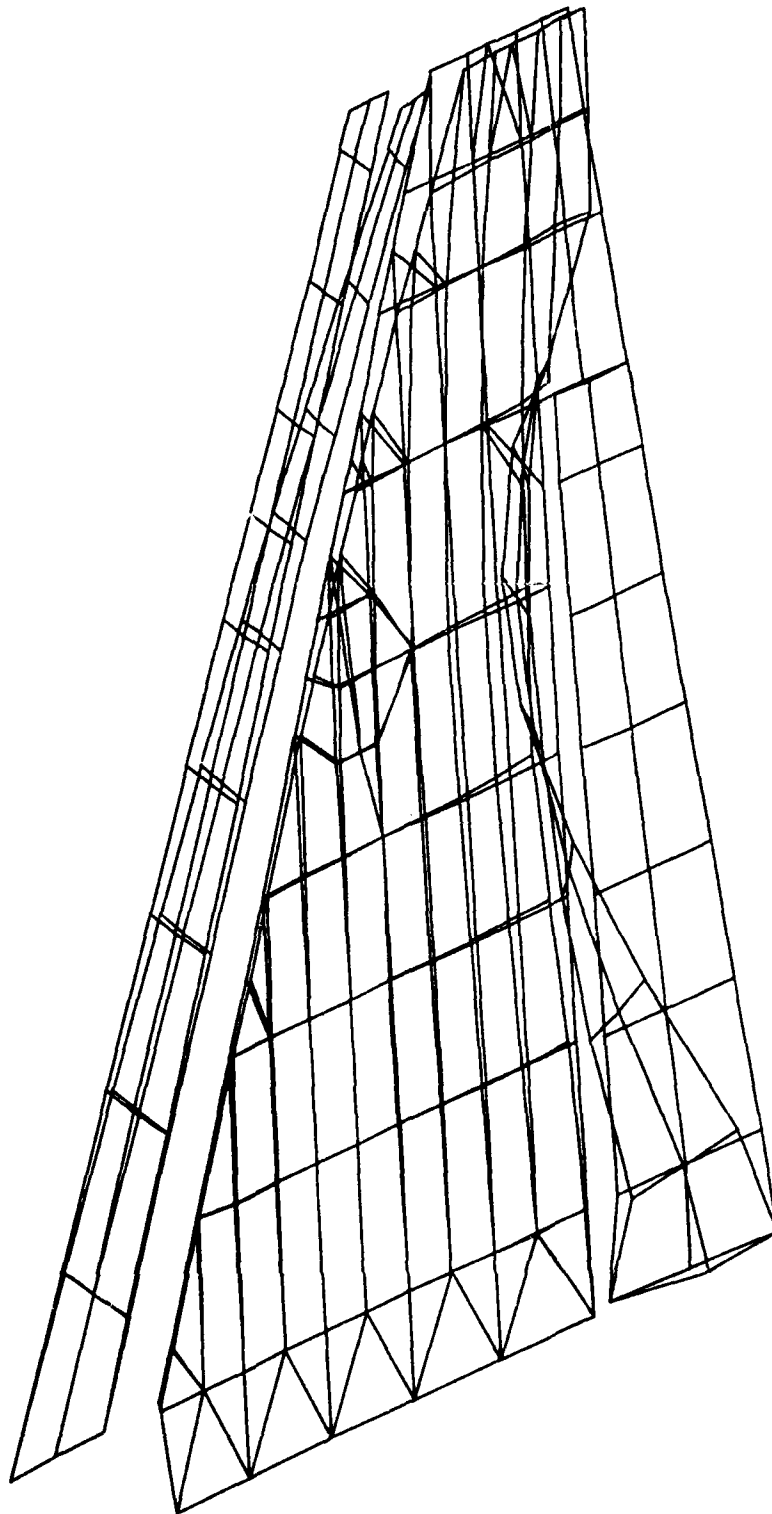
Figure A-10.   2nd Wing Bending Mode (Model D-2)

A-11

Symmetric Normal Modes for F-16 Wing Model D-2

Givens Method   Mode 3   Frequency = 32.99 Hertz
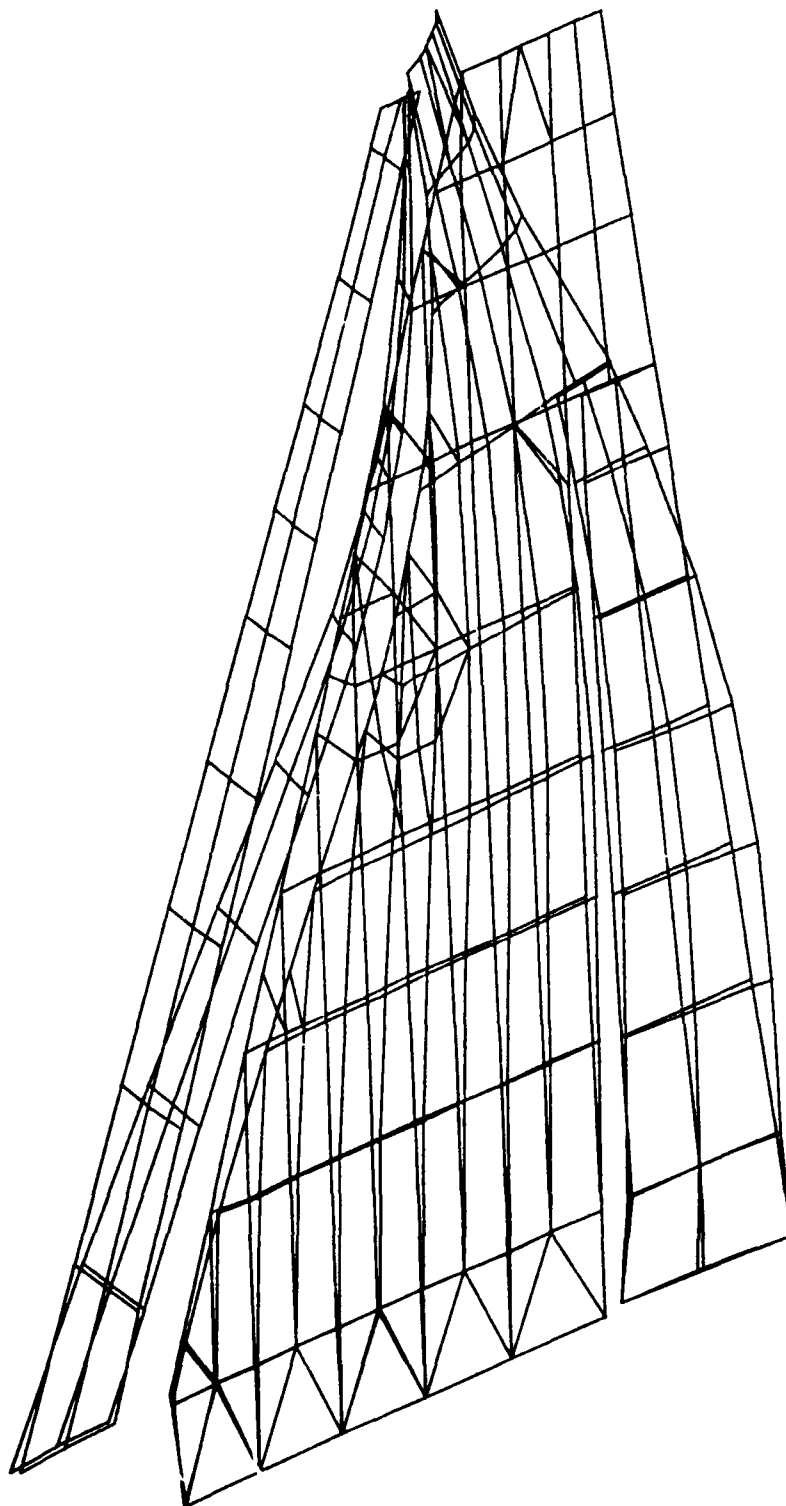
Figure A-11.   1st Torsional Mode (Model D-2)

A-12

Symmetric Normal Modes for F-16 Wing Model D-2

Givens Method   Mode 4   Frequency = 41.44 Hertz
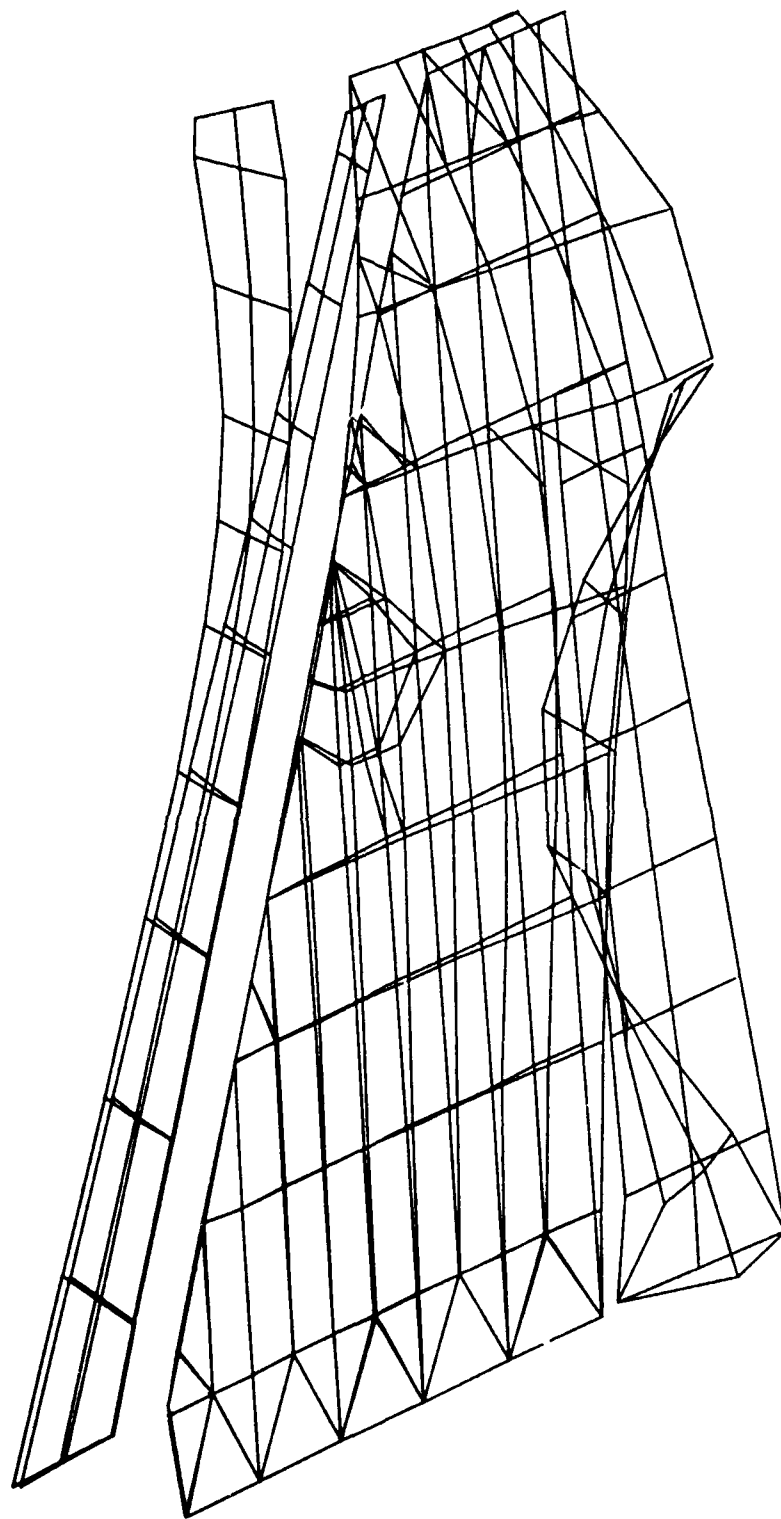
Figure A-12.   2nd Torsional Mode (Model D-2)

Symmetric Normal Modes for F-16 Wing Model D-3
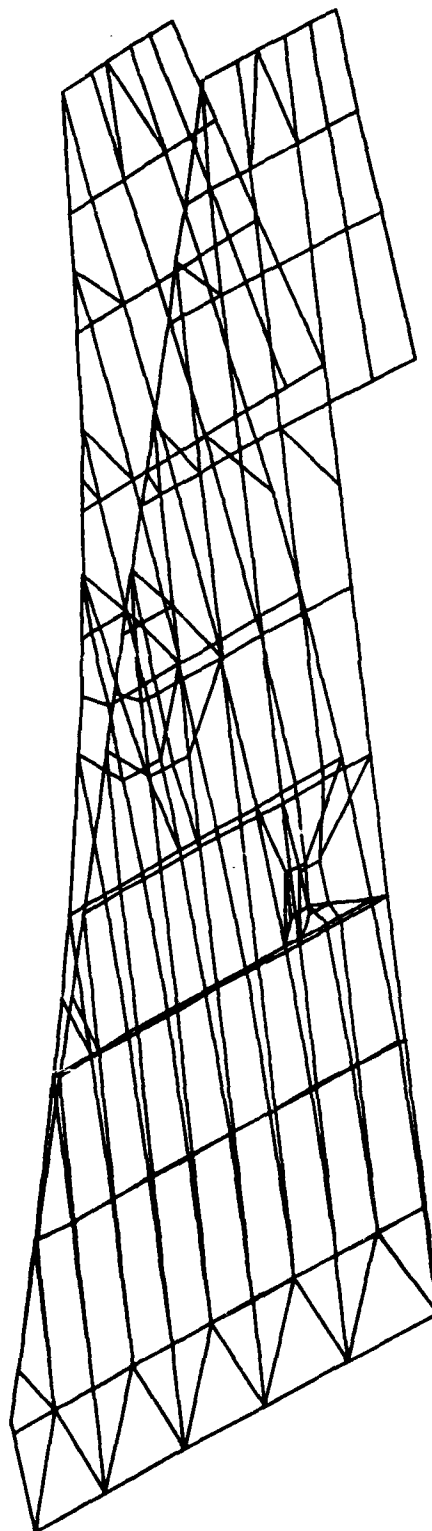Givens Method Mode 1 Frequency = 10.52 Hertz.
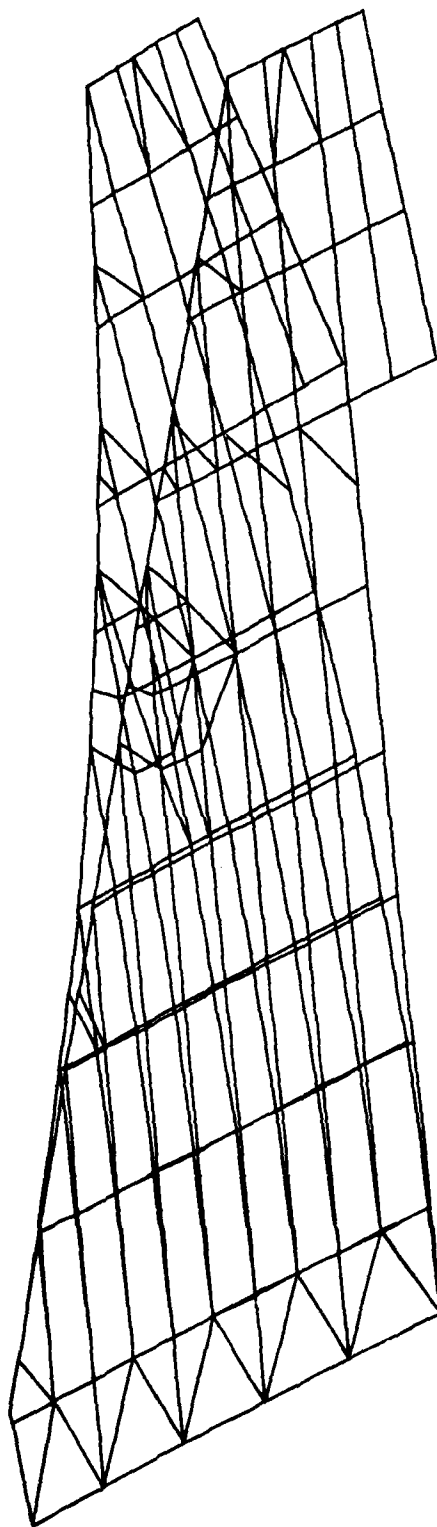
Figure A-13. 1st Wing Bending Mode (Model D-3)

Symmetric Normal Modes for F-16 Wing Model D-3
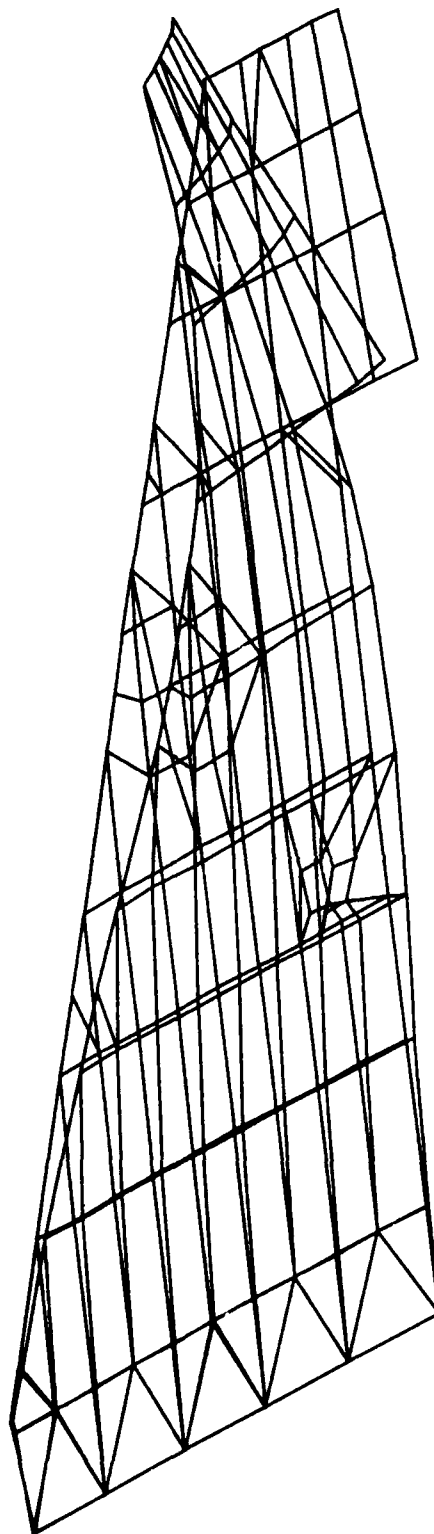
Givens Method Mode 2 Frequency = 35.29 Hertz
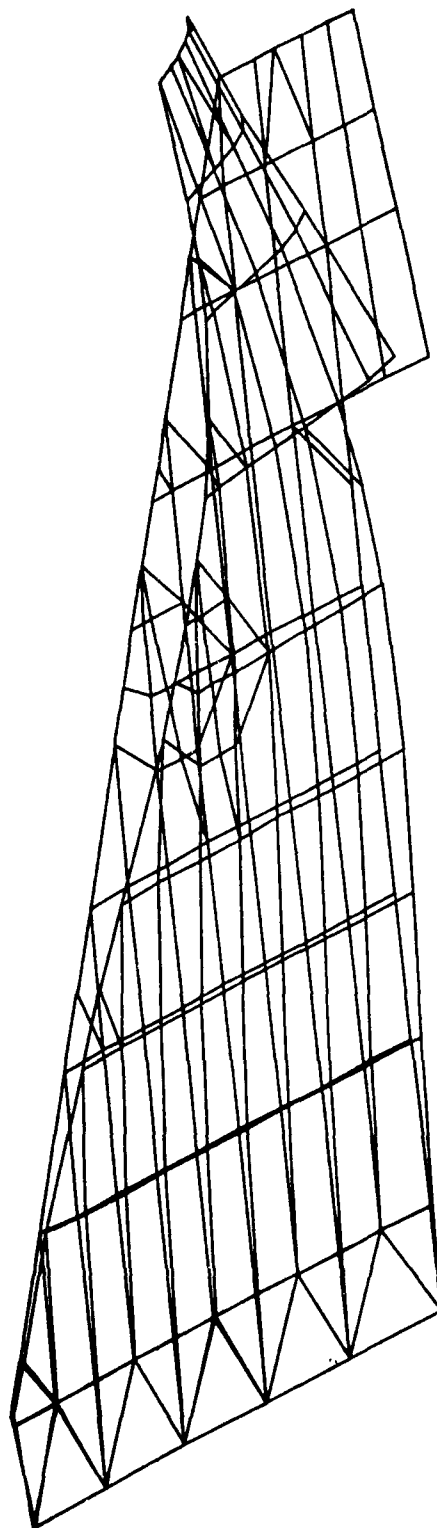
Figure A-14. 2nd Wing Bending Mode (Model D-3)

Symmetric Normal Modes for F-16 Wing Model D-3

Givens Method   Mode 3   Frequency = 45.59 Hertz
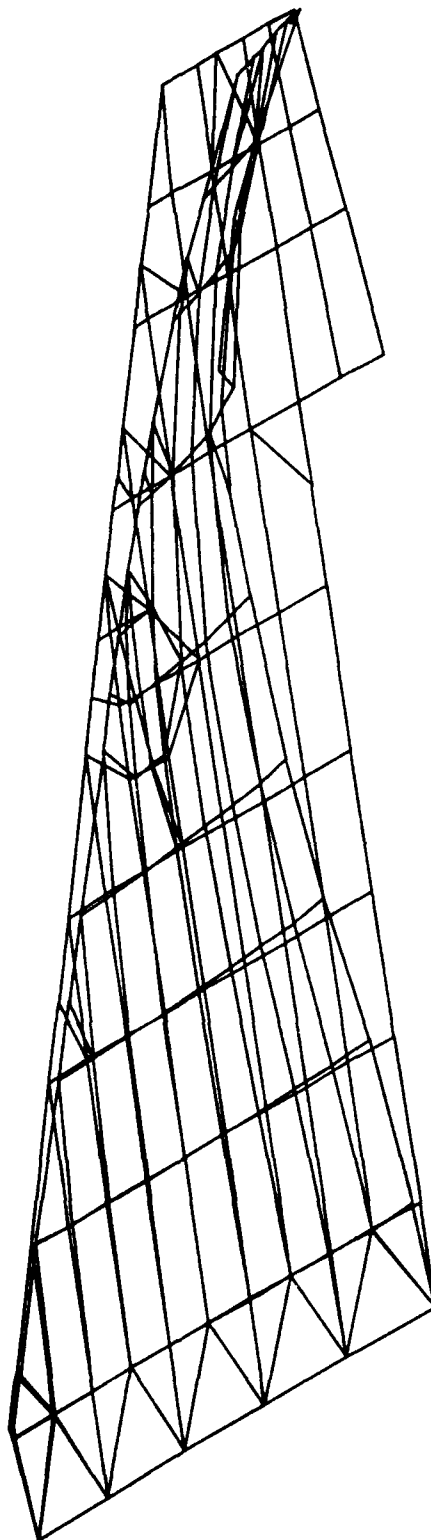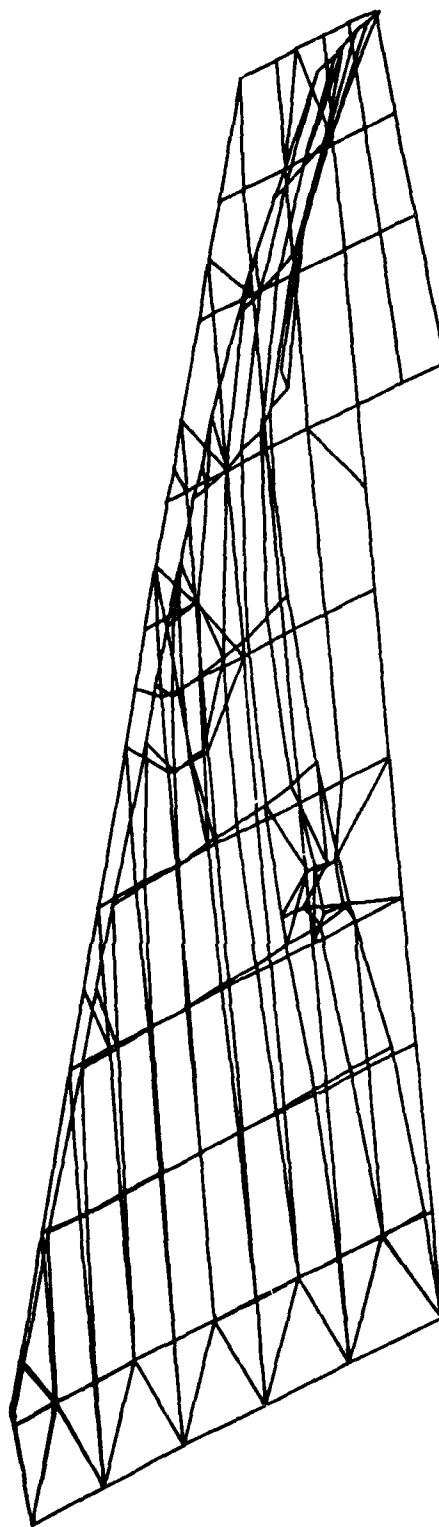

Figure A-15.   1st Torsional Mode (Model D-3)

Symmetric Normal Modes for F-16 Wing Model D-3

Givens Method   Mode 4   Frequency = 70.47 Hertz
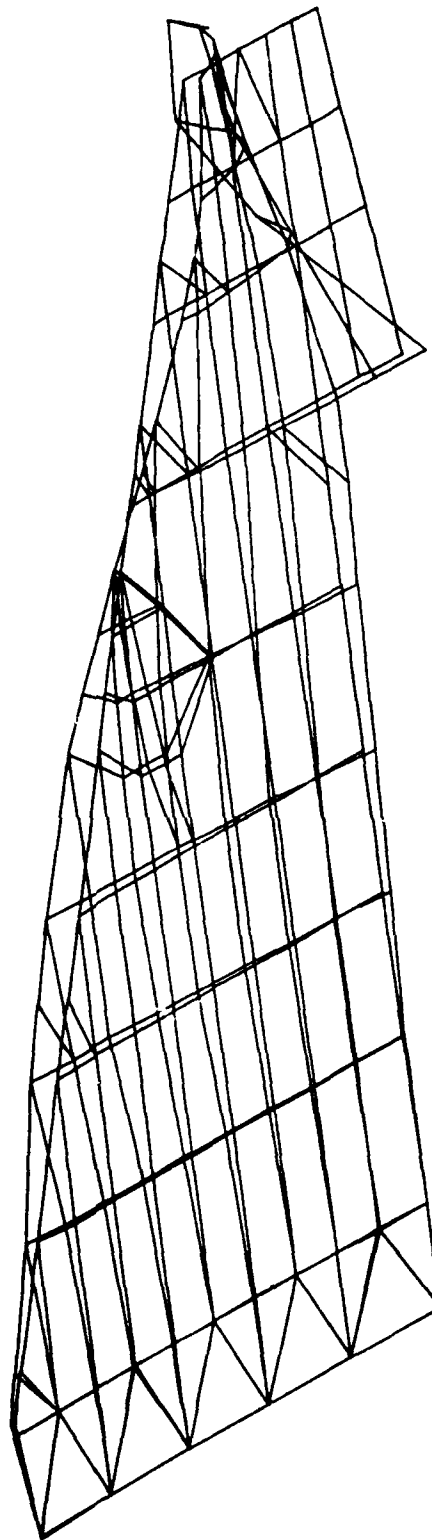
Figure A-16.   2nd Torsional Mode (Model D-3)

Symmetric Normal Modes for F-16 Wing Model D-4

Givens Method   Mode 1   Frequency = 10.94 Hertz
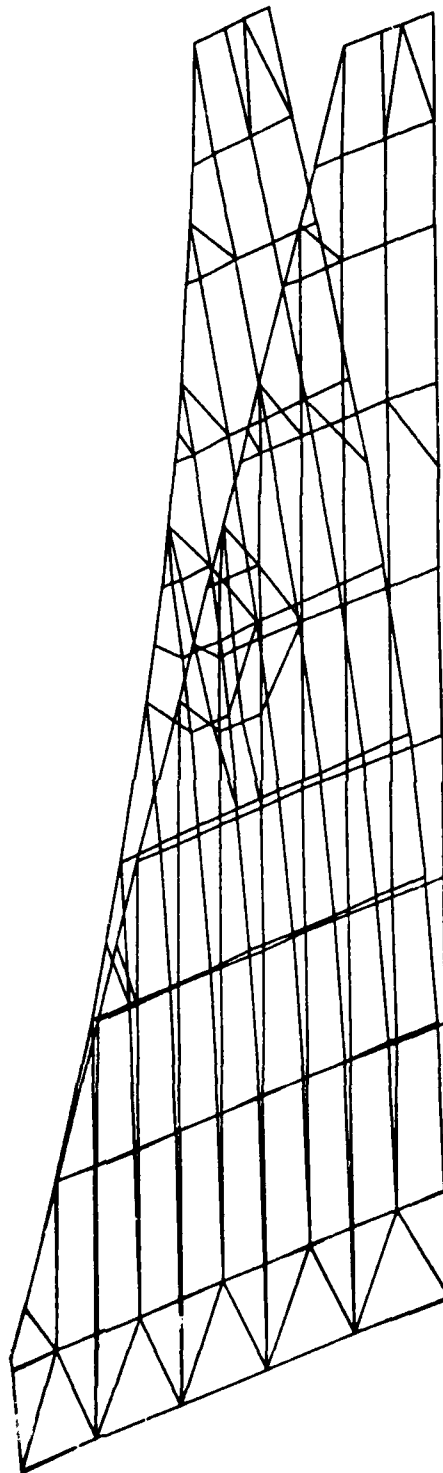
Figure A-17.   1st Wing Bending Mode (Model D-4)

Symmetric Normal Modes for F-16 Wing Model D-4

Givens Method Mode 2 Frequency = 37.28 Hertz
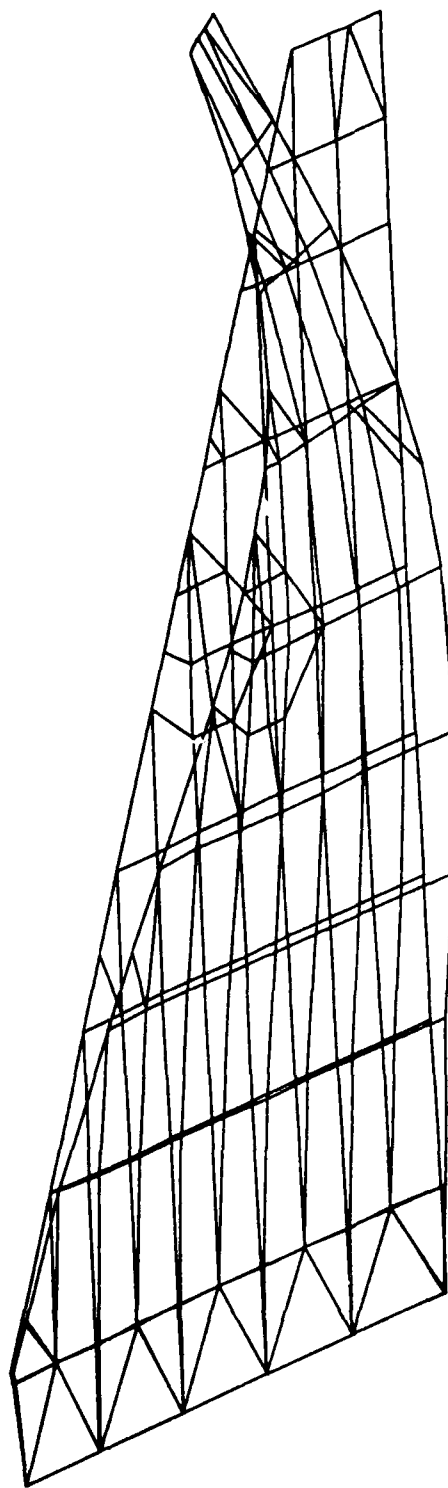
Figure A-18. 2nd Wing Bending Mode (Model D-4)

A-19

Symmetric Normal Modes for F-16 Wing Model D-4

Givens Method   Mode 3   Frequency = 48.15 Hertz
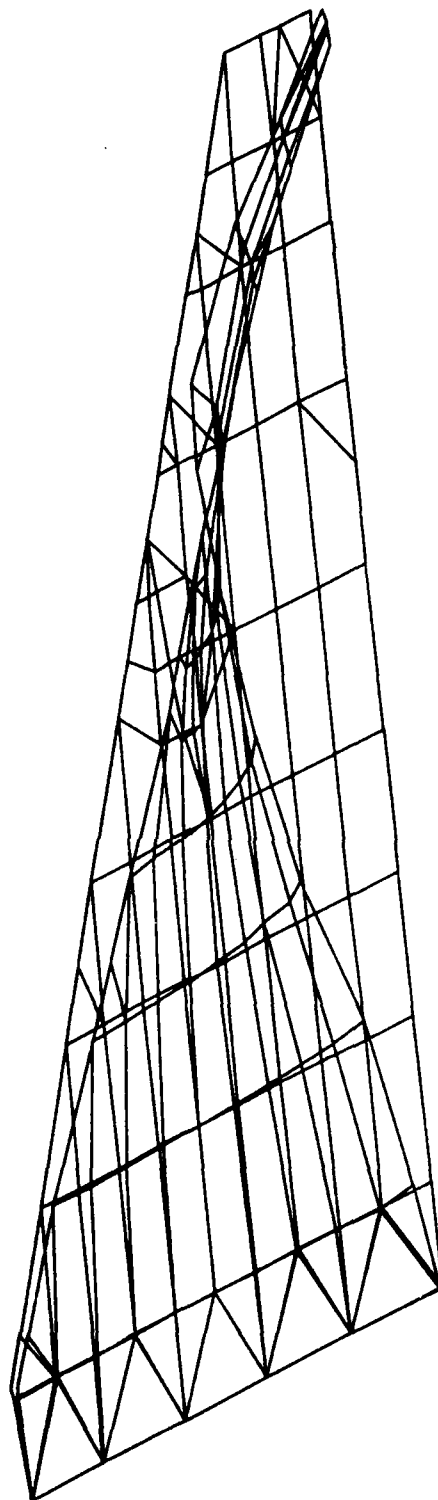
Figure A-19.   1st Torsional Mode (Model D-4)

Symmetric Normal Modes for F-16 Wing Model D-4

Givens Method   Mode 4   Frequency = 77.87 Hertz
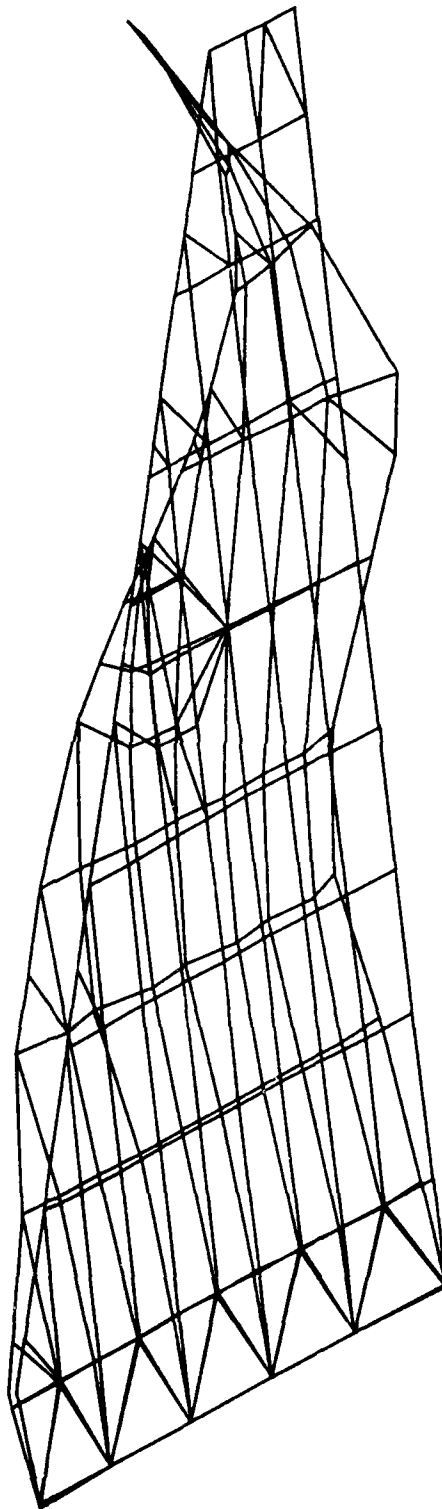
Figure A-20.   2nd Torsional Mode (Model D-4)

APPENDIX B

STATIC ANALYSIS OF UNDAMAGED WING MODELS

Figure B-1. Upper Wing Surface (Undamaged Model D-3)
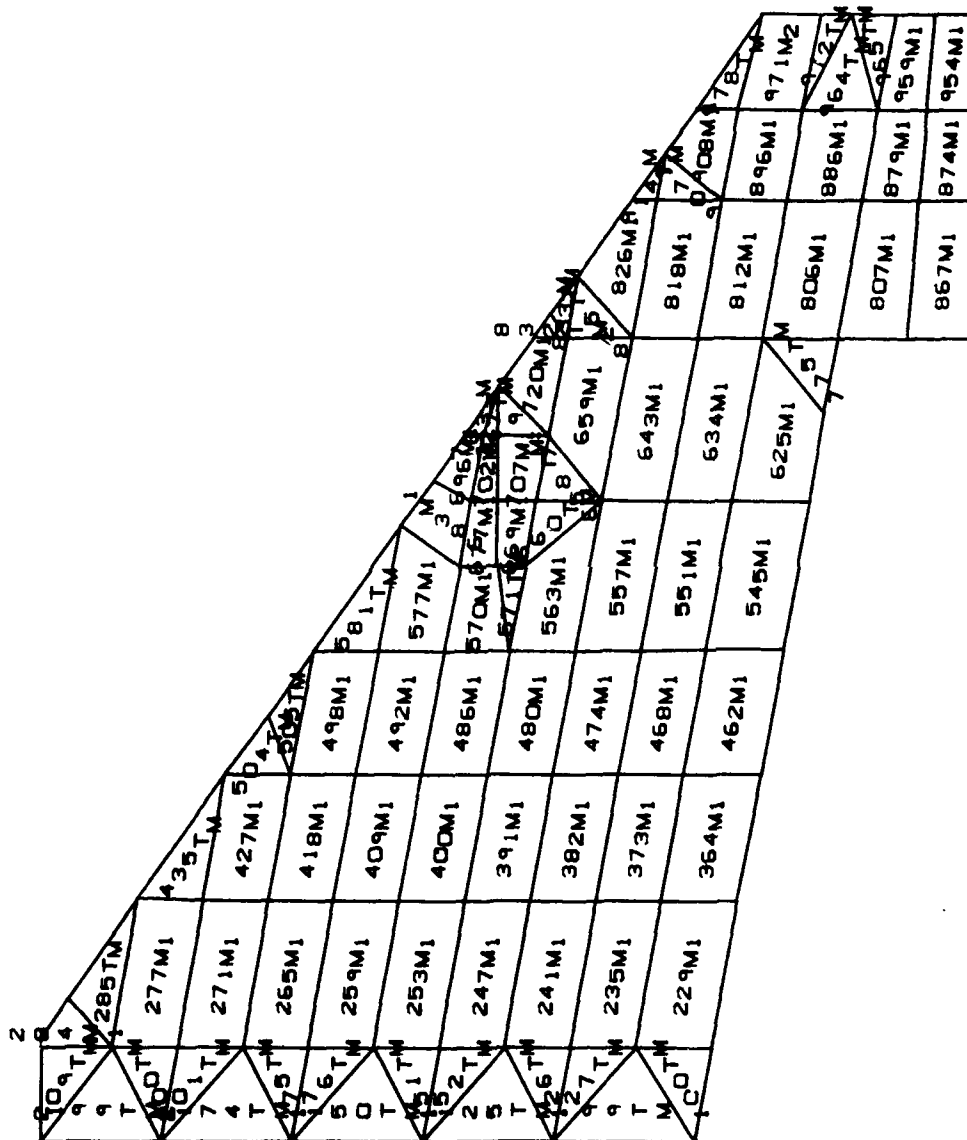
Figure B-2. Lower Wing Surface (Undamaged Model D-3)

CONTOUR SYMBOLS
PSI-Compression

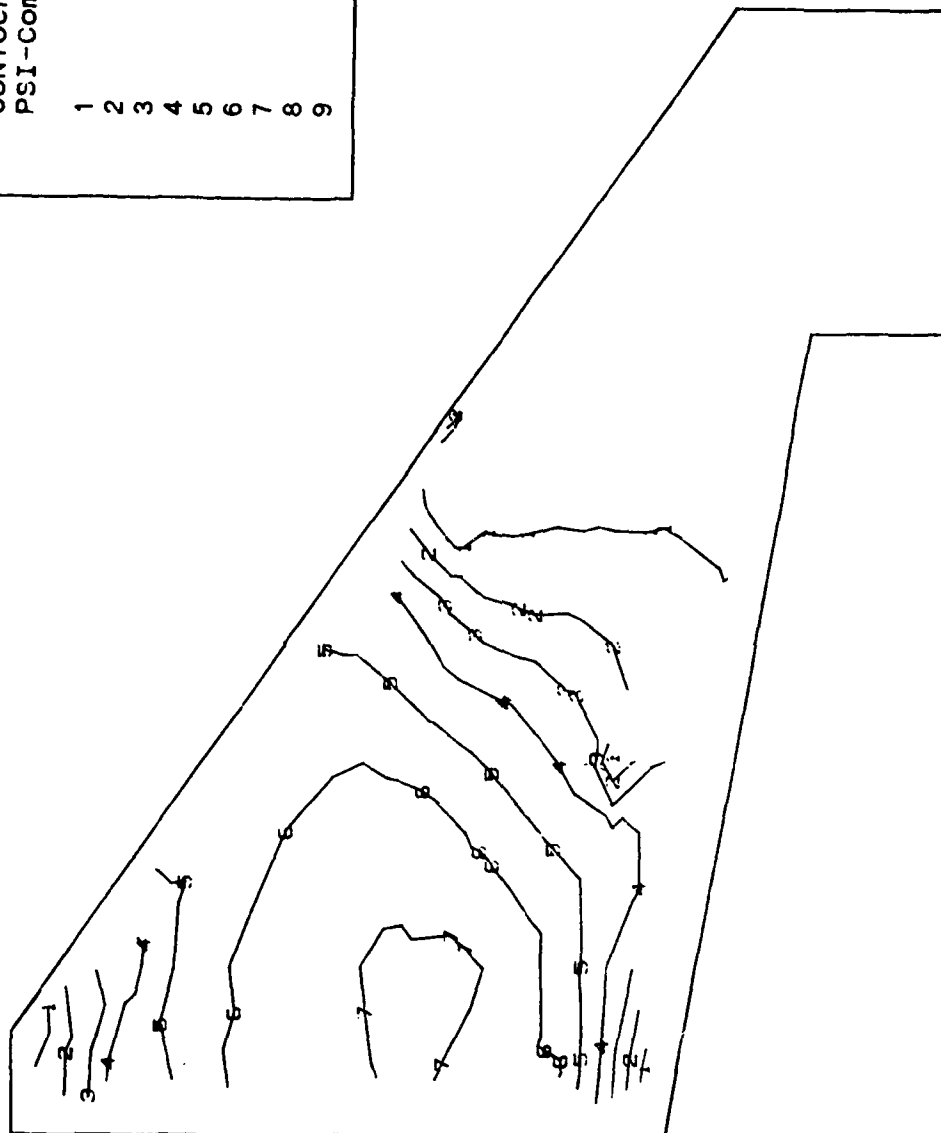|	
1	3,000
2	6,000
3	9,000
4	12,000
5	15,000
6	18,000
7	21,000
8	23,000
9	25,000
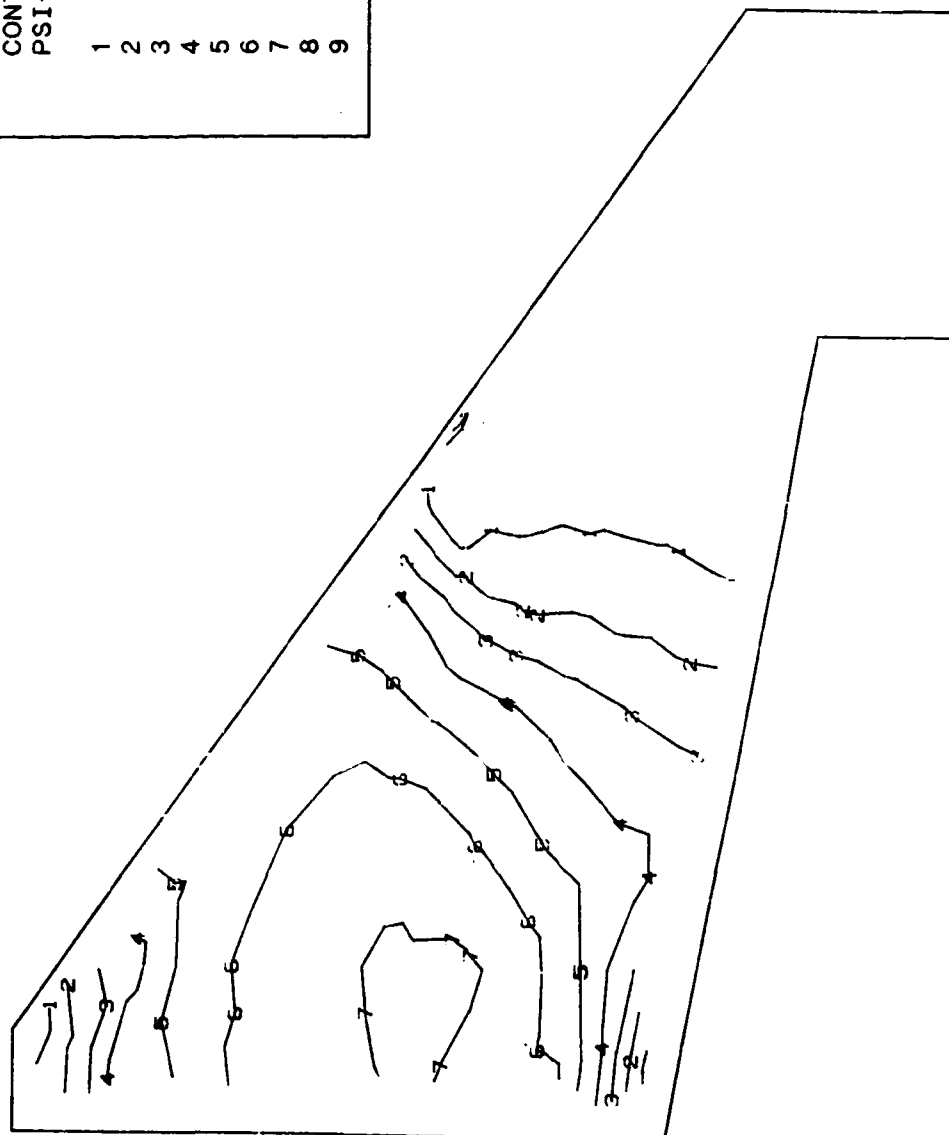
Figure B-3. Stress Contours on Upper Wing Surface (Undamaged Model D-3)

CONTOUR SYMBOLS
PSI-Tension

1   3,000
2   6,000
3   9,000
4   12,000
5   15,000
6   17,000
7   19,000
8   21,000
9   23,000
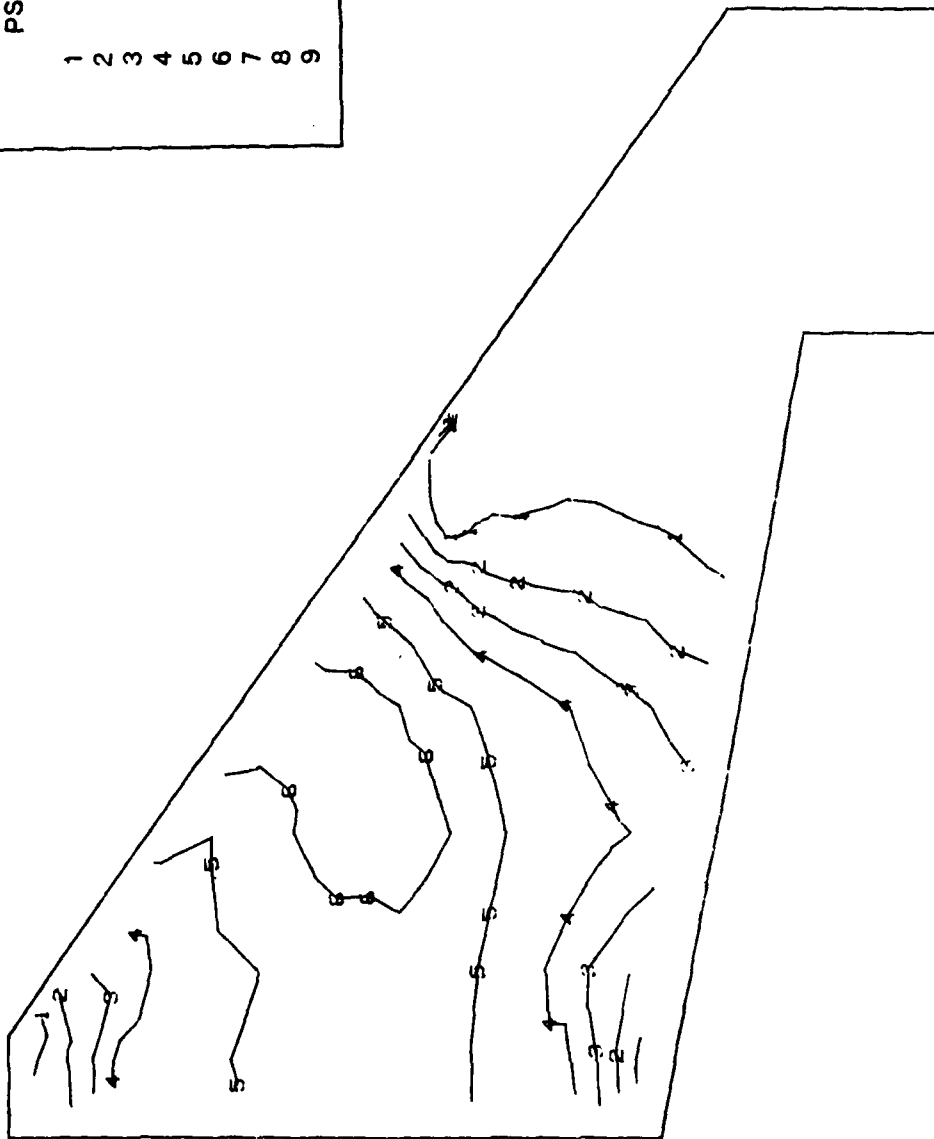
Figure B-4. Stress Contours on Lower Wing Surface (Undamaged Model D-3)
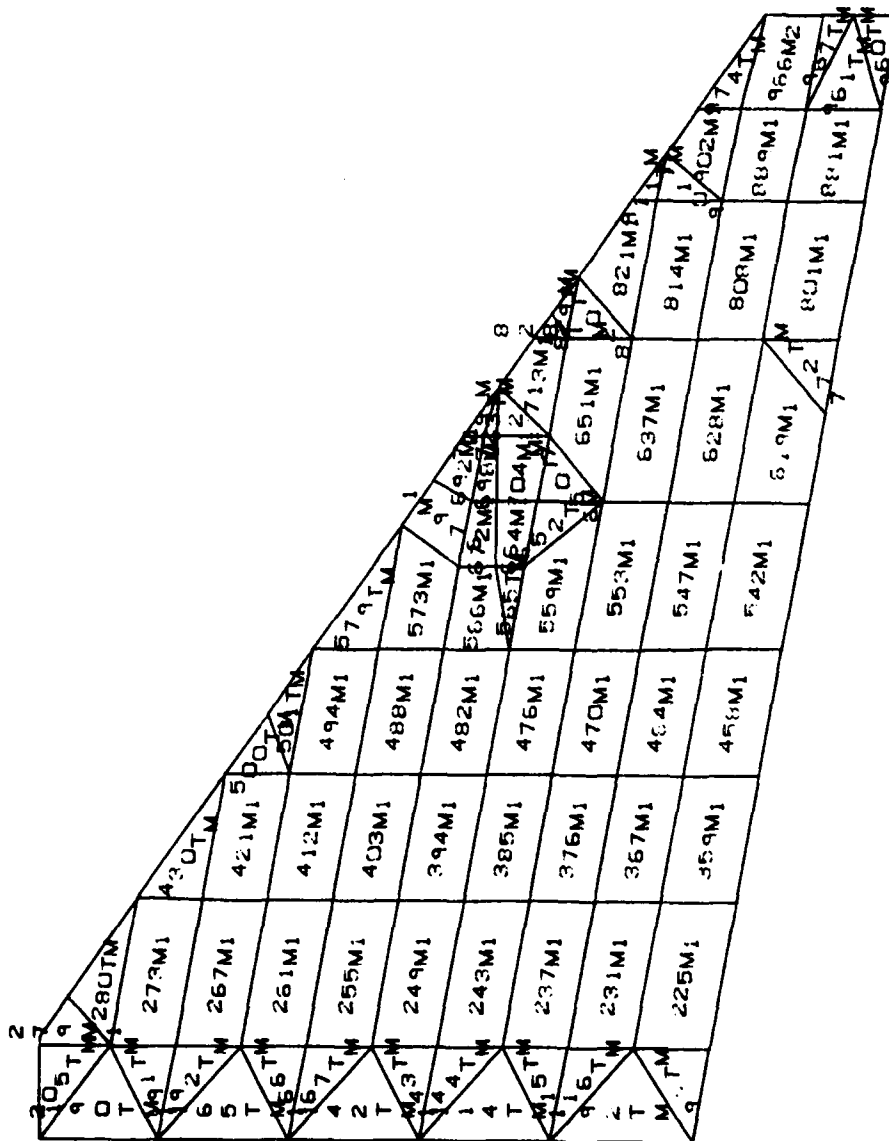
Figure B-5. Upper Wing Surface (Undamaged Model D-4)
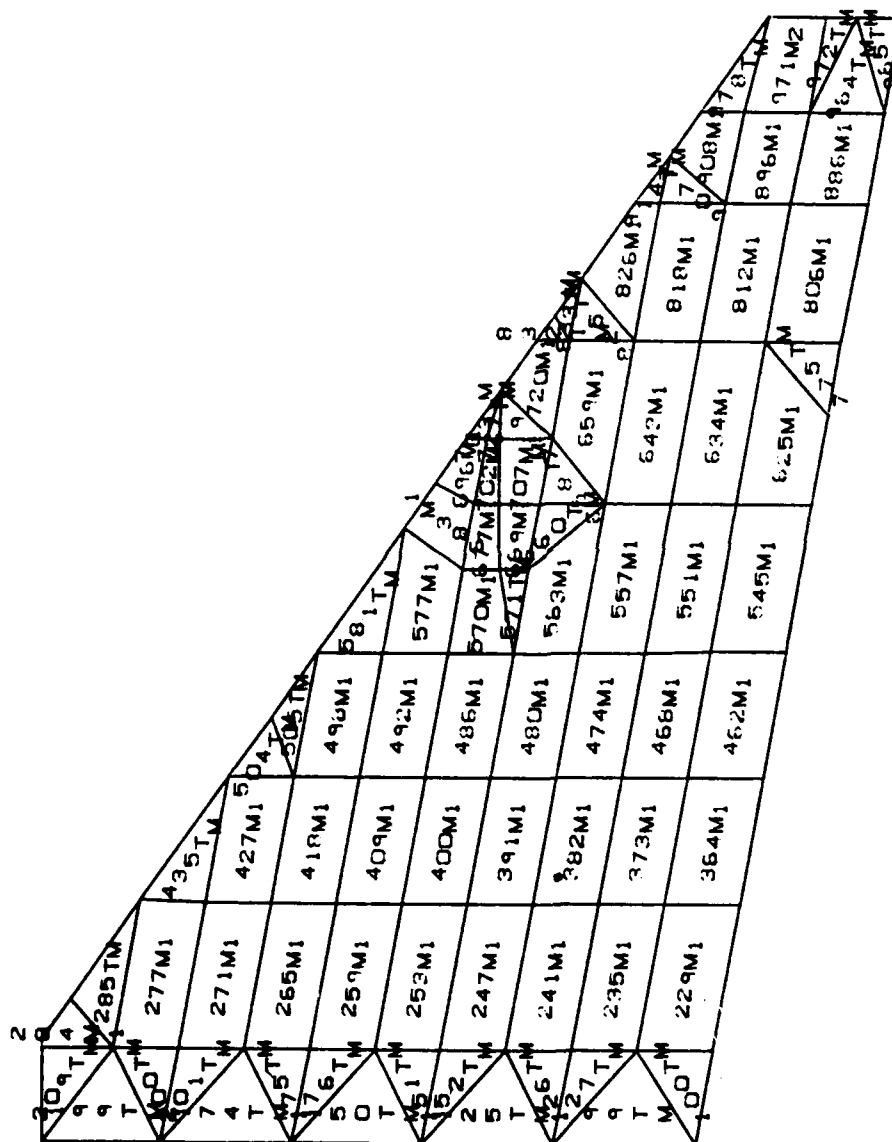
B-6

Figure B-6. Lower Wing Surface (Undamaged Model D-4)

B-7

CONTOUR SYMBOLS
PSI-Compression

1	3,000
2	6,000
3	9,000
4	12,000
5	15,000
6	18,000
7	21,000
8	23,000
9	25,000

Figure B-7. Stress Contours on Upper Wing Surface (Undamaged Model D-4)

CONTOUR SYMBOLS
PSI-Tension

1	3,000
2	6,000
3	9,000
4	12,000
5	15,000
6	17,000
7	19,000
8	21,000
9	23,000
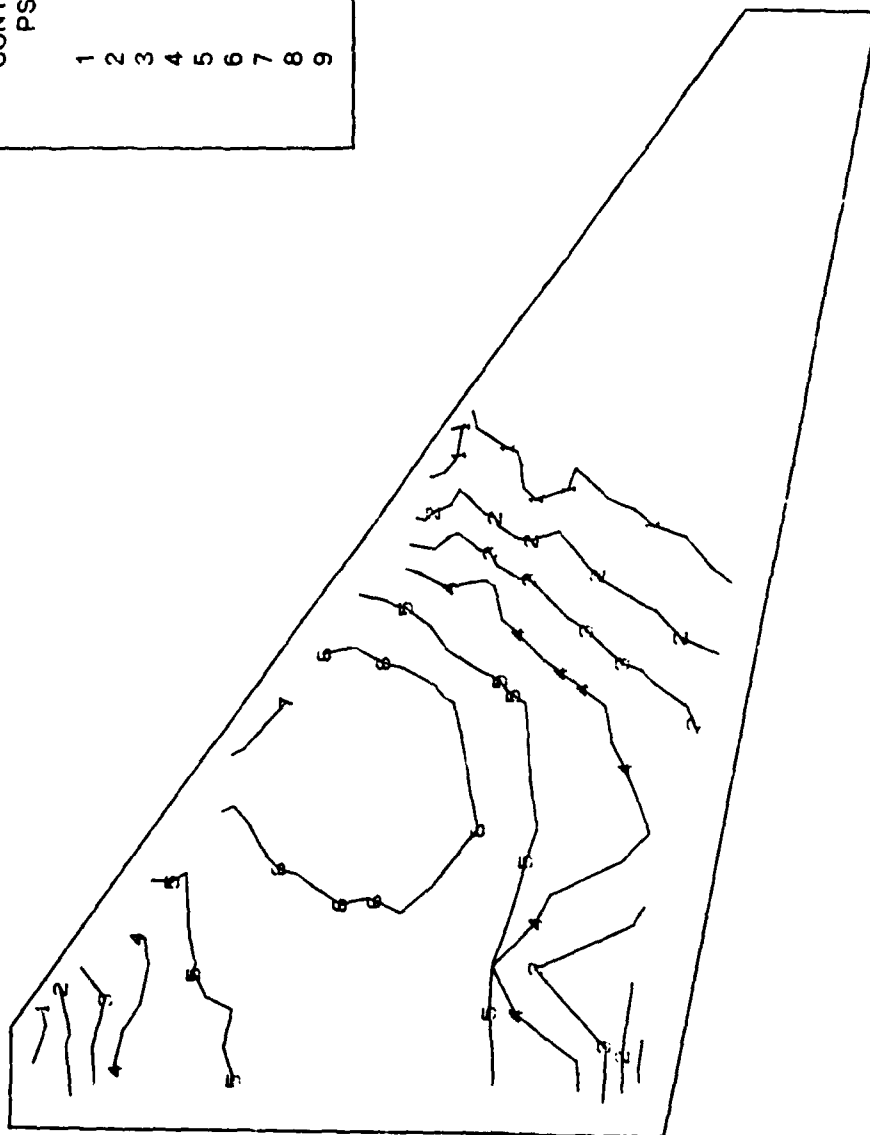
Figure B-8.   Stress Contours on Lower Wing Surface (Undamaged Model D-4)

APPENDIX C

ANALYSIS OF DAMAGE CASE #1

Plot of Wing Displacements at BL 120.0

--- Before Damage   ·— Damage Case   -- Repaired
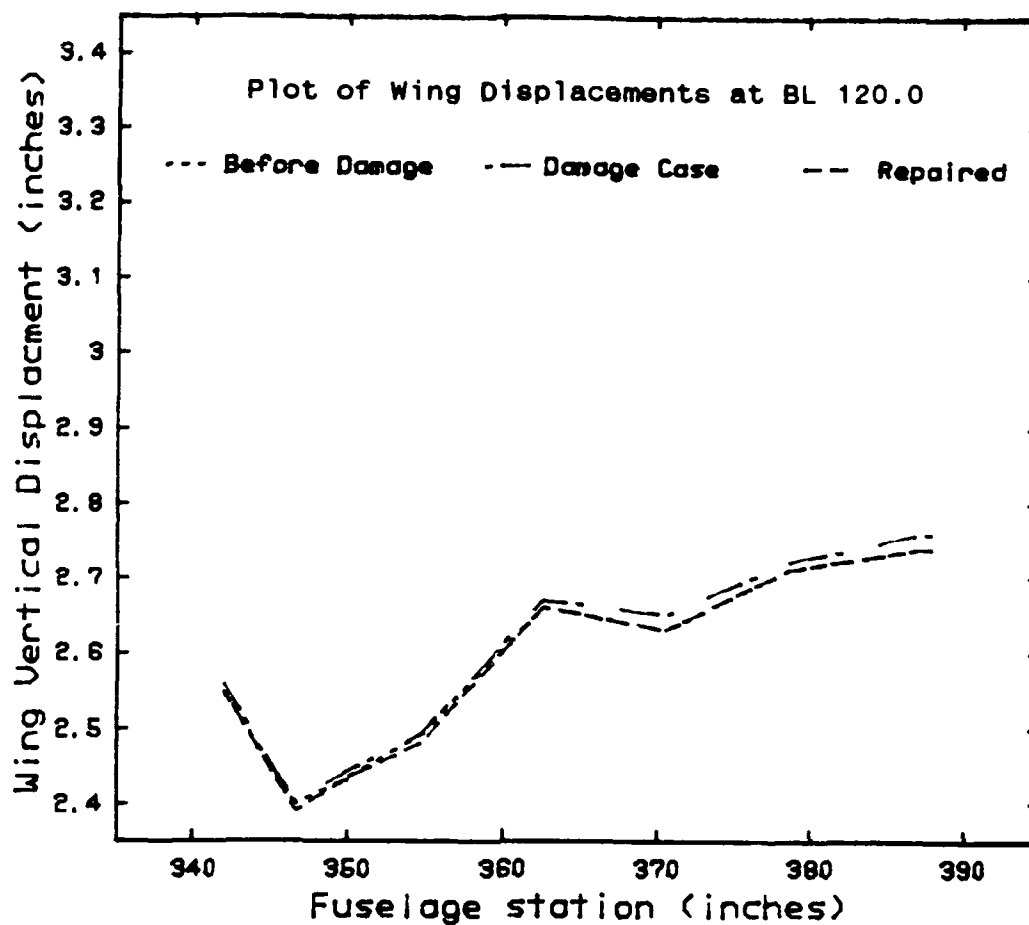
Tabulated Displacements

Fuselage St.	387.9	378.6	370.6	362.6	354.6	349.7	346.6	341.9
Model D-3	2.74	2.71	2.63	2.66	2.49	2.43	2.40	2.55
Model DC-1	2.76	2.72	2.65	2.67	2.49	2.44	2.40	2.56
Model DC-1R	2.74	2.71	2.63	2.66	2.48	2.43	2.39	2.55

Comparison of Residual Strength

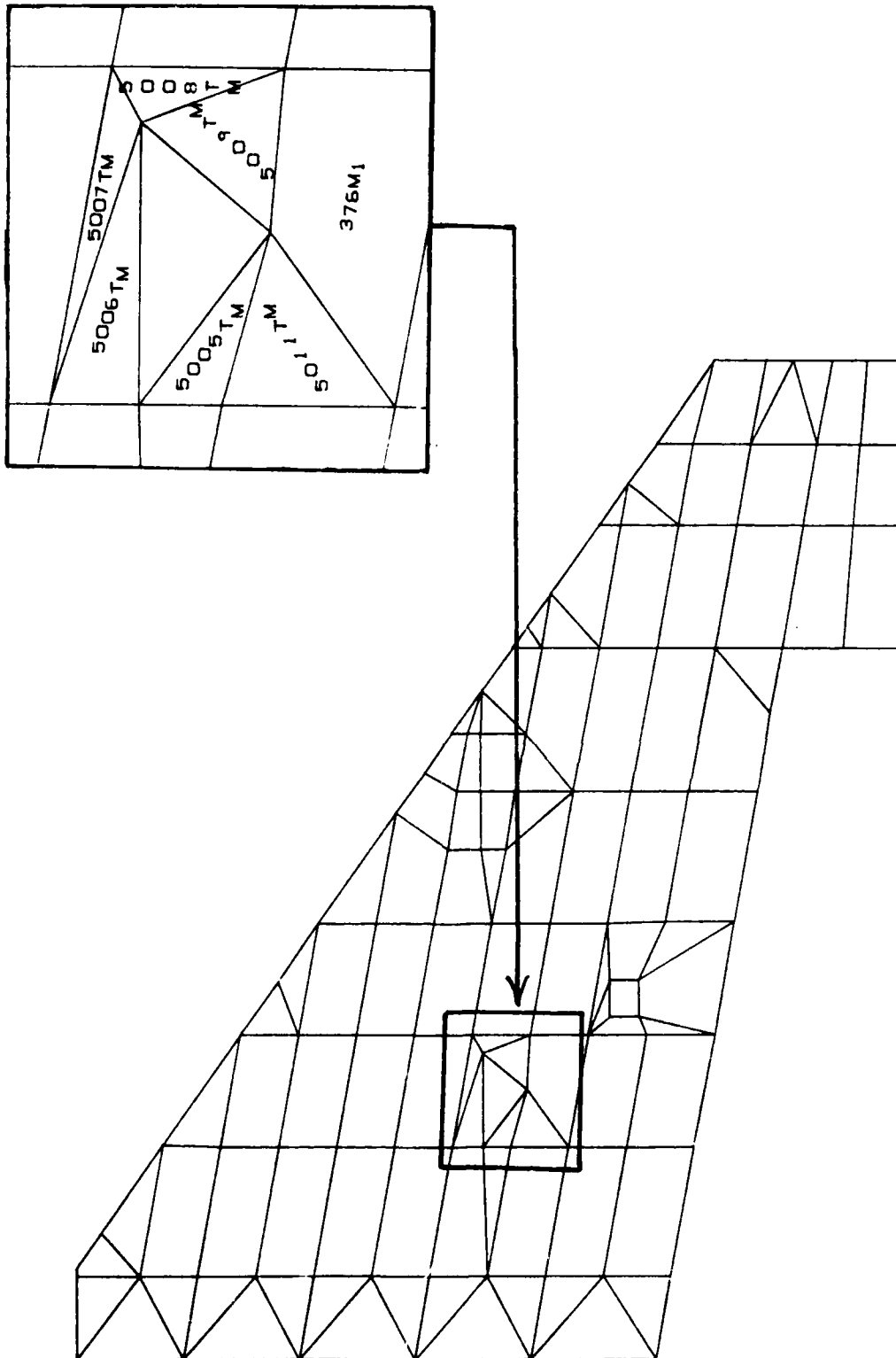|	Av Disp	% Change	Torsion mode	% Change
Model D-3	2.58		45.59	
Model DC-1	2.59	-0.4	45.15	-1.0
Model DC-1R	2.58	+0.4	45.62	+1.0

Figure C-1.   Summary of Damage Case #1 Results
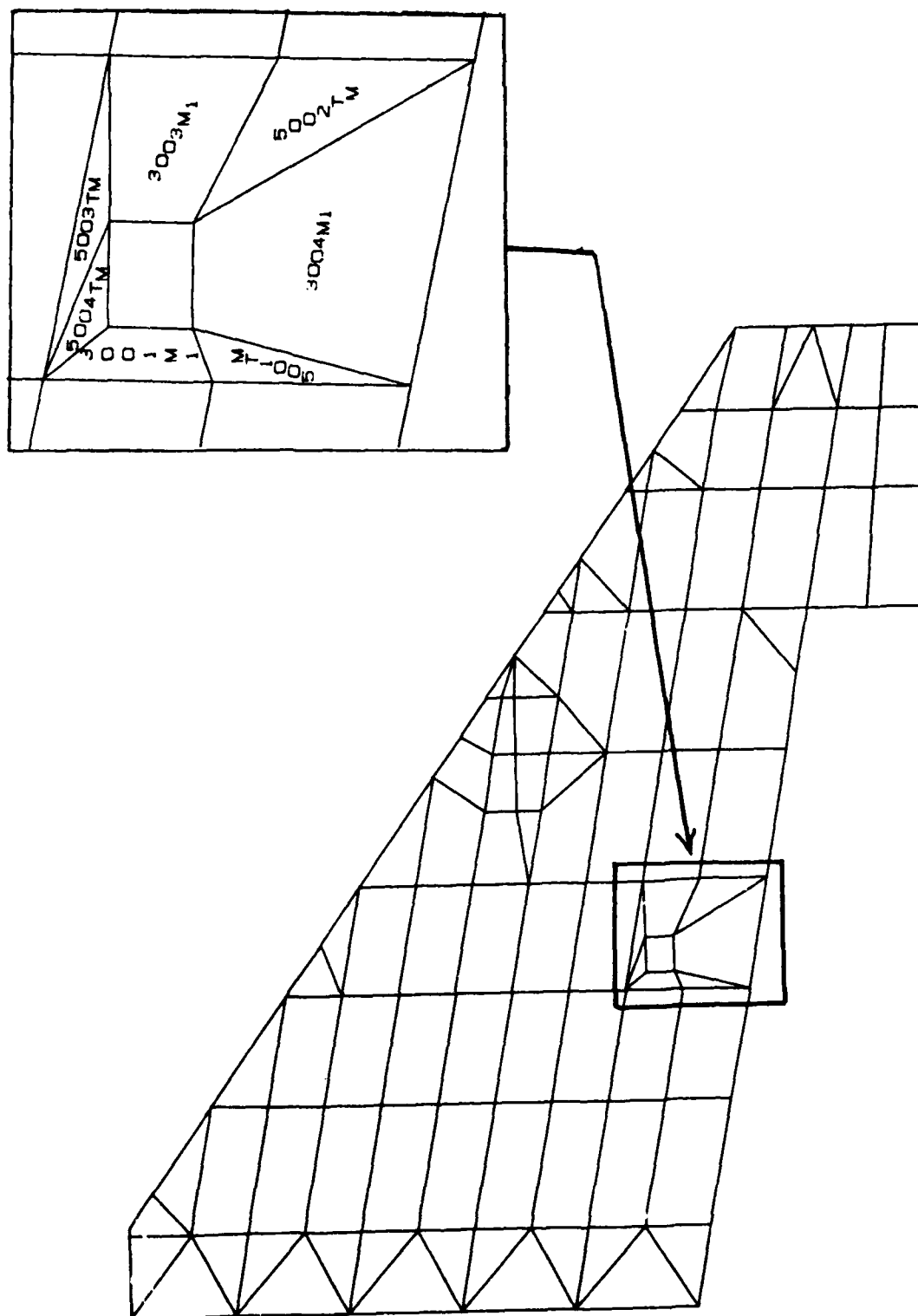
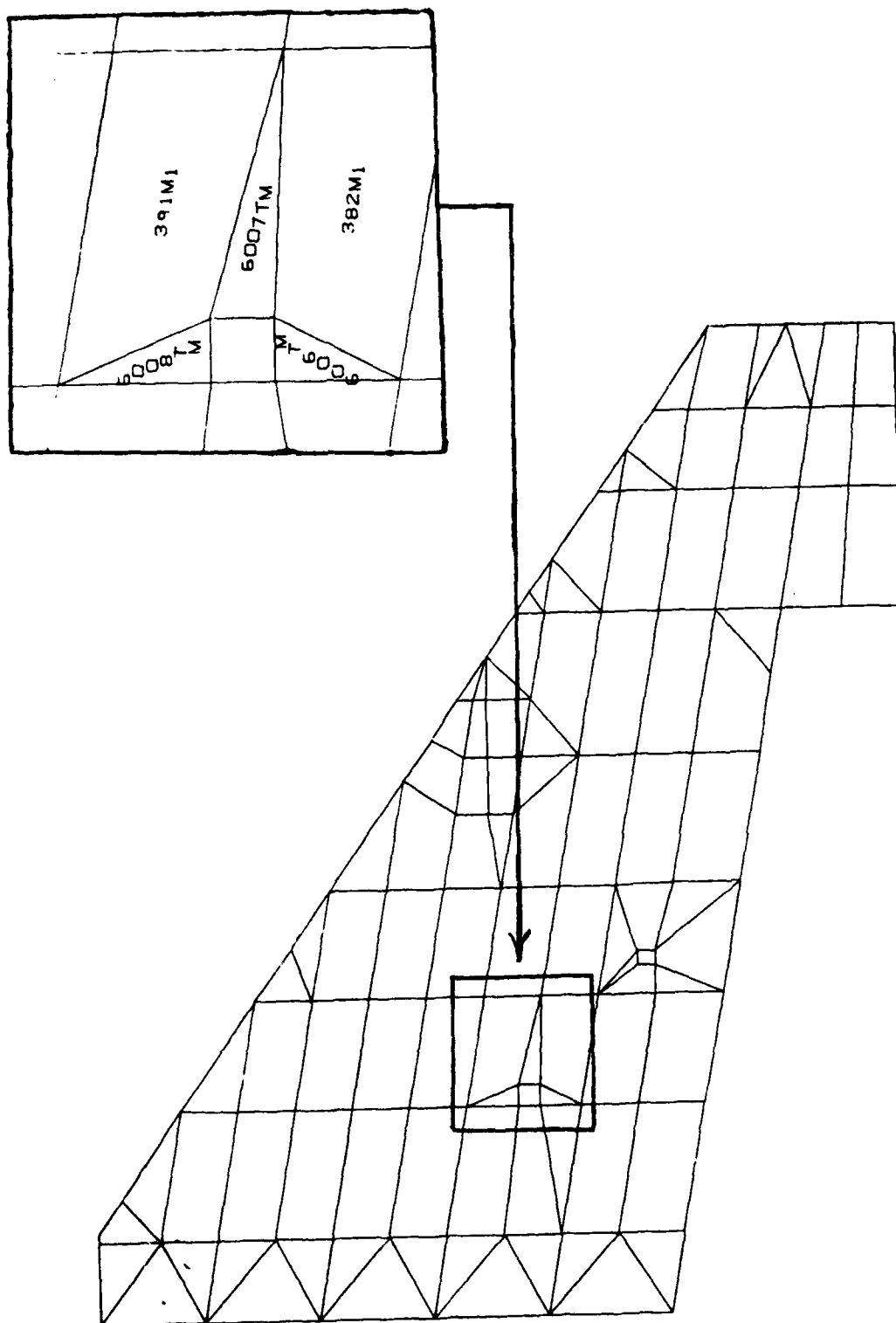Figure C-2. Upper Wing Surface (Model DC-1)
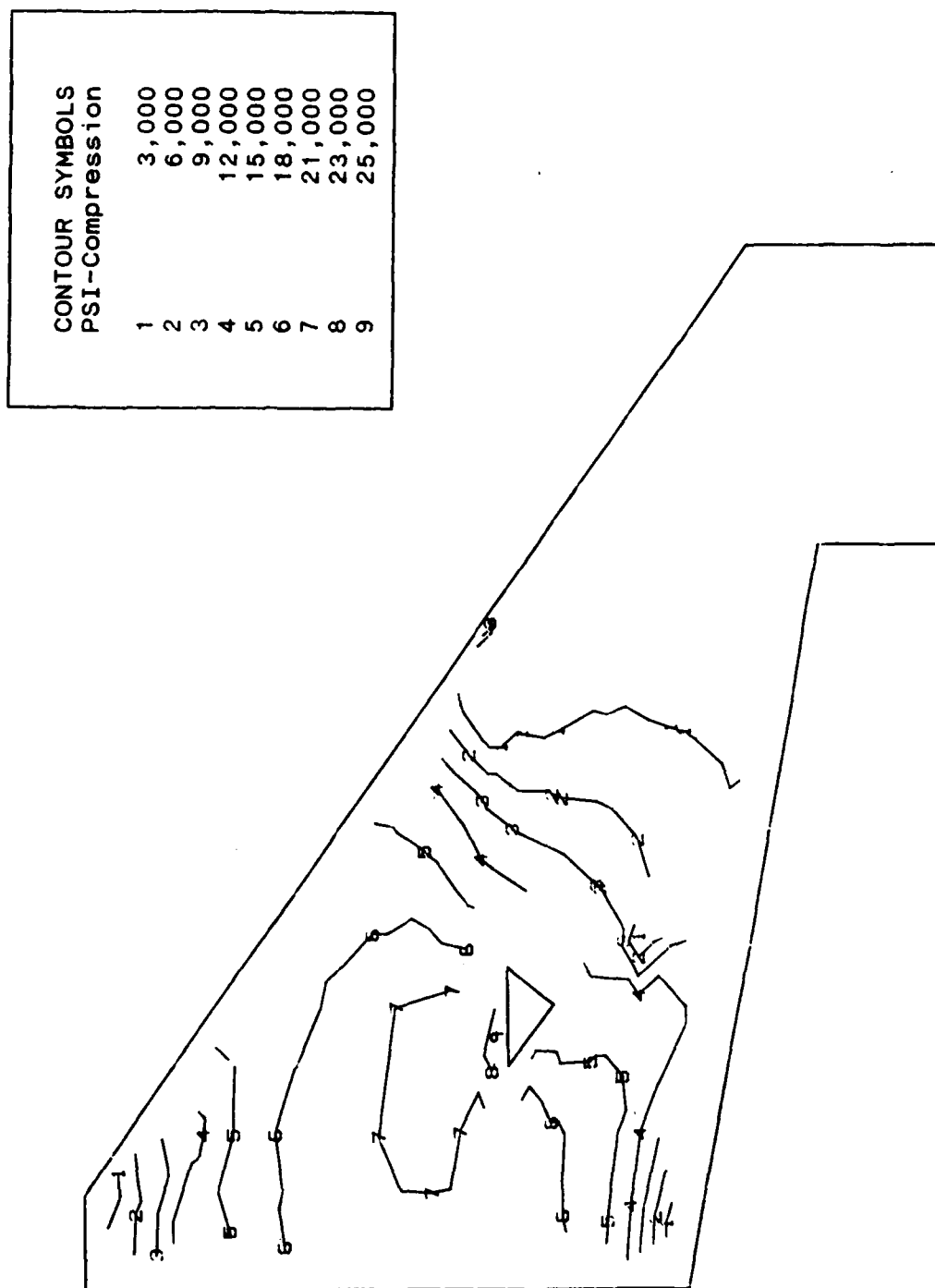
C-3
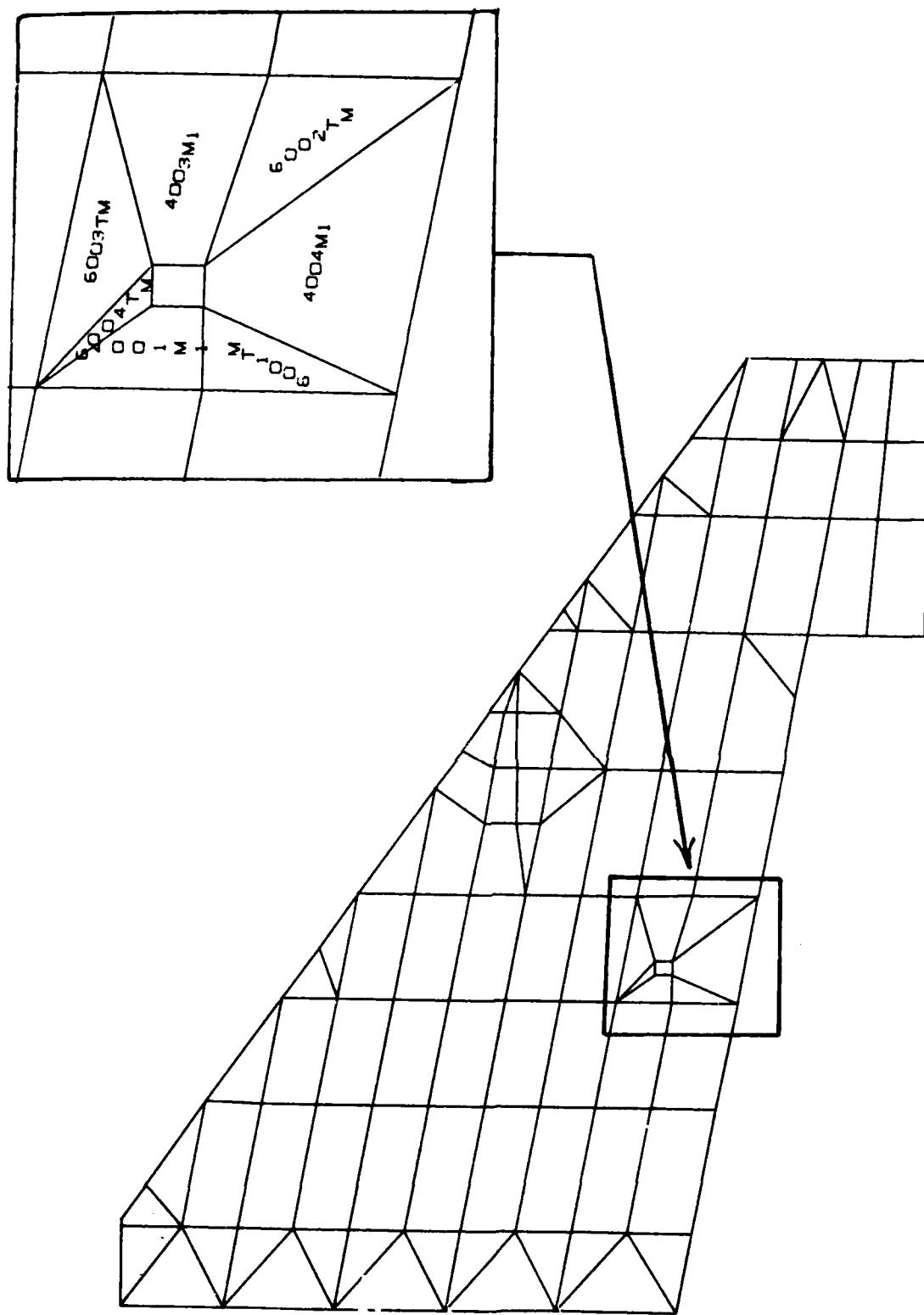
Figure C-3. Lower Wing Surface (Model DC-1)

CONTOUR SYMBOLS
PSI-Compression

1	3,000
2	6,000
3	9,000
4	12,000
5	15,000
6	18,000
7	21,000
8	23,000
9	25,000
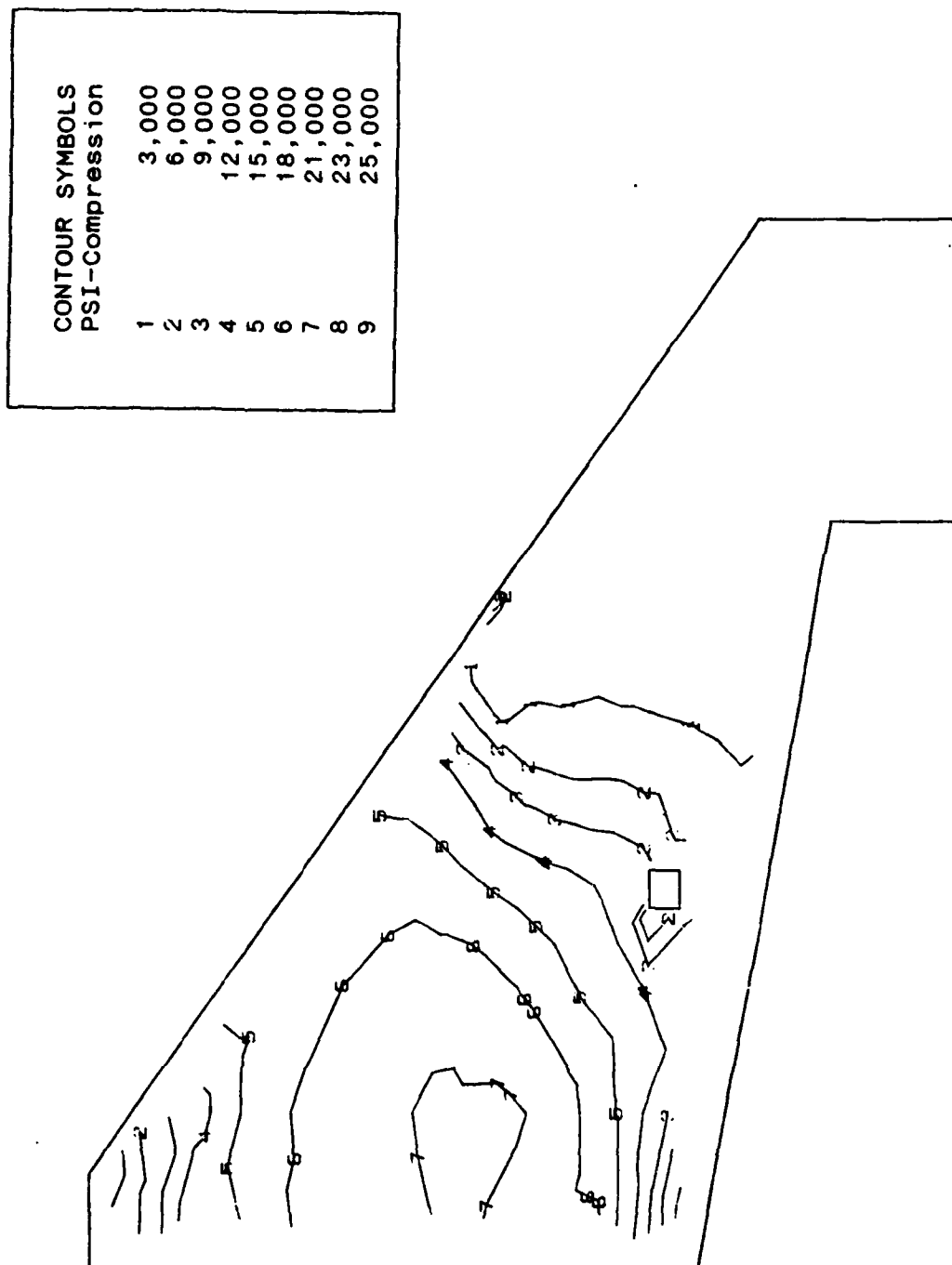
Figure C-4. Stress Contours on Upper Wing Surface (Model DC-1)

CONTOUR SYMBOLS
PSI-Tension

1	3,000
2	6,000
3	9,000
4	12,000
5	15,000
6	17,000
7	19,000
8	21,000
9	23,000
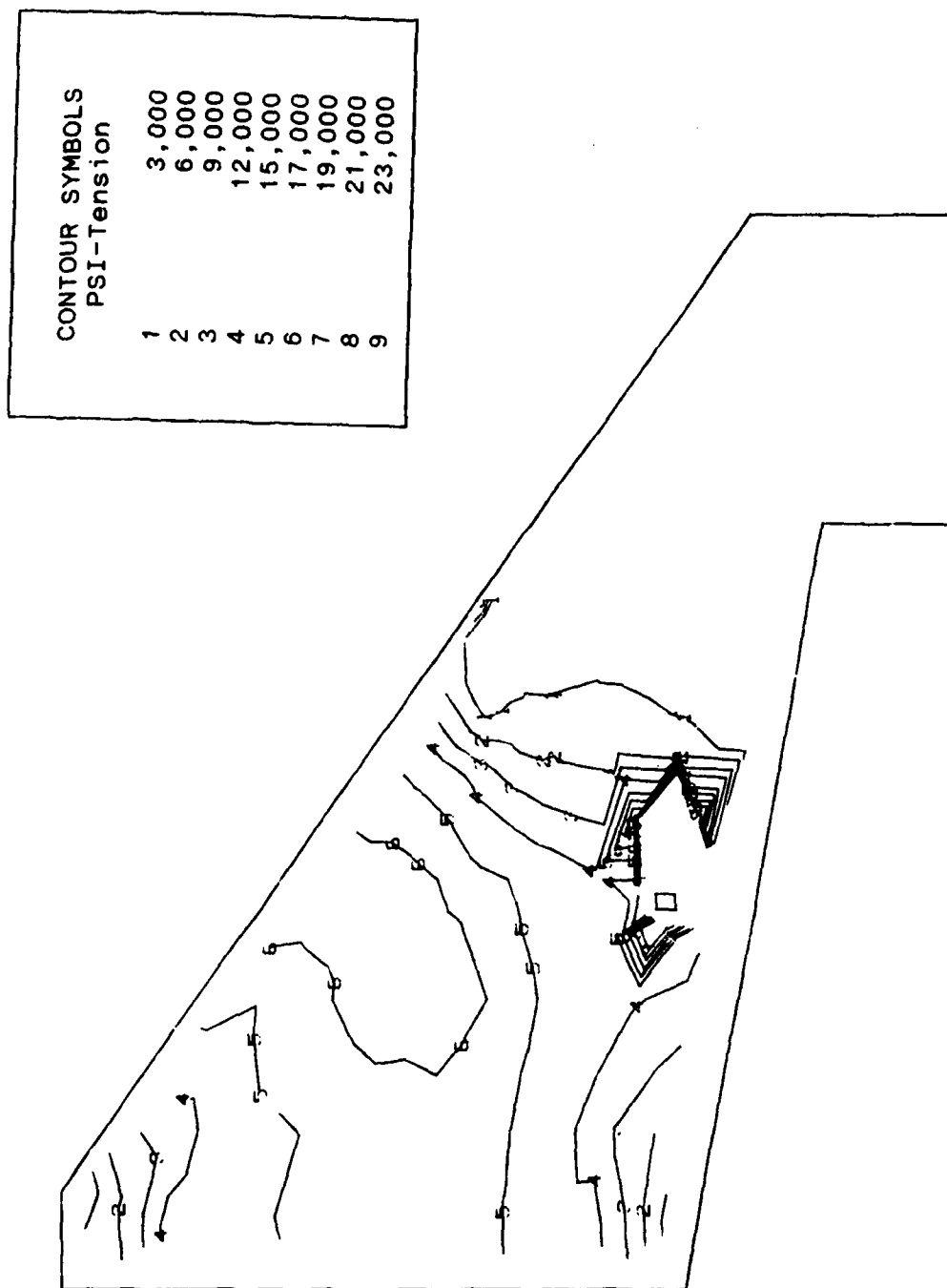
Figure C-5. Stress Contours on Lower Wing Surface (Model DC-1)

Symmetric Normal Modes for F-16 Wing Model DC-1
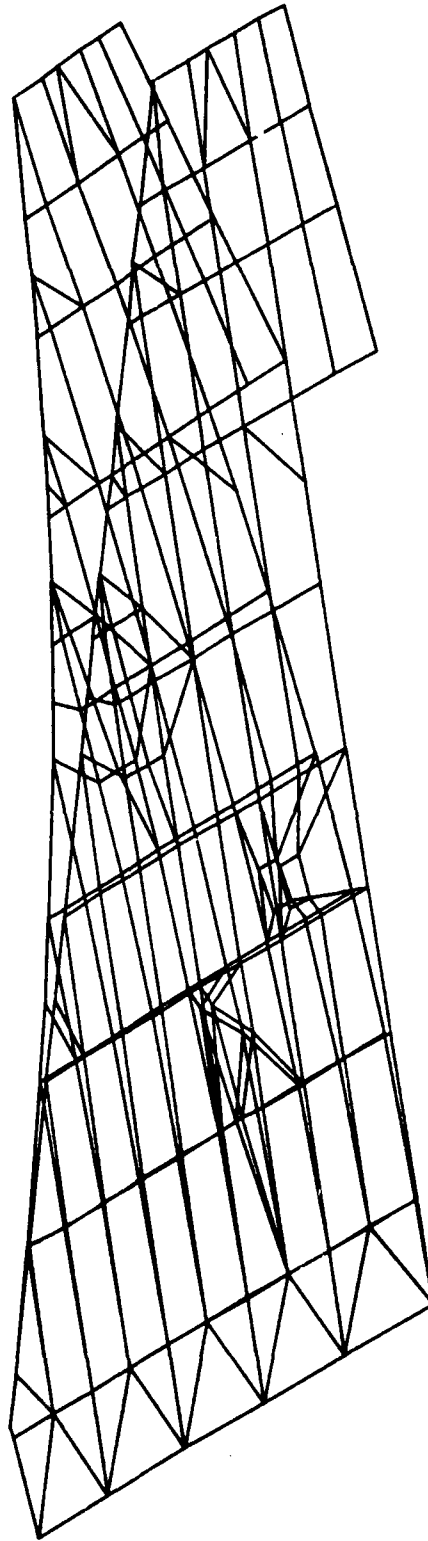
Givens Method   Mode 1   Frequency = 10.49 Hertz

Figure C-6.   1st Wing Bending Mode (Model DC-1)

Symmetric Normal Modes for F-16 Wing Model DC-1

Givens Method   Mode 2   Frequency = 35.26 Hertz
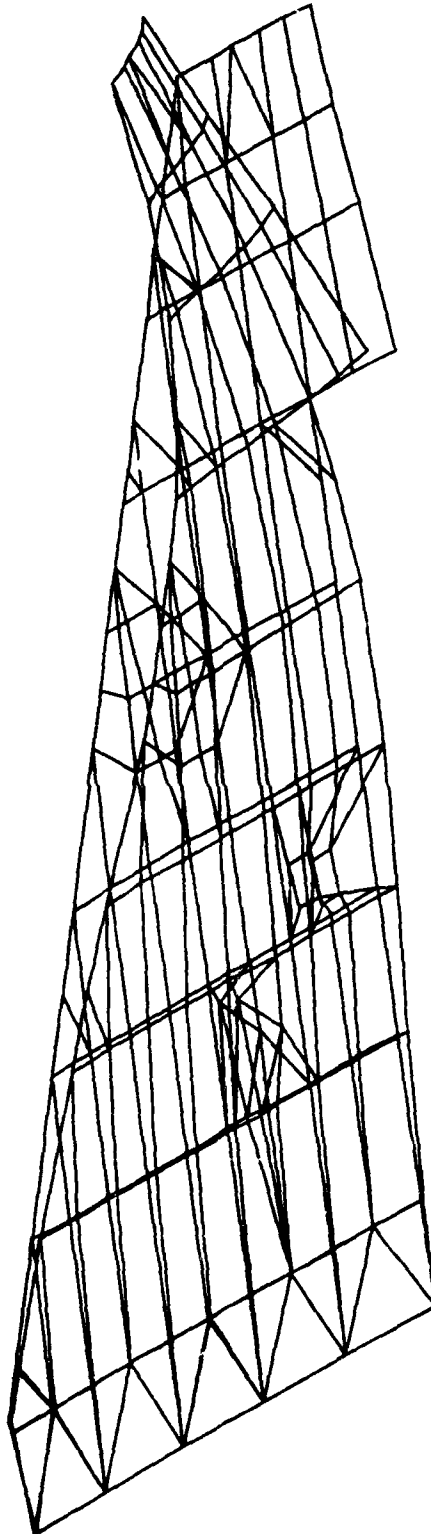
Figure C-7.   2nd Wing Bending Mode (Model DC-1)

Symmetric Normal Modes for F-16 Wing Model DC-1
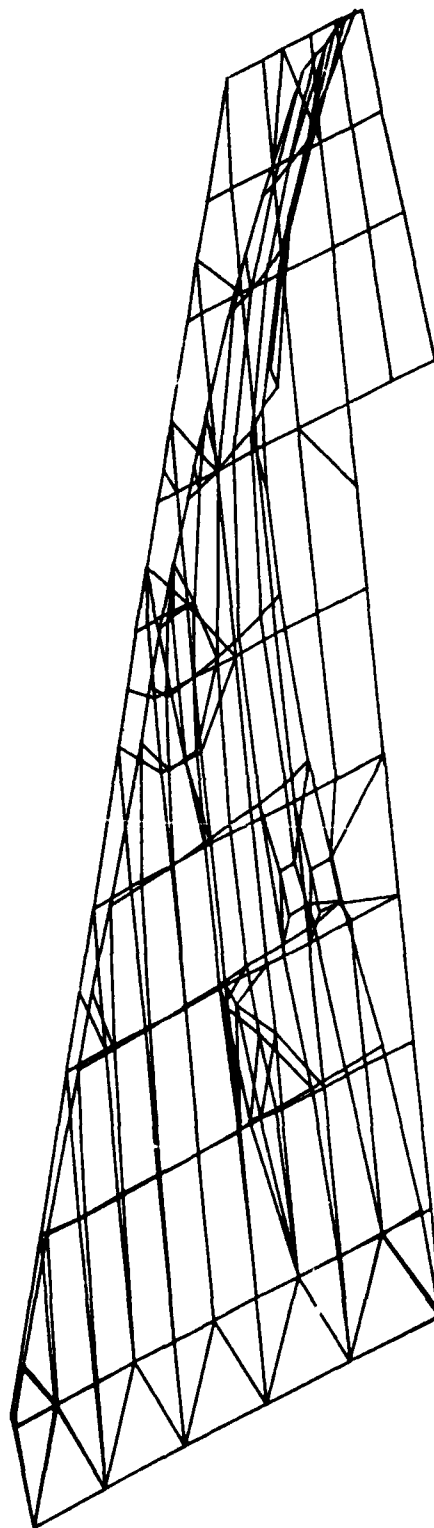
Givens Method   Mode 3   Frequency = 45.15 Hertz

Figure C-8. 1st Torsional Mode (Model DC-1)

Symmetric Normal Modes for F-16 Wing Model DC-1

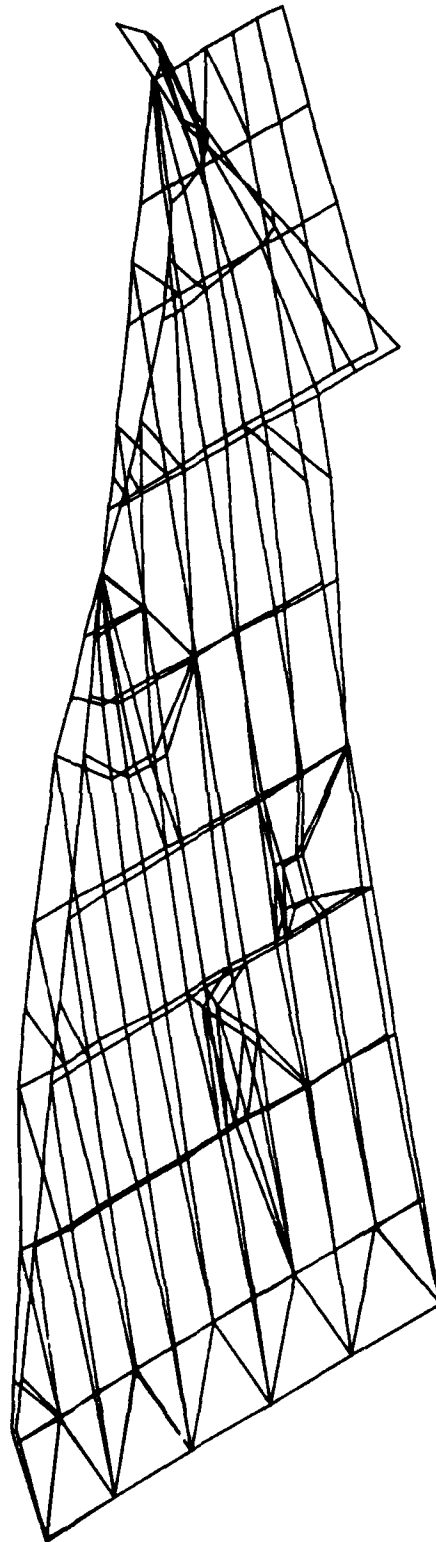Givens Method   Mode 4   Frequency = 70.21 Hertz
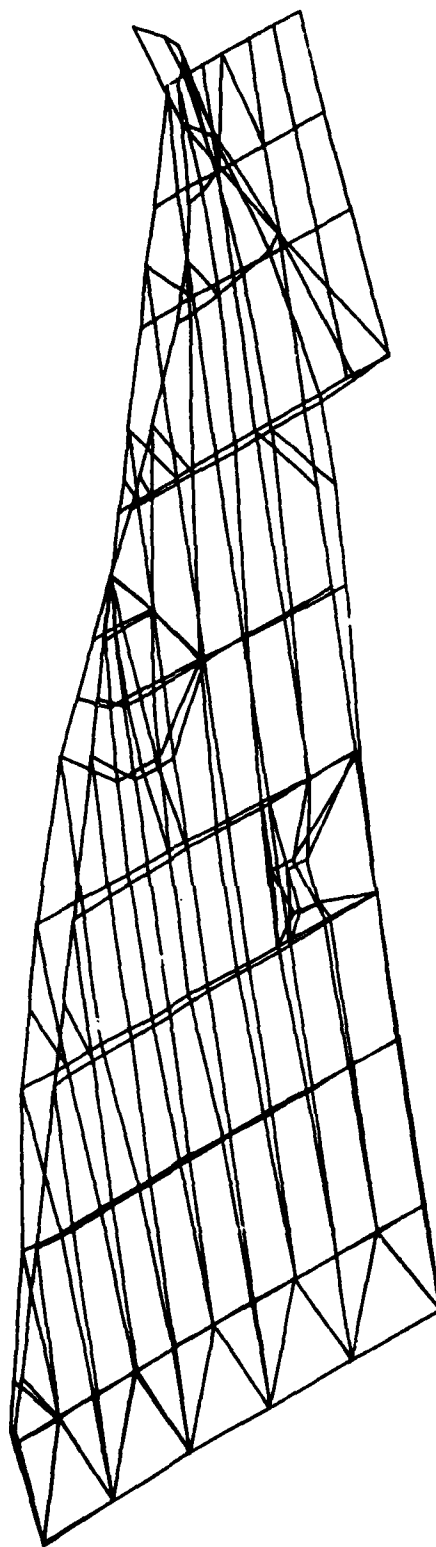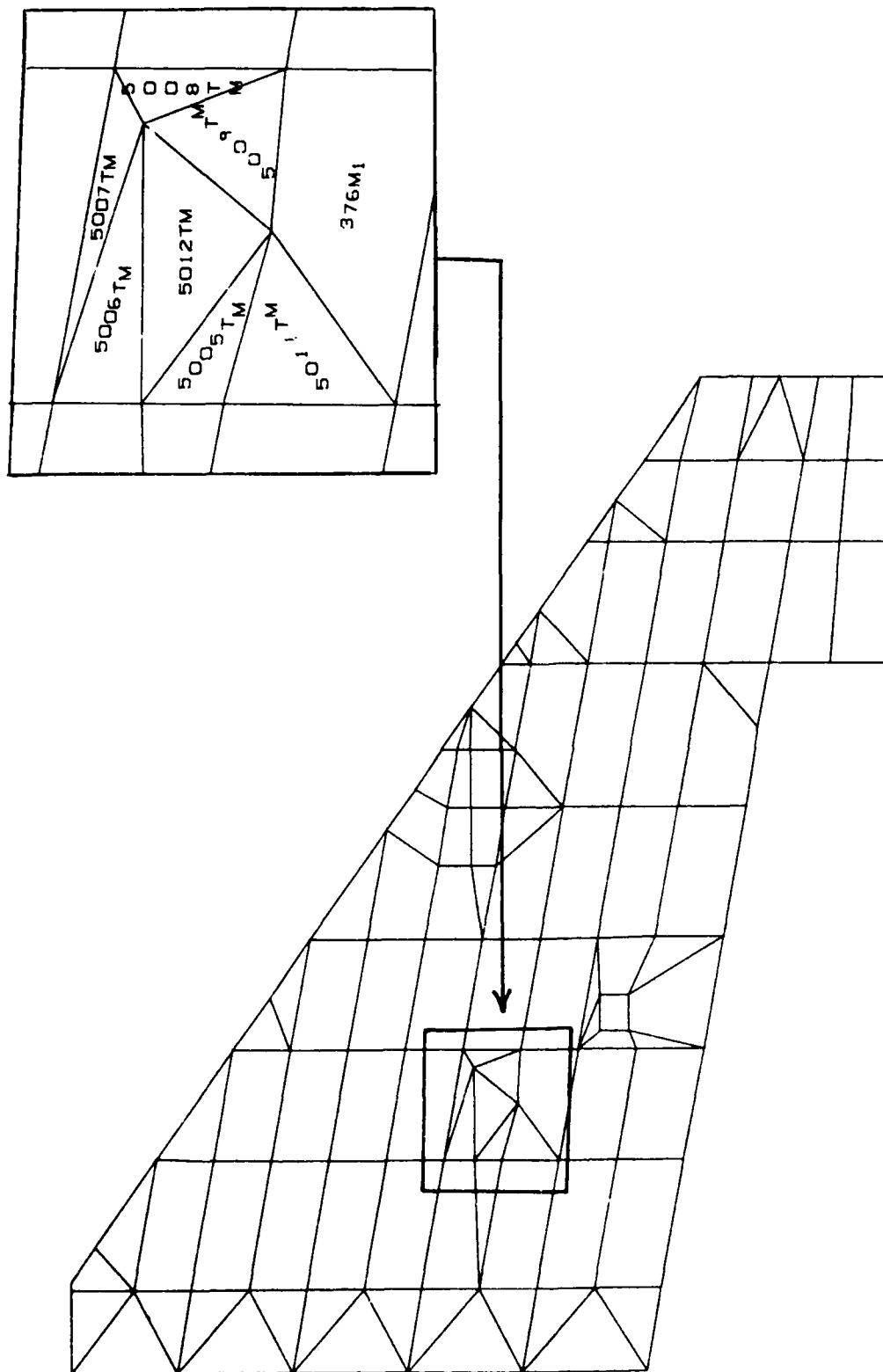
Figure C-9.   2nd Torsional Mode (Model DC-1)
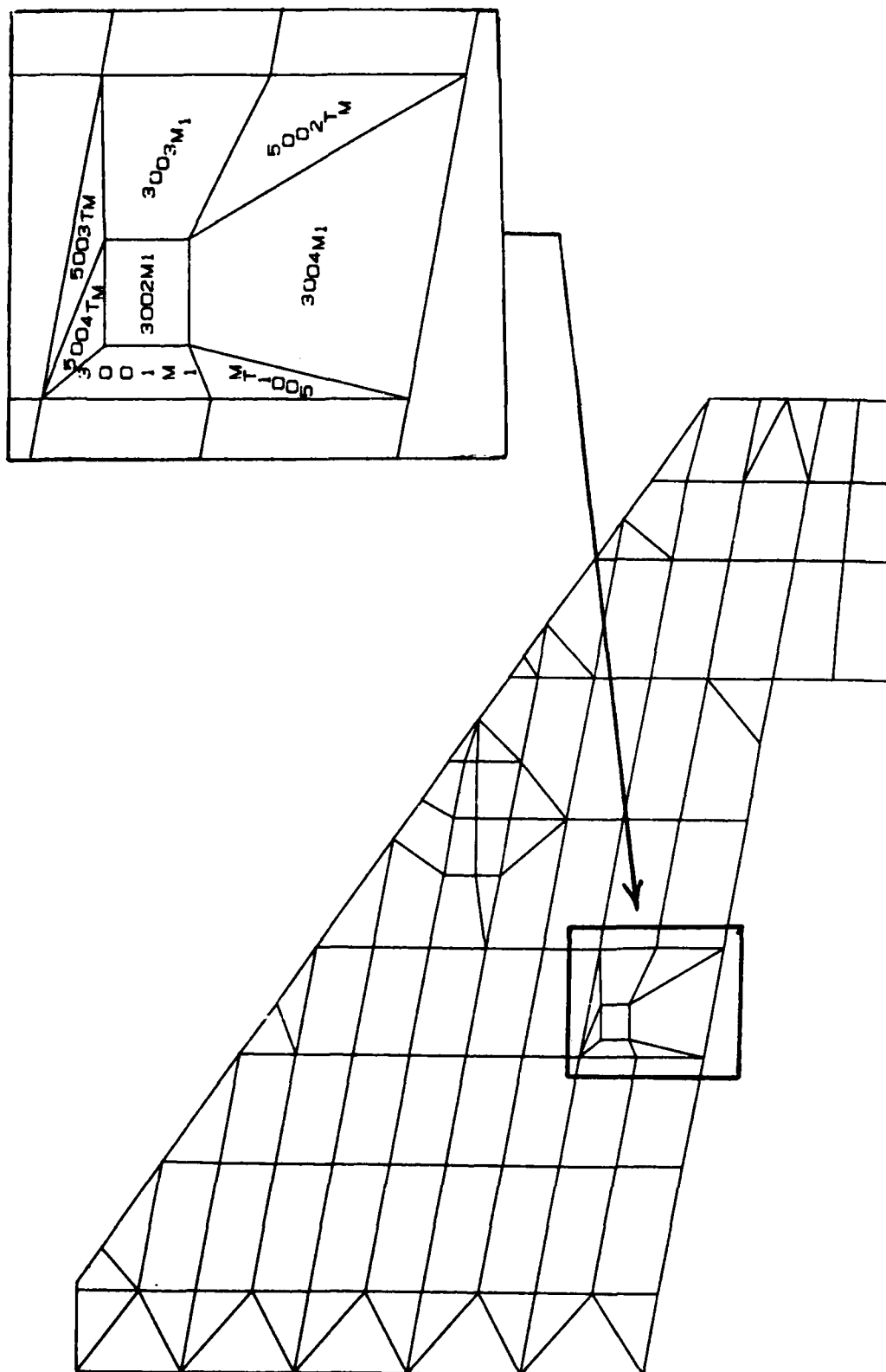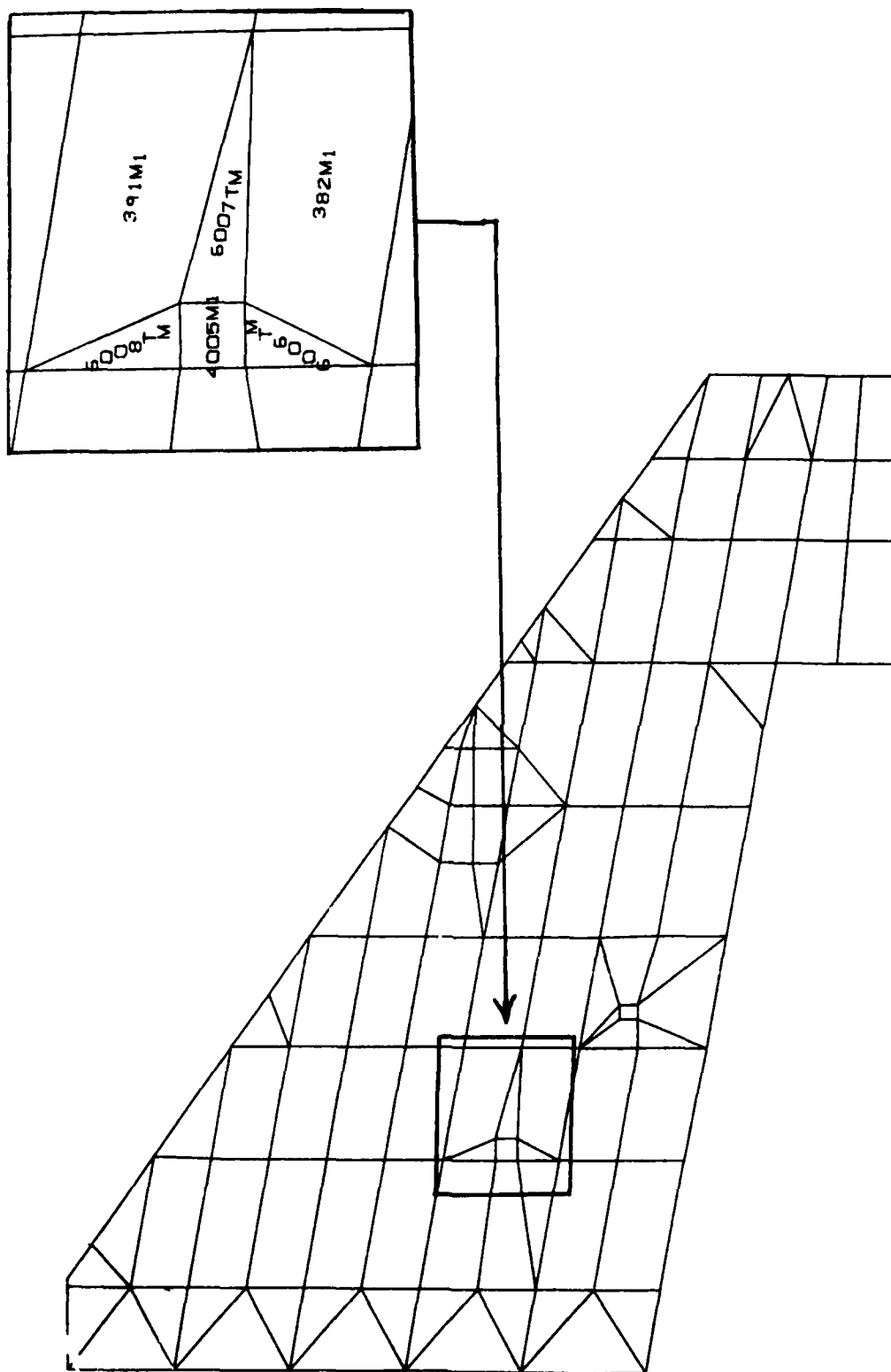
Figure C-10. Upper Wing Surface (Model DC-1R)
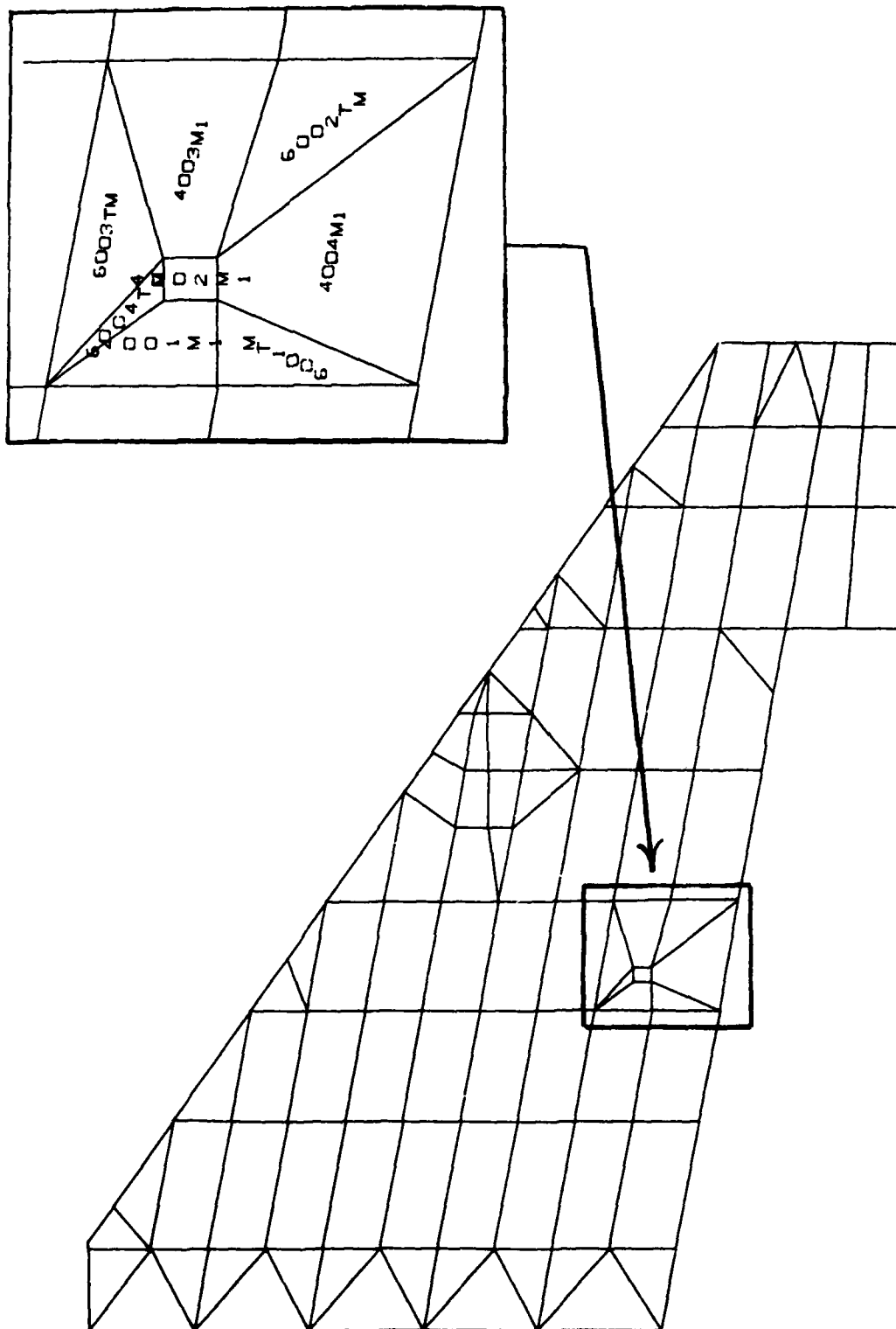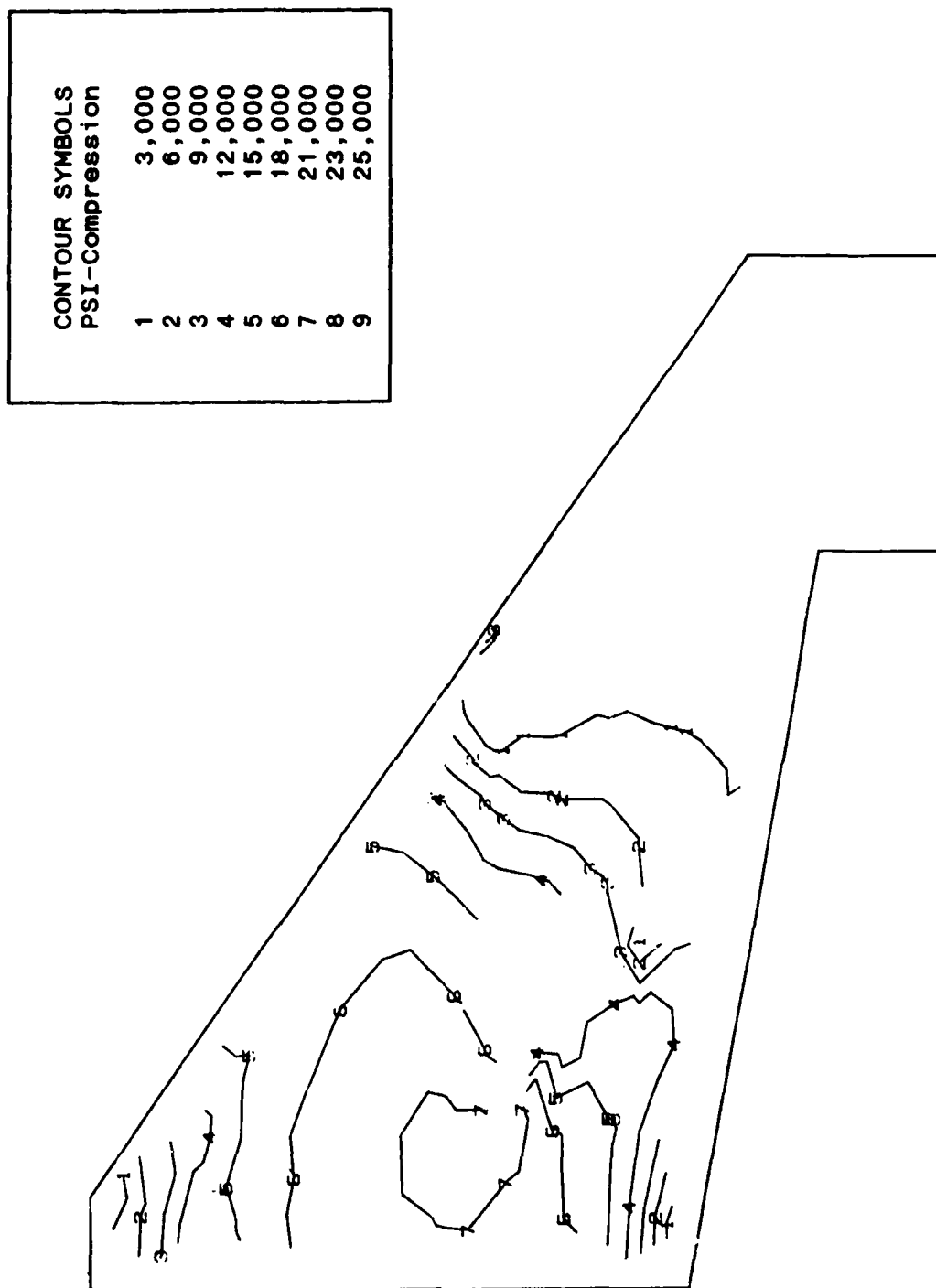
Figure C-11. Lower Wing Surface (Model DC-1R)

CONTOUR SYMBOLS
PSI-Compression

1	3,000
2	6,000
3	9,000
4	12,000
5	15,000
6	18,000
7	21,000
8	23,000
9	25,000

Figure C-12. Stress Contours on Upper Wing Surface (Model DC-1R)

CONTOUR SYMBOLS
PSI-Tension

|	
1	3,000
2	6,000
3	9,000
4	12,000
5	15,000
6	17,000
7	19,000
8	21,000
9	23,000
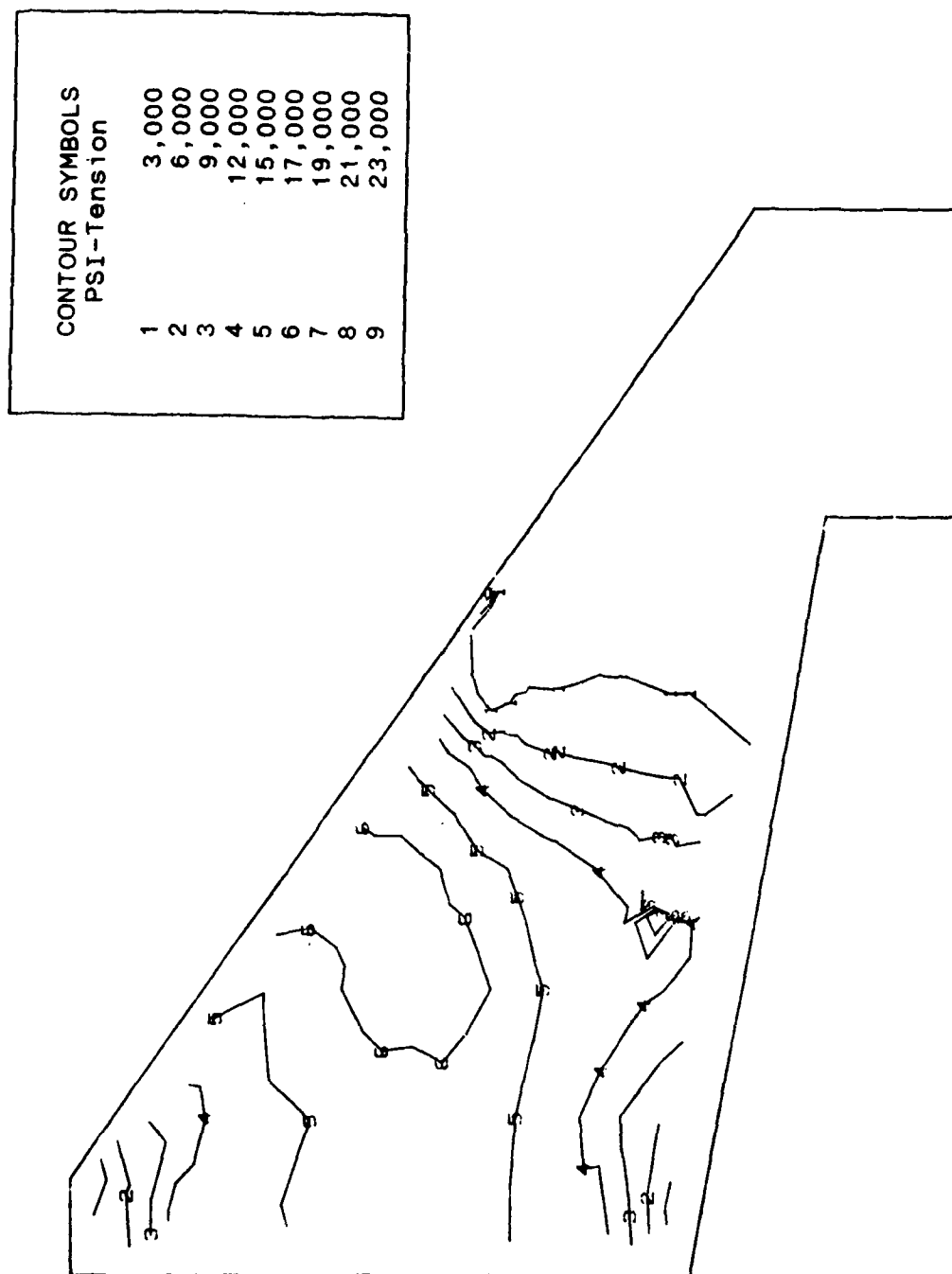
Figure C-13. Stress Contours on Lower Wing Surface (Model DC-1R)

Symmetric Normal Modes for F-16 Wing Model DC-1R

Givens Method   Mode 1   Frequency = 10.54 Hertz
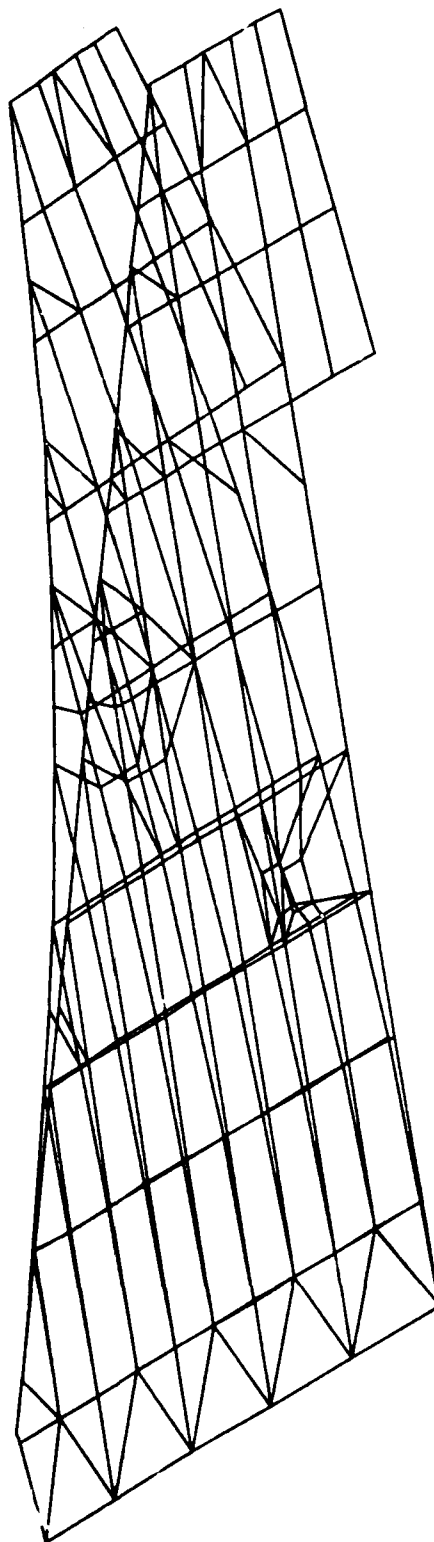
Figure C-14.   1st Wing Bending Mode (Model DC-1R)

Symmetric Normal Modes for F-16 Wing Model DC-1R

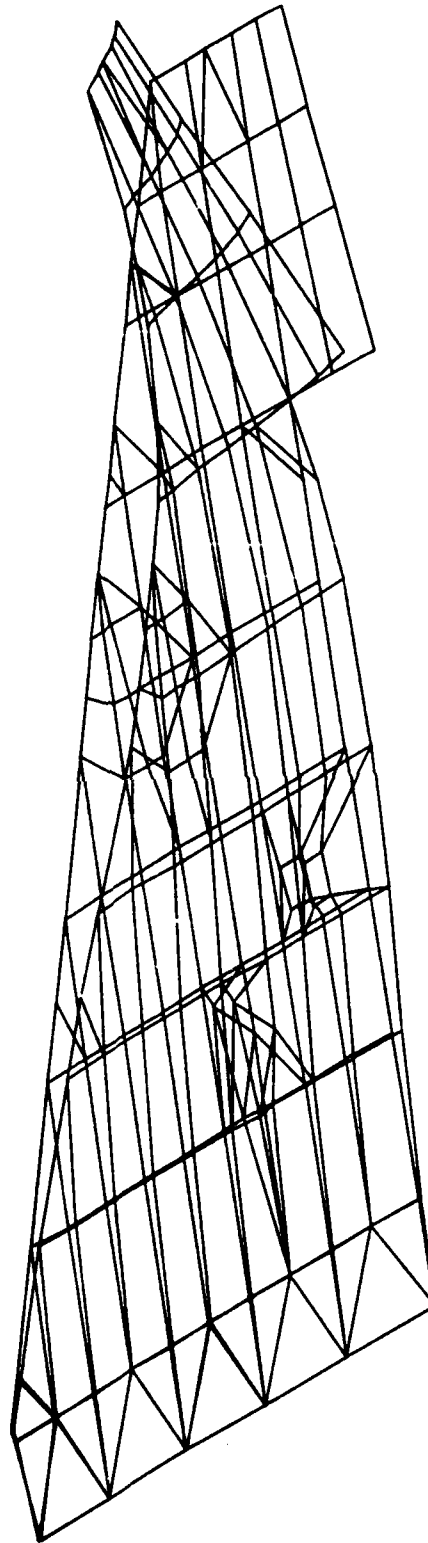Givens Method Mode 2 Frequency = 35.28 Hertz
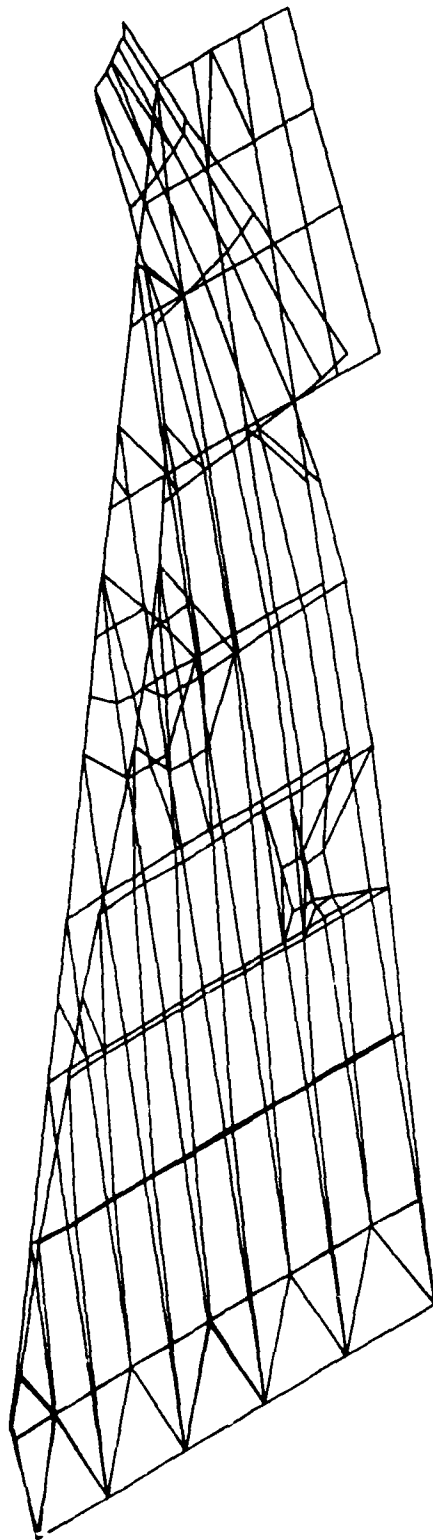
Figure C-15. 2nd Wing Bending Mode (Model DC-1R)

Symmetric Normal Modes for F-16 Wing Model DC-1R
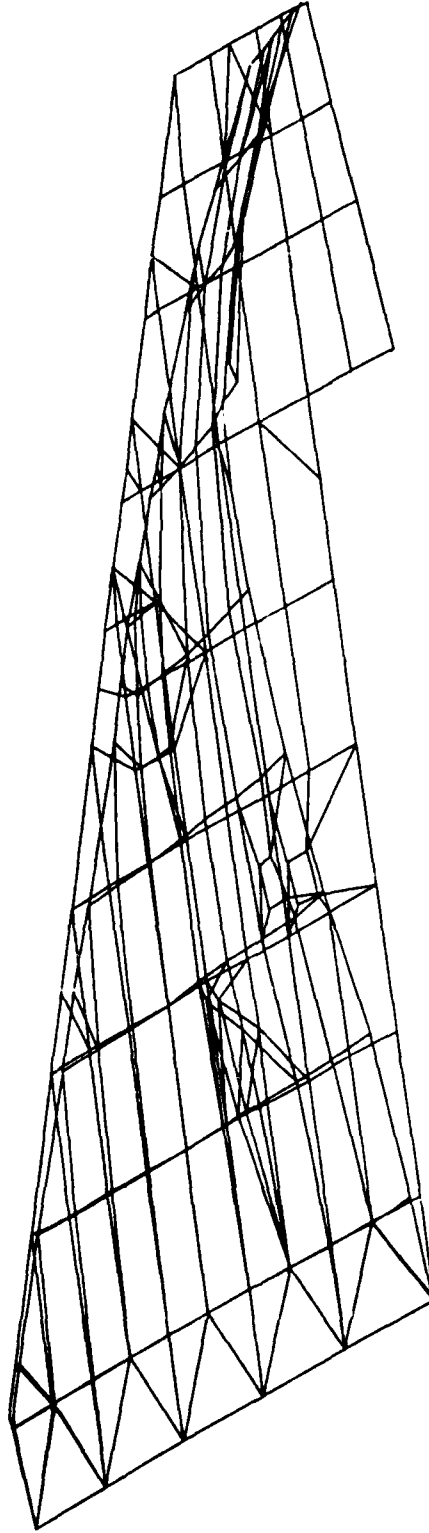
Givens Method   Mode 3   Frequency = 45.62 Hertz
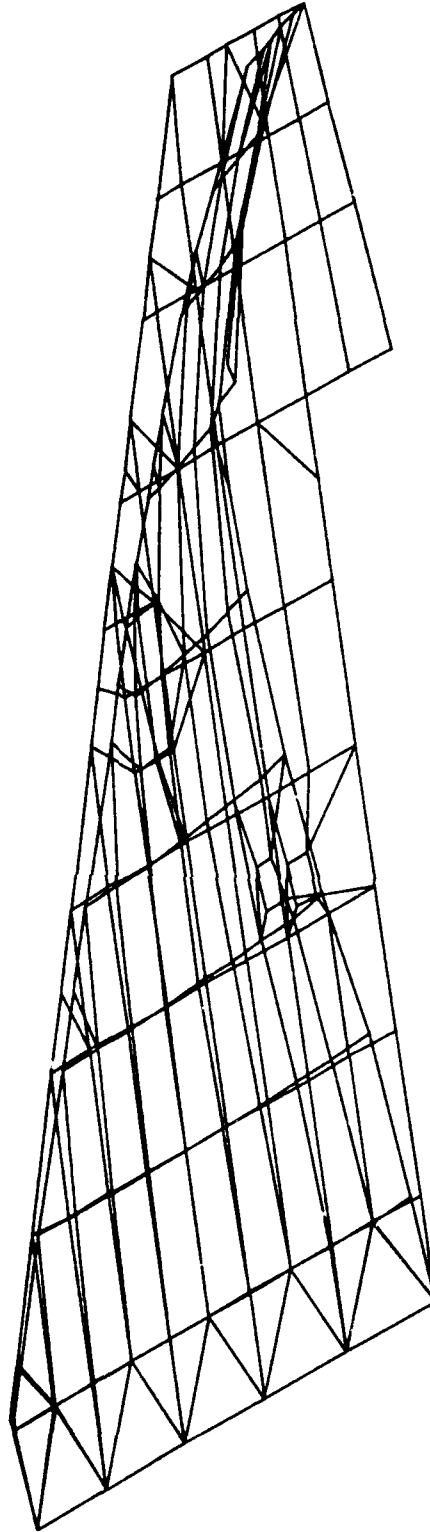
Figure C-16. 1st Torsional Mode (Model DC-1R)

Symmetric Normal Modes for F-16 Wing Model DC-1R
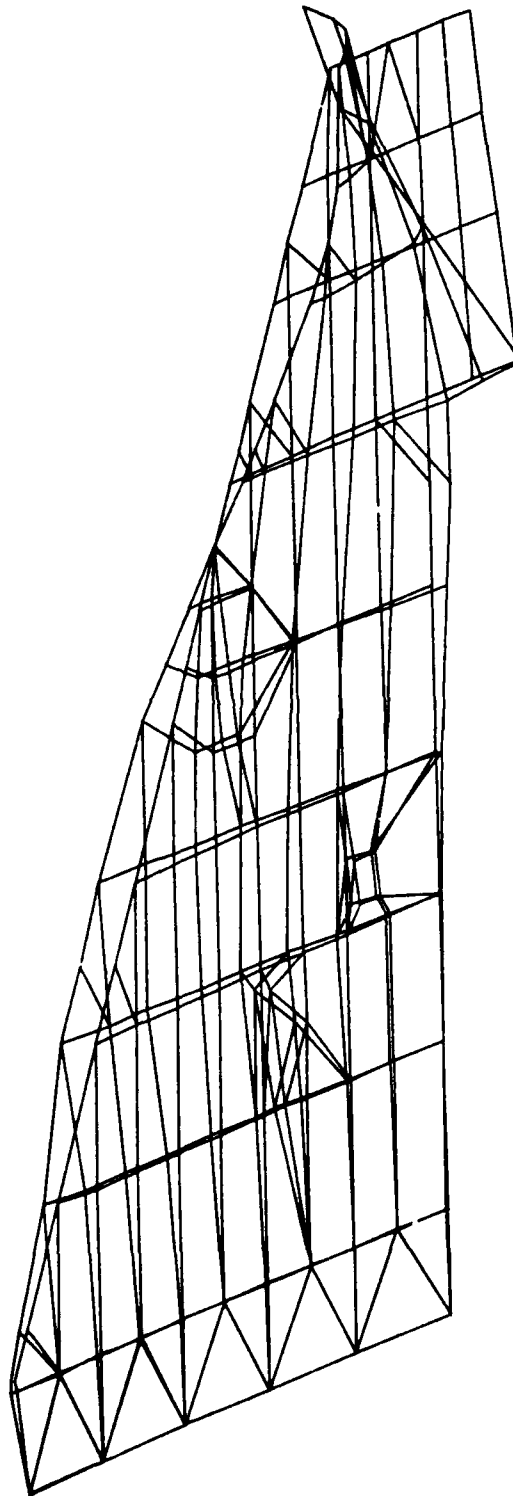
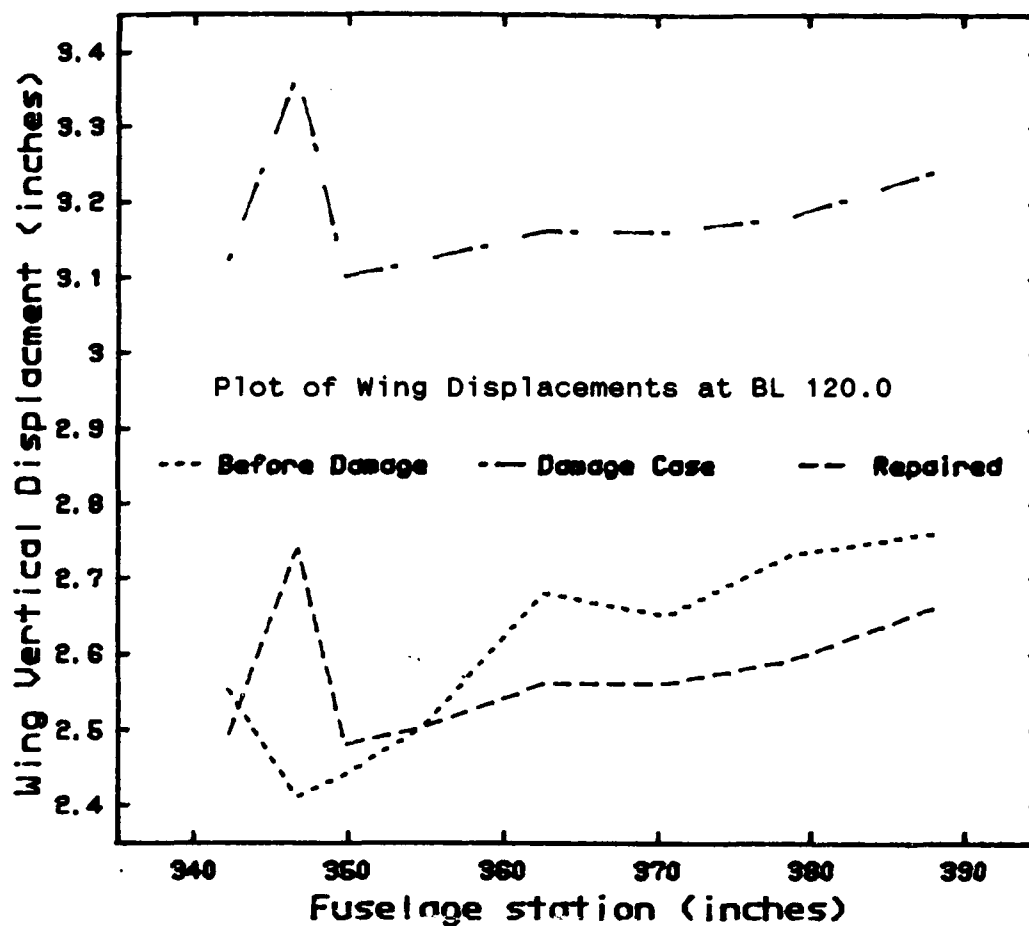Givens Method   Mode 4   Frequency = 70.48 Hertz
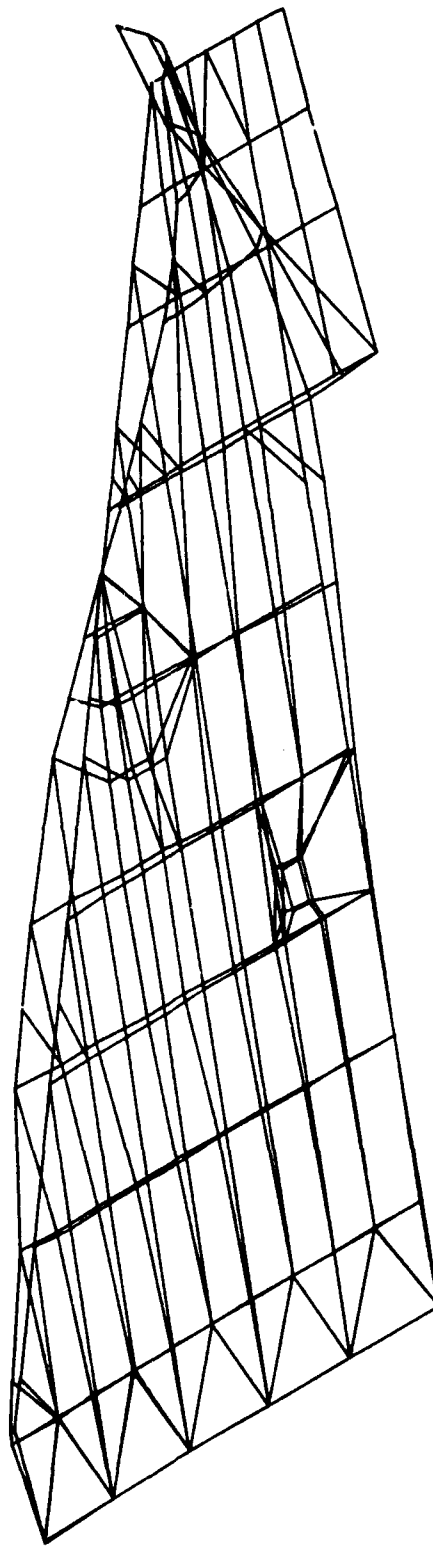
Figure C-17. 2nd Torsional Mode (Model DC-1R)

APPENDIX D

ANALYSIS OF DAMAGE CASE #2

Plot of Wing Displacements at BL 120.0

··· Before Damage   ·—· Damage Case   —— Repaired

Wing Vertical Displacement (inches)

Fuselage station (inches)
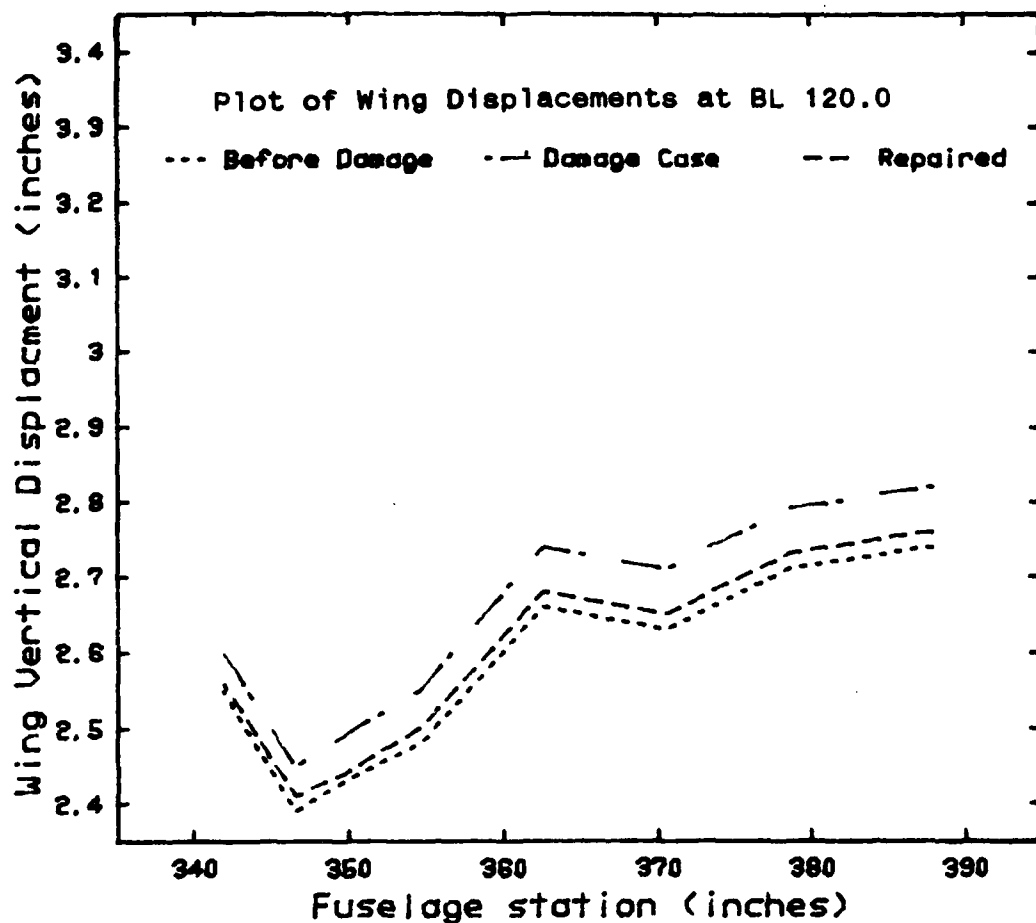
Tabulated Displacements

Fuselage St.	387.9	378.6	370.6	362.6	354.6	349.7	346.6	341.9
Model DC-1R	2.74	2.71	2.63	2.66	2.48	2.43	2.39	2.55
Model DC-2	2.82	2.79	2.71	2.74	2.55	2.49	2.45	2.60
Model DC-2R	2.76	2.73	2.65	2.68	2.50	2.44	2.41	2.56

Comparison of Residual Strength

	Av Disp	% Change	Torsion mode	% Change
Model D-1R	2.58		45.62	
Model DC-2	2.64	-2.3	44.75	-1.9
Model DC-2R	2.59	+1.9	45.56	+1.8

Figure D-1.   Summary of Damage Case #2 Results
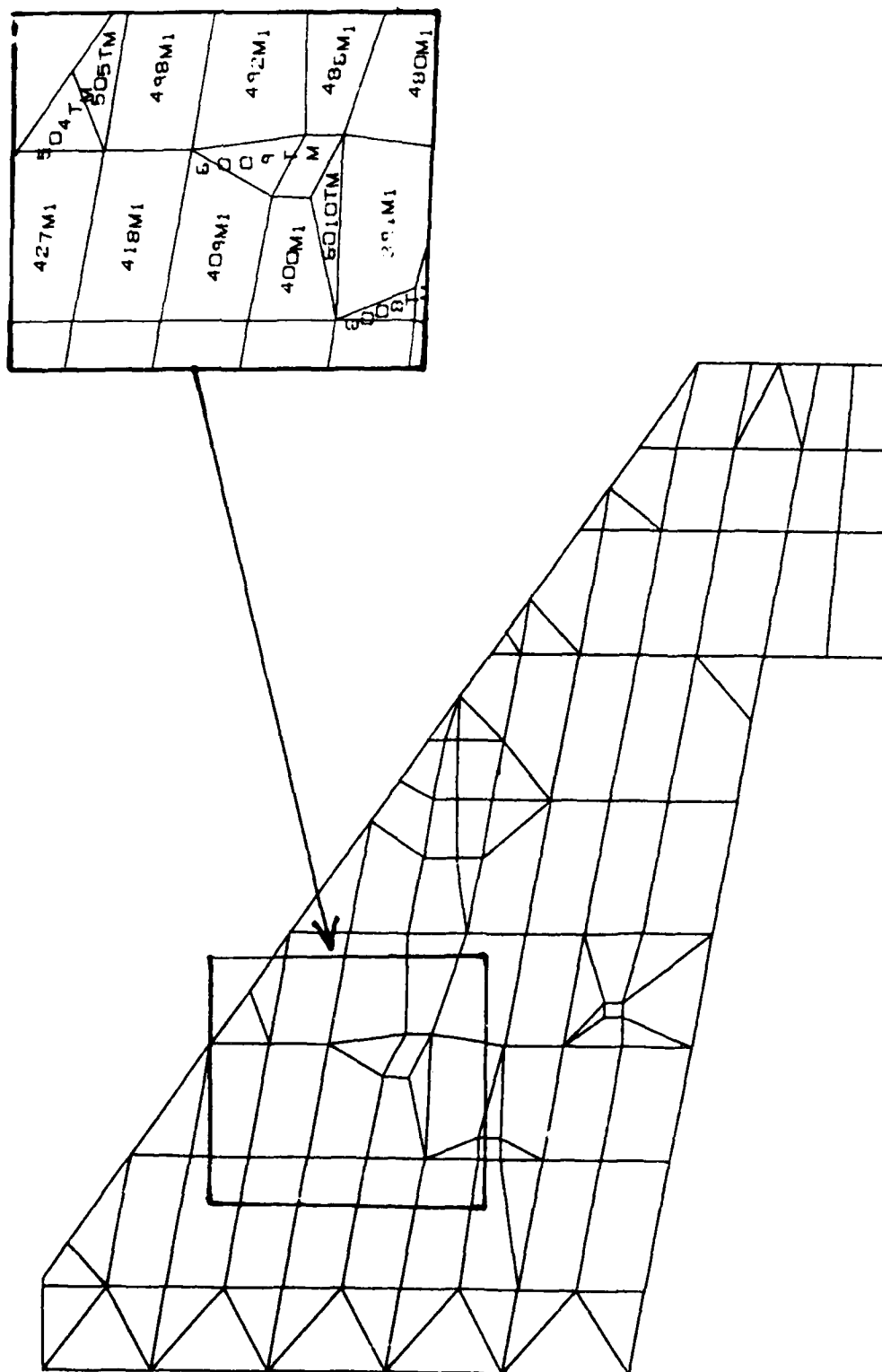
D-2

Figure D-2. Upper Wing Surface (Model DC-2)

D-3

Figure D-3. Lower Wing Surface (Model DC-2)

CONTOUR SYMBOLS
PSI-Compression

1	3,000
2	6,000
3	9,000
4	12,000
5	15,000
6	18,000
7	21,000
8	23,000
9	25,000

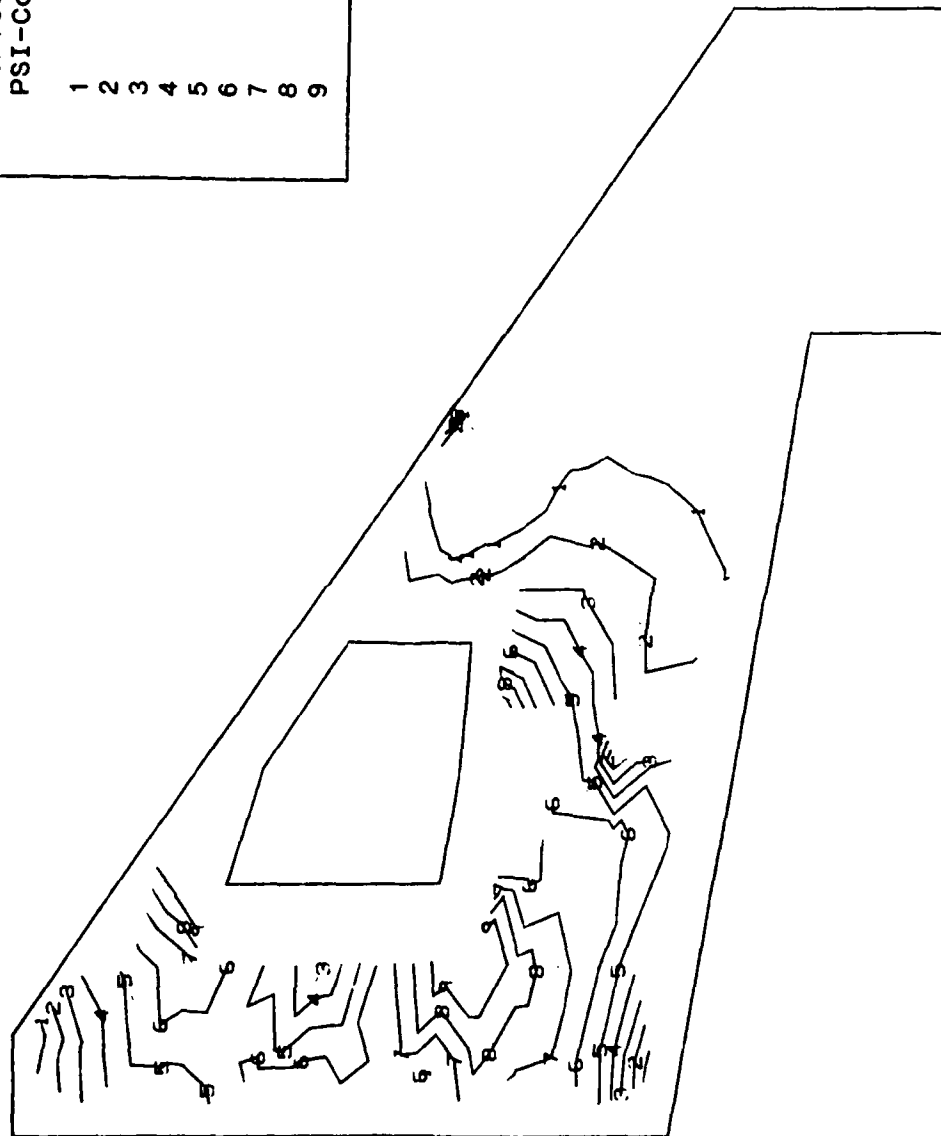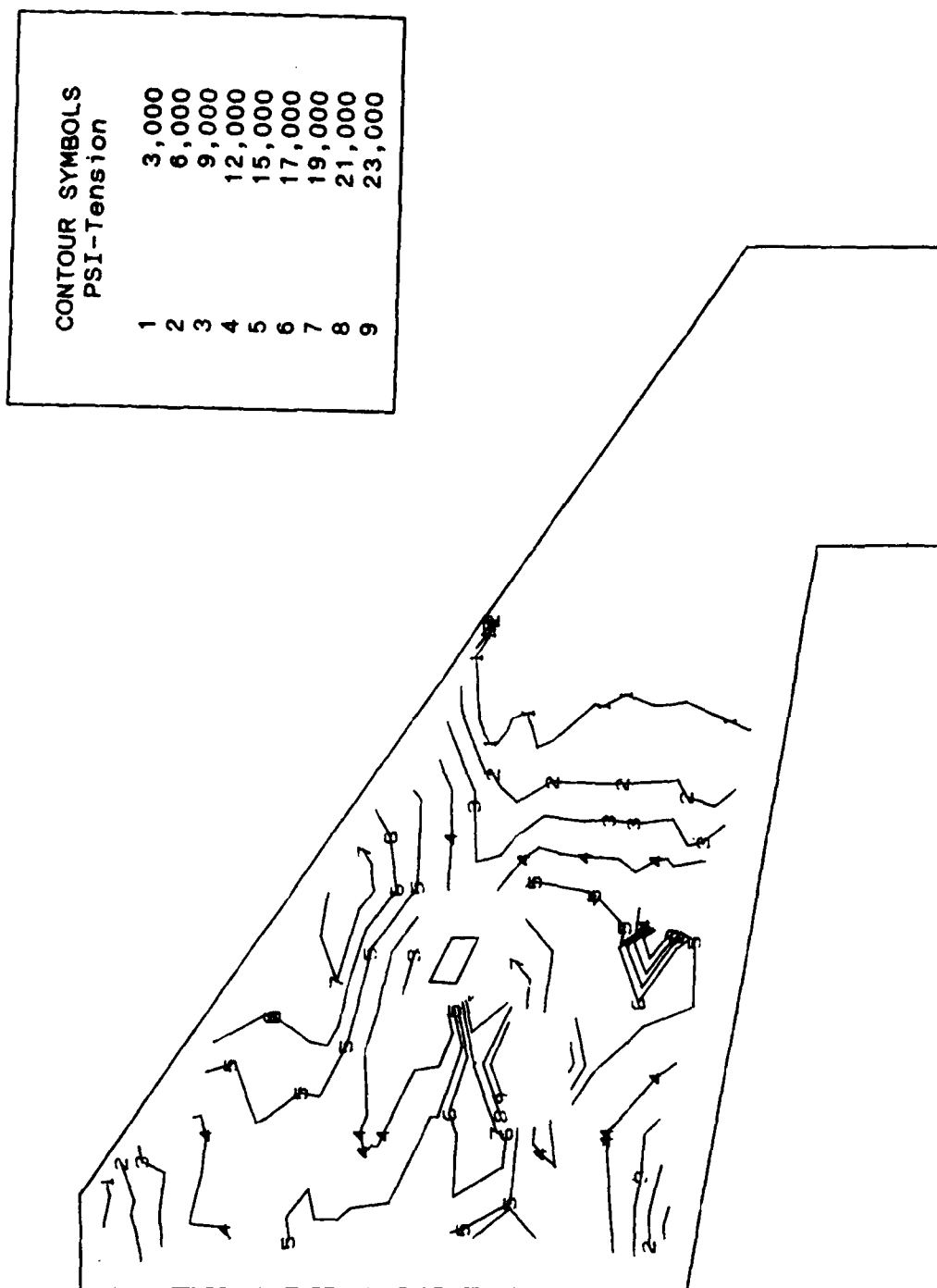Figure D-4. Stress Contours on Upper Wing Surface (Model DC-2)

CONTOUR SYMBOLS
PSI-Tension

1	3,000
2	6,000
3	9,000
4	12,000
5	15,000
6	17,000
7	19,000
8	21,000
9	23,000
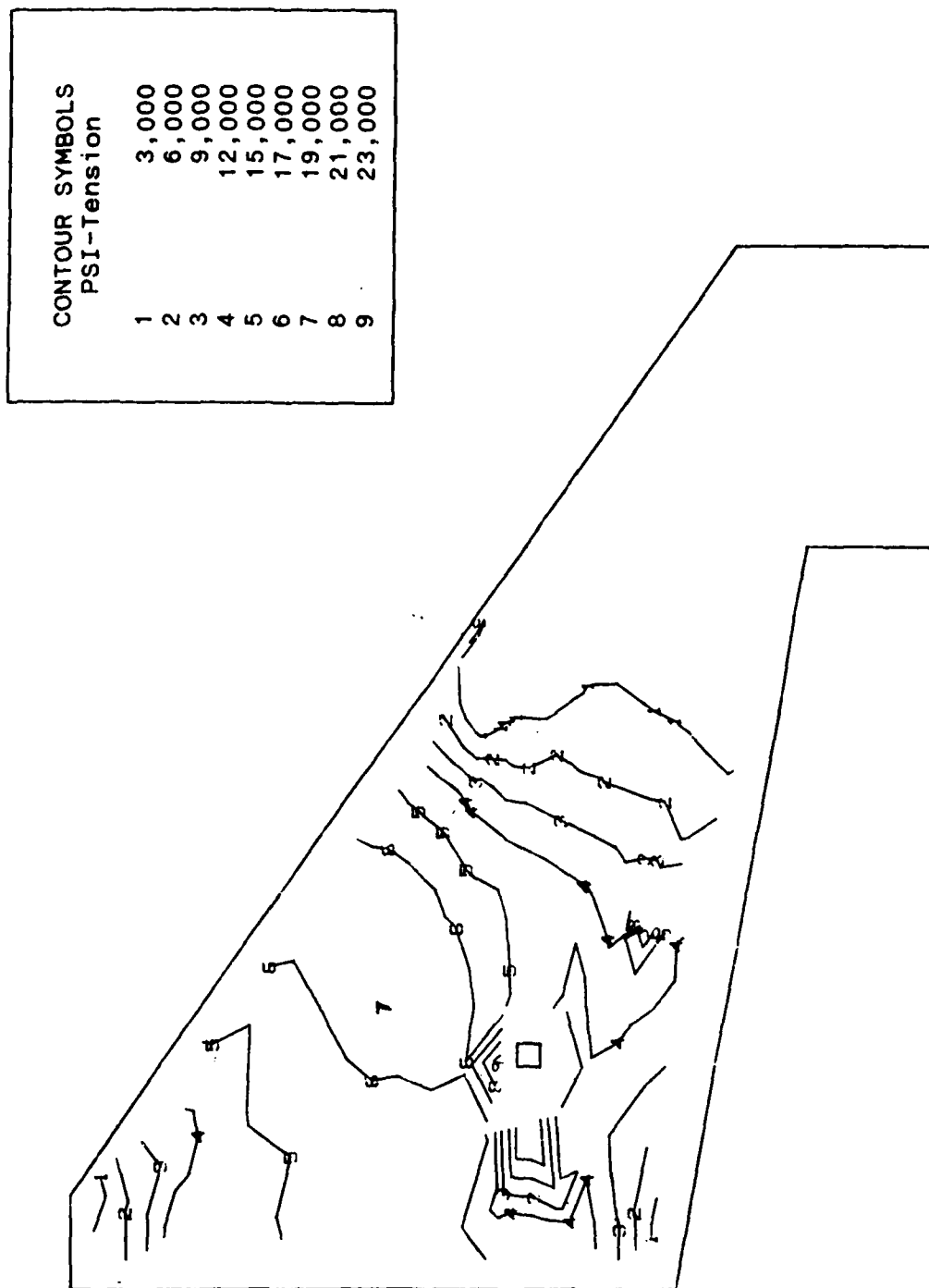
Figure D-5.   Stress Contours on Lower Wing Surface (Model DC-2)

Symmetric Normal Modes for F-16 Wing Model DC-2

Givens Method   Mode 1   Frequency = 10.45 Hertz

Figure D-8.   1st Wing Bending Mode (Model DC-2)

Symmetric Normal Modes for F-16 Wing Model DC-2
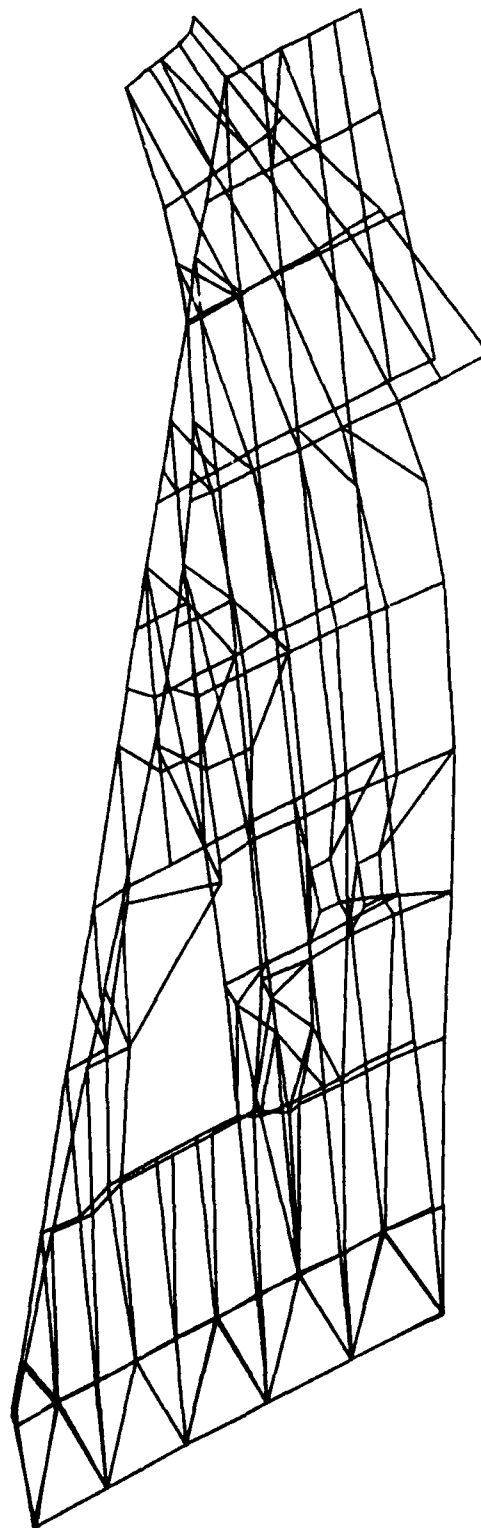
Givens Method   Mode 2   Frequency = 34.94 Hertz

Figure D-7. 2nd Wing Bending Mode (Model DC-2)

D-8

Symmetric Normal Modes for F-16 Wing Model DC-2
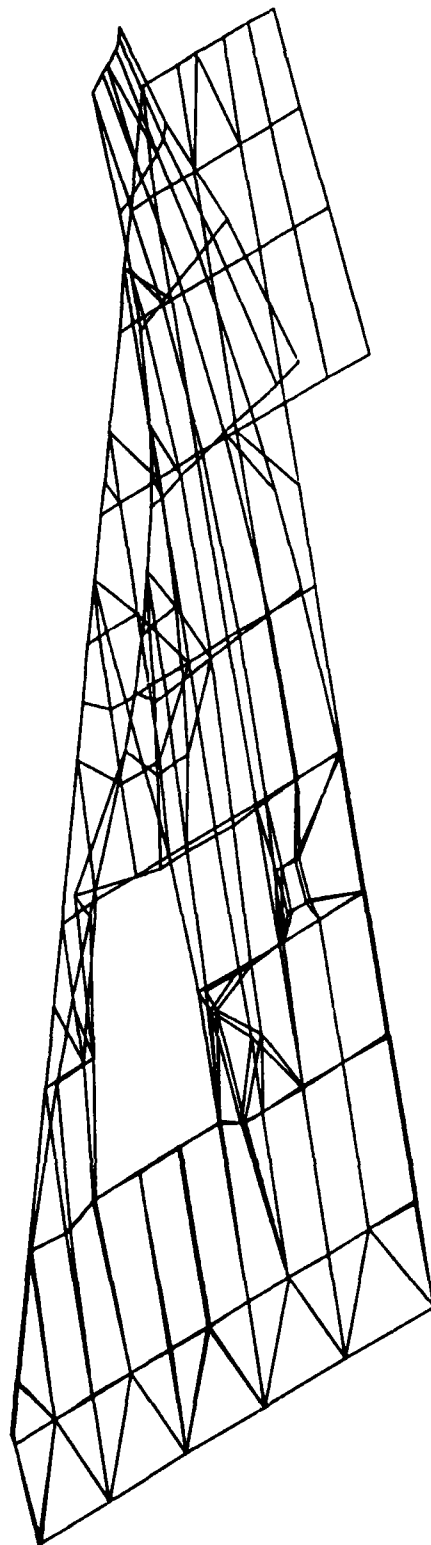
Givens Method   Mode 3   Frequency = 44.75 Hertz

Figure D-8.   1st Torsional Mode (Model DC-2)

Symmetric Normal Modes for F-16 Wing Model DC-2

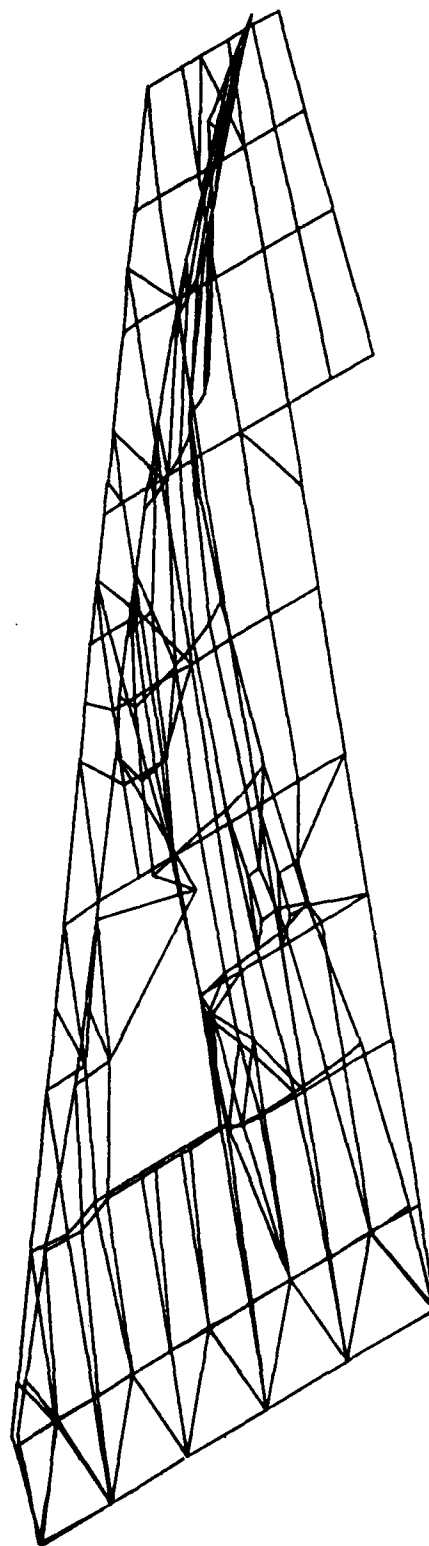Givens Method   Mode 4   Frequency = 66.75 Hertz

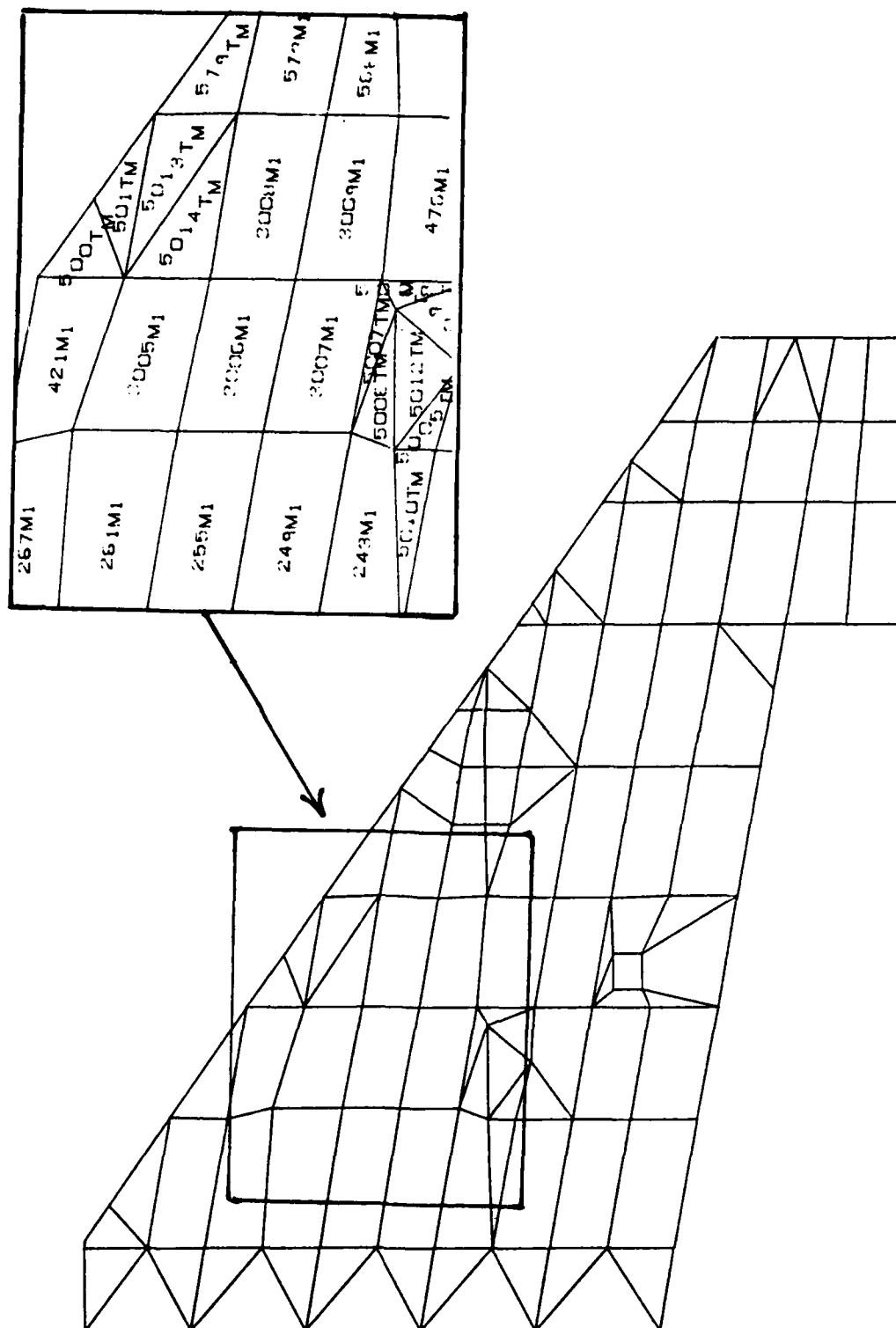Figure D-9.   2nd Torsional Mode (Model DC-2)
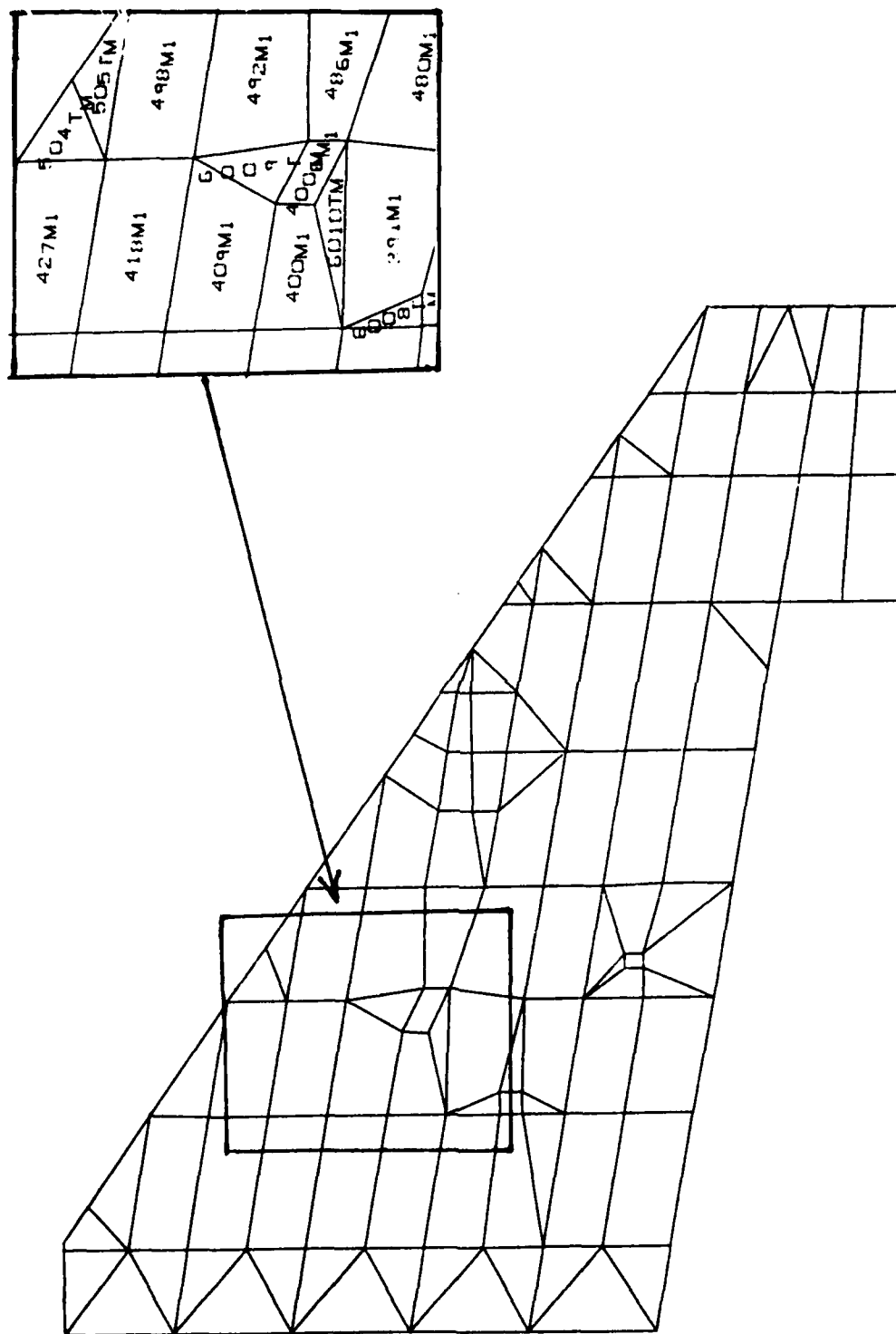
Figure D-10. Upper Wing Surface (Model DC-2R)
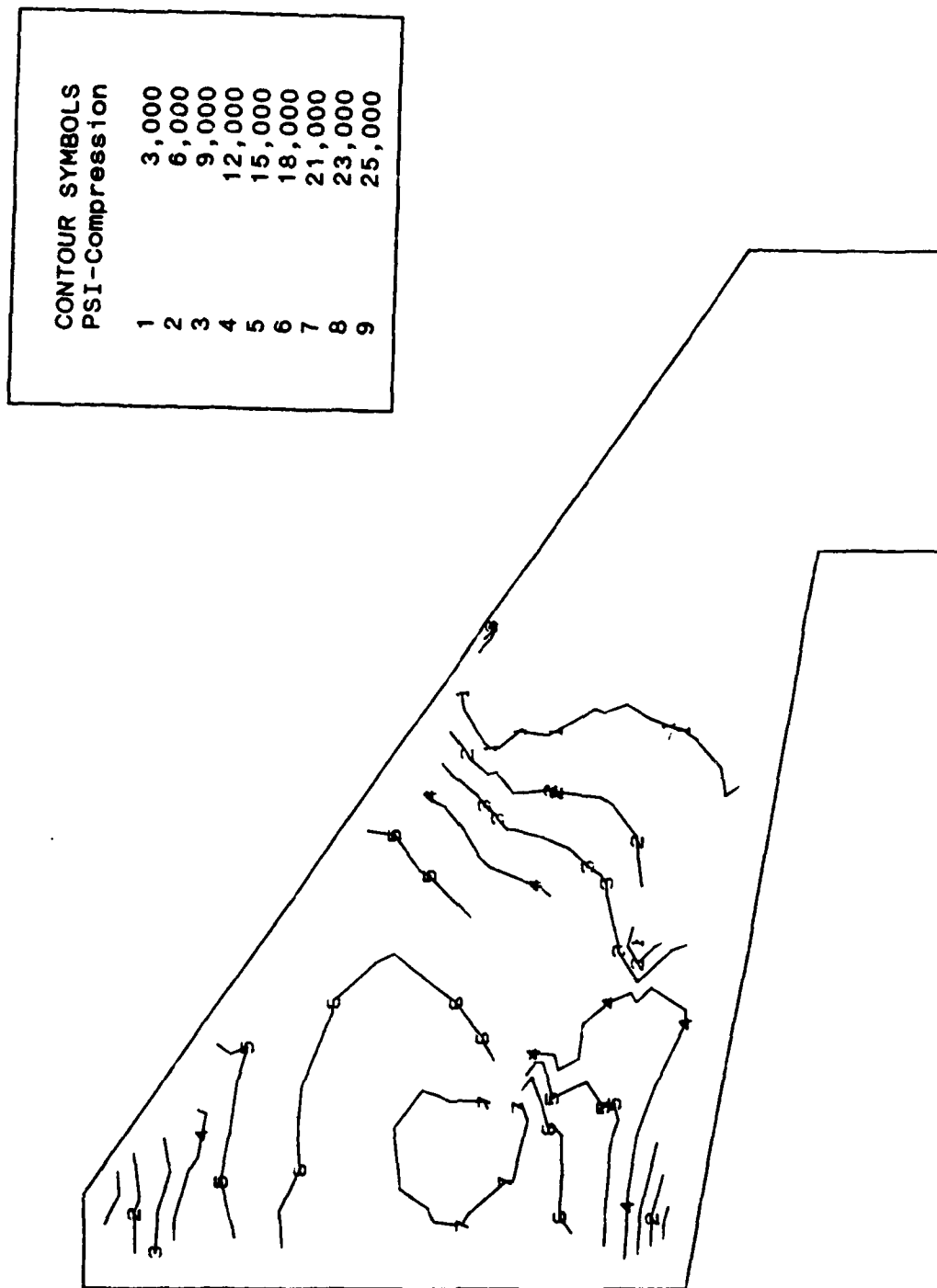
Figure D-11. Lower Wing Surface (Model DC-2R)

CONTOUR SYMBOLS
PSI-Compression

1	3,000
2	6,000
3	9,000
4	12,000
5	15,000
6	18,000
7	21,000
8	23,000
9	25,000

Figure D-12. Stress Contours on Upper Wing Surface (Model DC-2R)

CONTOUR SYMBOLS
PSI-Tension

1	3,000
2	6,000
3	9,000
4	12,000
5	15,000
6	17,000
7	19,000
8	21,000
9	23,000
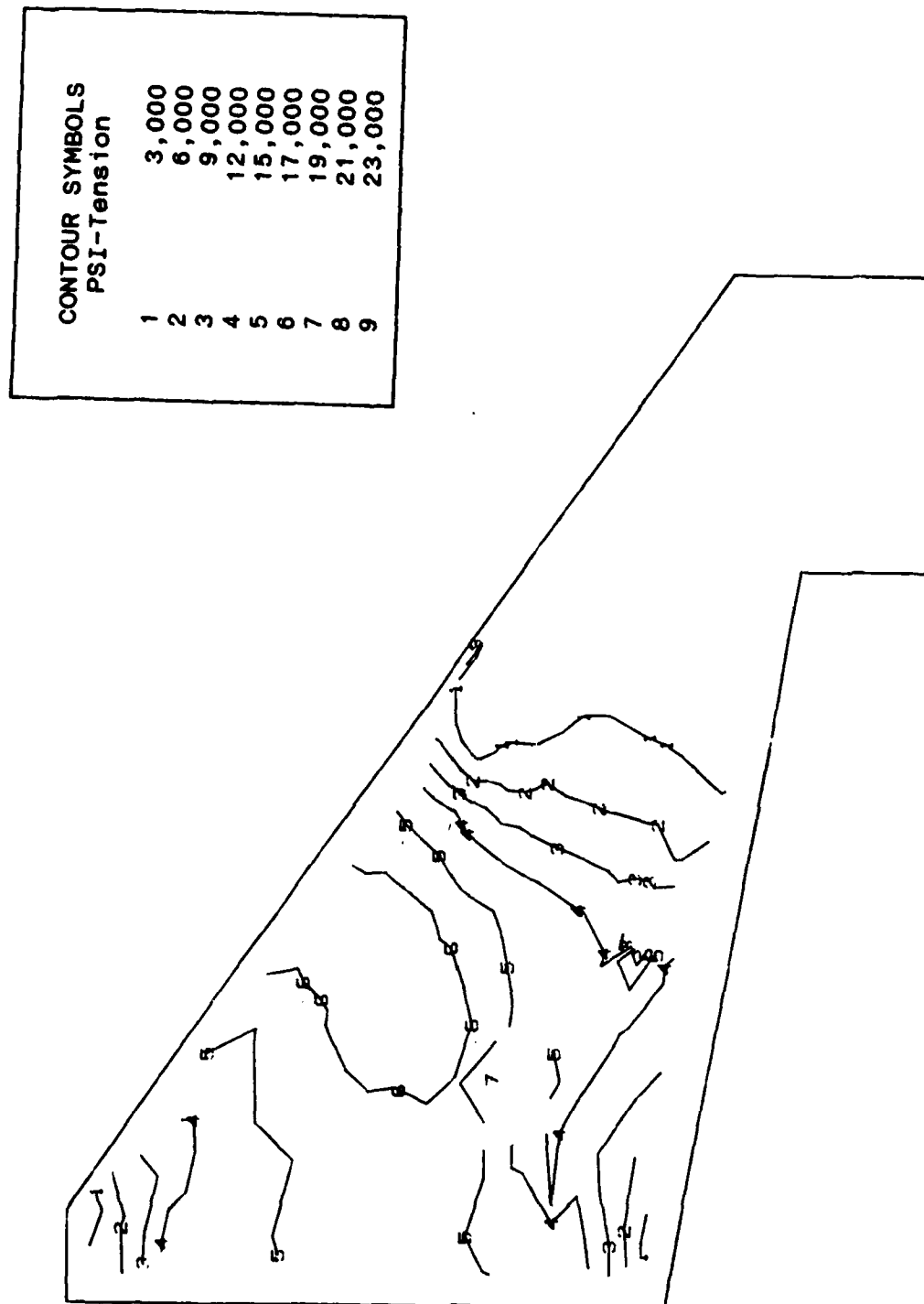
Figure D-13.   Stress Contours on Lower Wing Surface (Model DC-2R)

D-14

Symmetric Normal Modes for F-16 Wing Model DC-2R

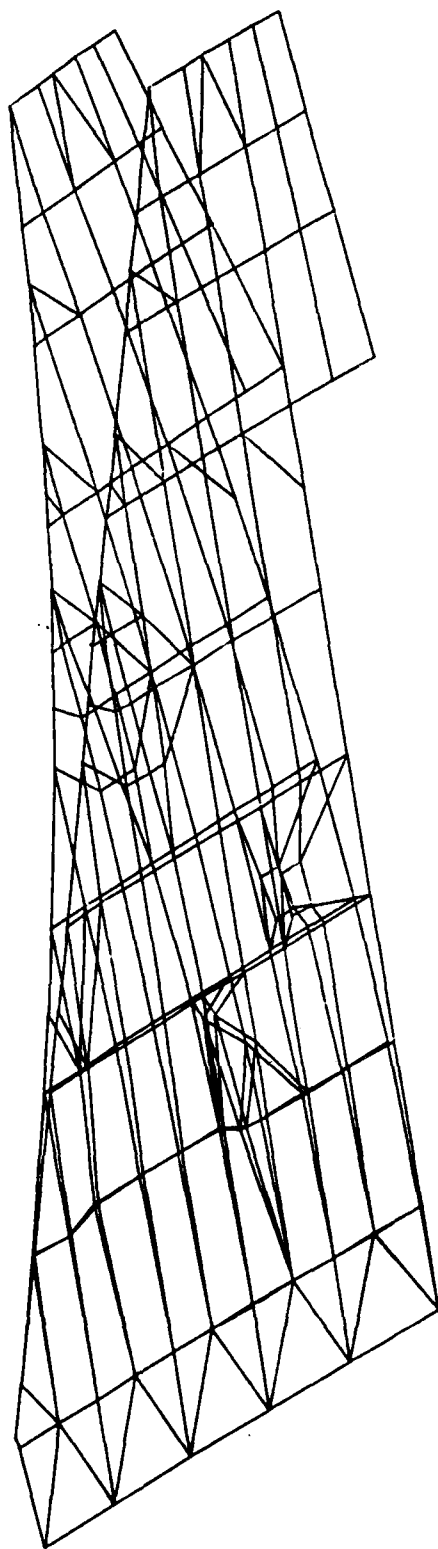Givens Method   Mode 1   Frequency = 10.55 Hertz
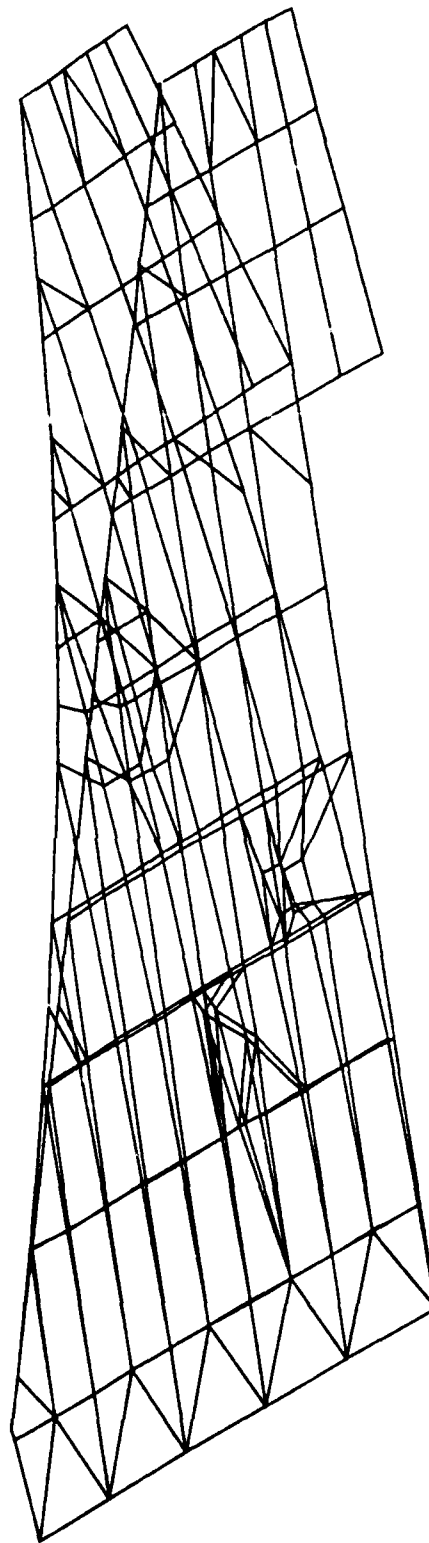
Figure D-14.   1st Wing Bending Mode (Model DC-2R)

D-15

Symmetric Normal Modes for F-16 Wing Model DC-2R
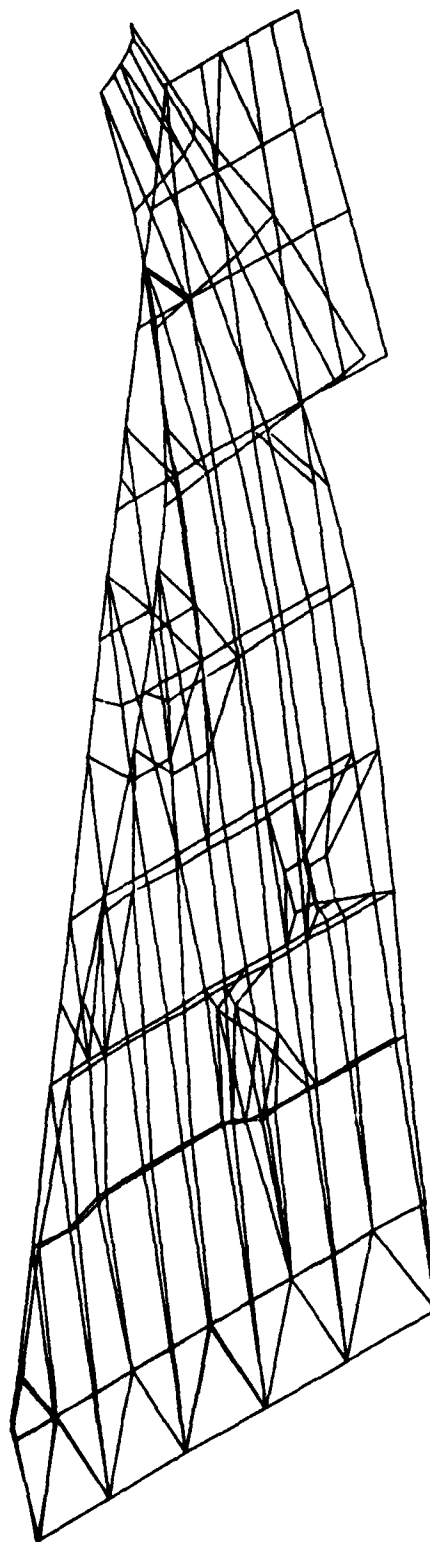
Givens Method Mode 2 Frequency = 35.05 Hertz

Figure D-15. 2nd Wing Bending Mode (Model DC-2R)

Symmetric Normal Modes for F-16 Wing Model DC-2R
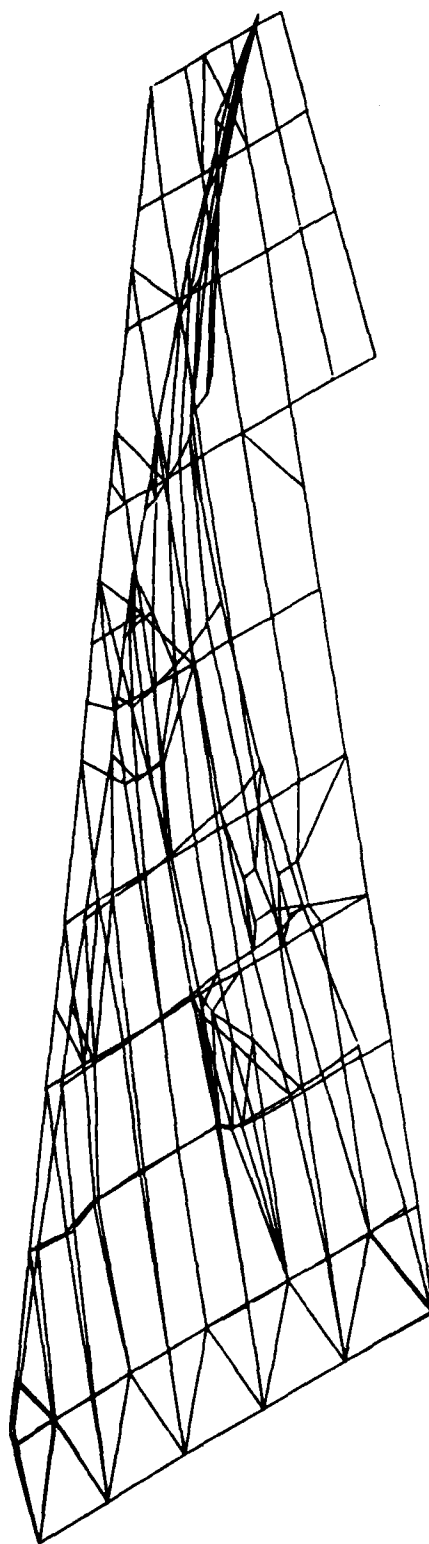
Givens Method   Mode 3   Frequency = 45.56 Hertz

D-17

Figure D-16. 1st Torsional Mode (Model DC-2R)

Symmetric Normal Modes for F-16 Wing Model DC-2R

Givens Method   Mode 4   Frequency = 70.38 Hertz

Figure D-17.   2nd Torsional Mode (Model DC-2R)

D-18

APPENDIX E

ANALYSIS OF DAMAGE CASE #3

Plot of Wing Displacements at BL 120.0

··· Before Damage   ·— Damage Case   —— Repaired

Wing Vertical Displacment (inches) vs Fuselage station (inches)

Tabulated Displacements

Fuselage St.	387.9	378.6	370.6	352.6	354.6	349.7	346.6	341.9
Model DC-2R	2.76	2.73	2.65	2.68	2.50	2.44	2.41	2.56
Model DC-3	3.24	3.18	3.16	3.16	3.12	3.10	3.37	3.11
Model DC-3R	2.66	2.59	2.56	2.56	2.50	2.48	2.74	2.48

Comparison of Residual Strength

	Av Disp	% Change	Torsion mode	% Change
Model D-2R	2.59		45.56	
Model DC-3`	3.18	-22.8	29.64	-34.9
Model DC-3R	2.57	+23.6	47.02	+38.1

Figure E-1.   Summary of Damage Case #3 Results
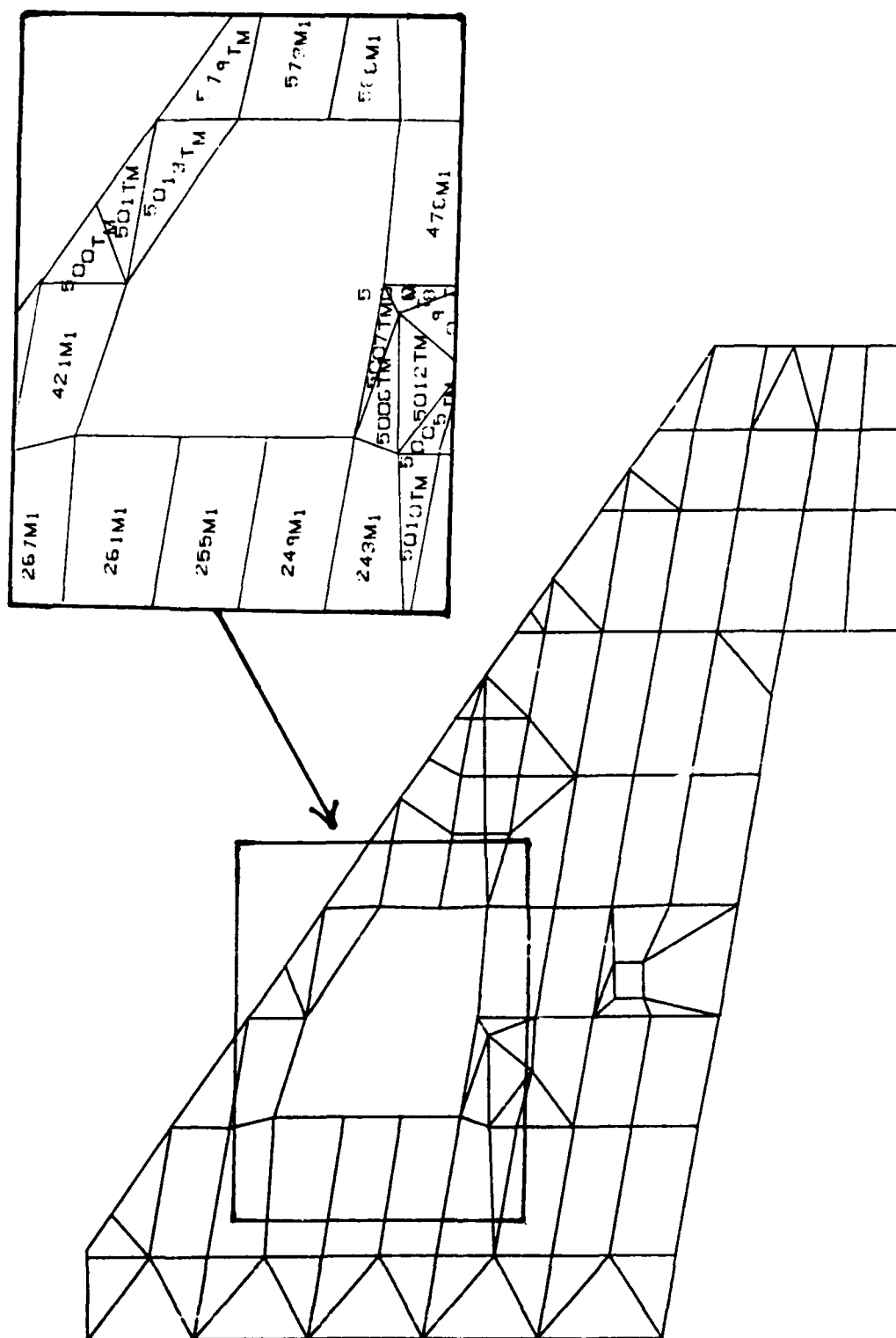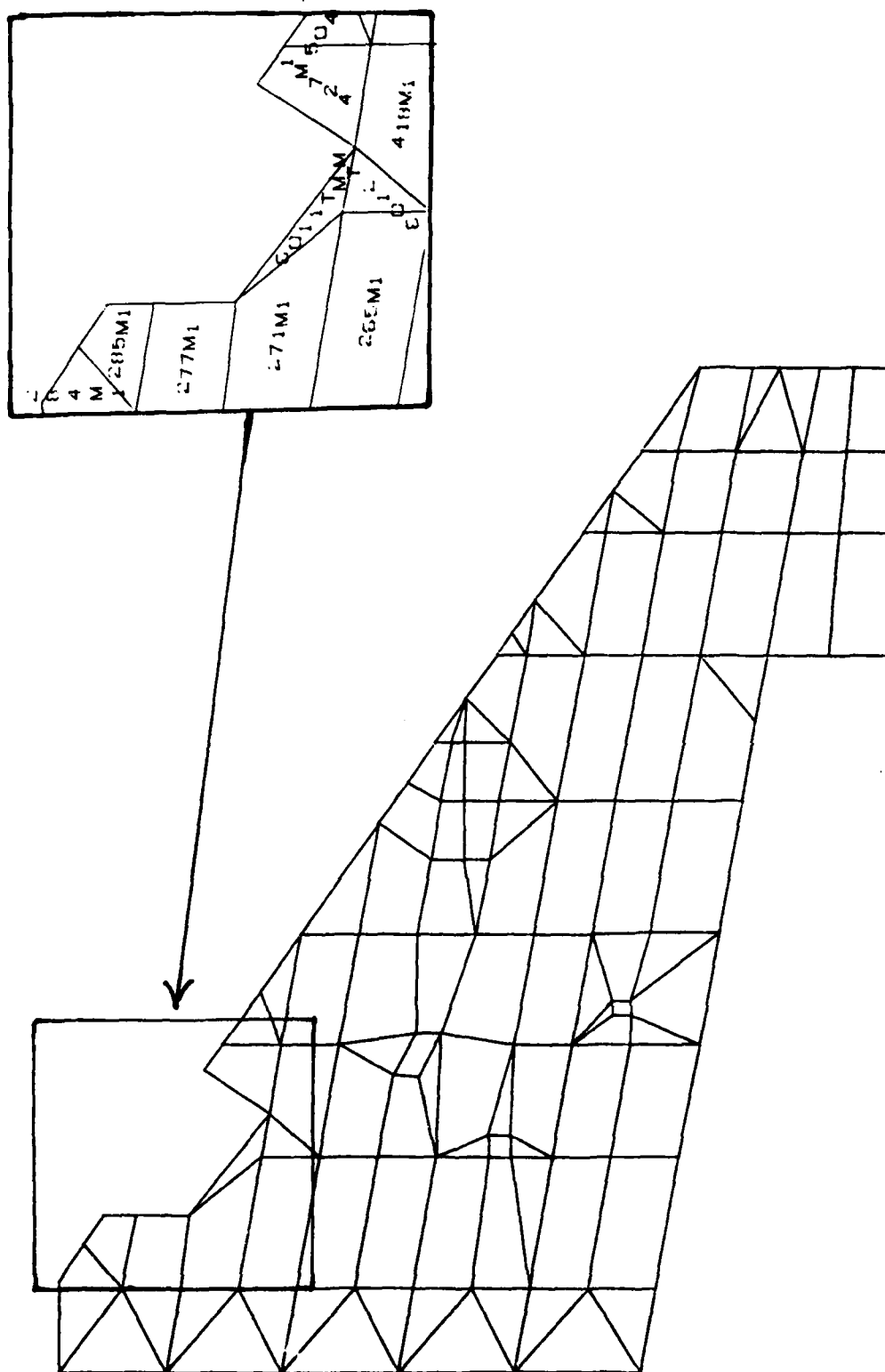
Figure E-2. Upper Wing Surface (Model DC-3)
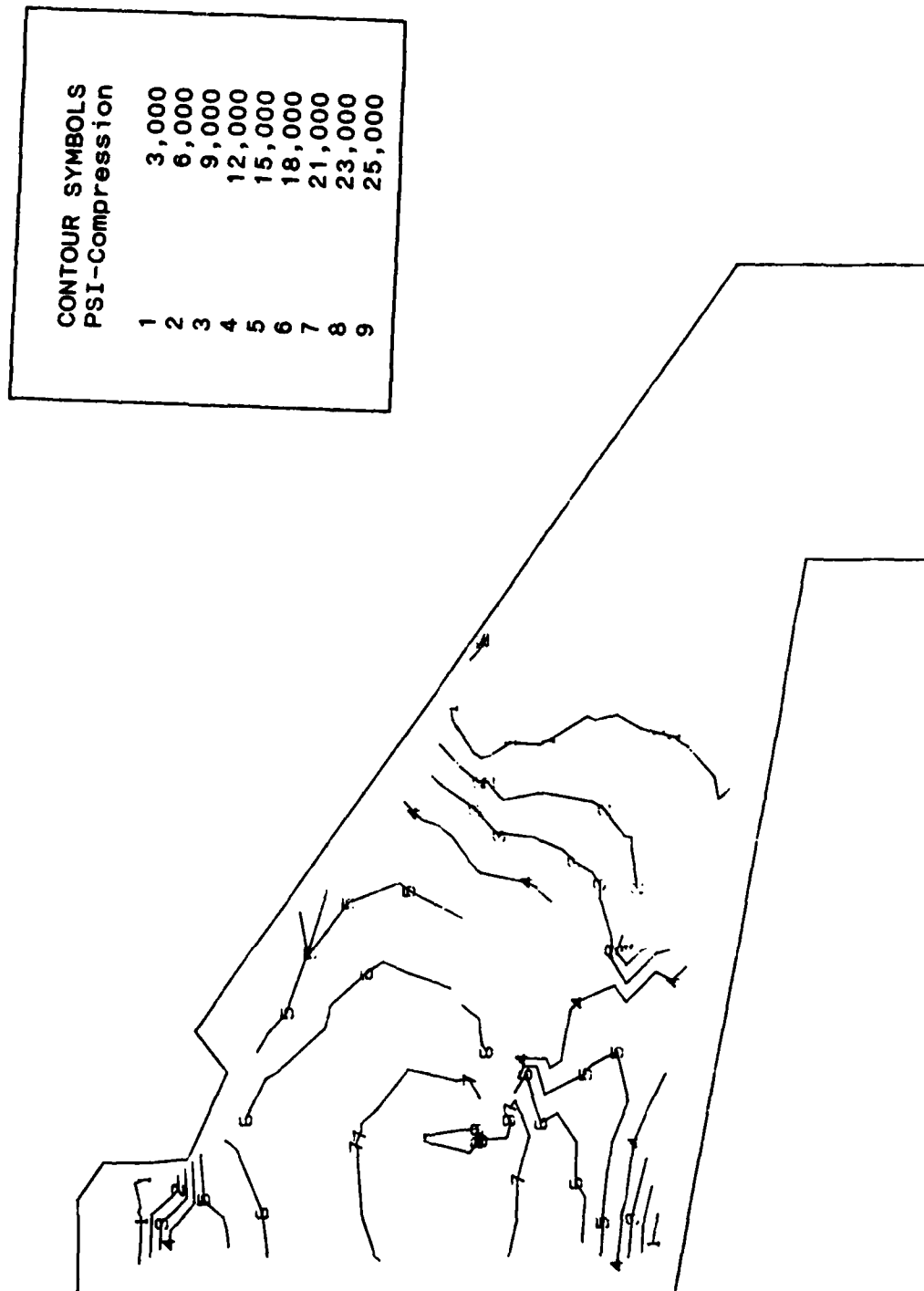
Figure E-3. Lower Wing Surface (Model DC-3)

CONTOUR SYMBOLS
PSI-Compression

1	3,000
2	6,000
3	9,000
4	12,000
5	15,000
6	18,000
7	21,000
8	23,000
9	25,000

Figure E-4. Stress Contours on Upper Wing Surface (Model DC-3)

CONTOUR SYMBOLS
PSI-Tension

| 1 | 3,000 |
2	6,000
3	9,000
4	12,000
5	15,000
6	17,000
7	19,000
8	21,000
9	23,000

Figure E-5.   Stress Contours on Lower Wing Surface (Model DC-3)

Symmetric Normal Modes for F-16 Wing Model DC-3
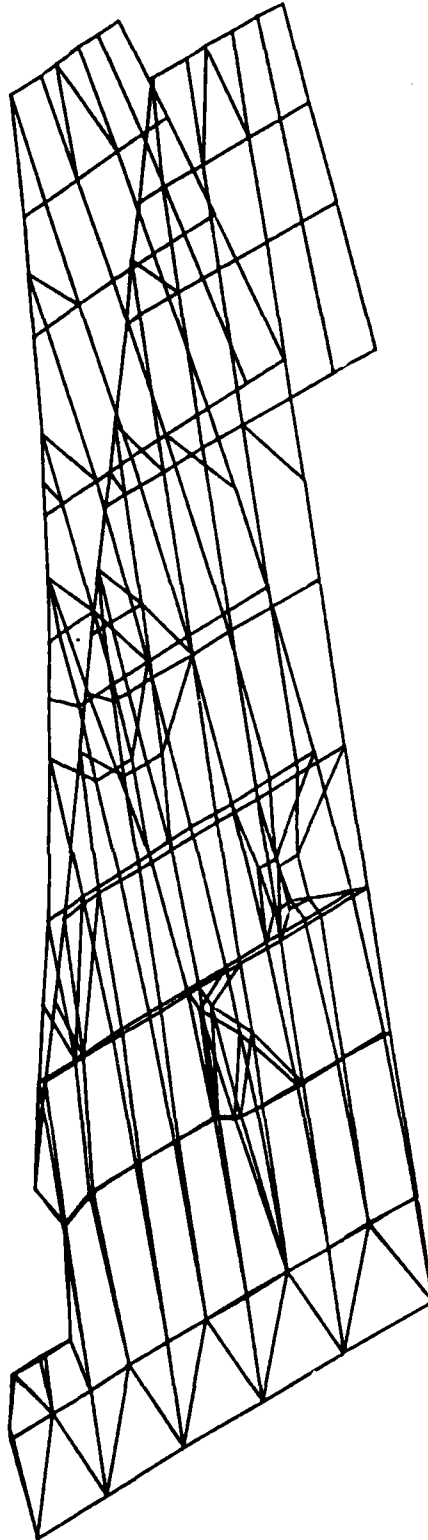
Givens Method   Mode 1   Frequency = 9.54 Hertz
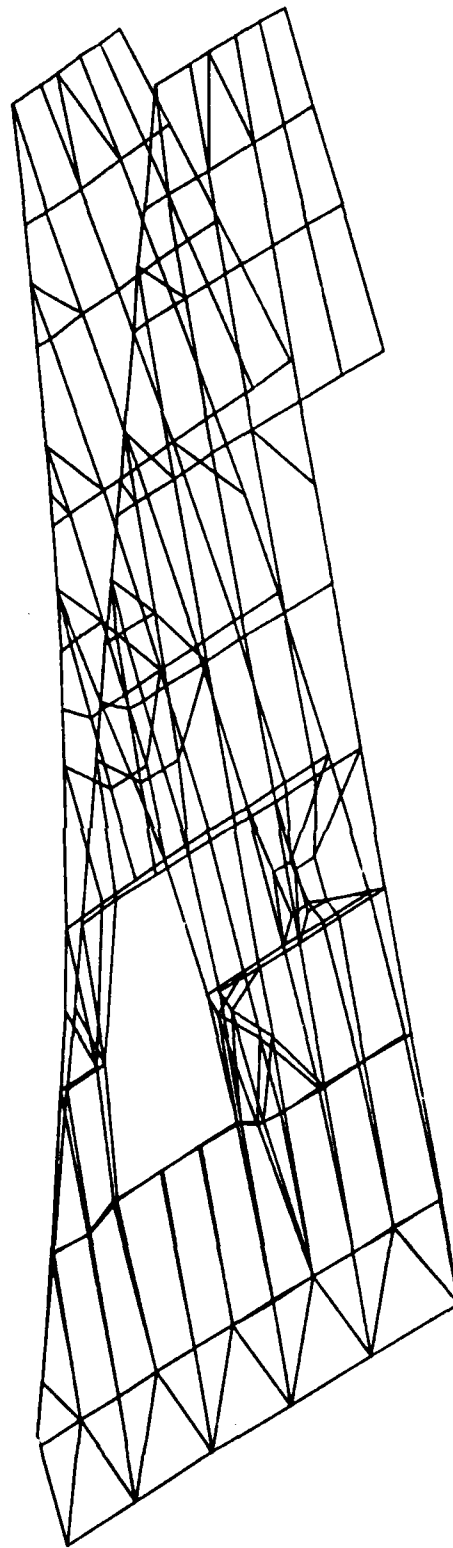
Figure E-6.   1st Wing Bending Mode (Model DC-3)

Symmetric Normal Modes for F-16 Wing Model DC-3
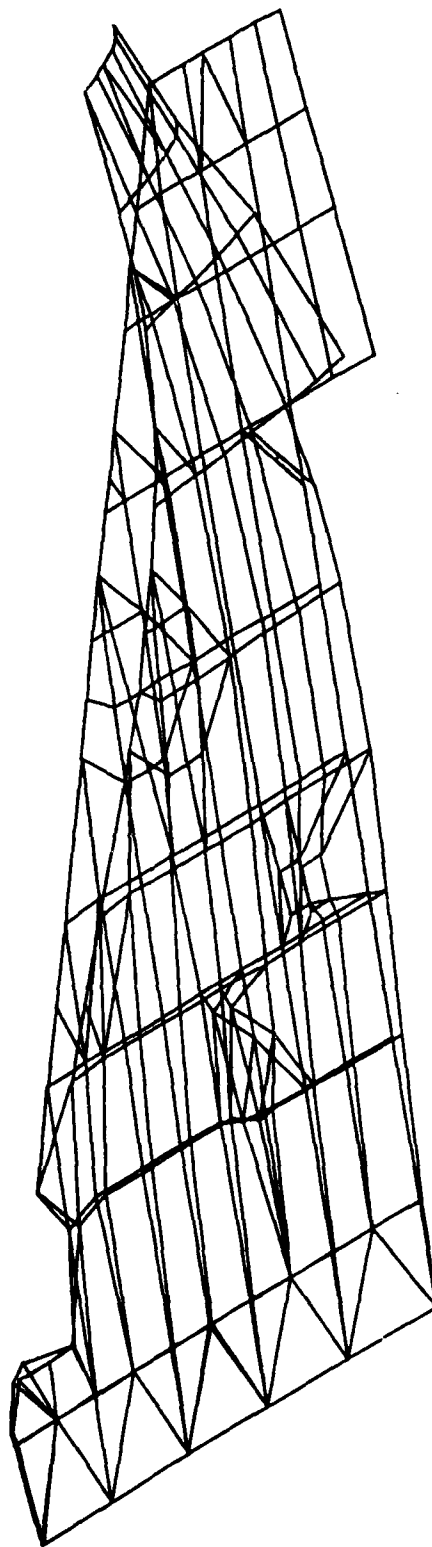Givens Method   Mode 3   Frequency = 38.11 Hertz

Figure E-7.   2nd Wing Bending Mode (Model DC-3)

Symmetric Normal Modes for F-16 Wing Model DC-3

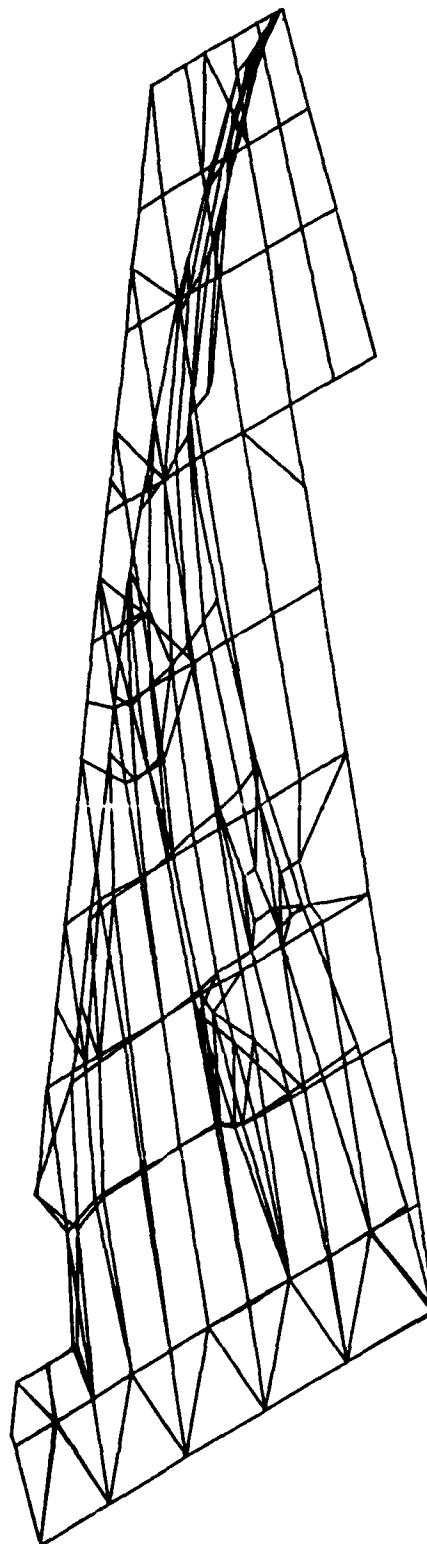Givens Method   Mode 2   Frequency = 29.64 Hertz

Figure E-8.   1st Torsional Mode (Model DC-3)

Symmetric Normal Modes for F-16 Wing Model DC-3

Givens Method   Mode 4   Frequency = 47.23 Hertz

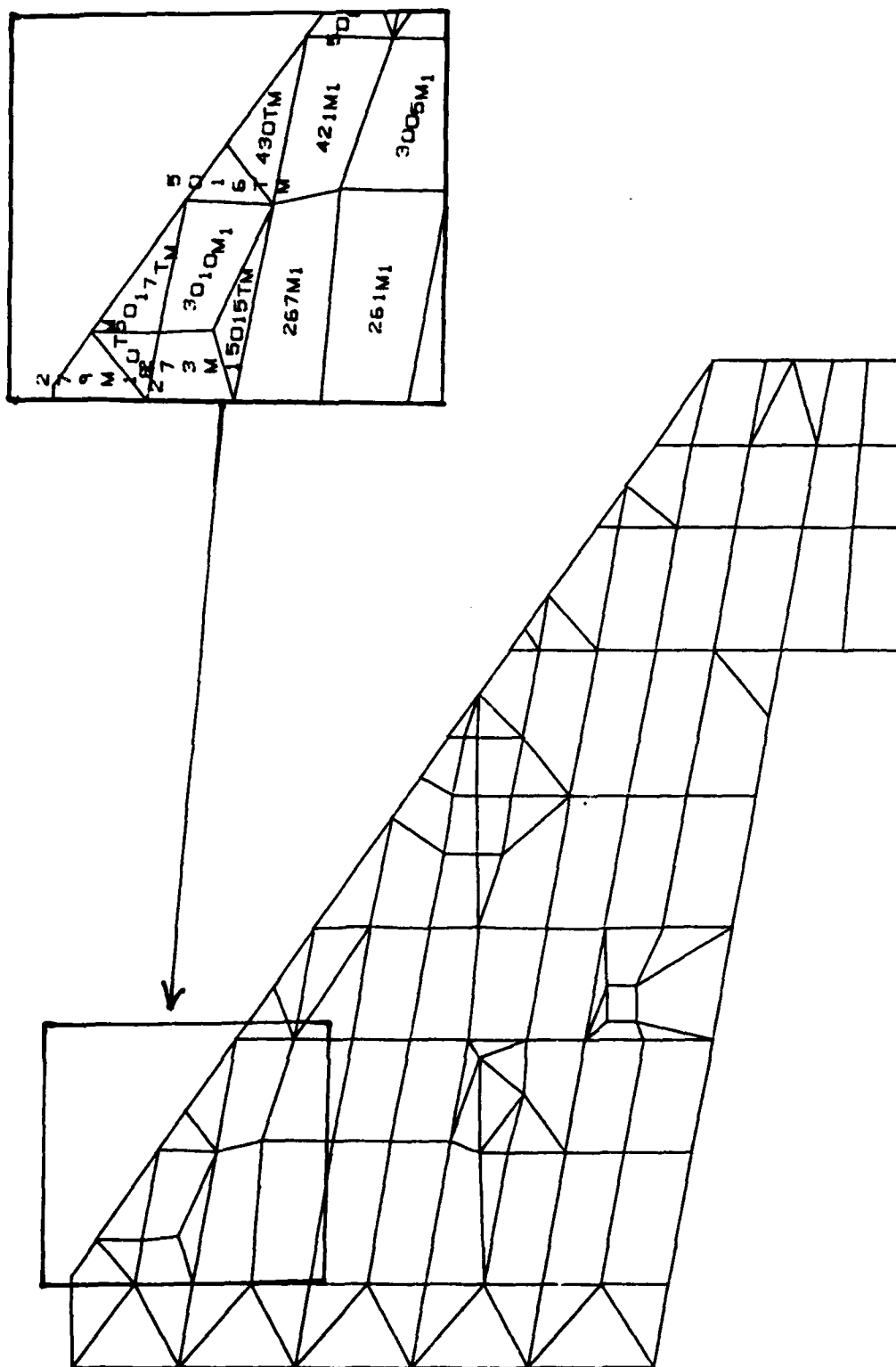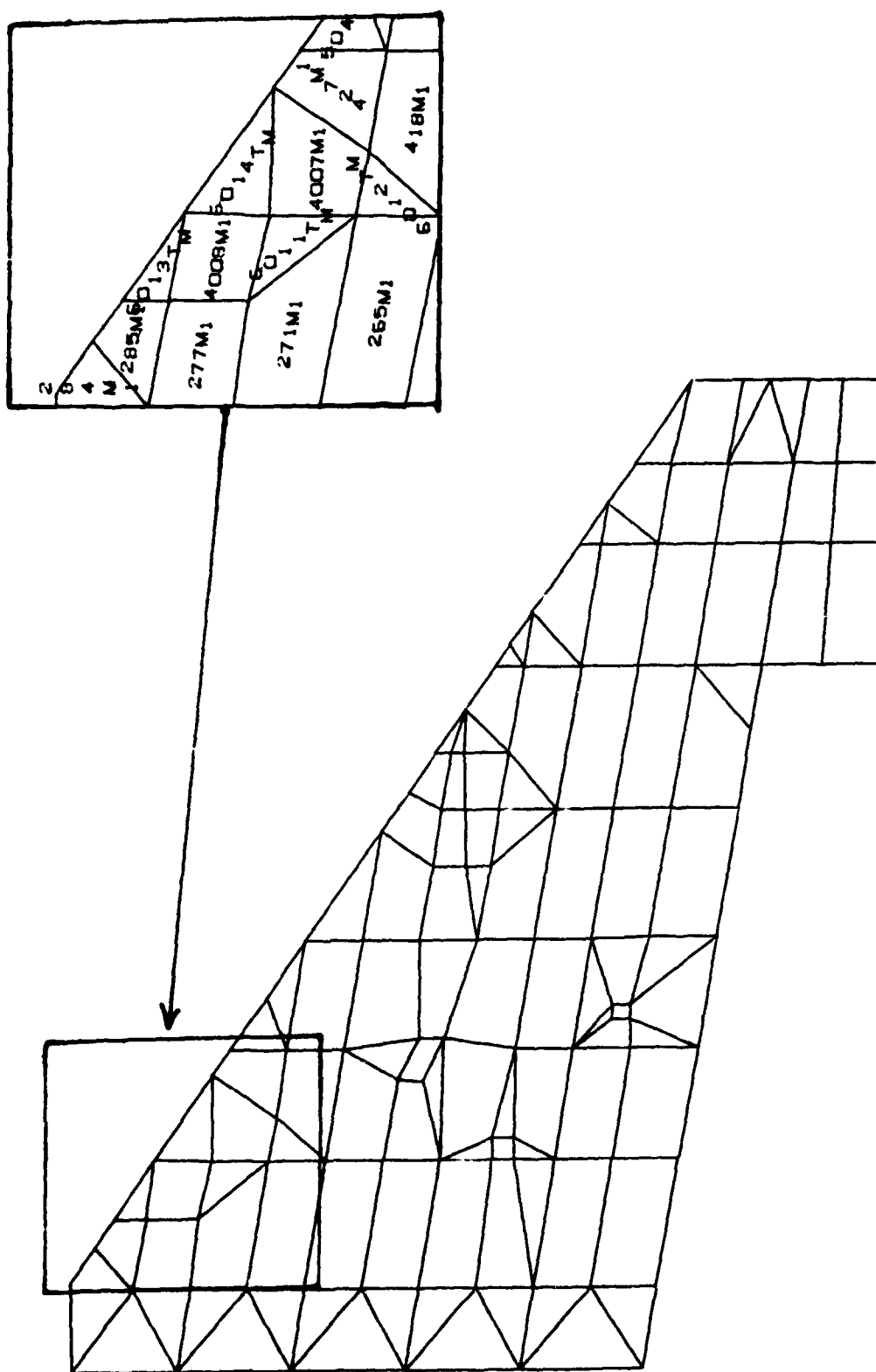Figure E-9.   2nd Torsional Mode (Model DC-3)

Figure E-10. Upper Wing Surface (Model DC-3R)

Figure E-11. Lower Wing Surface (Model DC-3R)

CONTOUR SYMBOLS
PSI-Compression

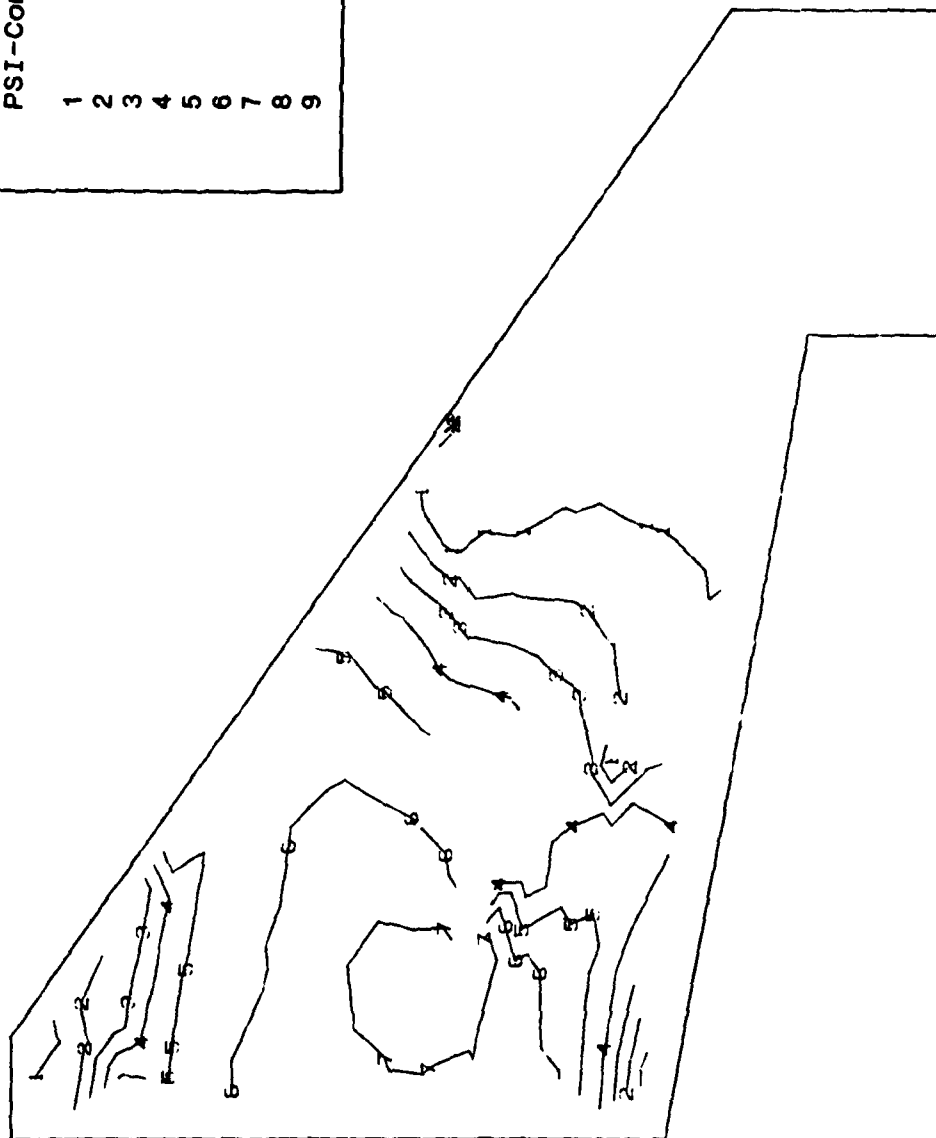| 1	3,000
2	6,000
3	9,000
4	12,000
5	15,000
6	18,000
7	21,000
8	23,000
9	25,000

Figure E-12. Stress Contours on Upper Wing Surface (Model DC-3R)

E-13

CONTOUR SYMBOLS
PSI-Tension

1	3,000
2	6,000
3	9,000
4	12,000
5	15,000
6	17,000
7	19,000
8	21,000
9	23,000
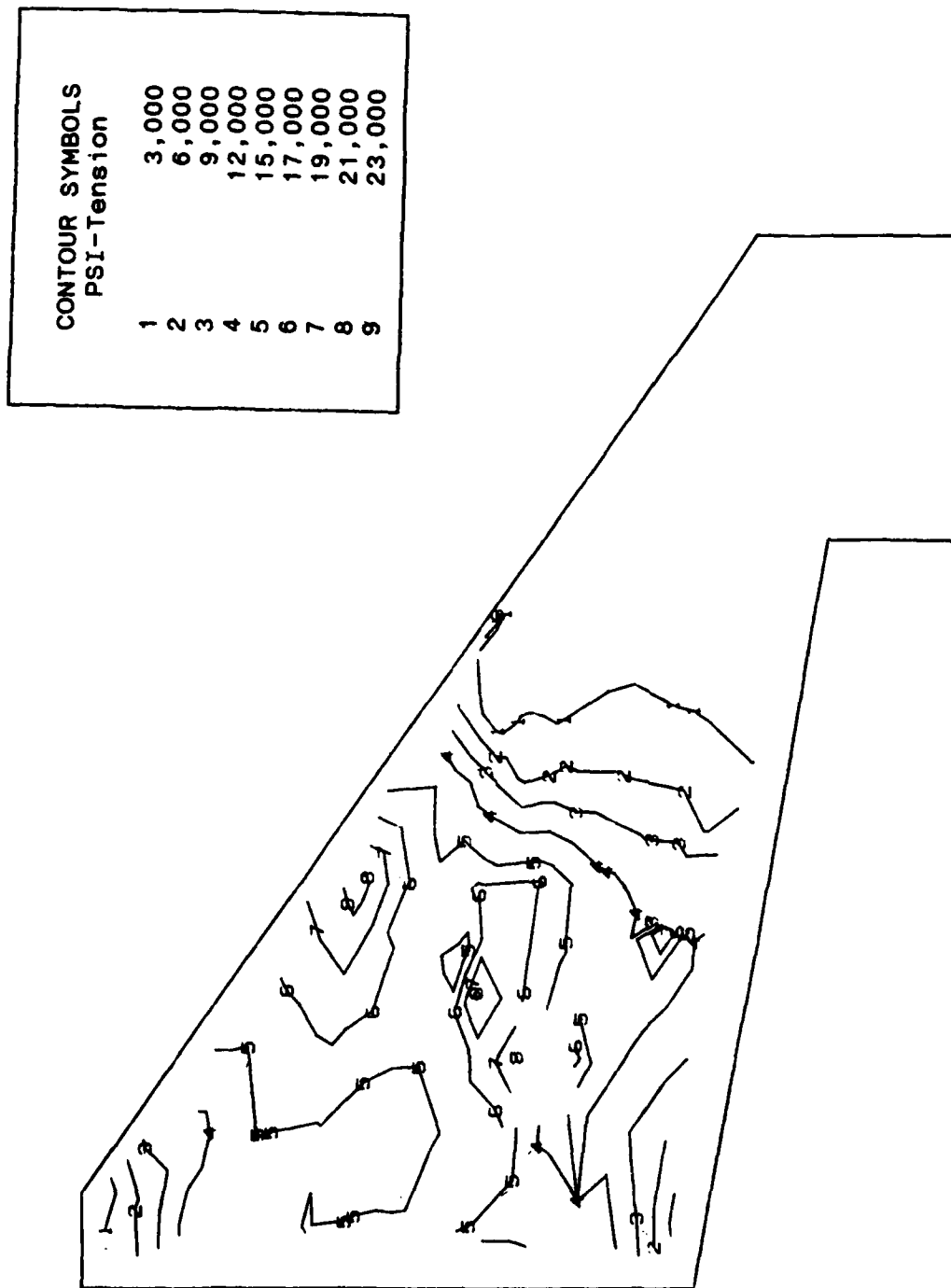
Figure E-13.   Stress Contours on Lower Wing Surface (Model DC-3R)

E-14

Symmetric Normal Modes for F-16 Wing Model DC-3R

Givens Method   Mode 1   Frequency = 10.54 Hertz
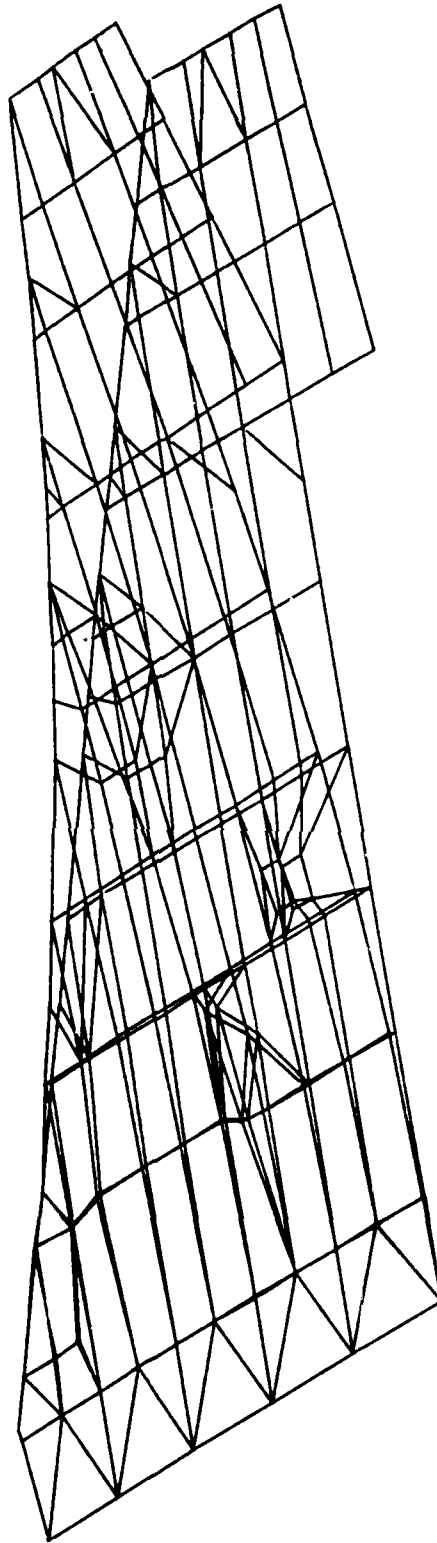
Figure E-14.   1st Wing Bending Mode (Model DC-3R)

Symmetric Normal Modes for F-16 Wing Model DC-3R
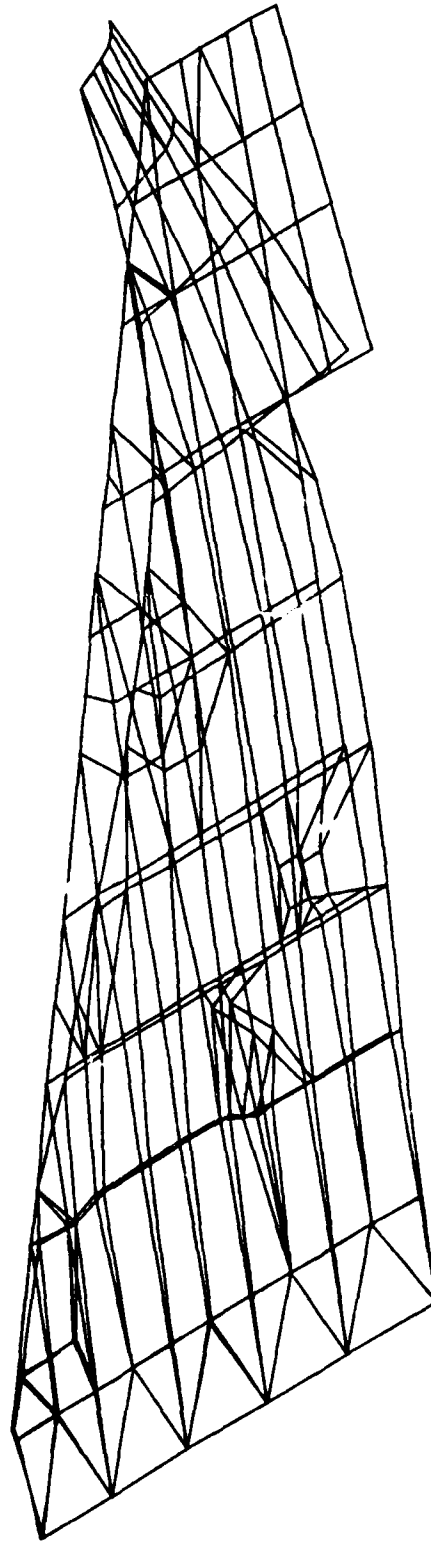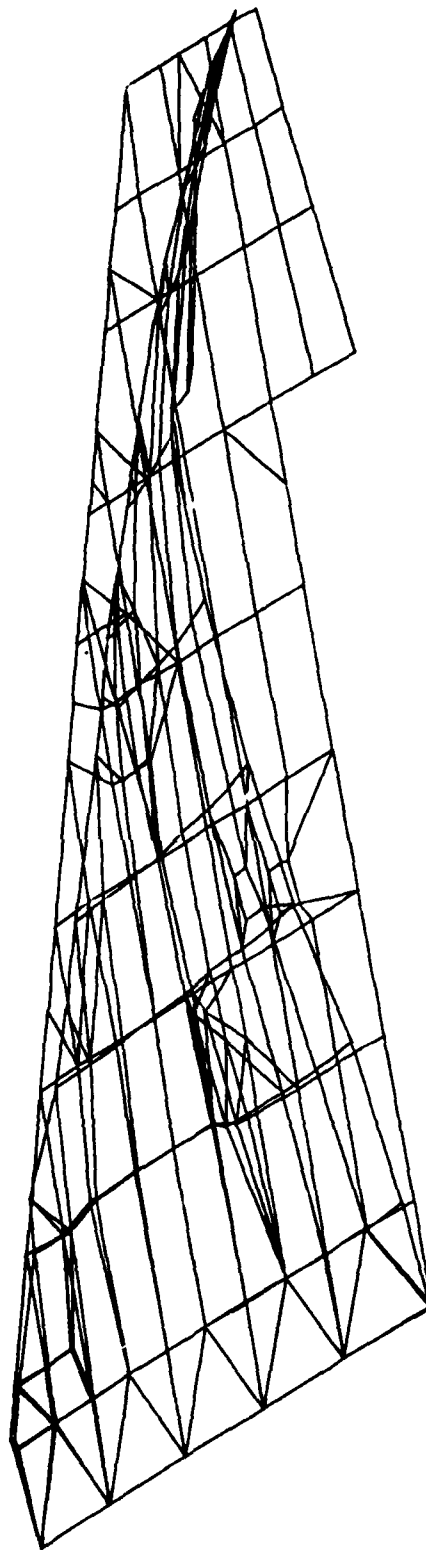
Givens Method   Mode 2   Frequency = 35.23 Hertz

Figure E-15.   2nd Wing Bending Mode (Model DC-3R)

Symmetric Normal Modes for F-16 Wing Model DC-3R

Givens Method   Mode 3   Frequency = 47.02 Hertz

Figure E-16.   1st Torsional Mode (Model DC-3R)

Symmetric Normal Modes for F-16 Wing Model DC-3R
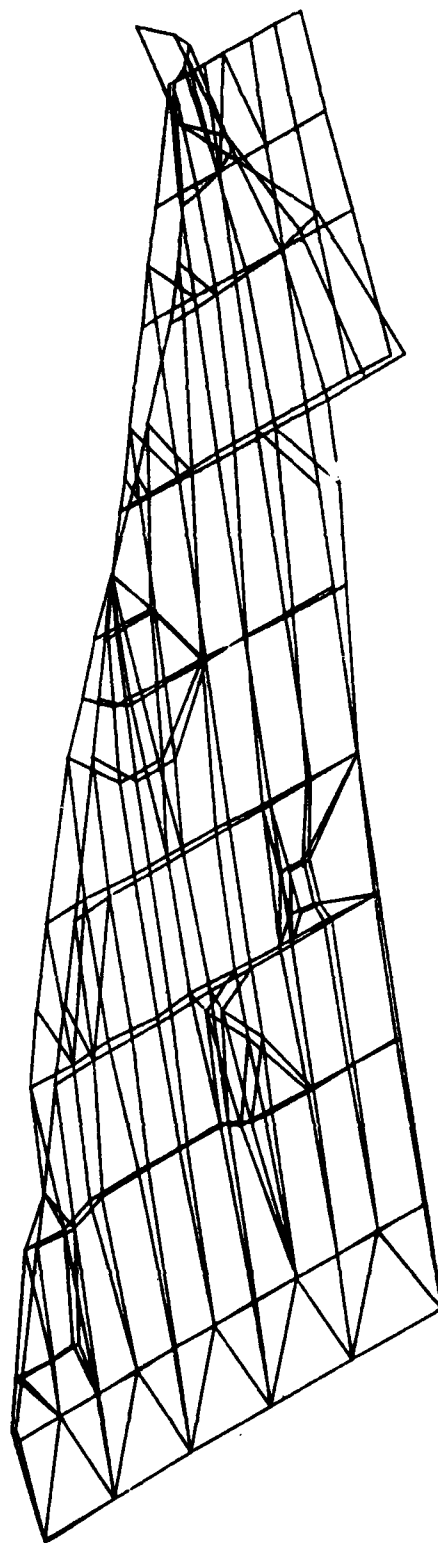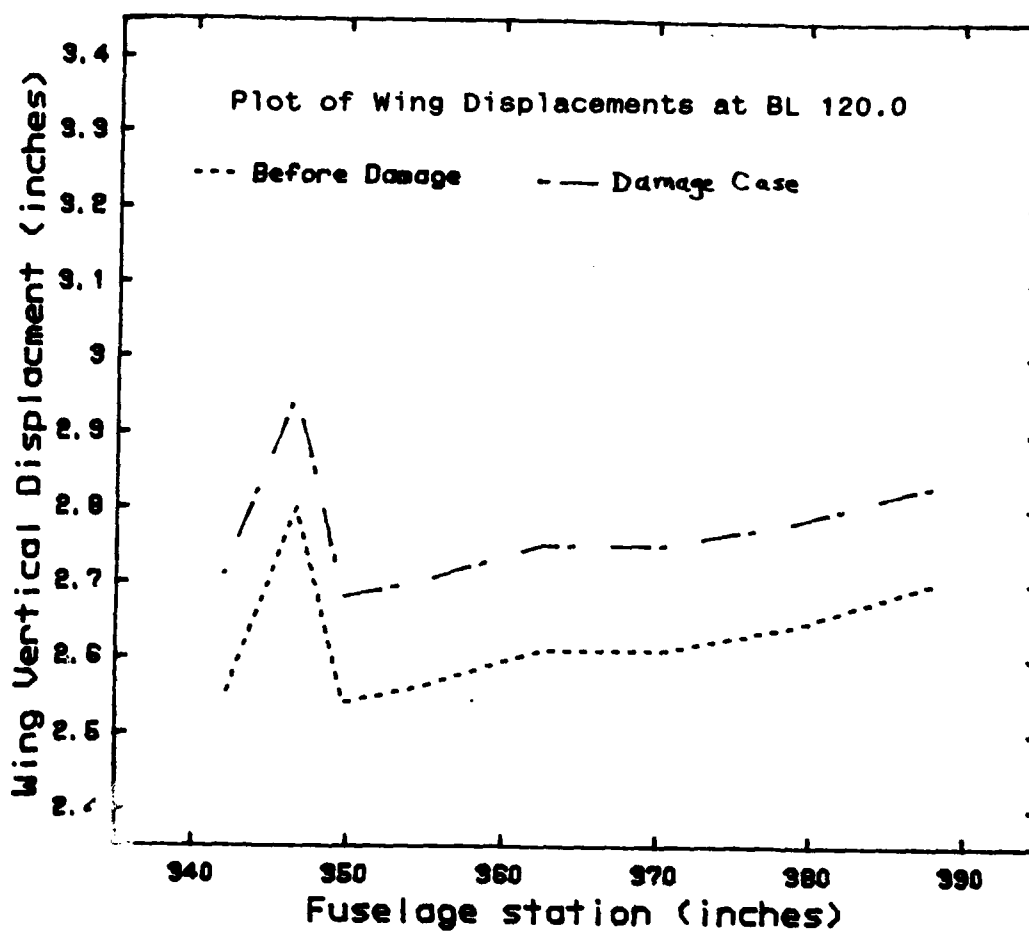
Givens Method   Mode 4   Frequency = 70.67 Hertz
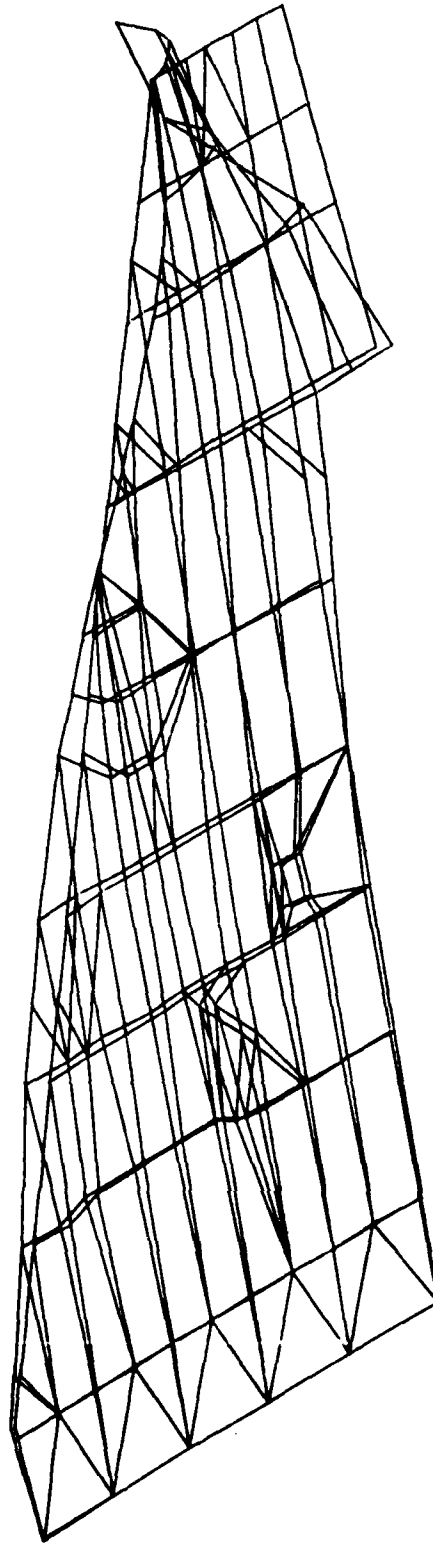
Figure E-17.   2nd Torsional Mode (Model DC-3R)

APPENDIX F

ANALYSIS OF DAMAGE CASE #4

Plot of Wing Displacements at BL 120.0

··· Before Damage   ·— Damage Case   —— Repaired
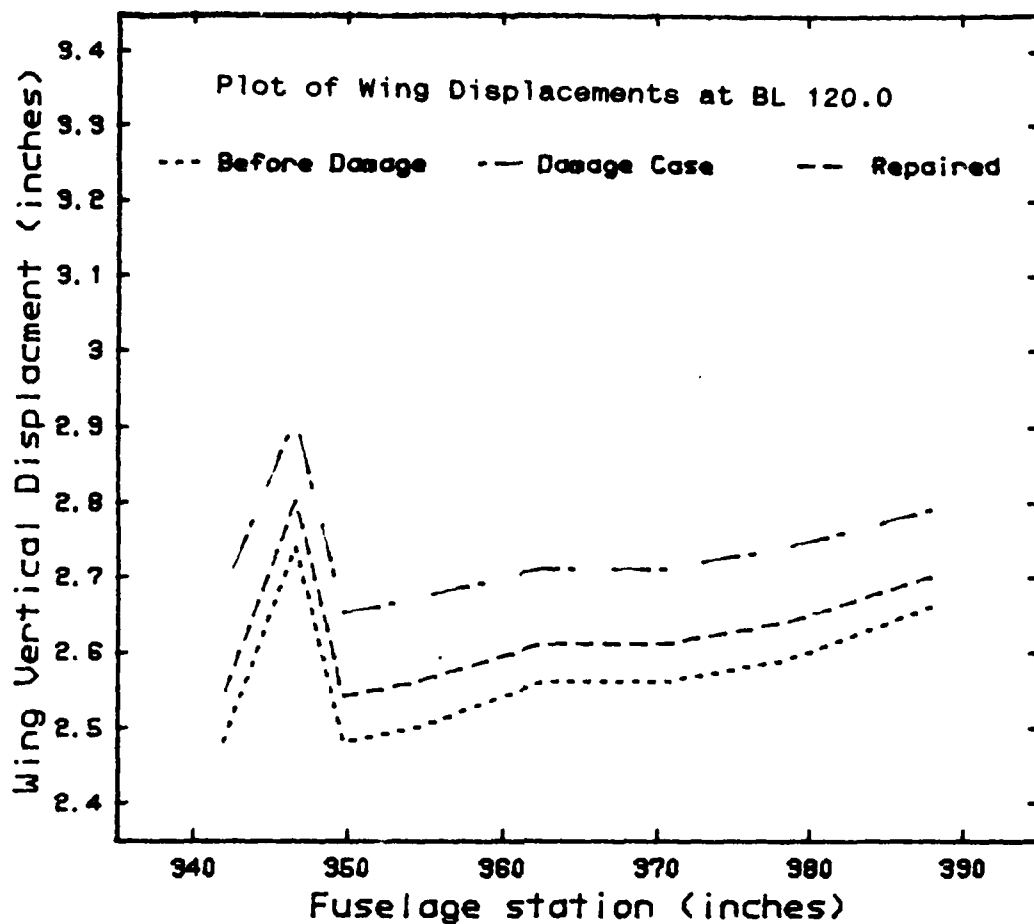
Tabulated Displacements

Fuselage St.	387.9	378.6	370.6	362.6	354.6	349.7	346.6	341.9
Model DC-3R	2.66	2.59	2.56	2.56	2.50	2.48	2.74	2.48
Model DC-4	2.79	2.74	2.71	2.71	2.67	2.65	2.91	2.68
Model DC-4R	2.70	2.64	2.61	2.61	2.56	2.54	2.80	2.54

Comparison of Residual Strength

	Av Disp	% Change	Torsion mode	% Change
Model D-3R	2.57		47.02	
Model DC-4	2.73	-6.2	46.22	-1.7
Model DC-4R	2.63	+3.9	46.93	+1.5

Figure F-1.   Summary of Damage Case #4 Results
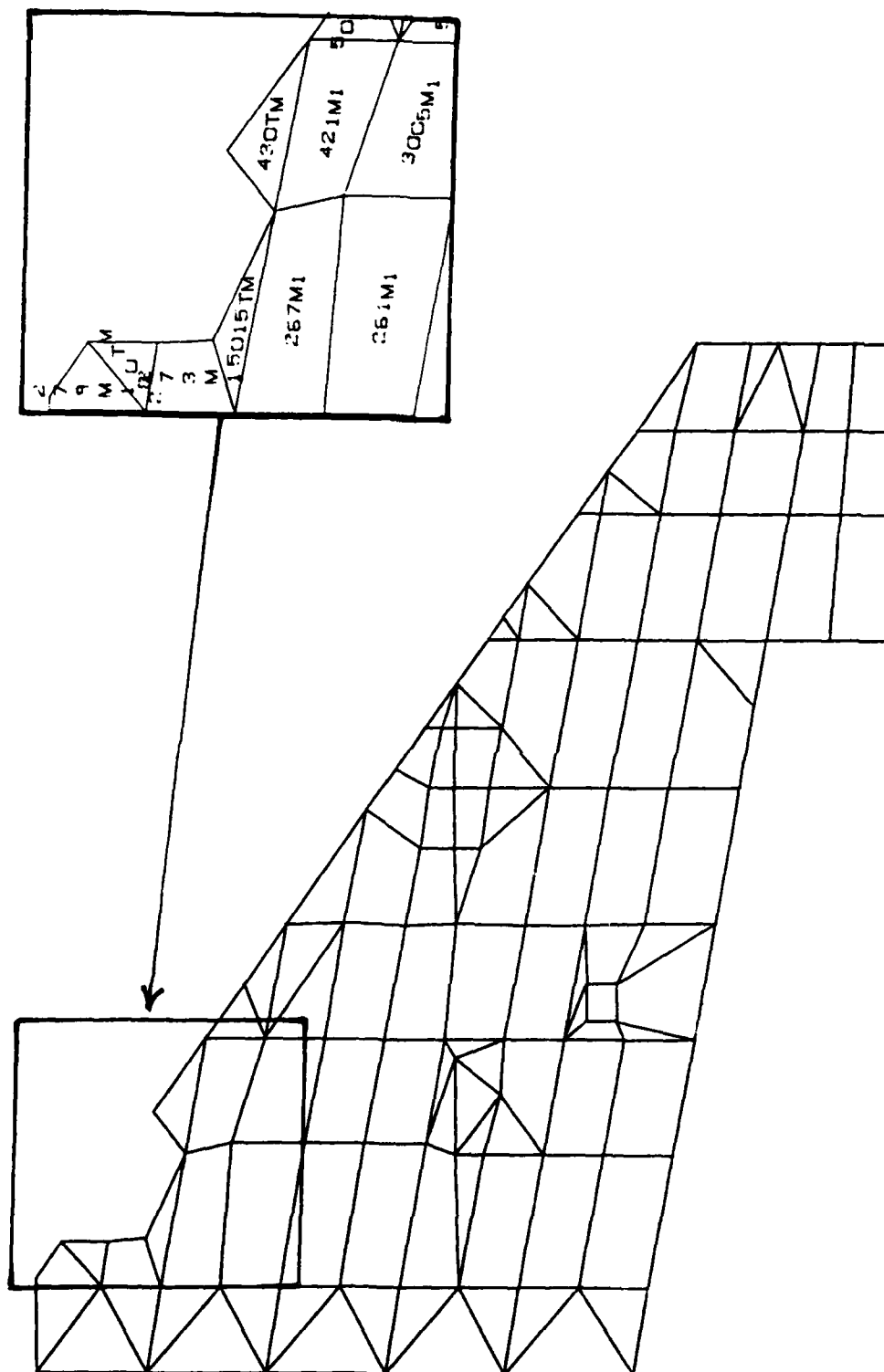
Figure F-2. Upper Wing Surface (Model DC-4)

F-3

Figure F-3.   Lower Wing Surface (Model DC-4)

CONTOUR SYMBOLS
PSI-Compression

1	3,000
2	6,000
3	9,000
4	12,000
5	15,000
6	18,000
7	21,000
8	23,000
9	25,000

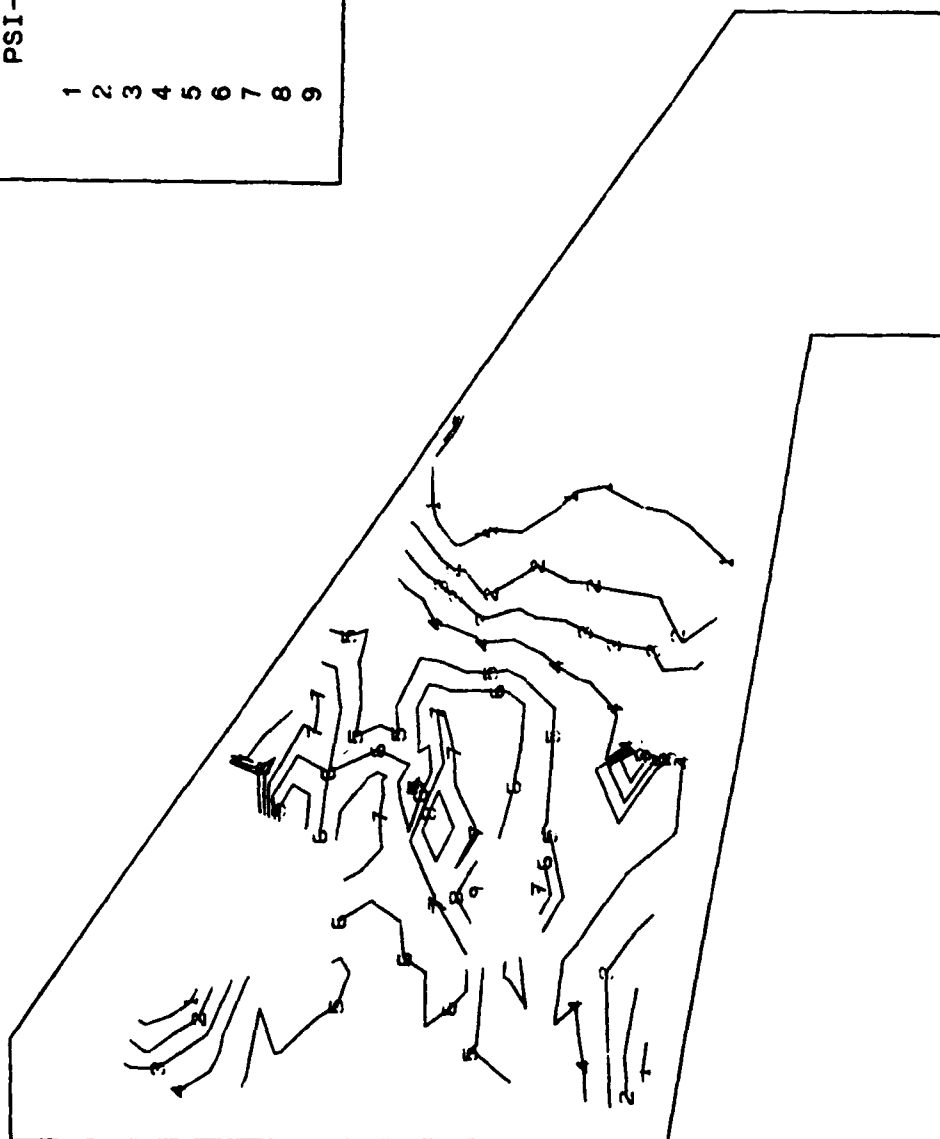Figure F-4. Stress Contours on Upper Wing Surface (Model DC-4)

F-5
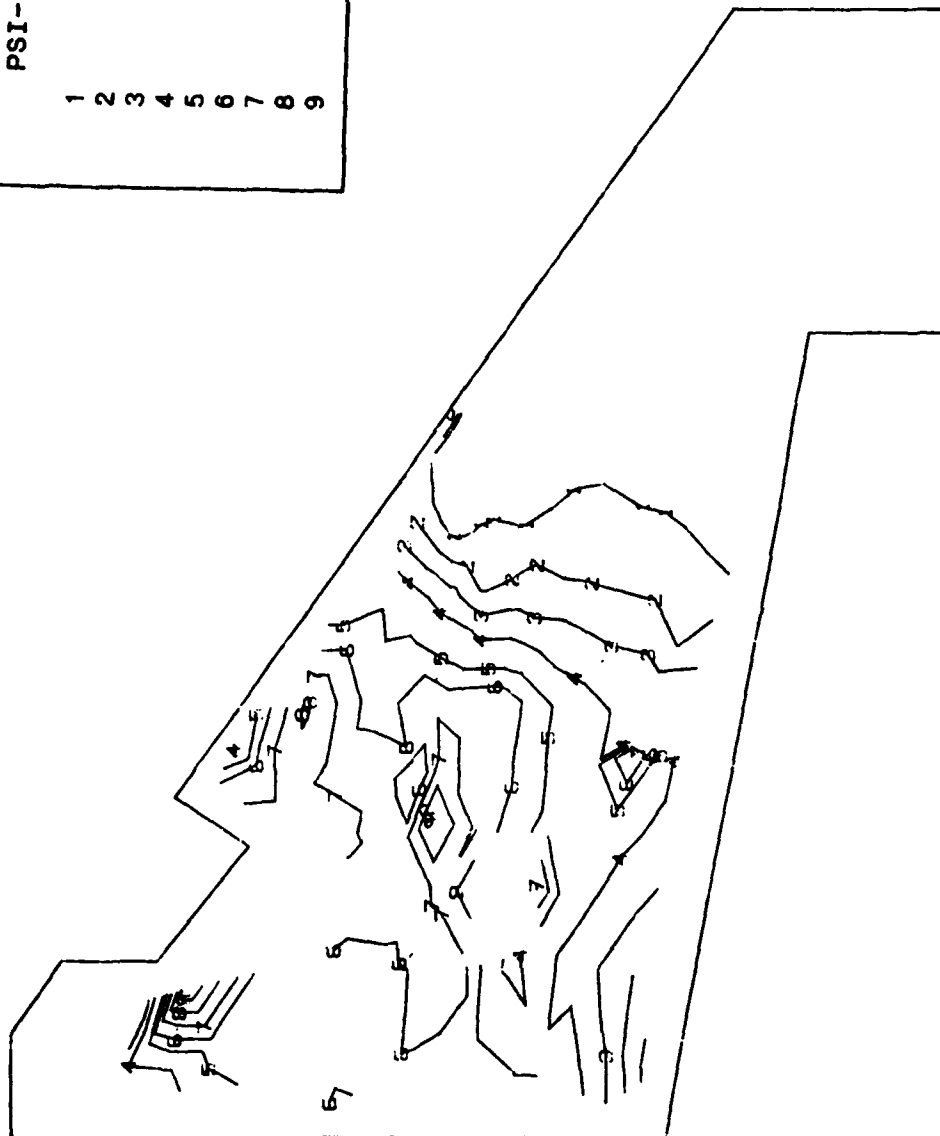
Figure F-5. Stress Contours on Lower Wing Surface (Model DC-4)

Symmetric Normal Modes for F-16 Wing Model DC-4

Givens Method   Mode 1   Frequency = 10.33 Hertz
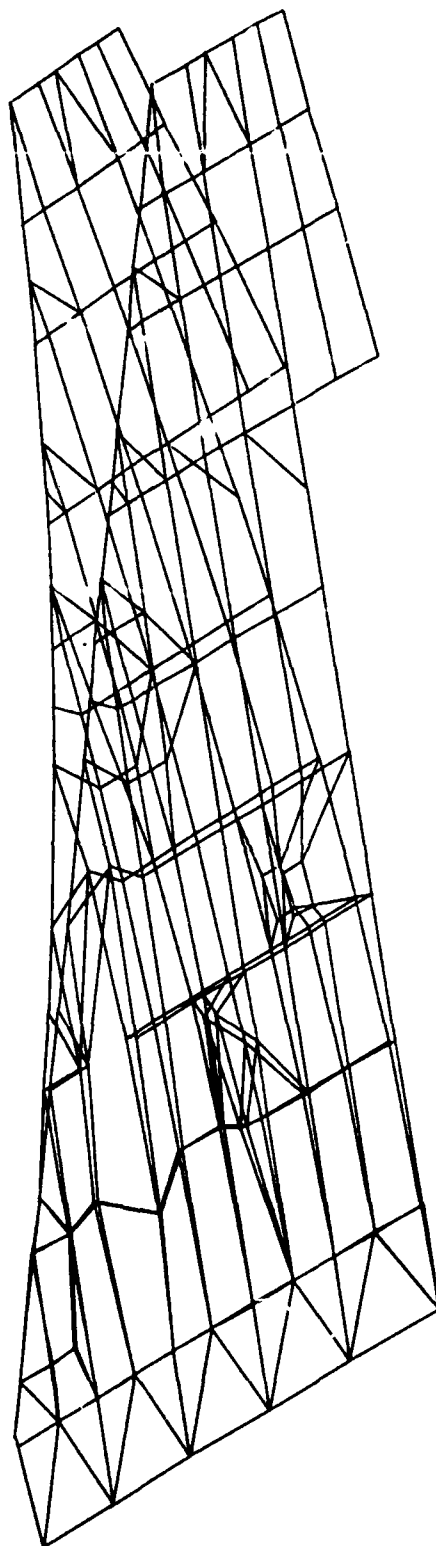

Figure F-6.   1st Wing Bending Mode (Model DC-4)

Symmetric Normal Modes for F-16 Wing Model DC-4

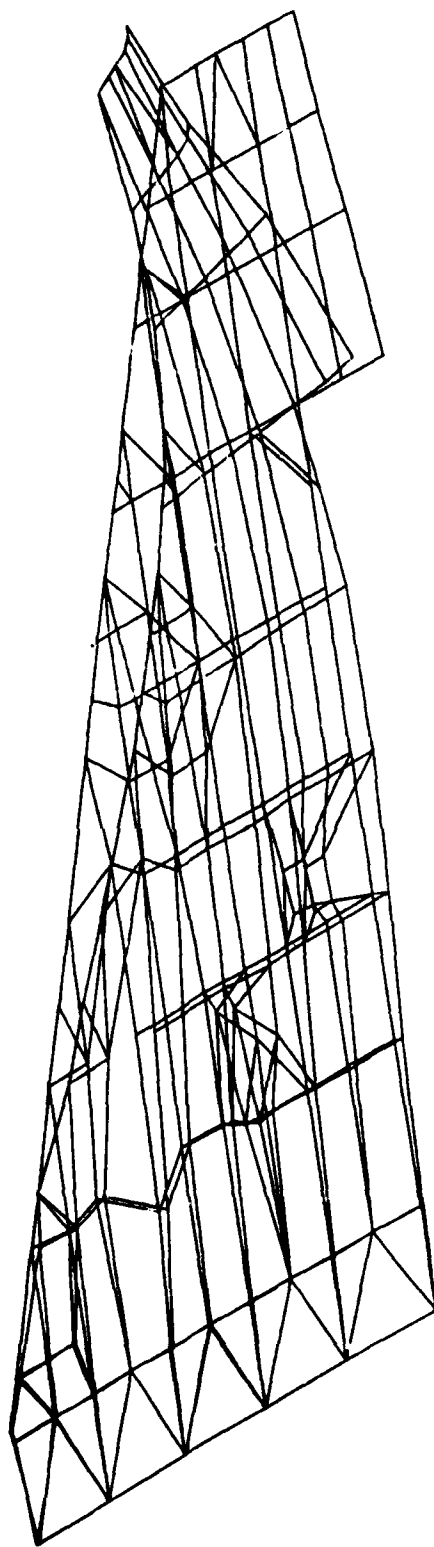Givens Method Mode 2 Frequency = 34.64 Hertz

Figure F-7. 2nd Wing Bending Mode (Model DC-4)

Symmetric Normal Modes for F-16 Wing Model DC-4

Givens Method   Mode 3   Frequency = 46.22 Hertz
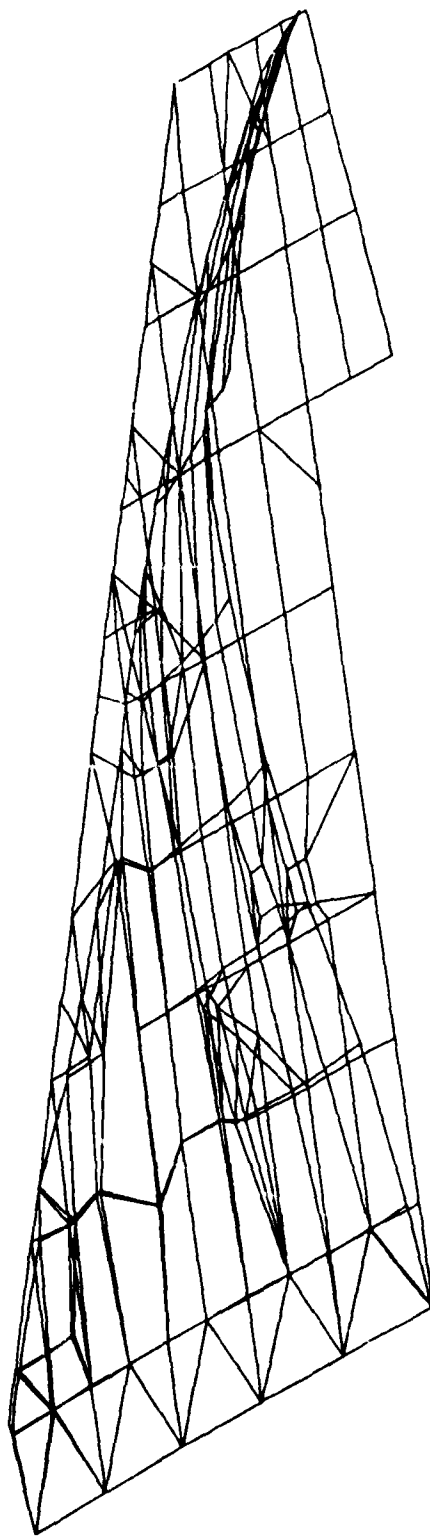
Figure F-8.   1st Torsional Mode (Model DC-4)

Symmetric Normal Modes for F-16 Wing Model DC-4

Givens Method   Mode 4   Frequency = 68.04 Hertz
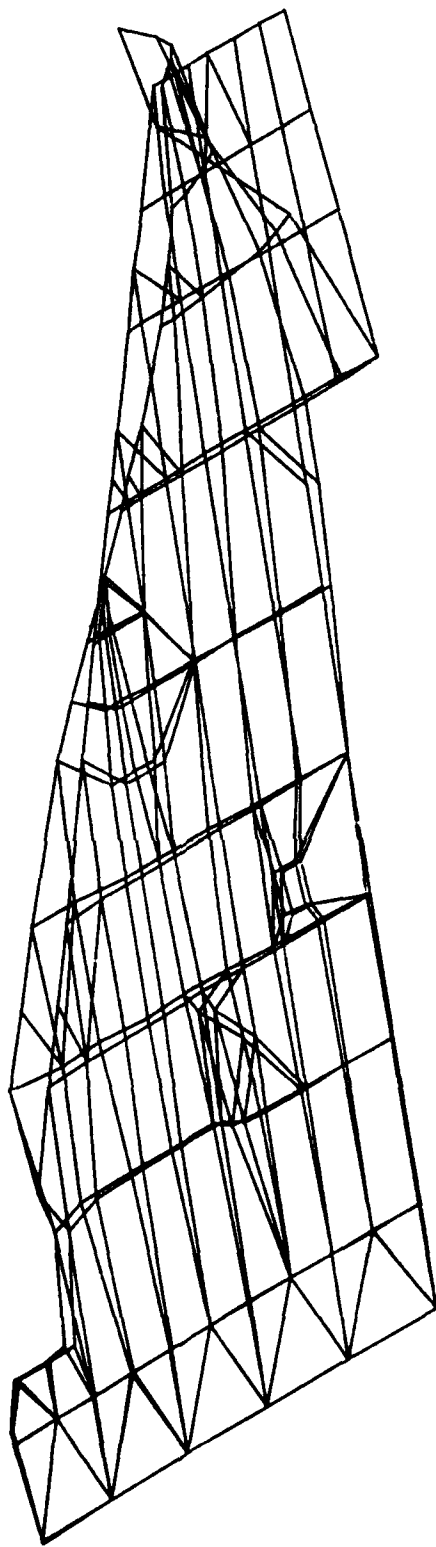
Figure F-9. 2nd Torsional Mode (Model DC-4)

Figure F-10. Upper Wing Surface (Model DC-4R)

Figure F-11. Lower Wing Surface (Model DC-4R)

CONTOUR SYMBOLS
PSI-Compression

1   3,000
2   6,000
3   9,000
4   12,000
5   15,000
6   18,000
7   21,000
8   23,000
9   25,000

Figure F-12.   Stress Contours on Upper Wing Surface (Model DC-4R)

CONTOUR SYMBOLS
PSI-Tension

1	3,000
2	6,000
3	9,000
4	12,000
5	15,000
6	17,000
7	19,000
8	21,000
9	23,000

Figure F-13. Stress Contours on Lower Wing Surface (Model DC-4R)

Symmetric Normal Modes for F-16 Wing Model DC-4R

Givens Method   Mode 1   Frequency = 10.47 Hertz

Figure F-14.   1st Wing Bending Mode (Model DC-4R)

Symmetric Normal Modes for F-16 Wing Model DC-4R

Givens Method   Mode 2   Frequency = 35.06 Hertz

Figure F-15.   2nd Wing Bending Mode (Model DC-4R)

Symmetric Normal Modes for F-16 Wing Model DC-4R

Givens Method   Mode 3   Frequency = 46.93 Hertz

Figure F-16. 1st Torsional Mode (Model DC-4R)

F-17

Symmetric Normal Modes for F-16 Wing Model DC-4R

Givens Method   Mode 4   Frequency = 70.42 Hertz

Figure F-17.   2nd Torsional Mode (Model DC-4R)

F-18

APPENDIX G

ANALYSIS OF DAMAGE CASE #7

Plot of Wing Displacements at BL 120.0

··· Before Damage   ·—· Damage Case

Wing Vertical Displacement (inches)

Fuselage station (inches)

Tabulated Displacements

Fuselage St.	387.9	378.6	370.6	362.6	354.6	349.7	346.6	341.9
Model DC-4R	2.70	2.64	2.61	2.61	2.56	2.54	2.80	2.54
Model DC-7	2.83	2.78	2.75	2.75	2.70	2.68	2.95	2.71

Comparison of Residual Strength

	Av Disp	% Change	Torsion mode	% Change
Model D-4R	2.63		46.93	
Model DC-7	2.77	-5.3	46.04	-1.9

Figure G-1. Summary of Damage Case #7 Results
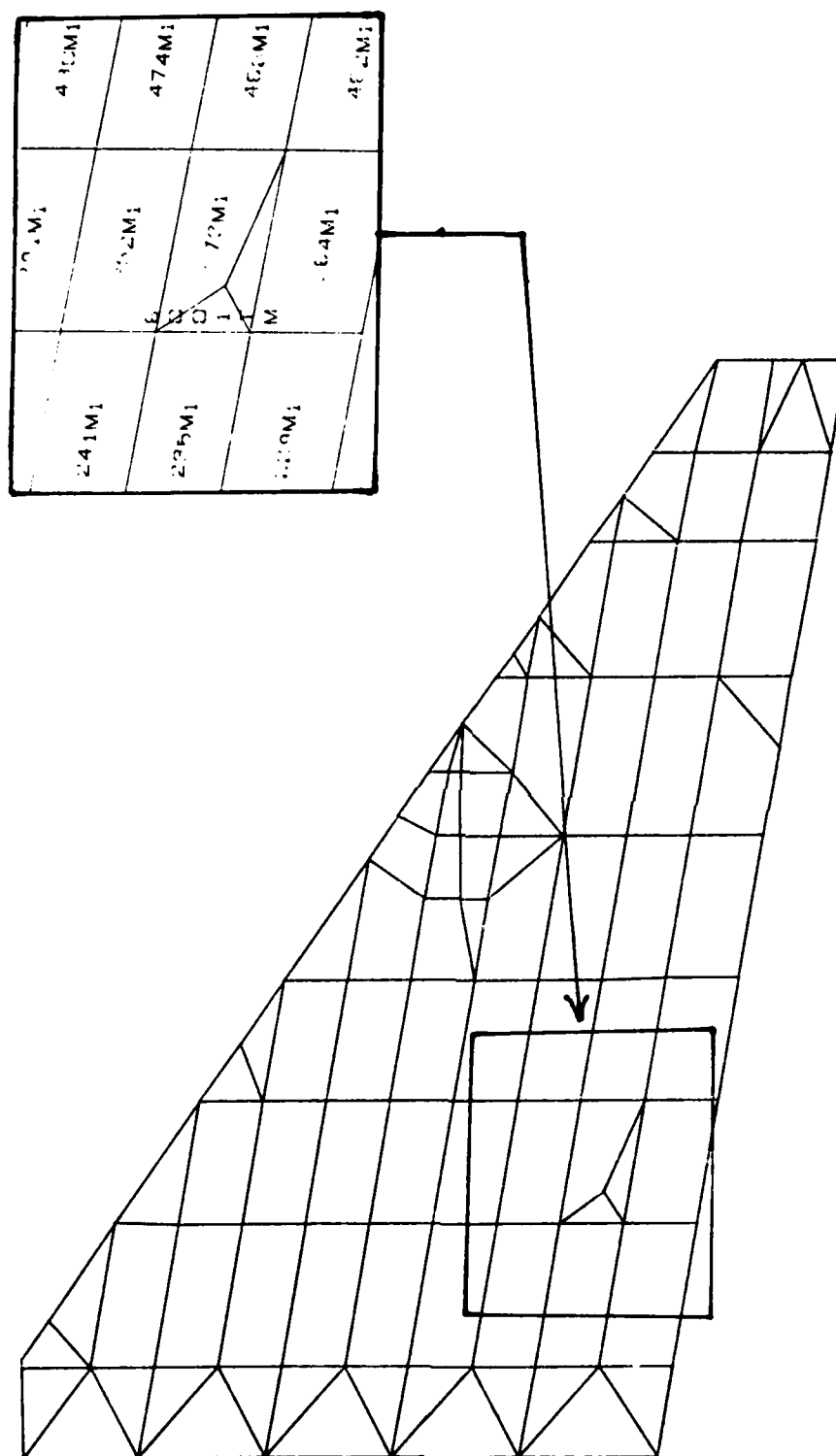
Figure G-2. Upper Wing Surface (Model DC-7)
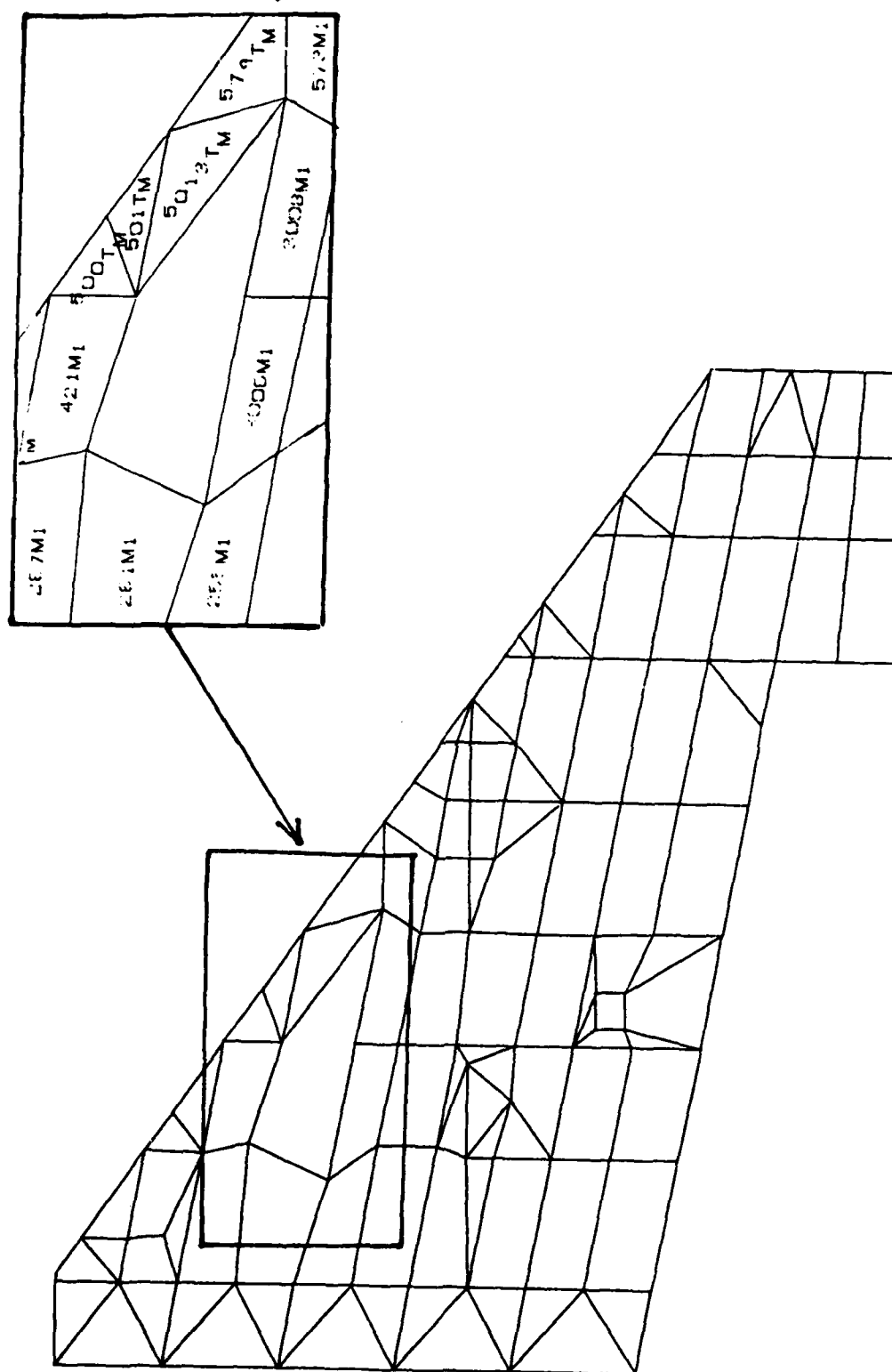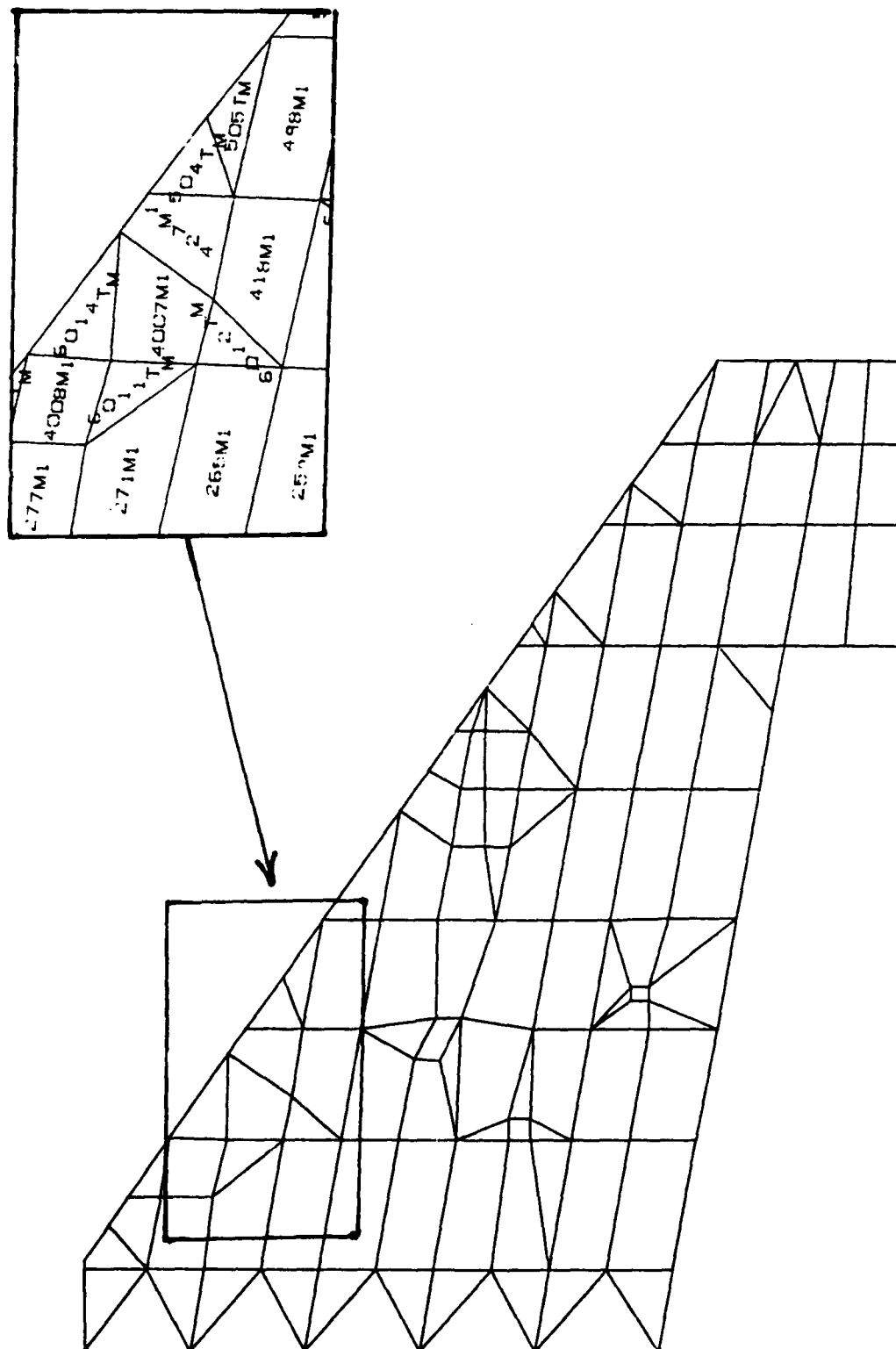
Figure G-3. Lower Wing Surface (Model DC-7)

CONTOUR SYMBOLS
PSI-Compression

1	3,000
2	6,000
3	9,000
4	12,000
5	15,000
6	18,000
7	21,000
8	23,000
9	25,000

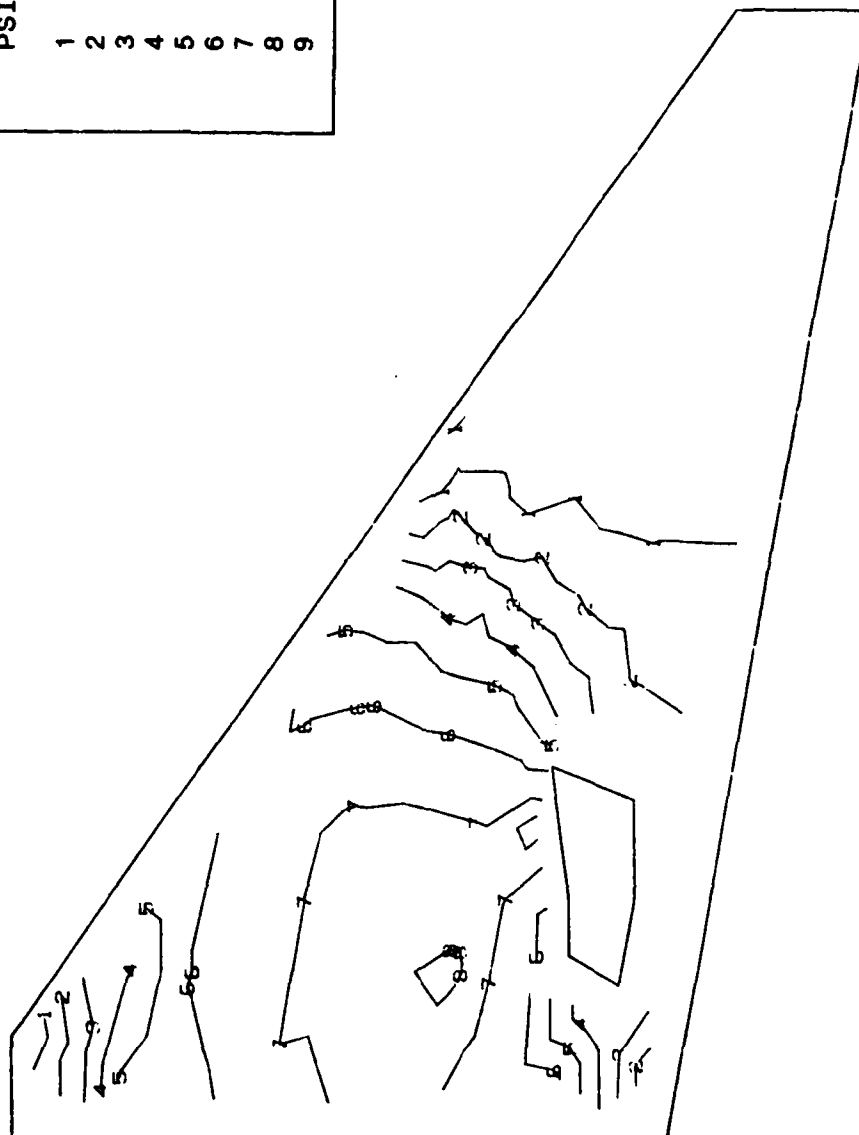Figure G-4.   Stress Contours on Upper Wing Surface (Model DC-7)

CONTOUR SYMBOLS
PSI-Tension

|	
1	3,000
2	6,000
3	9,000
4	12,000
5	15,000
6	17,000
7	19,000
8	21,000
9	23,000

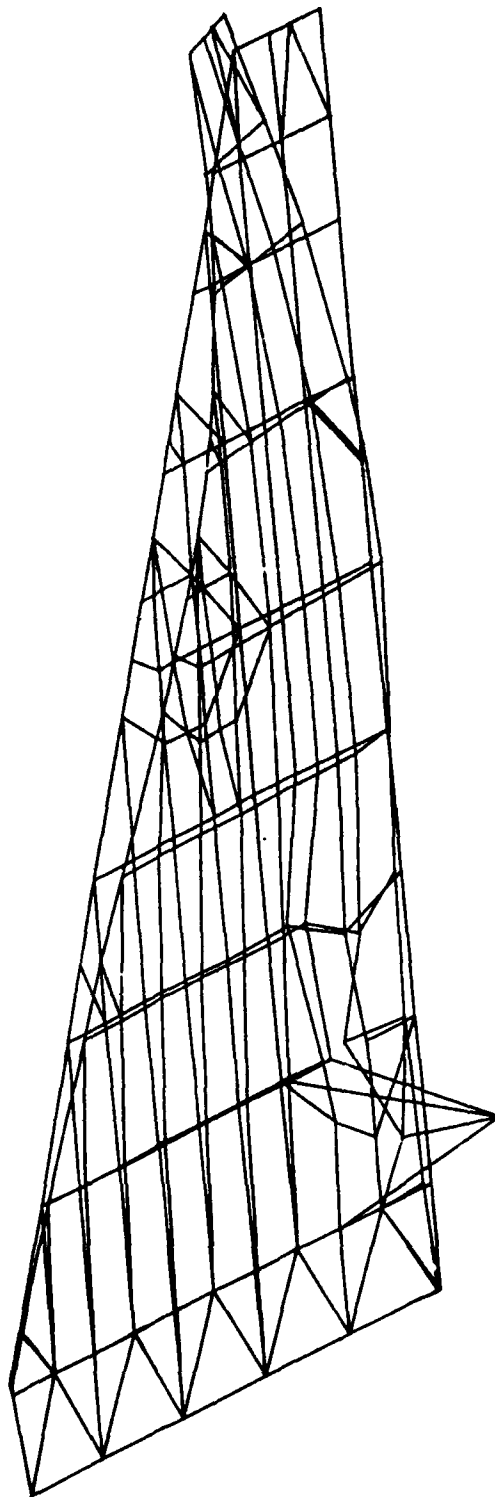Figure G-5. Stress Contours on Lower Wing Surface (Model DC-7)

Symmetric Normal Modes for F-16 Wing Model DC-7

Givens Method   Mode 1   Frequency = 10.24 Hertz

Figure G-6.   1st Wing Bending Mode (Model DC-7)

Symmetric Normal Modes for F-16 Wing Model DC-7

Givens Method   Mode 2   Frequency = 34.61 Hertz

Figure G-7.   2nd Wing Bending Mode (Model DC-7)

Symmetric Normal Modes for F-16 Wing Model DC-7

Givens Method   Mode 3   Frequency = 46.04 Hertz
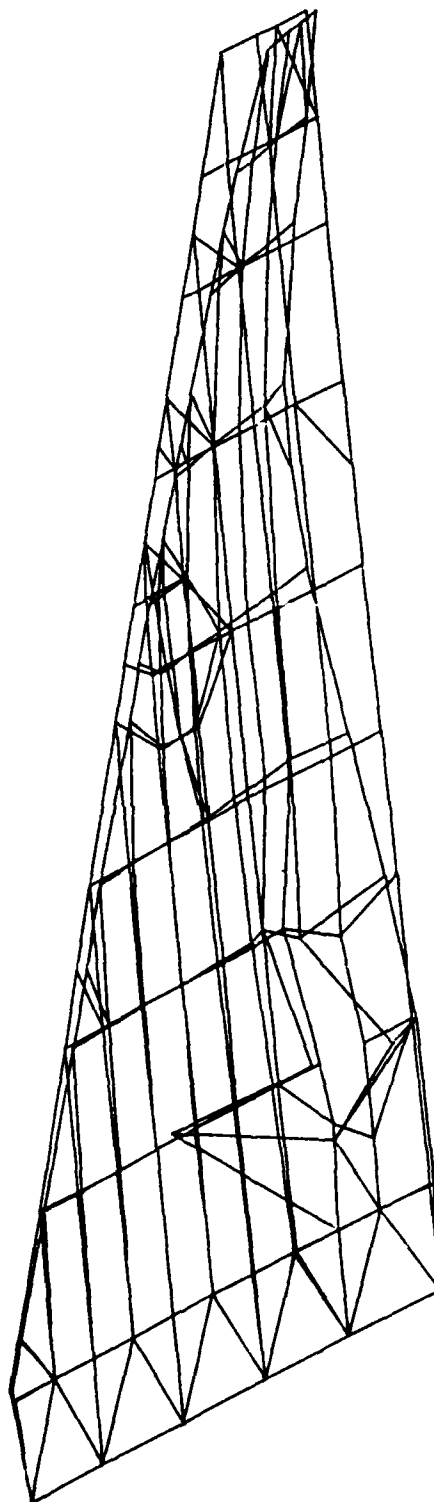
Figure G-8.   1st Torsional Mode (Model DC-7)

Symmetric Normal Modes for F-16 Wing Model DC-7

Givens Method Mode 4   Frequency = 67.33 Hertz
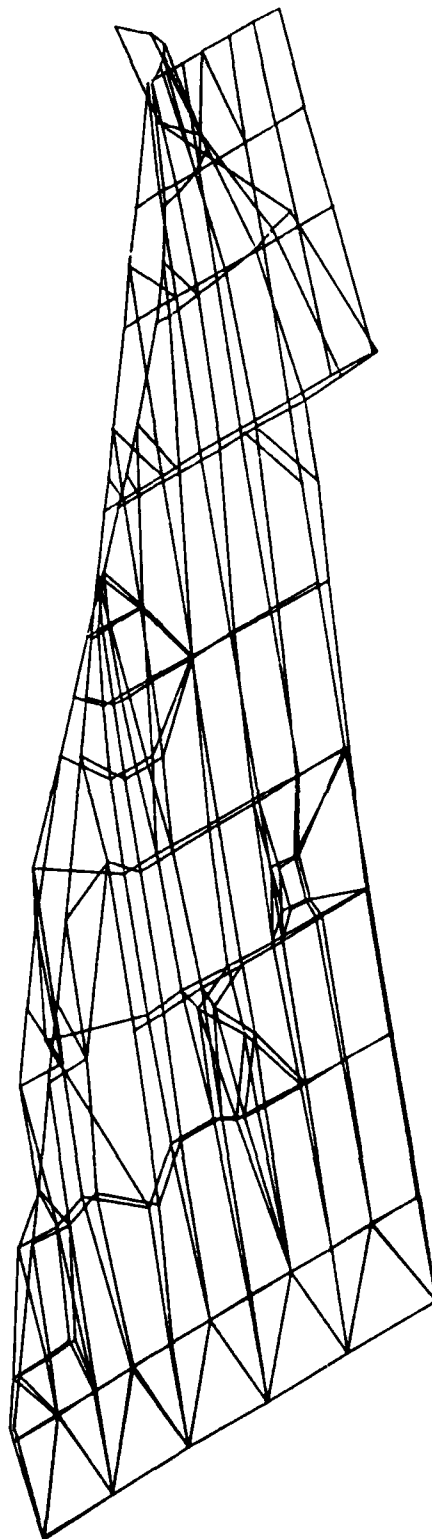
Figure G-9. 2nd Torsional Mode (Model DC-7)

APPENDIX H

ANALYSIS OF DAMAGE CASE #9
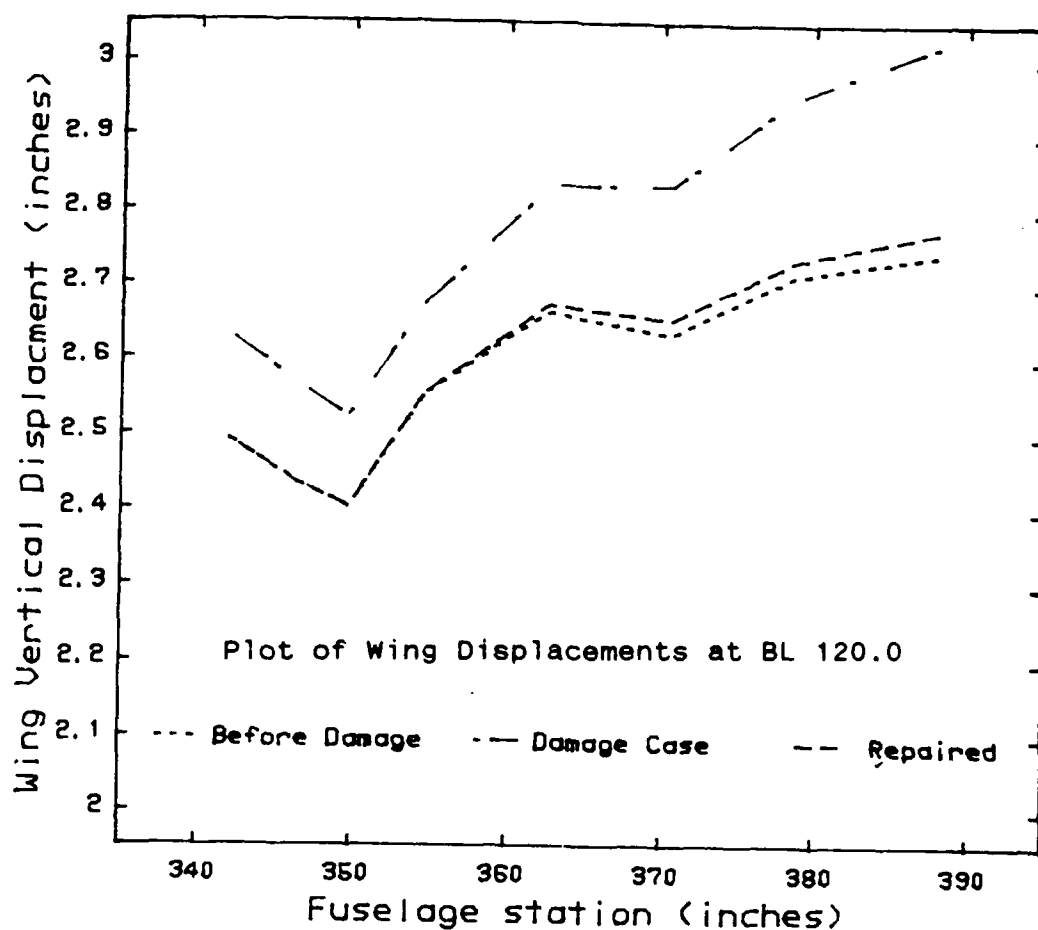
Plot of Wing Displacements at BL 120.0

--- Before Damage   ·— Damage Case   — — Repaired

Tabulated Displacements

Fuselage St.	387.9	378.6	370.6	362.6	354.6	349.7	346.6	341.9
Model D-4	2.74	2.71	2.63	2.66	2.55	2.40	2.43	2.49
Model DC-9	3.02	2.95	2.83	2.83	2.67	2.52	2.56	2.63
Model DC-9R	2.77	2.73	2.65	2.67	2.55	2.40	2.43	2.49

Comparison of Residual Strength

	Av Disp	% Change	Torsion mode	% Change
Model D-4	2.58		48.15	
Model DC-9	2.75	-6.6	35.02	-27.3
Model DC-9R	2.59	+6.2	45.67	+21.9

Figure H-1.   Summary of Damage Case #9 Results
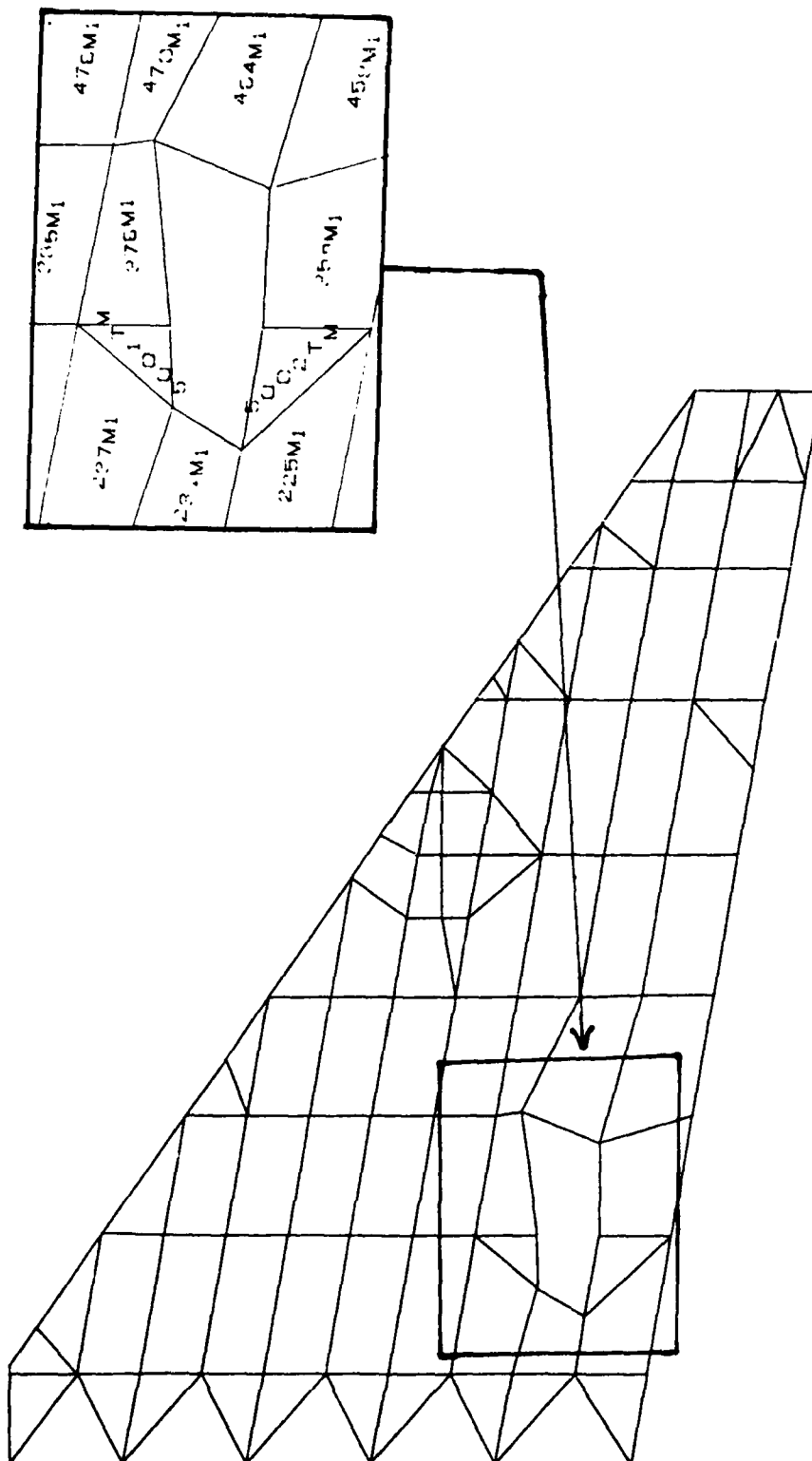
Figure H-2. Upper Wing Surface (Model DC-9)

Figure H-3. Lower Wing Surface (Model DC-9)

CONTOUR SYMBOLS
PSI-Compression

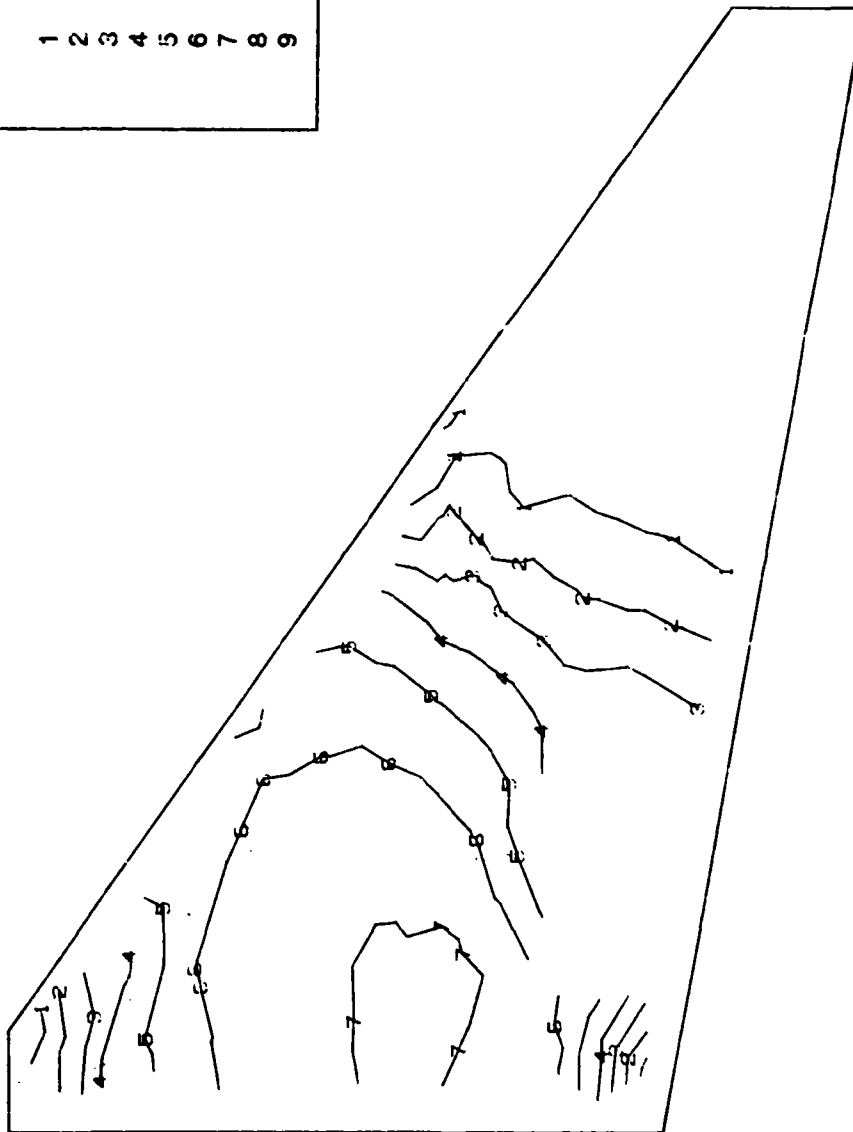|	
1	3,000
2	6,000
3	9,000
4	12,000
5	15,000
6	18,000
7	21,000
8	23,000
9	25,000

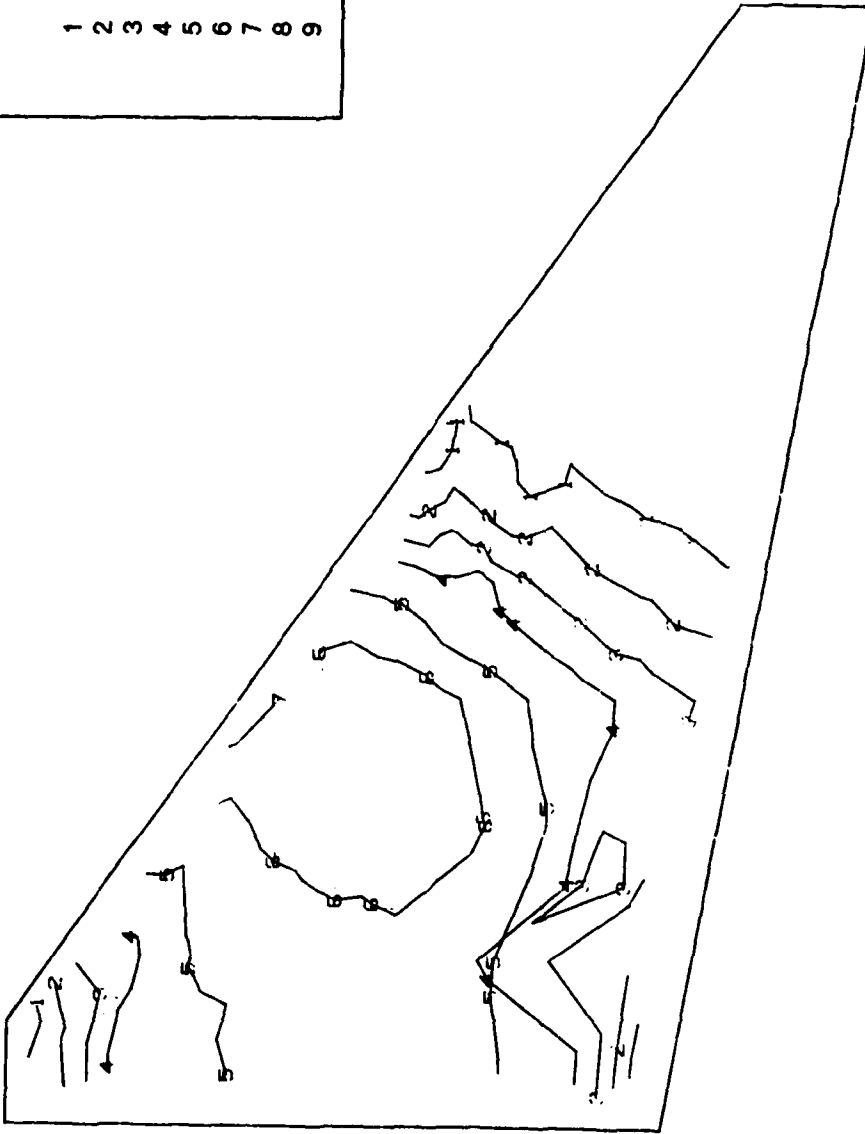Figure H-4. Stress Contours on Upper Wing Surface (Model DC-9)

CONTOUR SYMBOLS
PSI-Tension

1	3,000
2	6,000
3	9,000
4	12,000
5	15,000
6	17,000
7	19,000
8	21,000
9	23,000
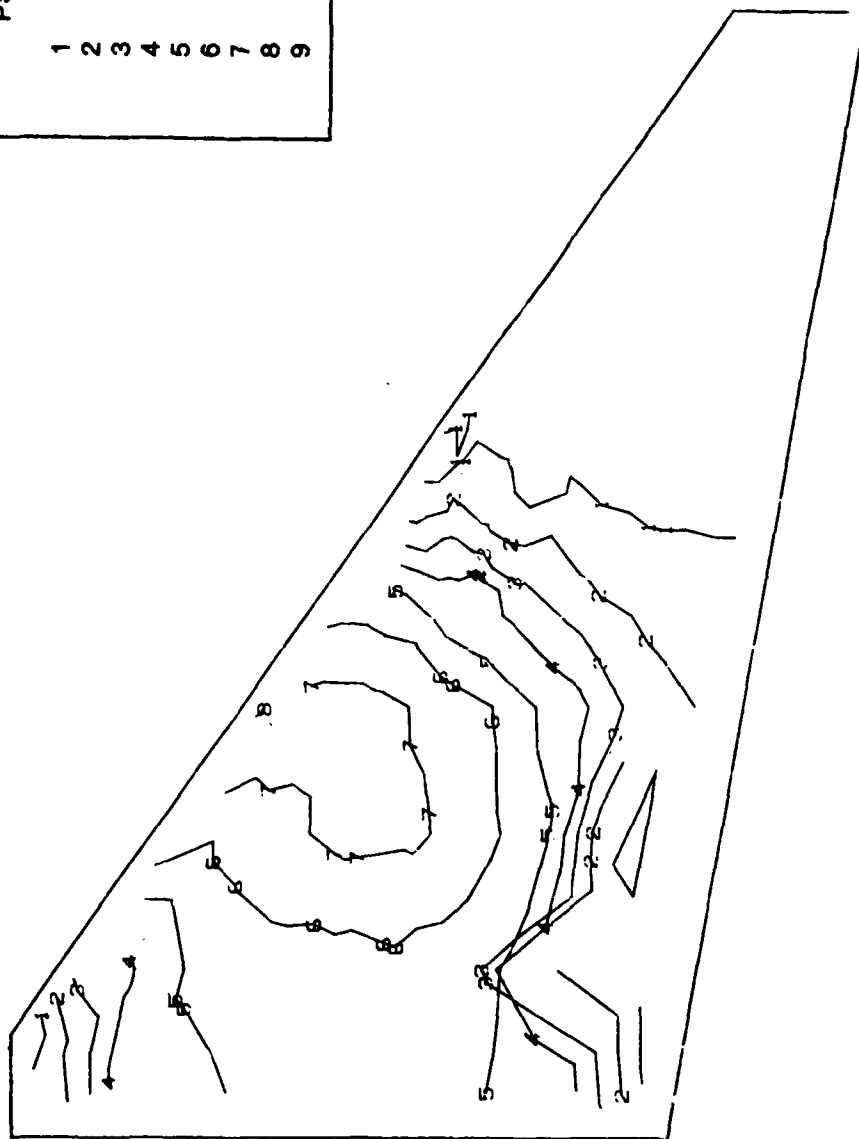
Figure H-5. Stress Contours on Lower Wing Surface (Model DC-9)
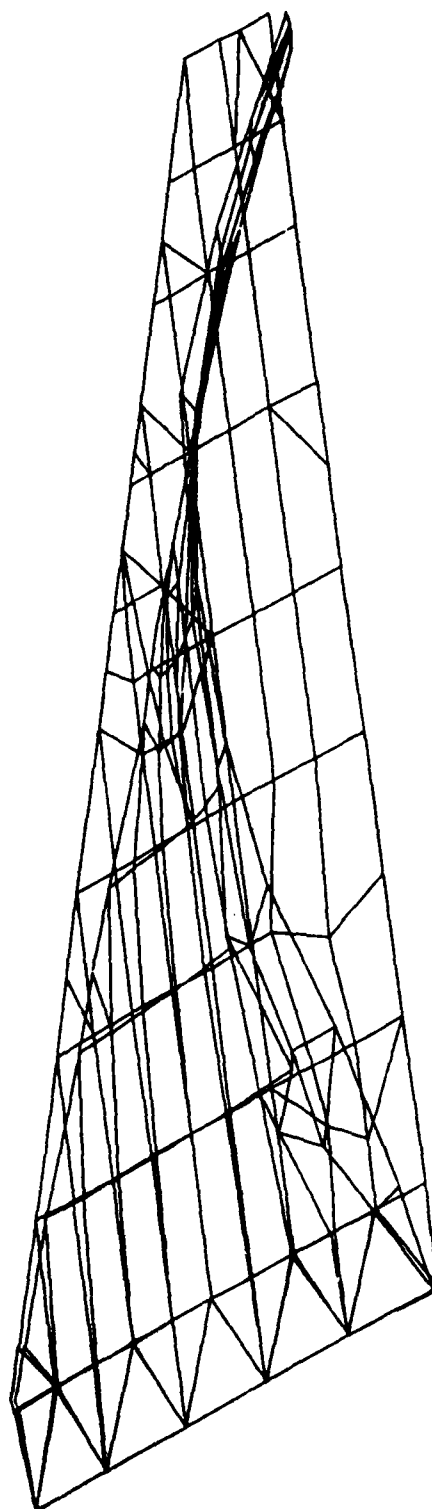
Symmetric Normal Modes for F-16 Wing Model DC-9

Givens Method   Mode 1   Frequency = 10.42 Hertz
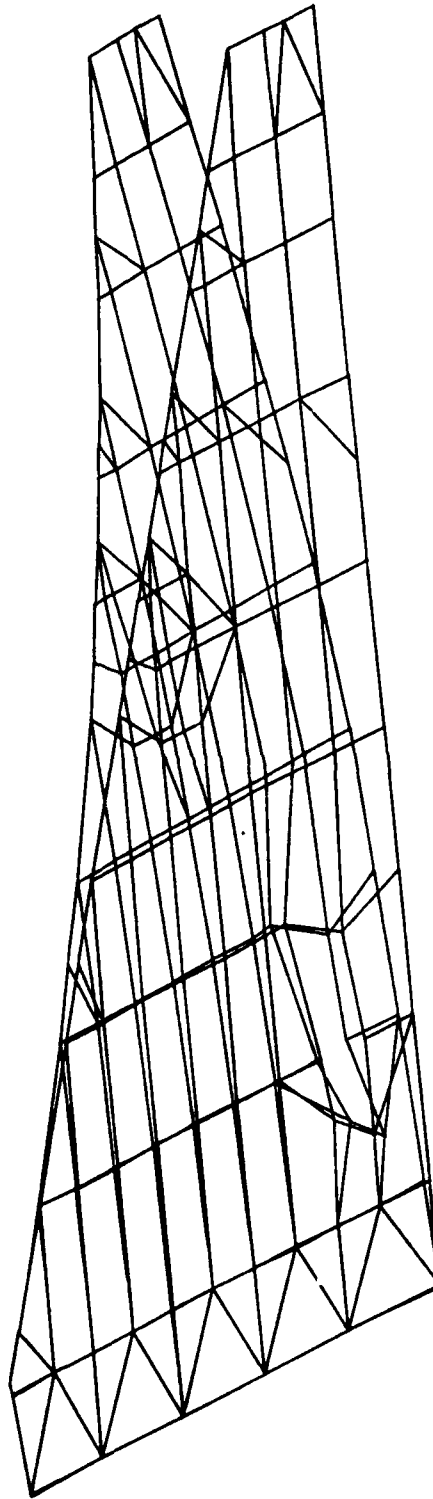
Figure H-6.   1st Wing Bending Mode (Model DC-9)

Symmetric Normal Modes for F-16 Wing Model DC-9

Givens Method   Mode 2   Frequency = 31.60 Hertz

Figure H-7.   2nd Wing Bending Mode (Model DC-9)

Symmetric Normal Modes for F-16 Wing Model DC-9

Givens Method   Mode 3   Frequency = 35.02 Hertz

Figure H-8. 1st Torsional Mode (Model DC-9)

Symmetric Normal Modes for F-16 Wing Model DC-9

Givens Method   Mode 4   Frequency = 48.06 Hertz
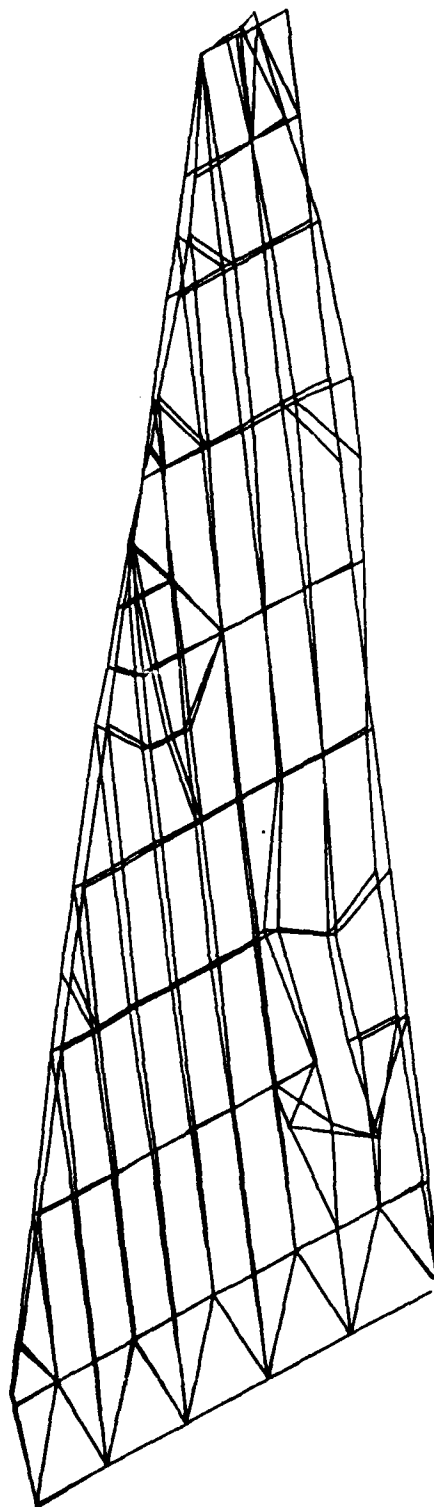
Figure H-9.   2nd Torsional Mode (Model DC-9)
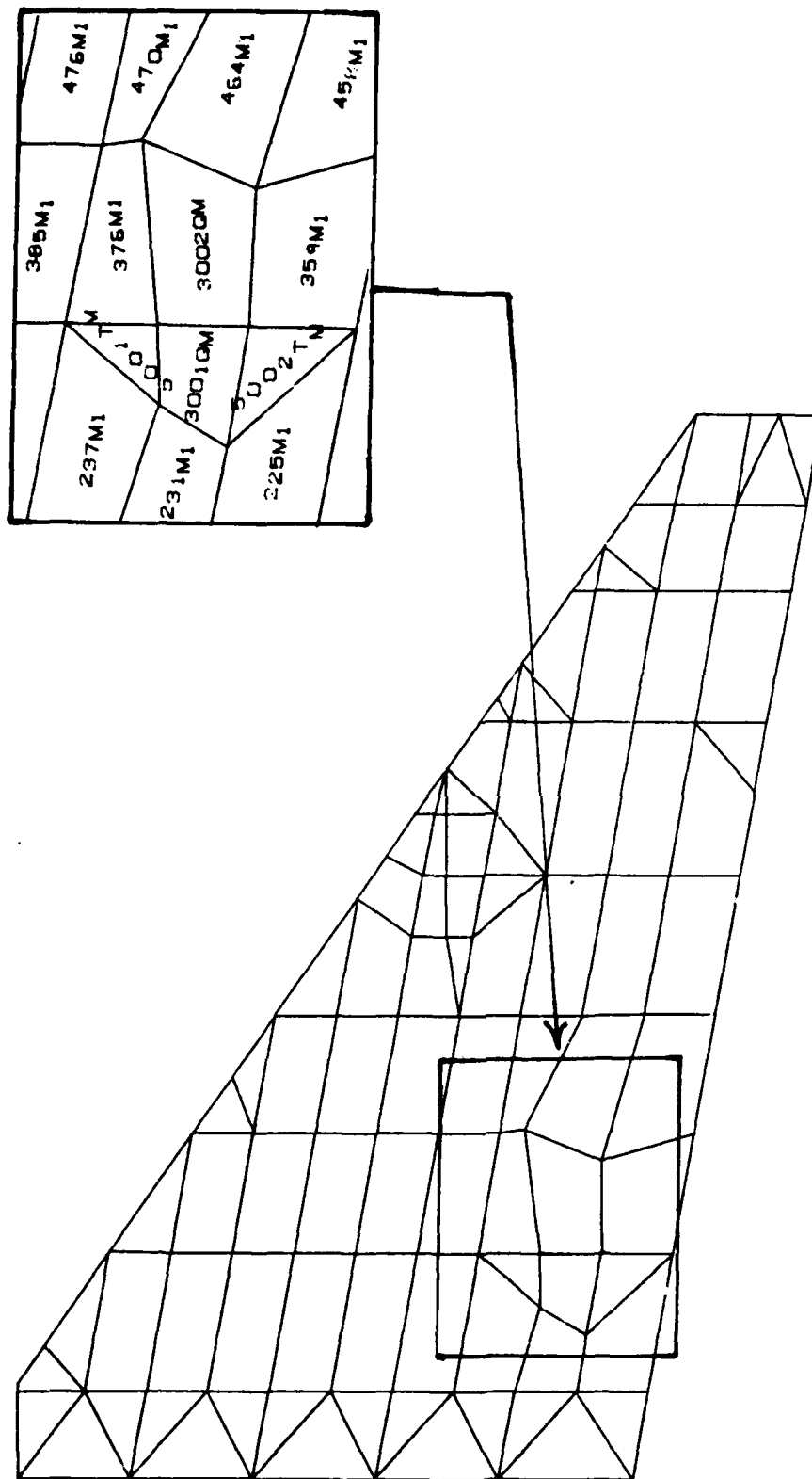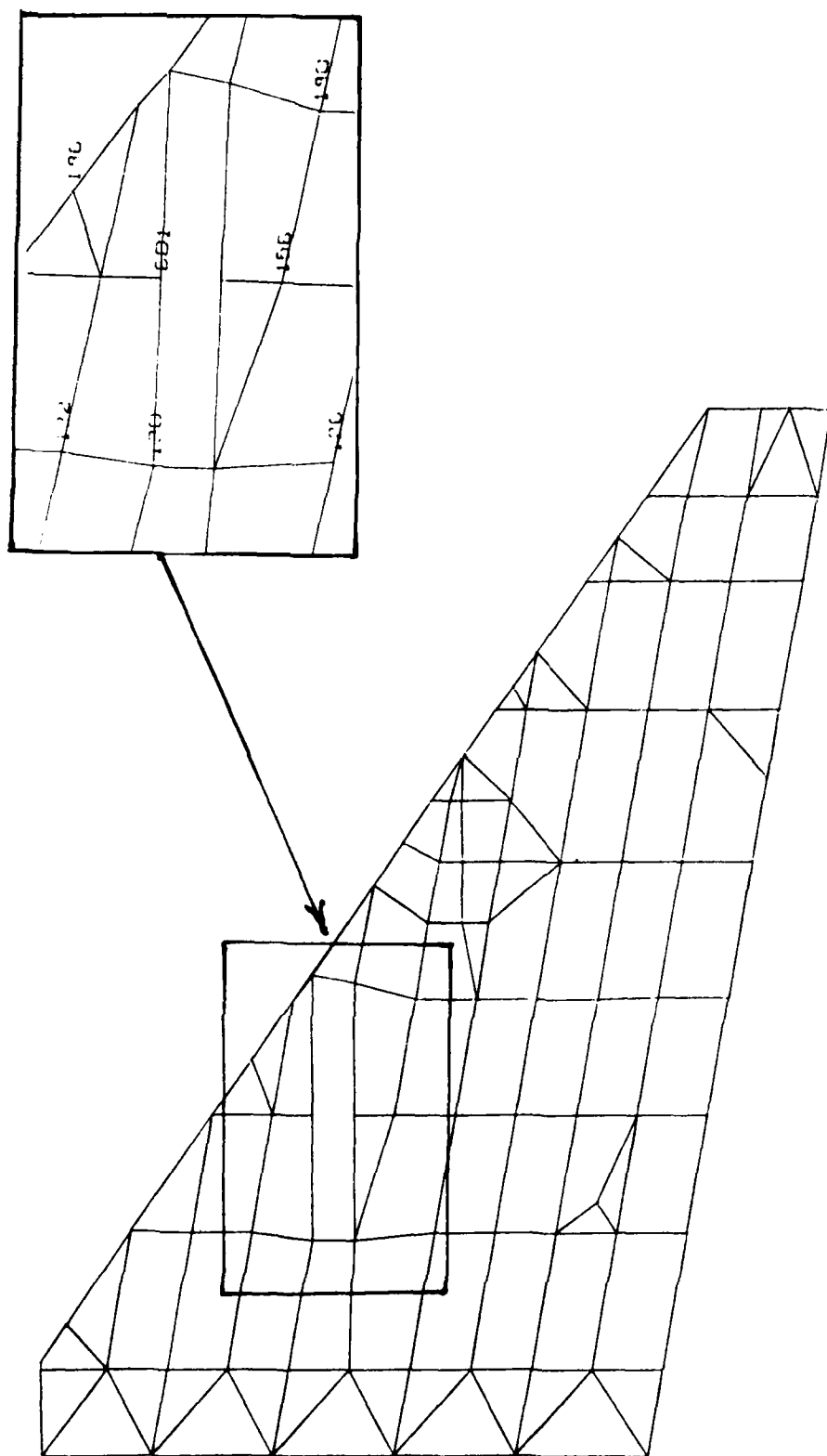
Figure H-10. Upper Wing Surface (Model DC-9R)
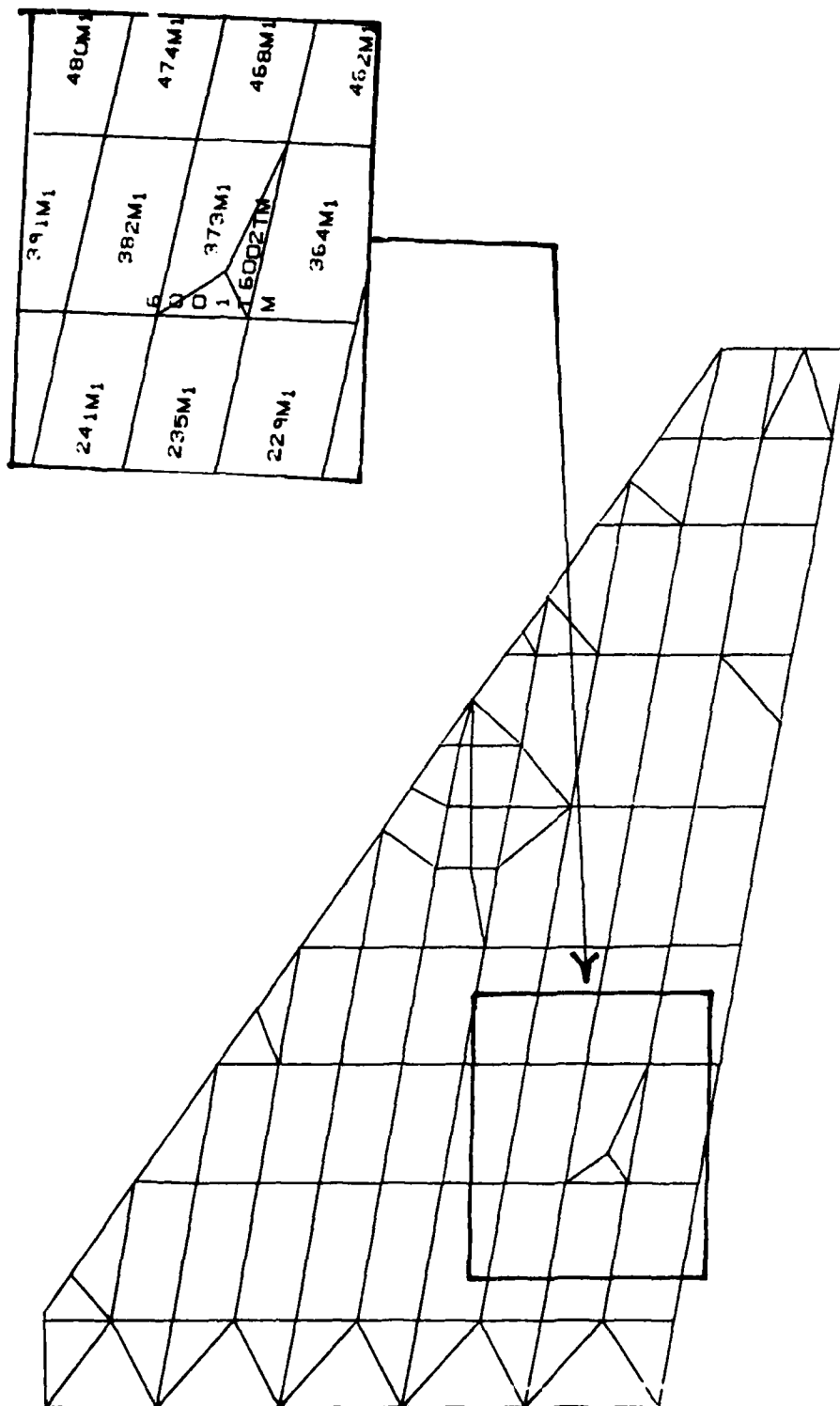
Figure H-11. Lower Wing Surface (Model DC-9R)

Figure H-12. Stress Contours on Upper Wing Surface (Model DC-9R)

CONTOUR SYMBOLS
PSI–Compression

1	3,000
2	6,000
3	9,000
4	12,000
5	15,000
6	18,000
7	21,000
8	23,000
9	25,000

Figure H-13. Stress Contours on Lower Wing Surface (Model DC-9R)

CONTOUR SYMBOLS
PSI-Tension

1	3,000
2	6,000
3	9,000
4	12,000
5	15,000
6	17,000
7	19,000
8	21,000
9	23,000

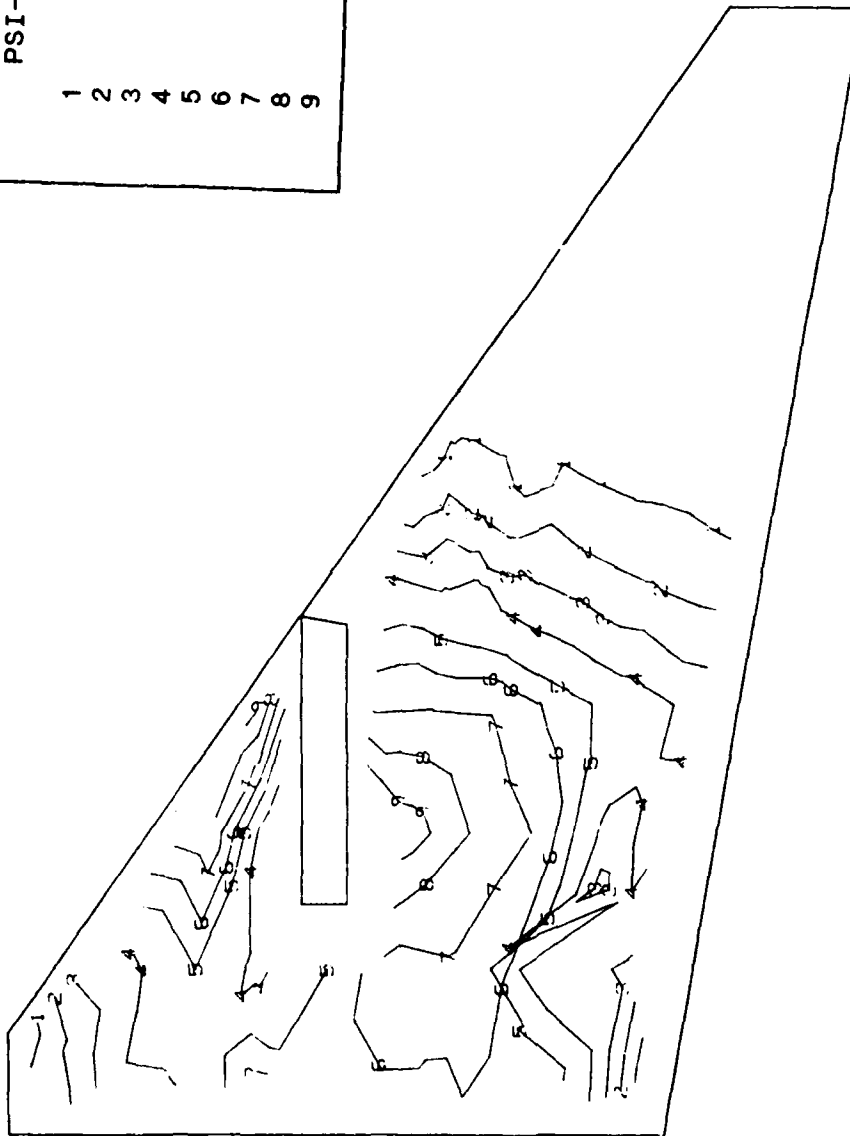Symmetric Normal Modes for F-16 Wing Model DC-9R

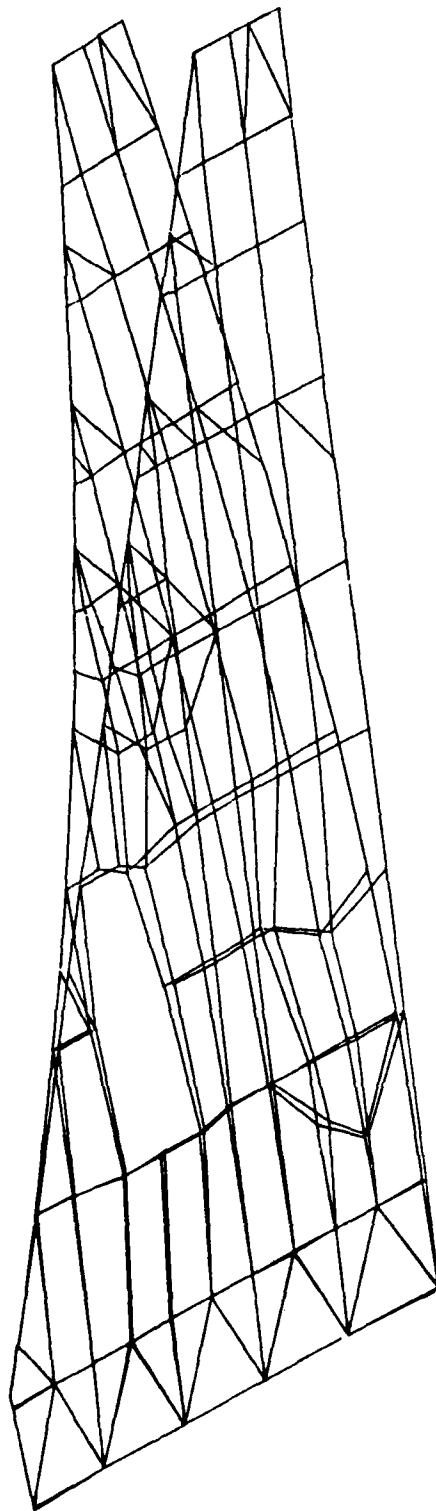Givens Method   Mode 1   Frequency = 10.70 Hertz
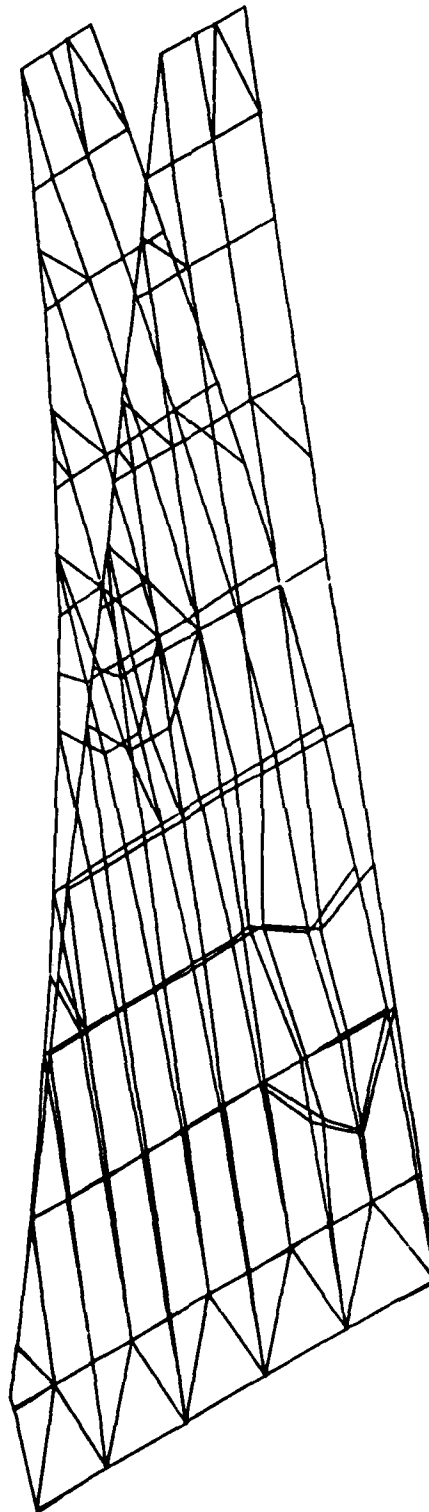
Figure H-14.   1st Wing Bending Mode (Model DC-9R)

Symmetric Normal Modes for F-16 Wing Model DC-9R

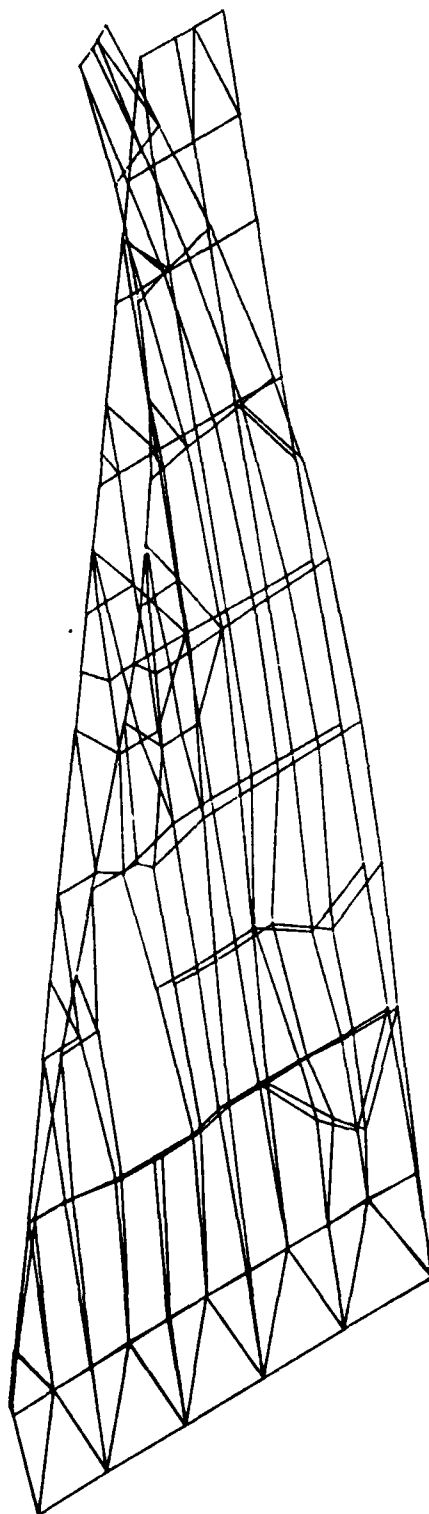Givens Method   Mode 2   Frequency = 35.06 Hertz
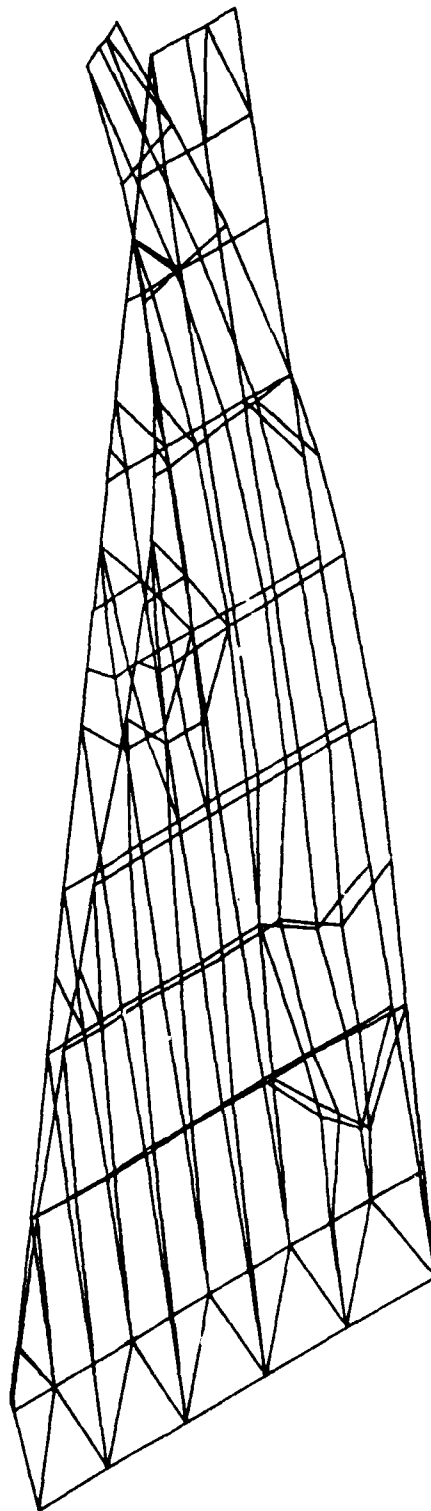
Figure H-15.   2nd Wing Bending Mode ((Model DC-9R)

Symmetric Normal Modes for F-16 Wing Model DC-9R

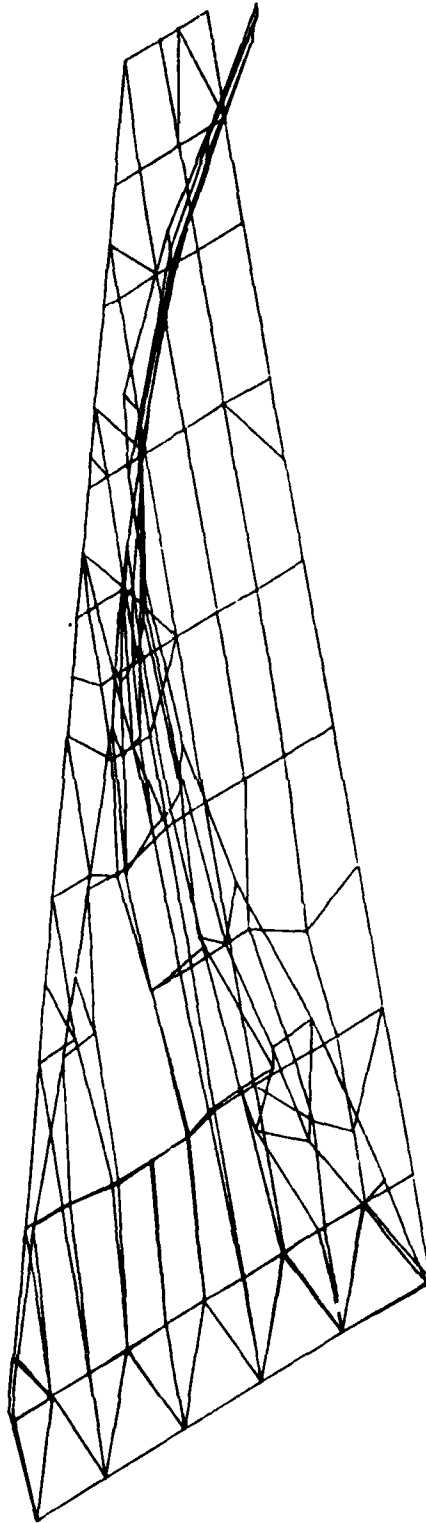Givens Method   Mode 3   Frequency = 45.67 Hertz

Figure H-16.   1st Torsional Mode (Model DC-9R)

H-17

Symmetric Normal Modes for F-16 Wing Model DC-9R

Givens Method   Mode 4   Frequency = 65.79 Hertz
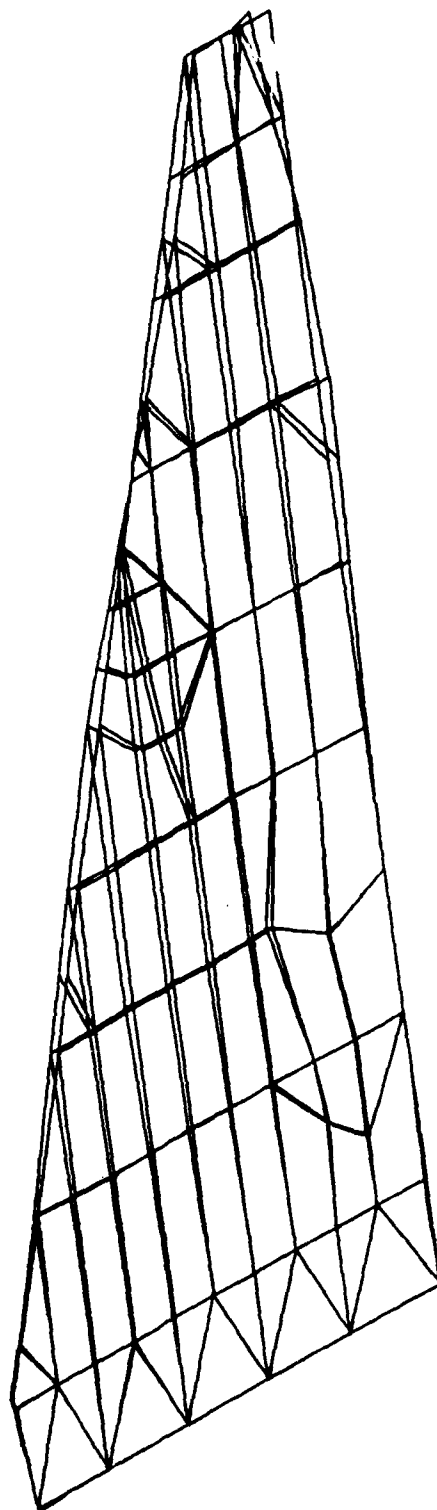
Figure H-17. 2nd Torsional Mode (Model DC-9R)

APPENDIX I

ANALYSIS OF DAMAGE CASE #12

Figure I-1. Summary of Damage Case #12 Results
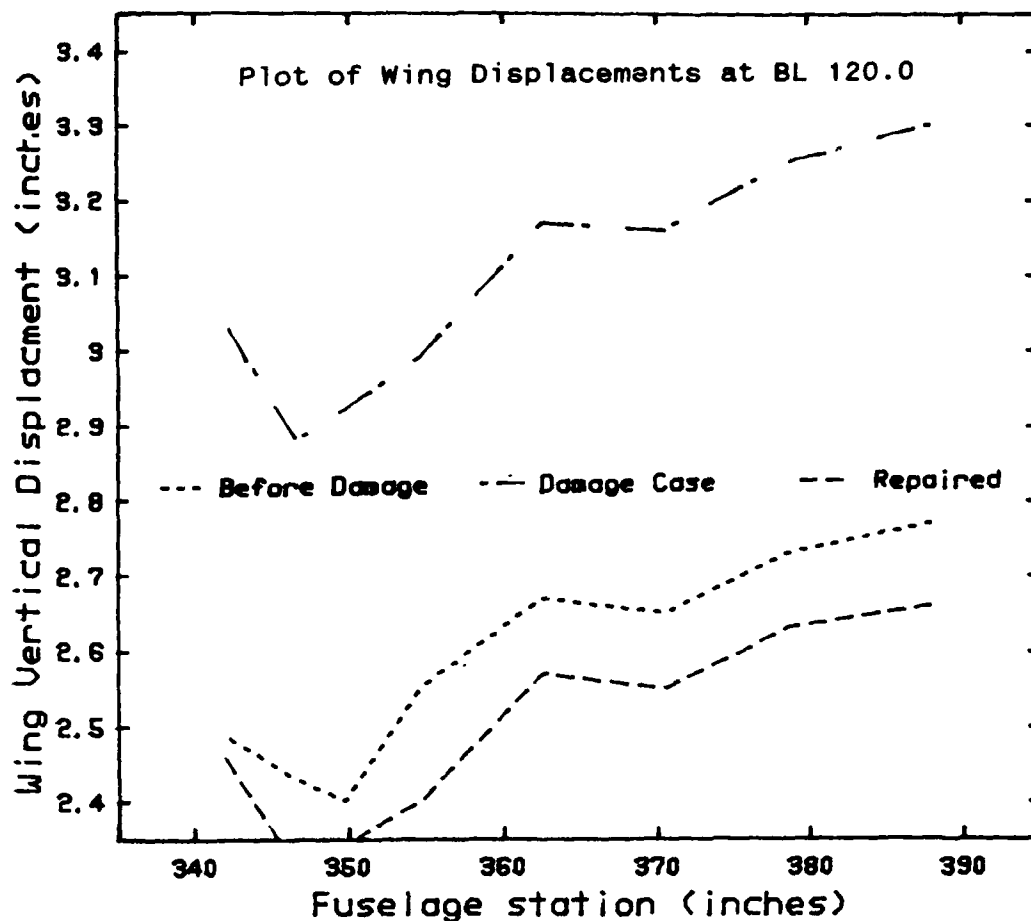
Tabulated Displacements

Fuselage St.	387.9	378.6	370.6	362.6	354.6	349.7	346.6	341.9
Model DC-9R	2.77	2.73	2.65	2.67	2.55	2.40	2.43	2.49
Model DC-12	3.30	3.25	3.16	3.17	2.99	2.92	2.88	3.04
Model DC-12R	2.66	2.63	2.55	2.57	2.40	2.34	2.31	2.46

Comparison of Residual Strength

	Av Disp	% Change	Torsion mode	% Change
Model DC-9	2.59		45.67	
Model DC-12	3.09	-19.3	43.87	-3.9
Model DC-9R	2.59	+23.2	45.54	+3.7
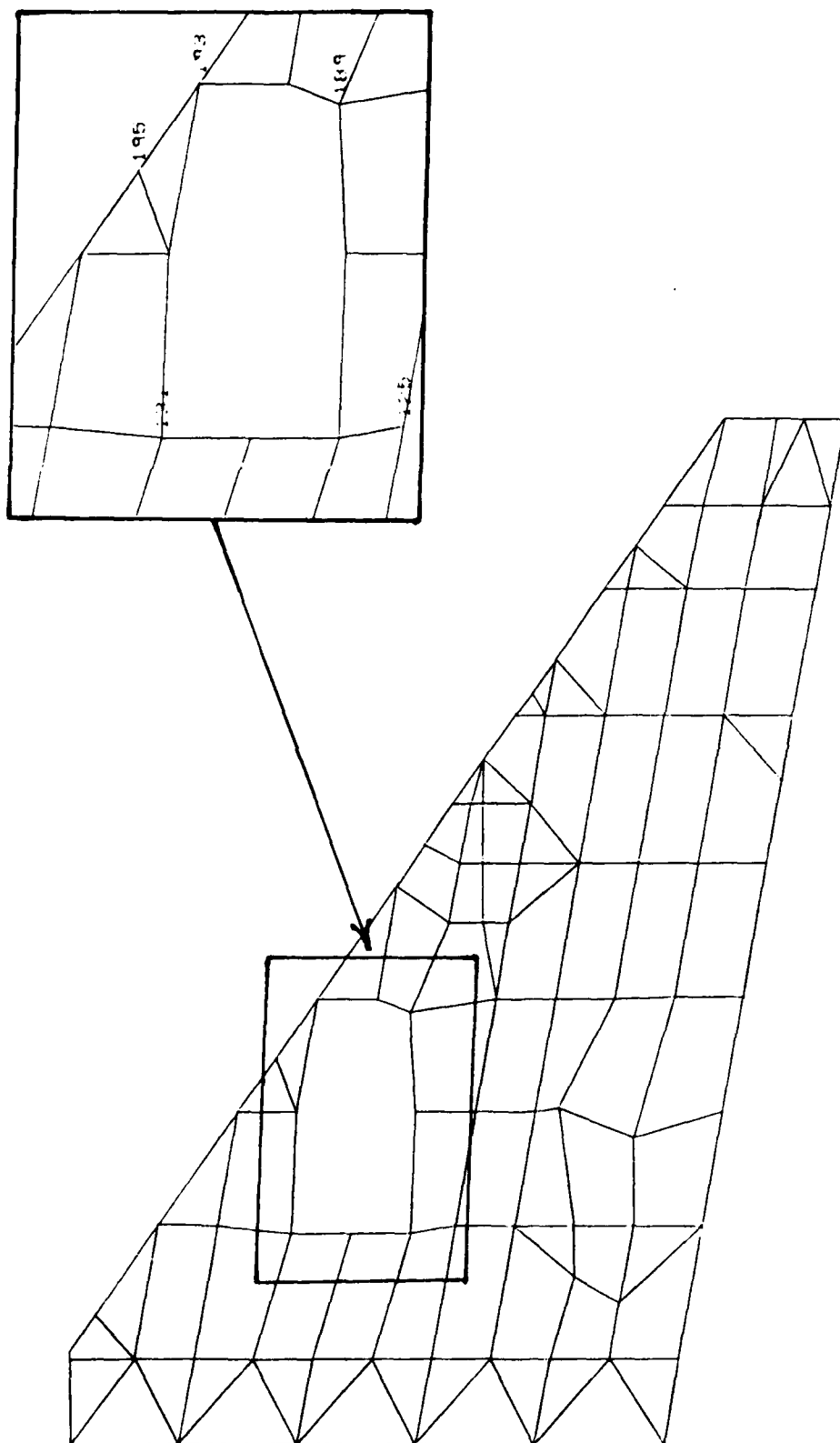
Figure I-2. Upper Wing Surface (Model DC-12)

Figure I-3. Lower Wing Surface (Model DC-12)

CONTOUR SYMBOLS
PSI-Compression

|	
1	3,000
2	6,000
3	9,000
4	12,000
5	15,000
6	18,000
7	21,000
8	23,000
9	25,000
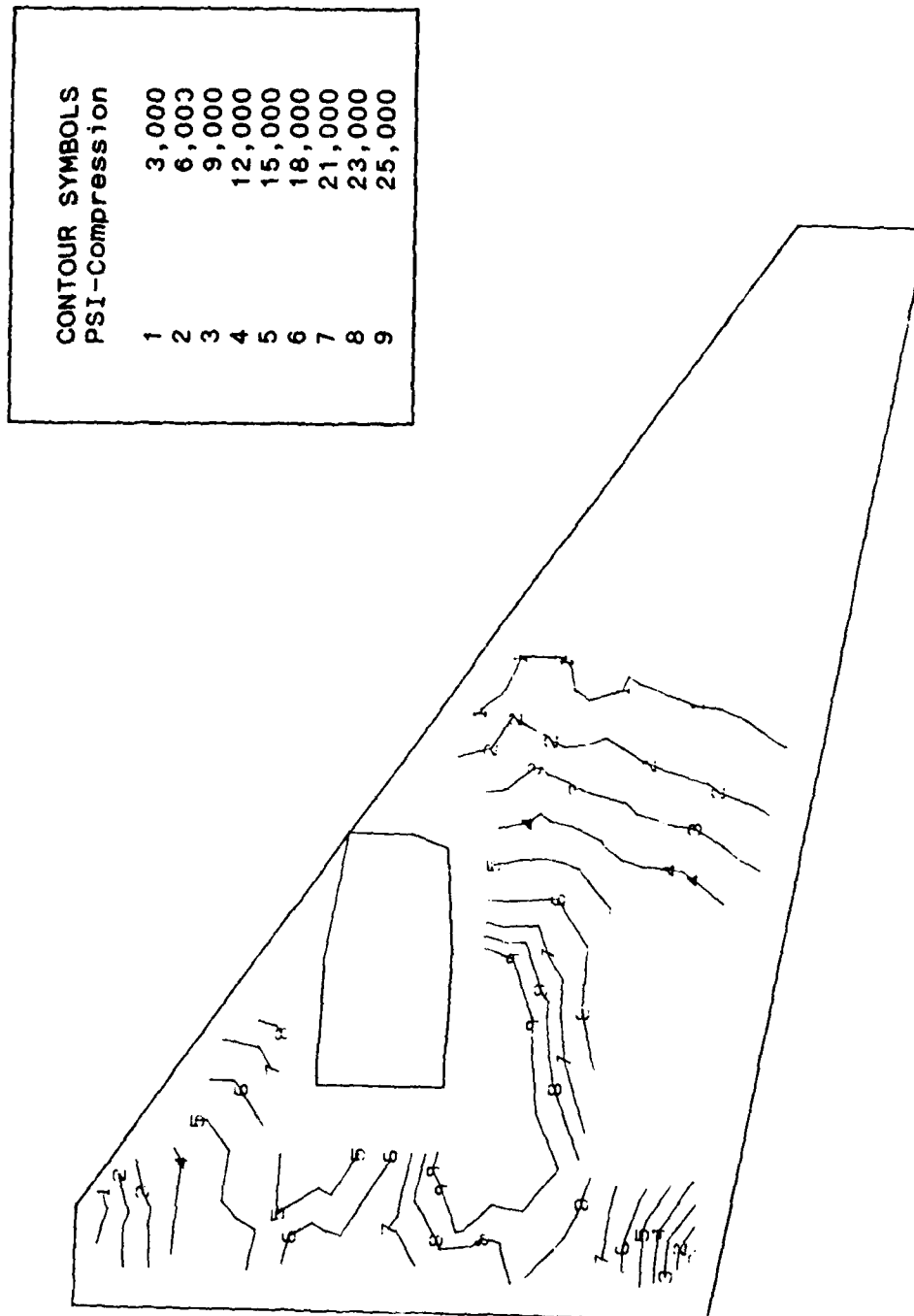
Figure I-4.   Stress Contours on Upper Wing Surface (Model DC-12)

CONTOUR SYMBOLS
PSI-Tension

1	3,000
2	6,000
3	9,000
4	12,000
5	15,000
6	17,000
7	19,000
8	21,000
9	23,000

Figure I-5. Stress Contours on Lower Wing Surface (Model DC-12)

Figure I-6. 1st Wing Bending Mode (Model DC-12)

Symmetric Normal Modes for F-16 Wing Model DC-12

Givens Method   Mode 1   Frequency = 9.88 Hertz

Symmetric Normal Modes for F-16 Wing Model DC-12

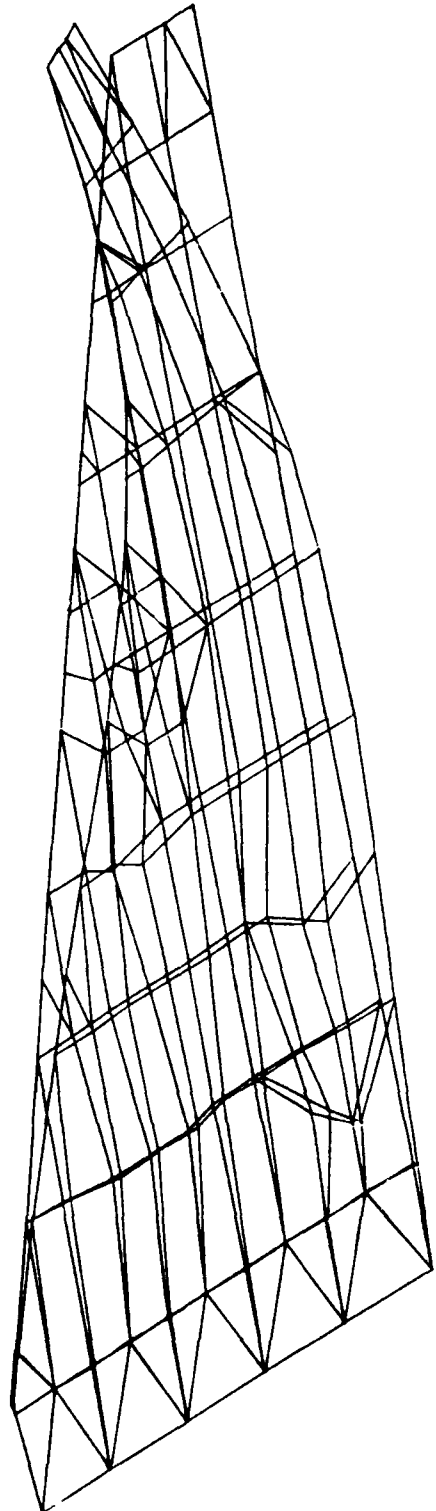Givens Method   Mode 2   Frequency = 34.14 Hertz

Figure I-7.   2nd Wing Bending Mode (Model DC-12)

Symmetric Normal Modes for F-16 Wing Model DC-12

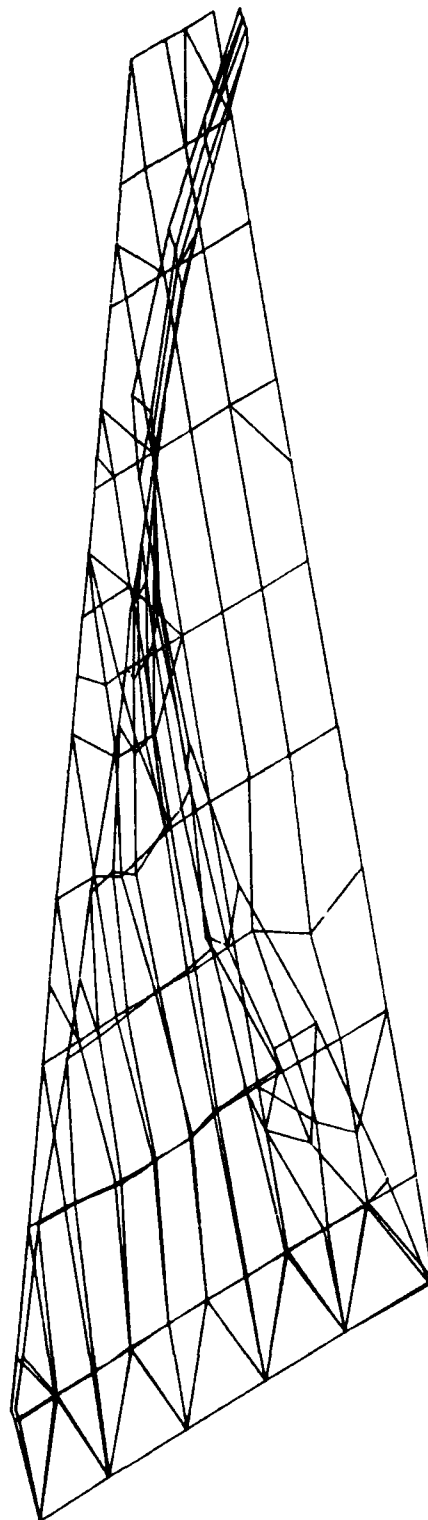Givens Method   Mode 3   Frequency = 43.87 Hertz

Figure I-8.   1st Torsional Mode (Model DC-12)

Symmetric Normal Modes for F-16 Wing Model DC-12

Givens Method   Mode 4   Frequency = 66.29 Hertz
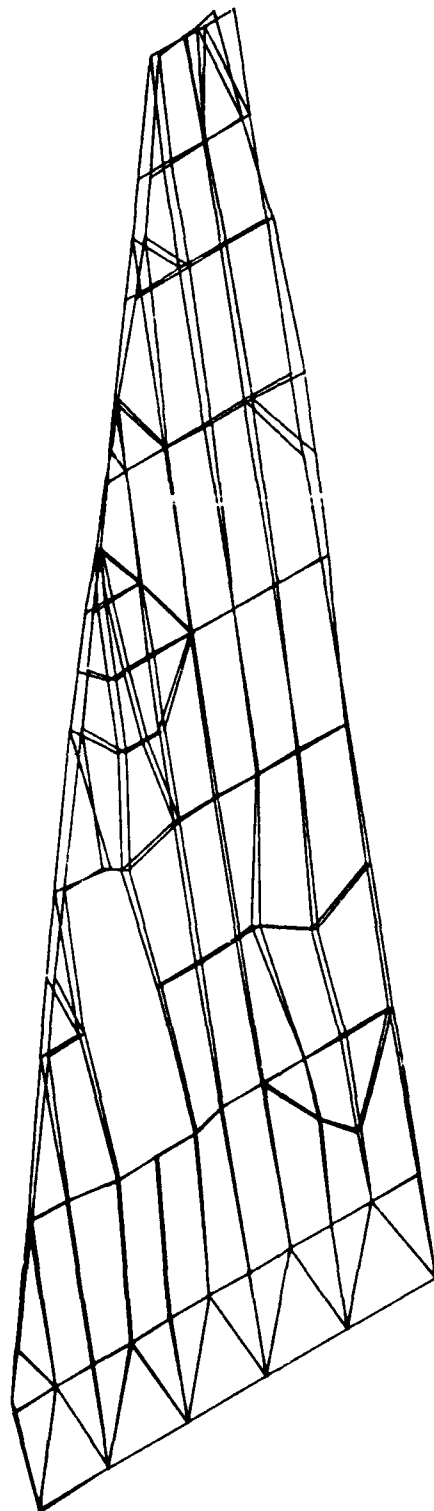
Figure I-9.   2nd Torsional Mode (Model DC-12)
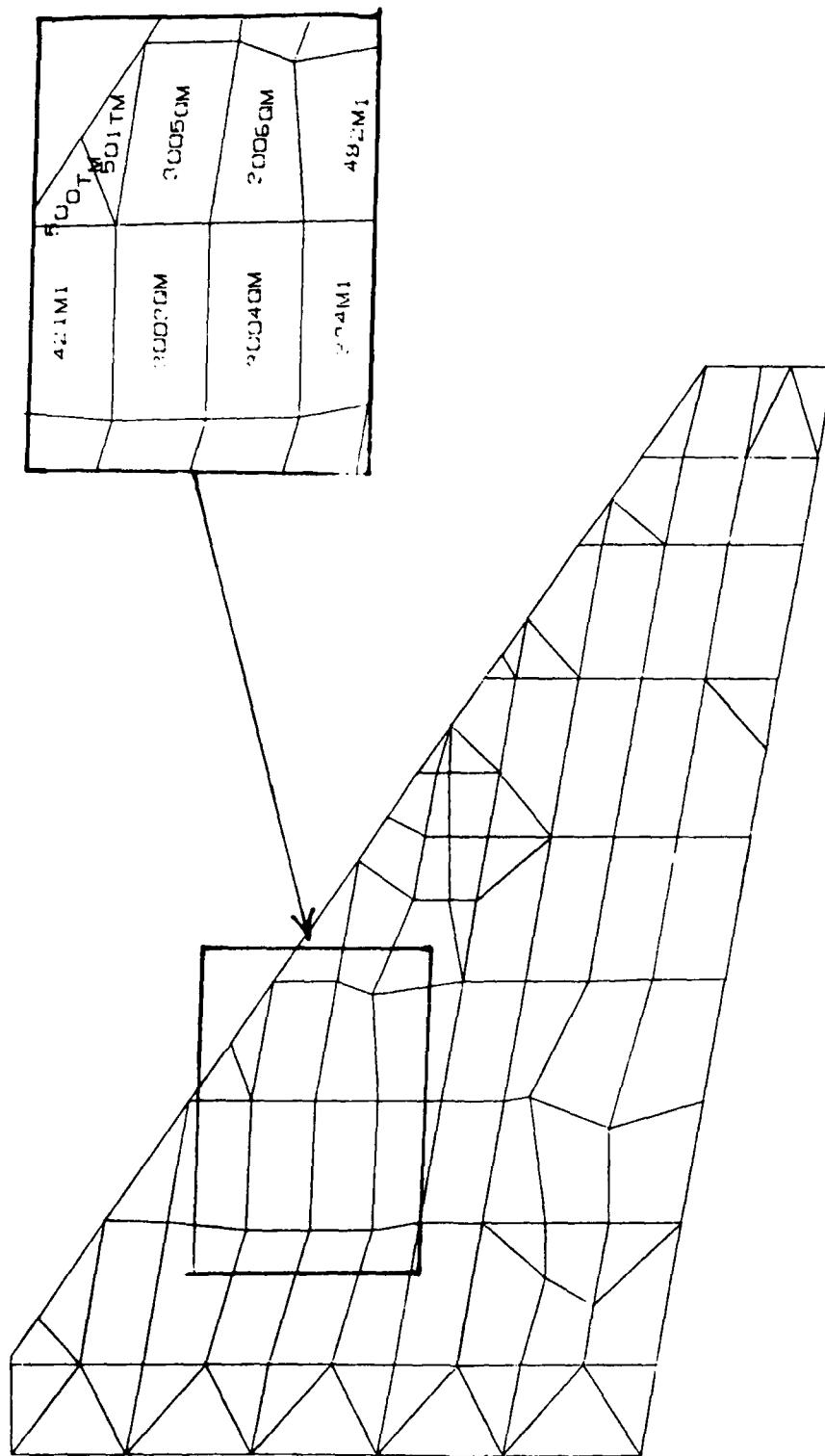
Figure I-10. Upper Wing Surface (Model DC-12R)

Figure I-11. Lower Wing Surface (Model DC-12R)

CONTOUR SYMBOLS
PSI-Compression

1	3,000
2	6,000
3	9,000
4	12,000
5	15,000
6	18,000
7	21,000
8	23,000
9	25,000
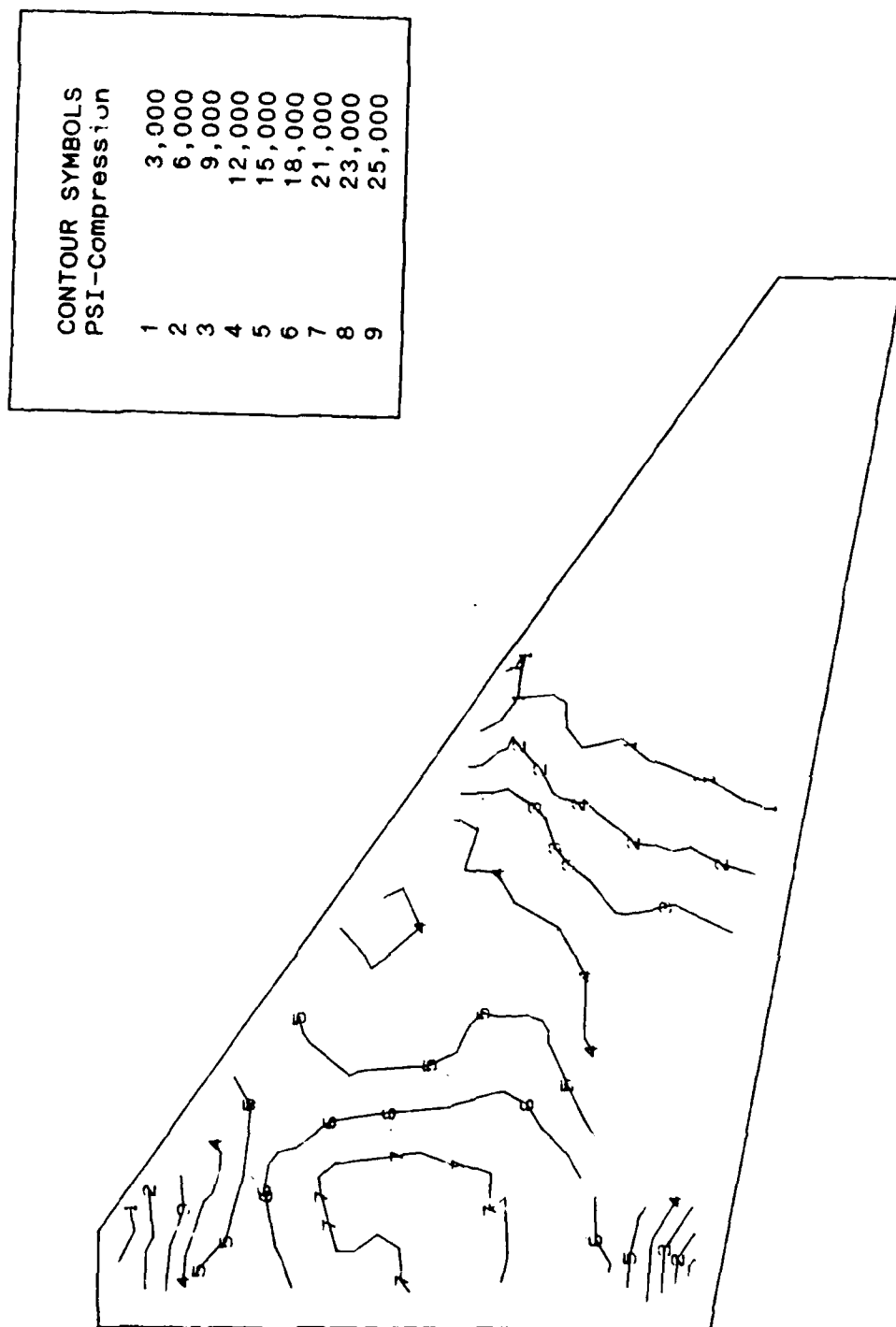
Figure I-12. Stress Contours on Upper Wing Surface (Model DC-12R)

I-13

CONTOUR SYMBOLS
PSI-Tension

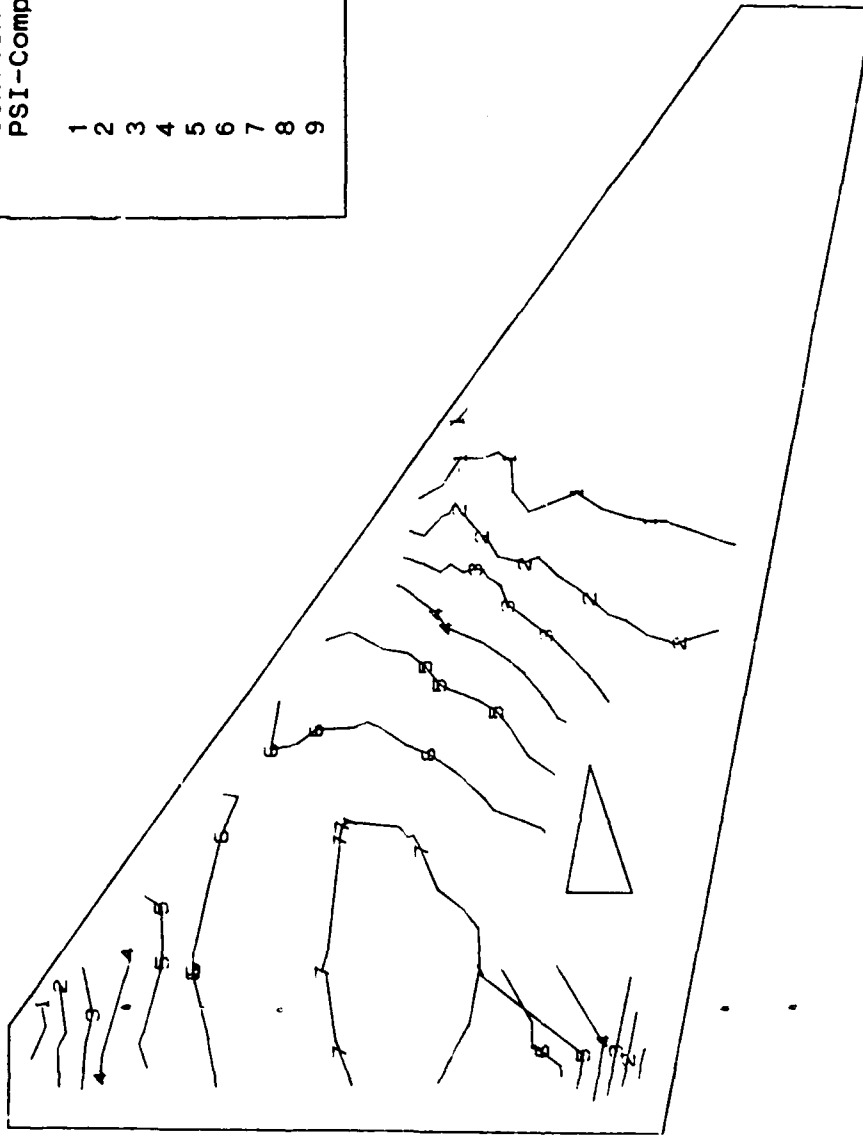|	
1	3,000
2	6,000
3	9,000
4	12,000
5	15,000
6	17,000
7	19,000
8	21,000
9	23,000
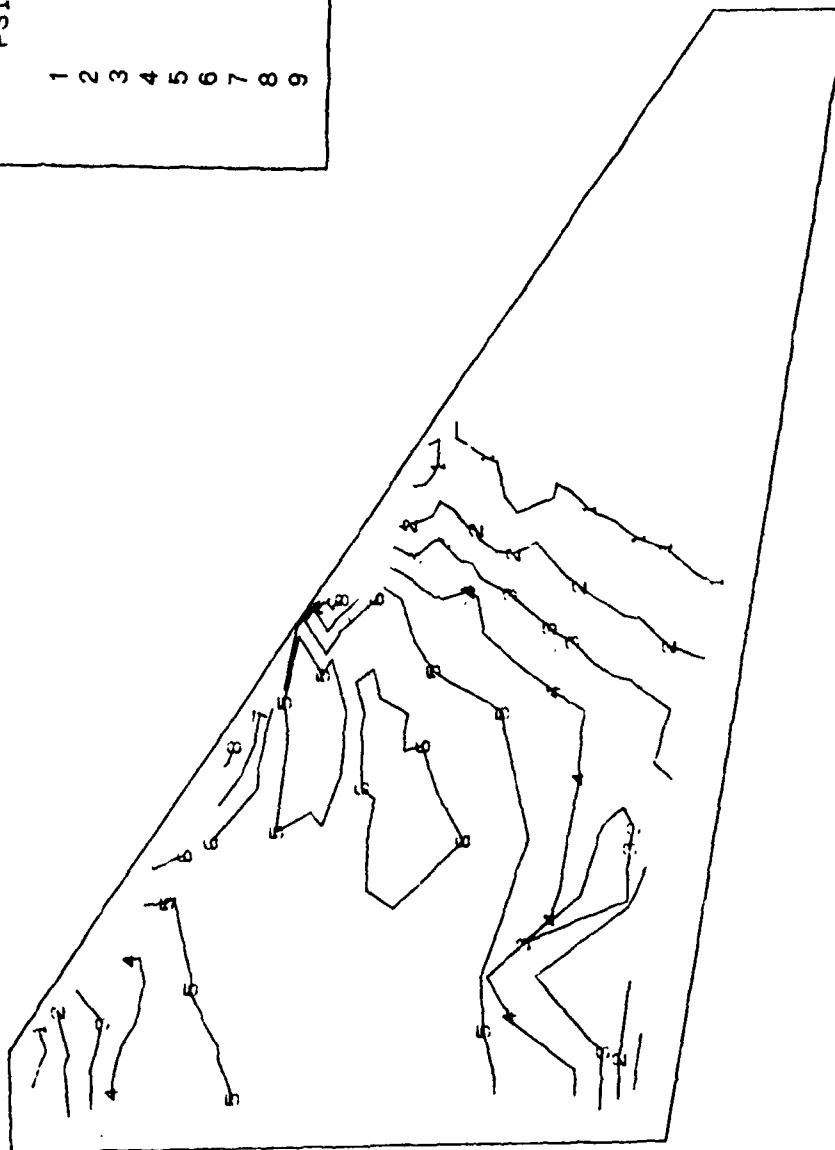
Figure I-13. Stress Contours on Lower Wing Surface (Model DC-12R)

Symmetric Normal Modes for F-16 Wing Model DC-12R

Givens Method   Mode 1   Frequency = 10.86 Hertz
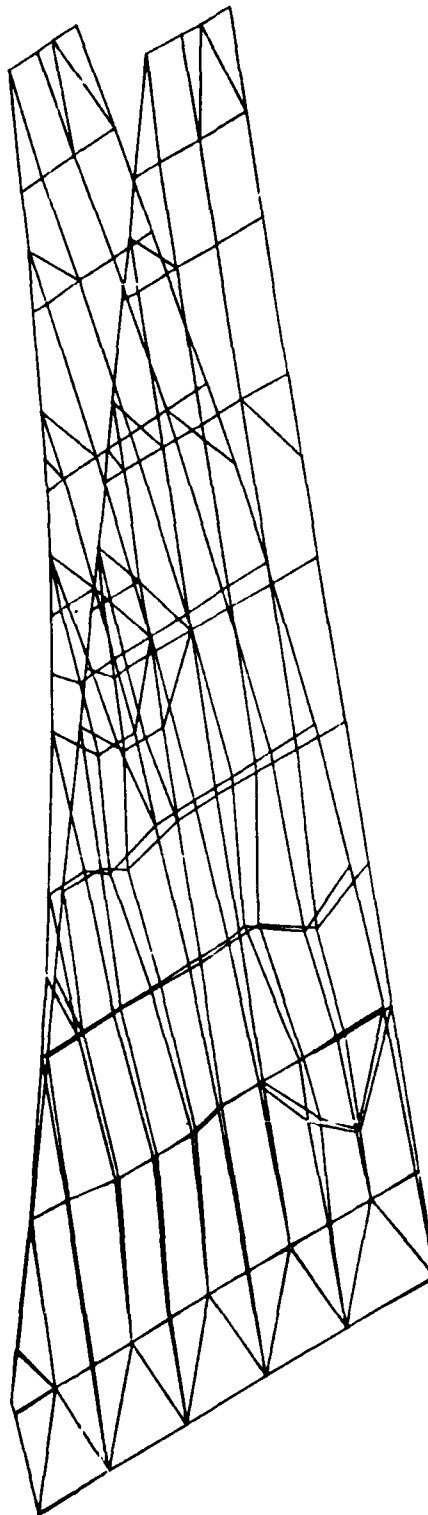
Figure I-14. 1st Wing Bending Mode (Model DC-12R)

Symmetric Normal Modes for F-16 Wing Model DC-12R

Givens Method Mode 2 Frequency = 34.87 Hertz

Figure I-15. 2nd Wing Bending Mode (Model DC-12R)

Symmetric Normal Modes for F-16 Wing Model DC-12R
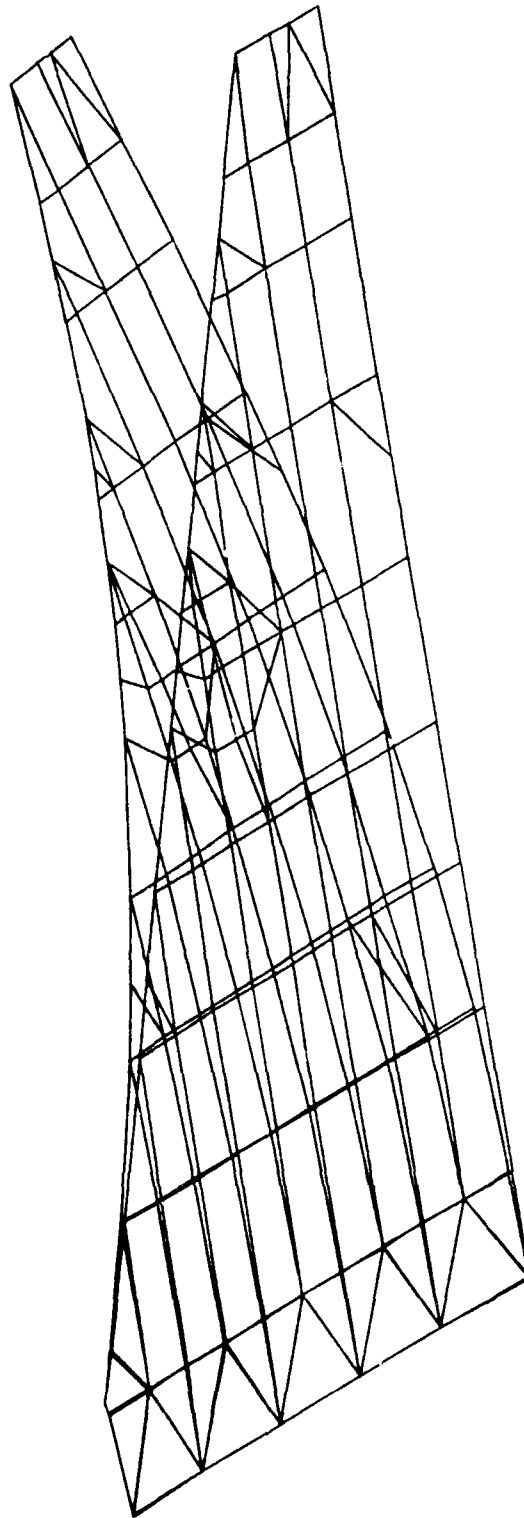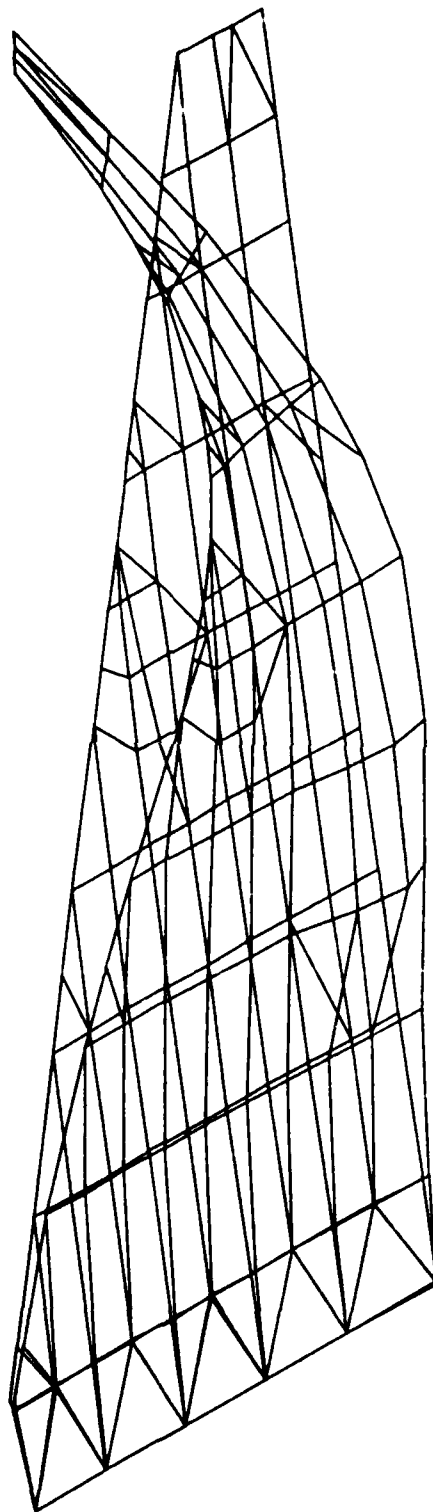
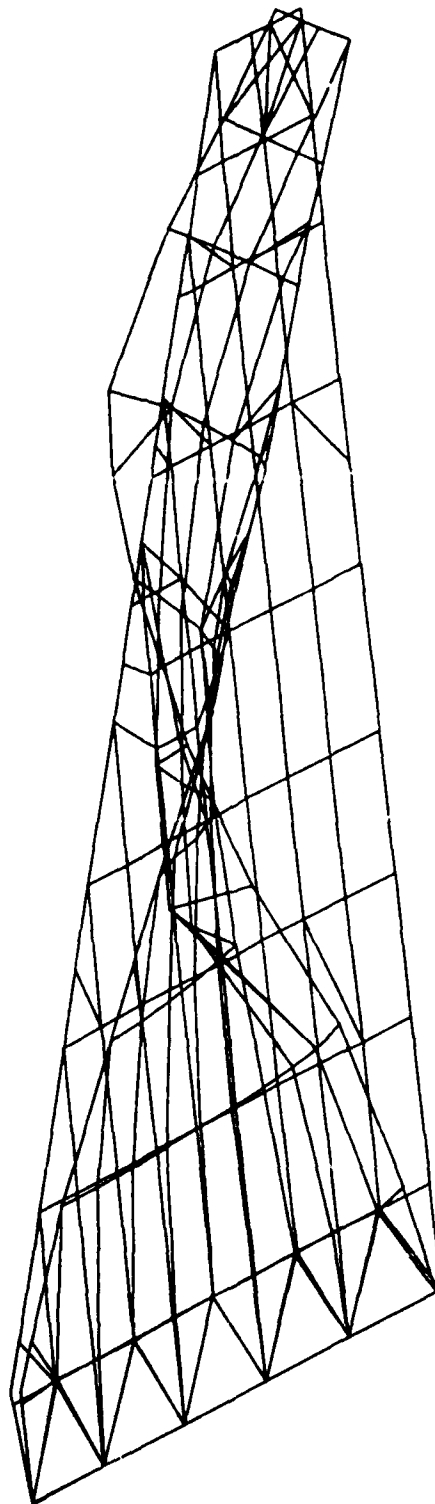Givens Method   Mode 3   Frequency = 45.54 Hertz

Figure I-16.   1st Torsional Mode (Model DC-12R)

Symmetric Normal Modes for F-16 Wing Model DC-12R

Givens Method   Mode 4   Frequency = 65.37 Hertz
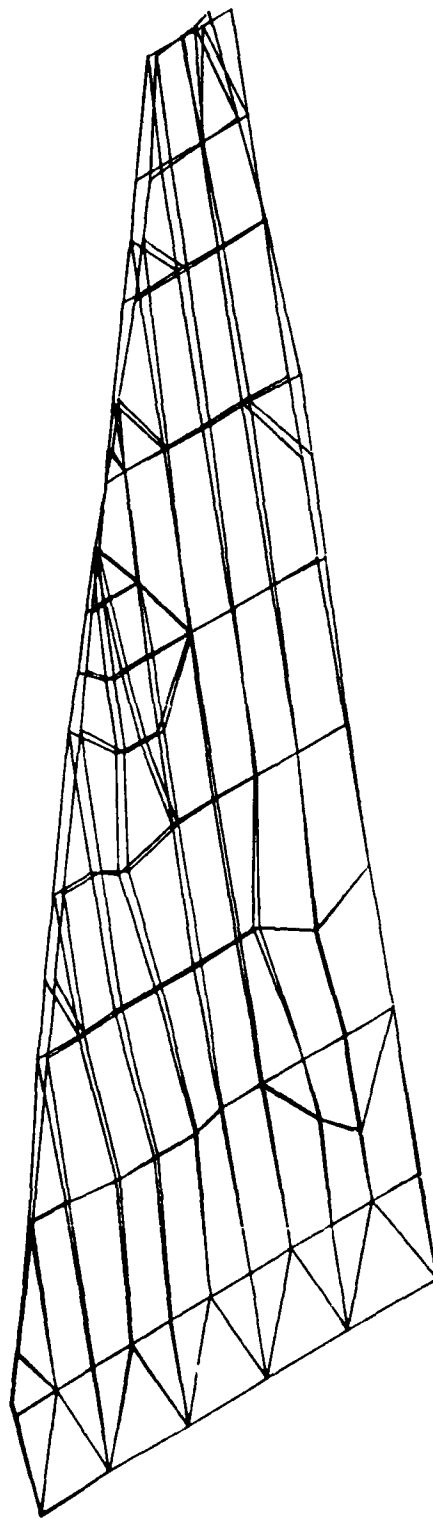
Figure I-17.   2nd Torsional Mode (Model DC-12R)

APPENDIX J

ANALYSIS OF DAMAGE CASE #15
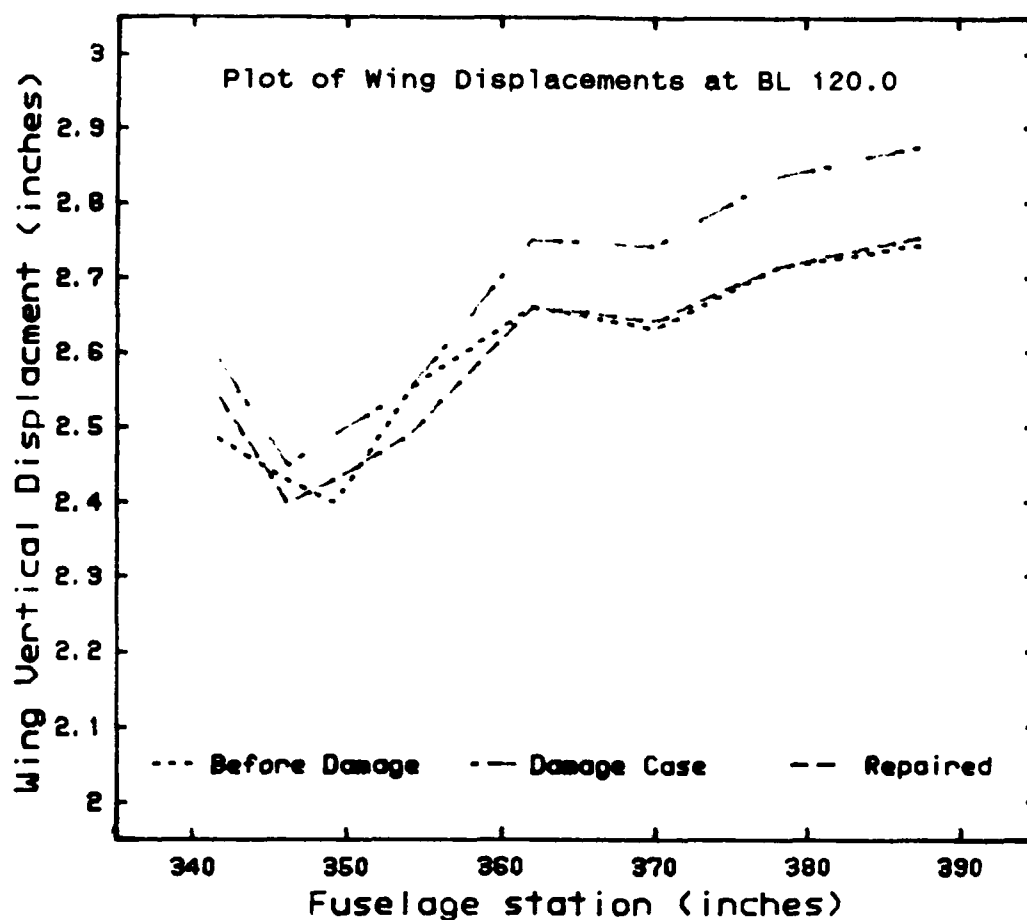
Plot of Wing Displacements at BL 120.0

Tabulated Displacements

Fuselage St.	387.9	378.6	370.6	362.6	354.6	349.7	346.6	341.9
Model D-4	2.74	2.71	2.63	2.66	2.55	2.40	2.43	2.49
Model DC-15	2.87	2.83	2.74	2.75	2.55	2.49	2.45	2.60
Model DC-15R	2.75	2.71	2.64	2.66	2.49	2.43	2.40	2.55

Comparison of Residual Strength

	Av Disp	% Change	Torsion mode	% Change
Model D-4	2.58		48.15	
Model DC-15	2.66	-3.1	46.10	-4.3
Model DC-15	2.58	+3.1	48.12	+4.2

Figure J-1. Summary of Damage Case #15 Results
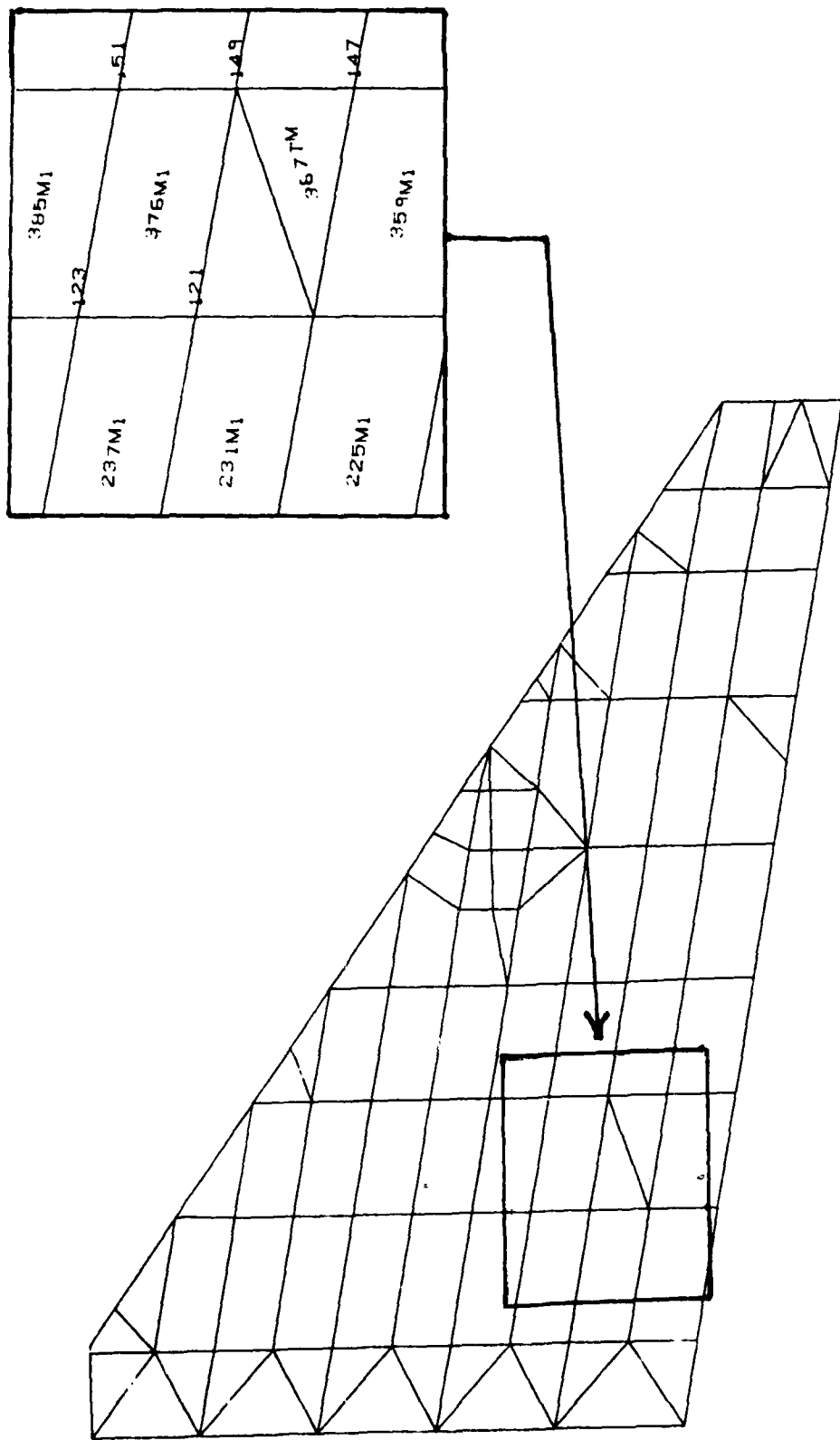
Figure J-2. Upper Wing Surface (Model DC-15)
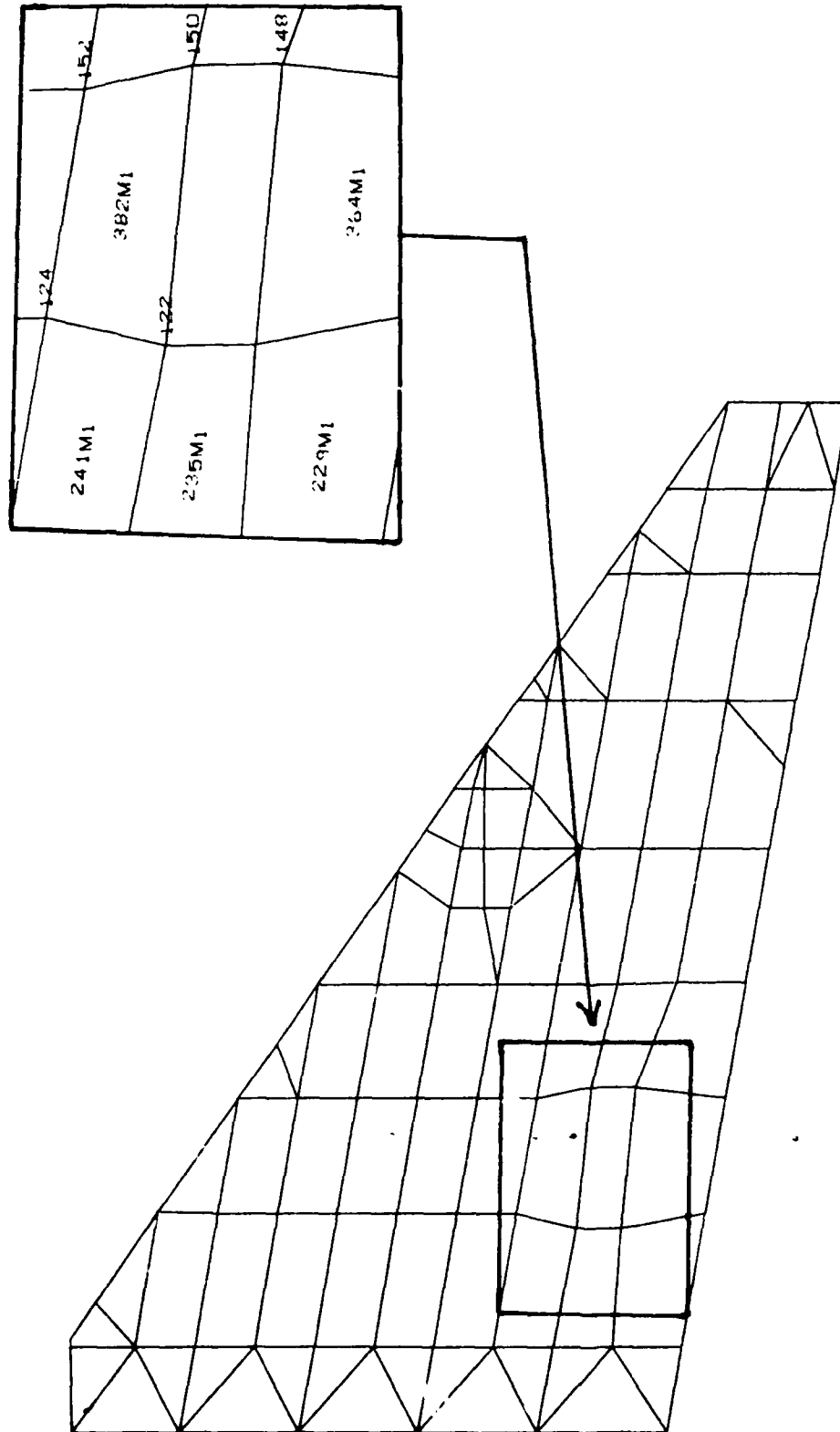
Figure J-3. Lower Wing Surface (Model DC-15)

CONTOUR SYMBOLS
PSI-Compression

1	3,000
2	6,000
3	9,000
4	12,000
5	15,000
6	18,000
7	21,000
8	23,000
9	25,000

Figure J-4. Stress Contours on Upper Wing Surface (Model DC-15)

CONTOUR SYMBOLS
PSI-Tension

1   3,000
2   6,000
3   9,000
4   12,000
5   15,000
6   17,000
7   19,000
8   21,000
9   23,000
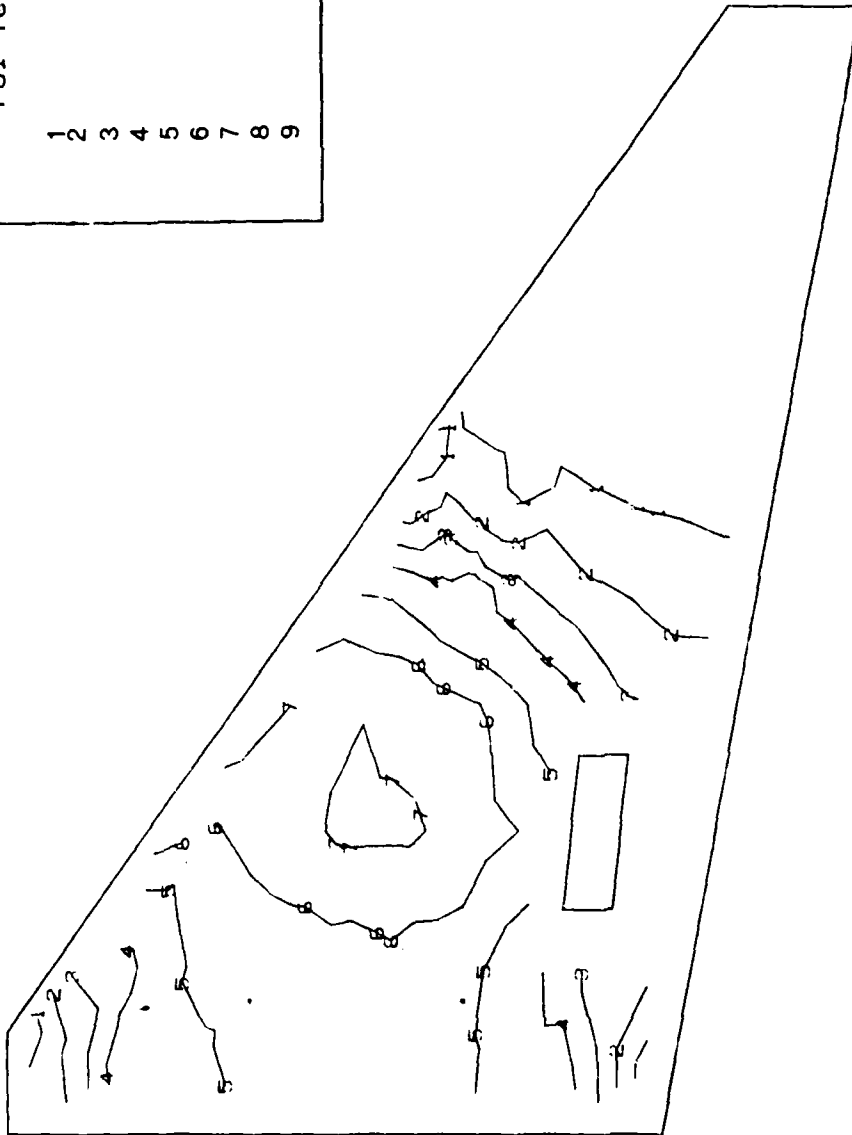
Figure J-5.   Stress Contours on Lower Wing Surface (Model DC-15)

Symmetric Normal Modes for F-16 Wing Model DC-15

Givens Method   Mode 1   Frequency = 10.82 Hertz

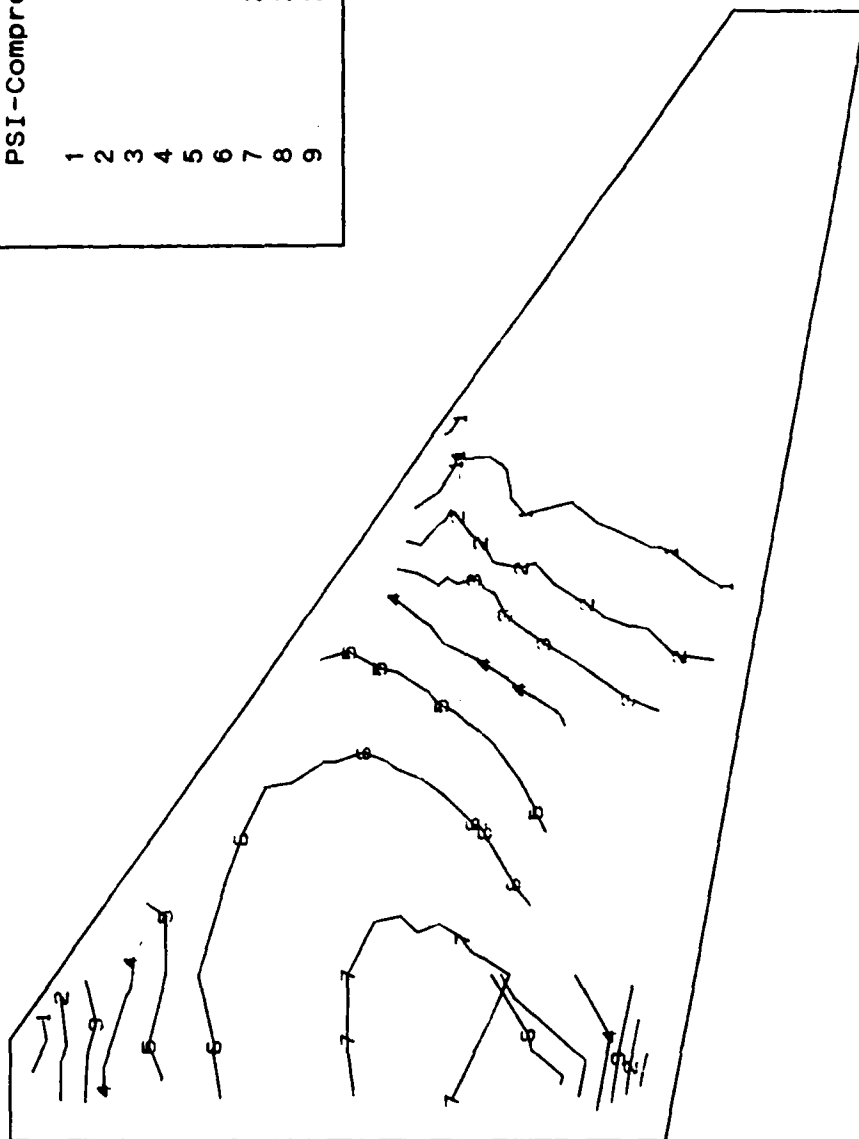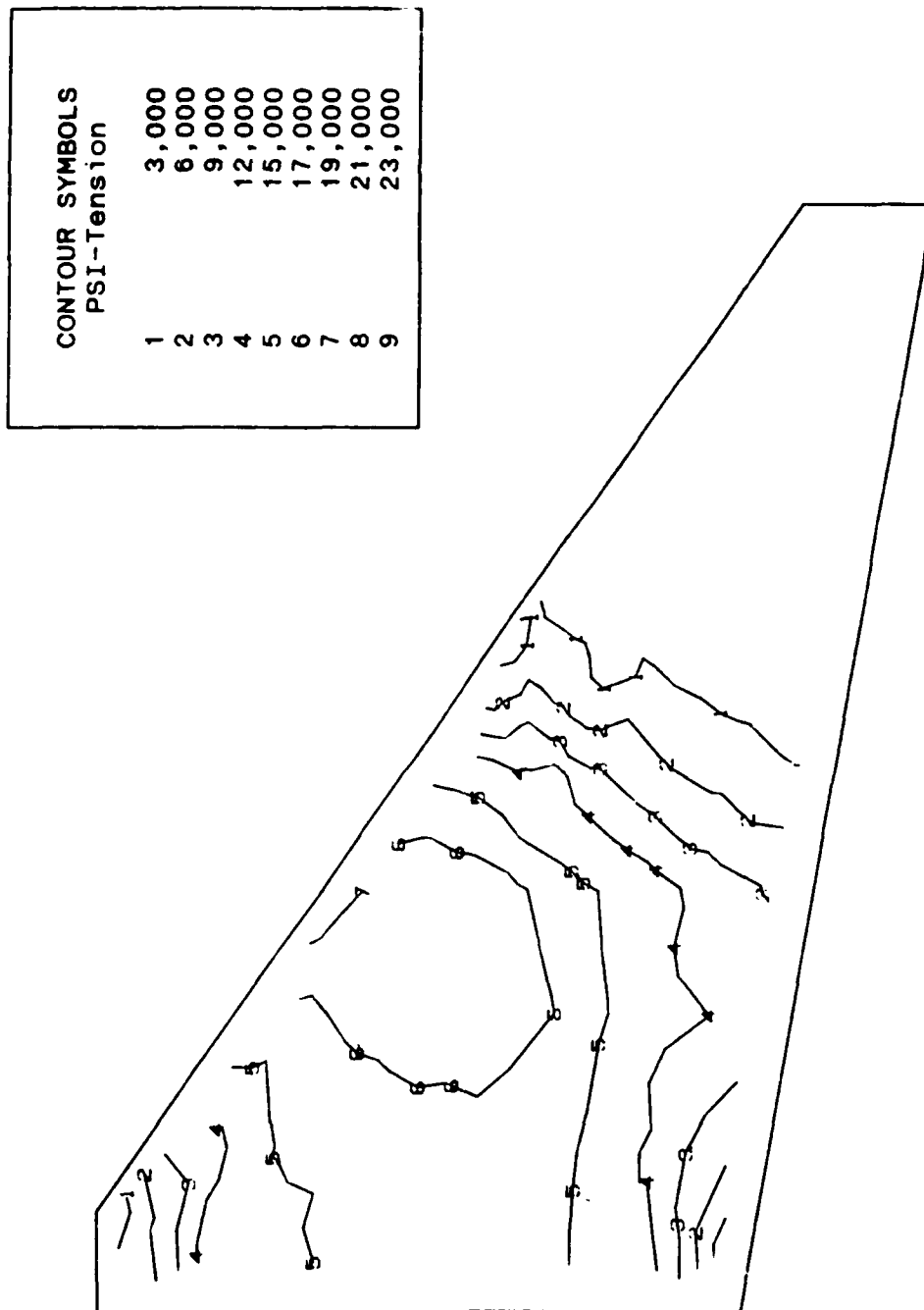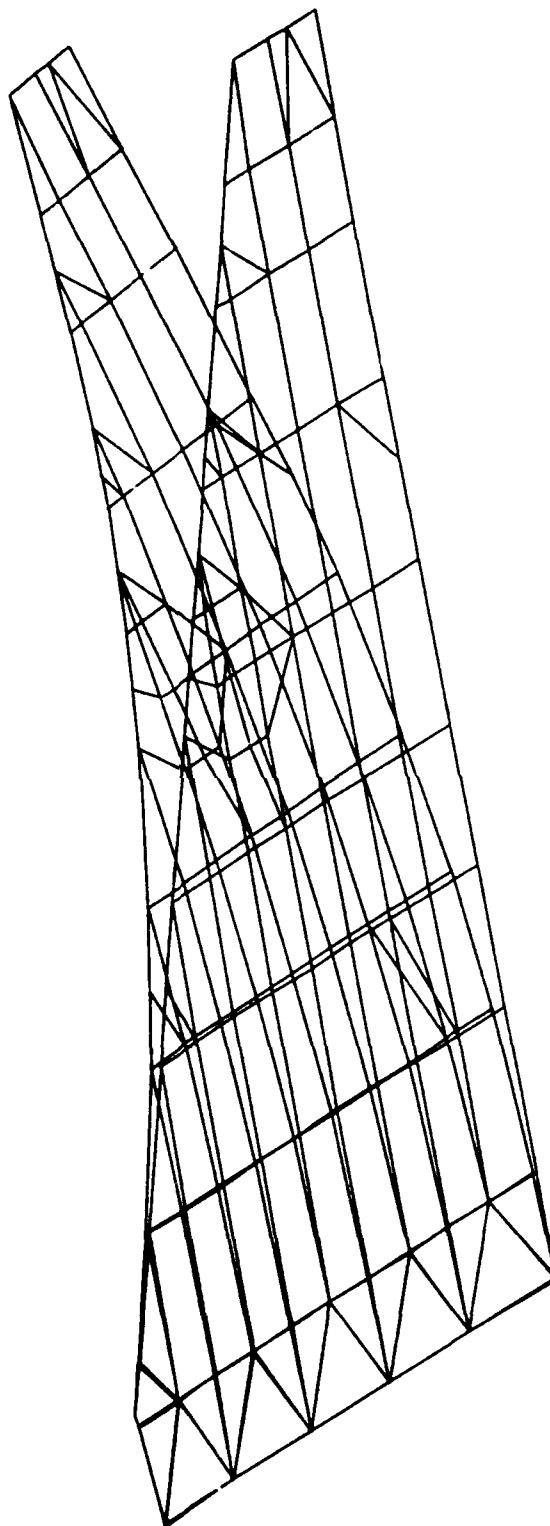Figure J-6.   1st Wing Bending Mode (Model DC-15)

Symmetric Normal Modes for F-16 Wing Model DC-15
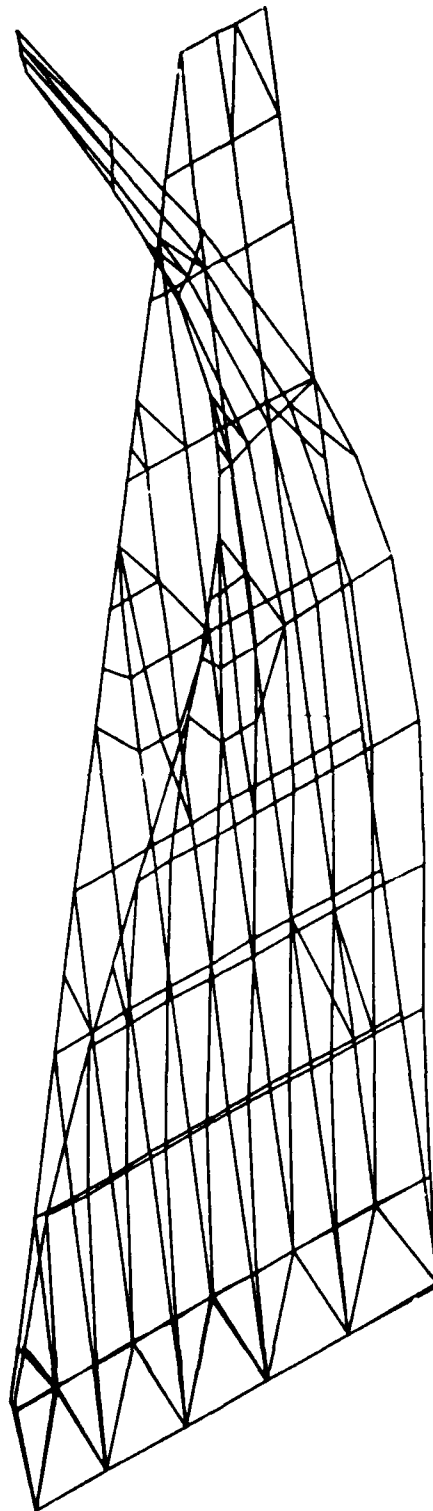
Givens Method   Mode 2   Frequency = 36.69 Hertz

Figure J-7.   2nd Wing Bending Mode (Model DC-15)

Symmetric Normal Modes for F-16 Wing Model DC-15
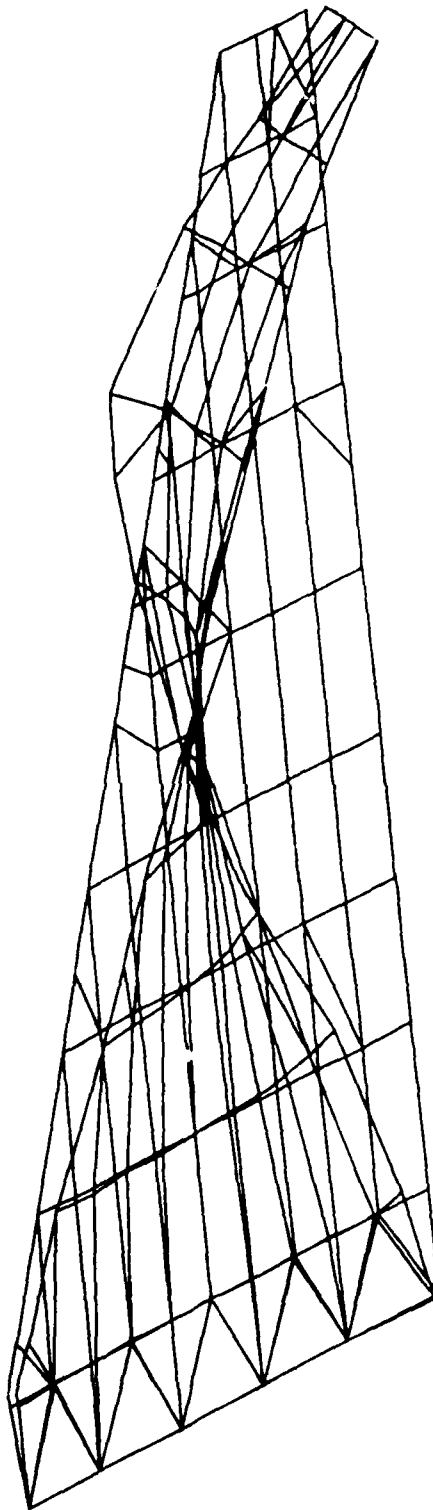
Givens Method   Mode 3   Frequency = 46.10 Hertz

Figure J-8.   1st Torsional Mode (Model DC-15)

Symmetric Normal Modes for F-16 Wing Model DC-15

Givens Method   Mode 4   Frequency = 73.39 Hertz
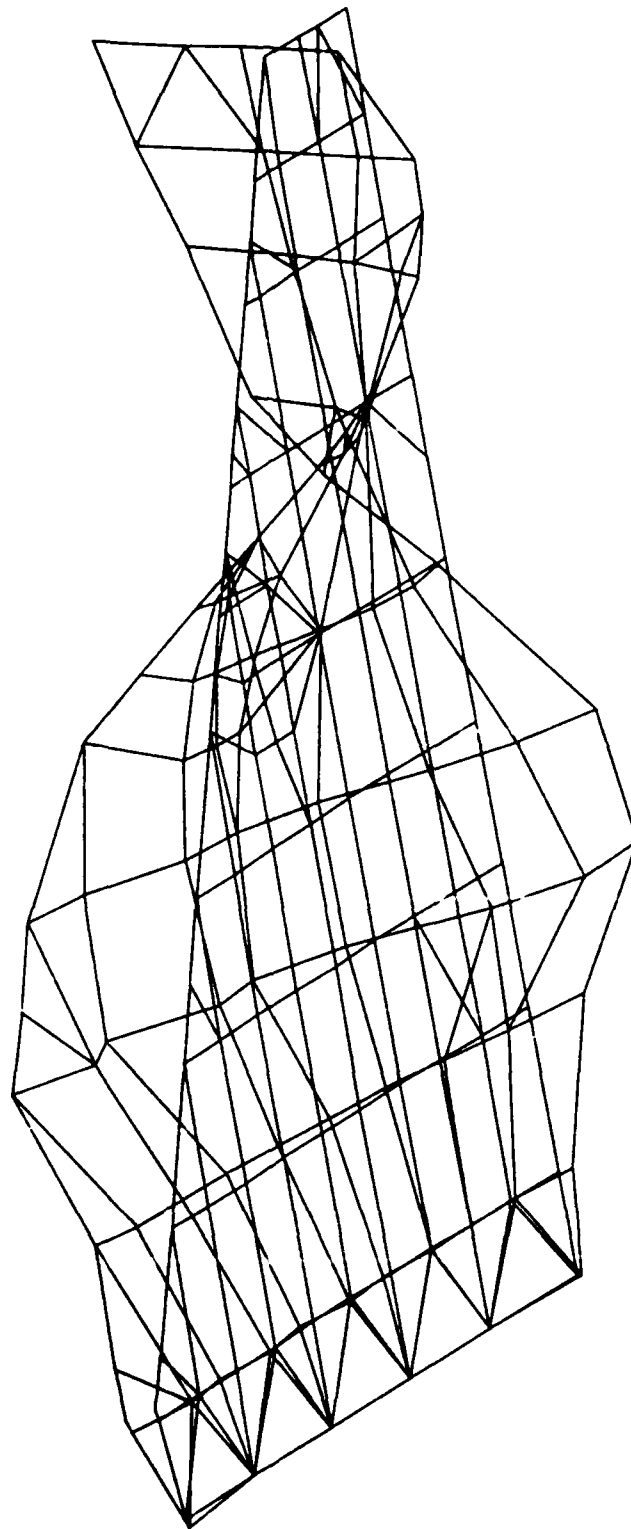
Figure J-9. 2nd Torsional Mode (Model DC-15)
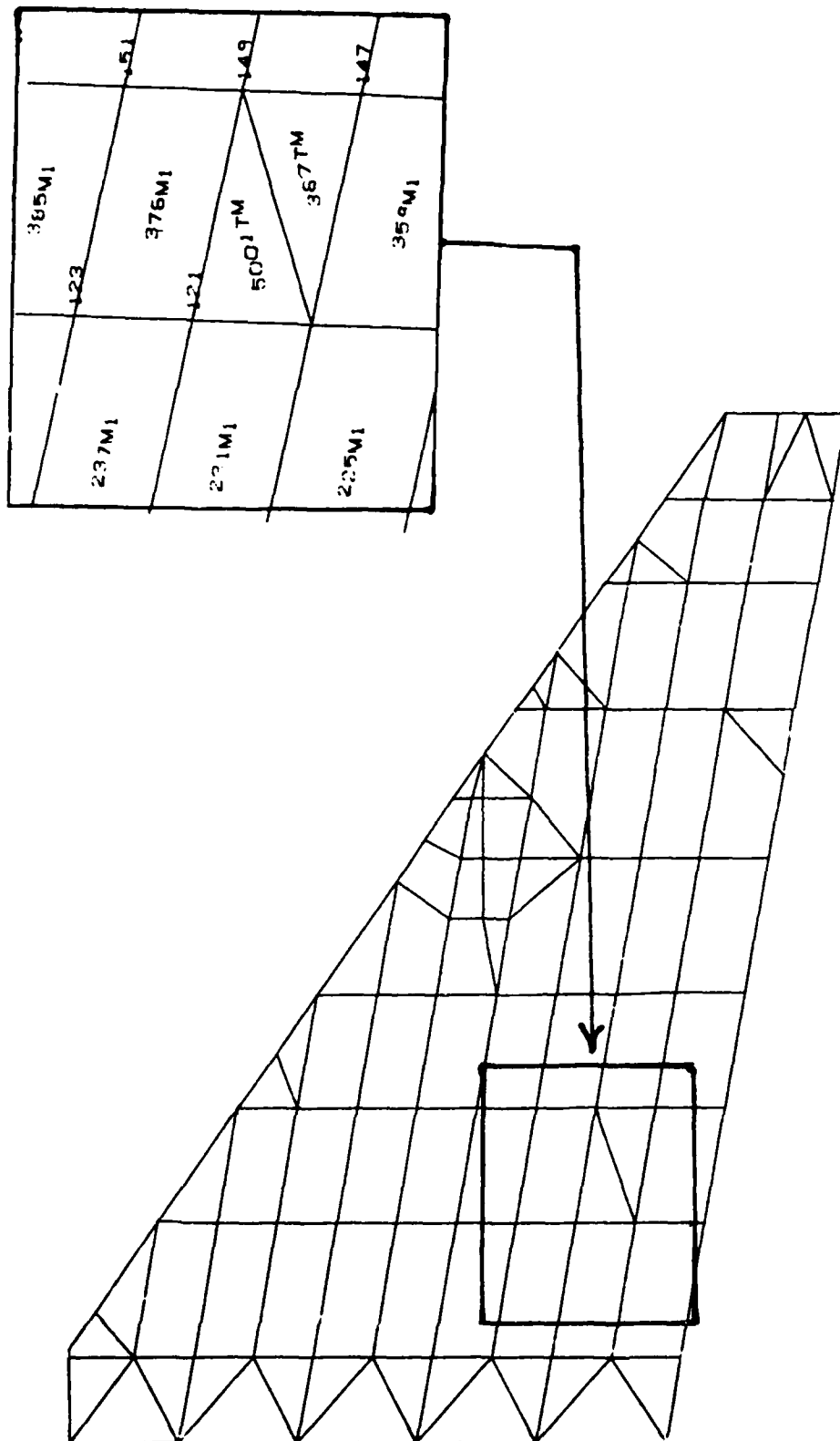
Figure J-10.   Upper Wing Surface (Model DC-15R)
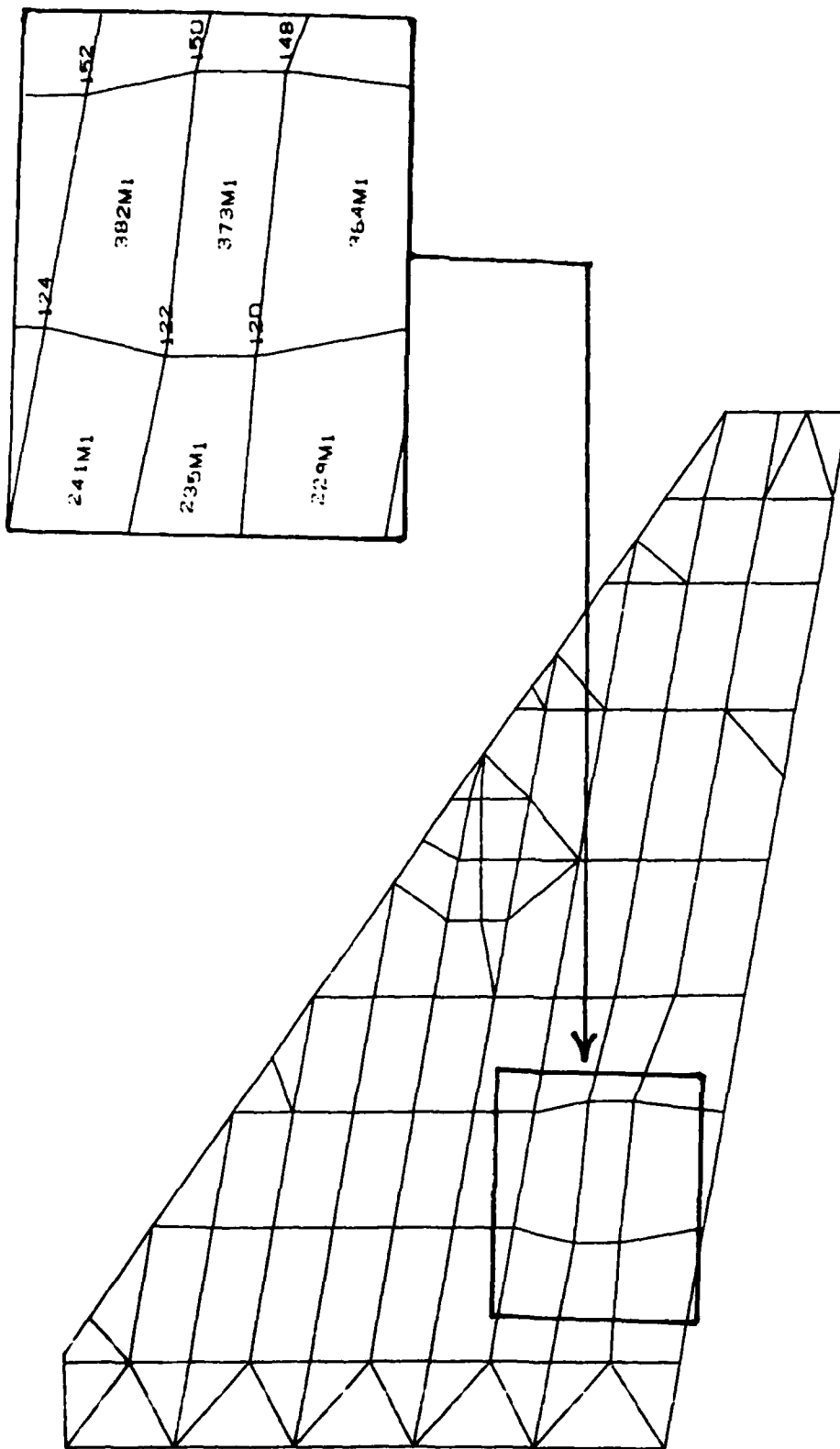
Figure J-11. Lower Wing Surface (Model DC-15R)

CONTOUR SYMBOLS
PSI-Compression

1   3,000
2   6,000
3   9,000
4   12,000
5   15,000
6   18,000
7   21,000
8   23,000
9   25,000

Figure J-12. Stress Contours on Upper Wing Surface (Model DC-12R)

CONTOUR SYMBOLS
PSI-Tension

1	3,000
2	6,000
3	9,000
4	12,000
5	15,000
6	17,000
7	19,000
8	21,000
9	23,000

Figure J-13. Stress Contours on Lower Wing Surface (Model DC-15R)

Symmetric Normal Modes for F-16 Wing Model DC-15R

Givens Method   Mode 1   Frequency = 10.93 Hertz

Figure J-14.   1st Wing Bending Mode (Model DC-15R)

Symmetric Normal Modes for F-16 Wing Model DC-15R

Givens Method   Mode 2   Frequency = 37.28 Hertz

Figure J-15.   2nd Wing Bending Mode (Model DC-15R)

Symmetric Normal Modes for F-16 Wing Model DC-15R

Givens Method   Mode 3   Frequency = 48.12 Hertz

Figure J-16.   1st Torsional Mode (Model DC-15R)

Symmetric Normal Modes for F-16 Wing Model DC-15R

Givens Method   Mode 4   Frequency = 77.50 Hertz
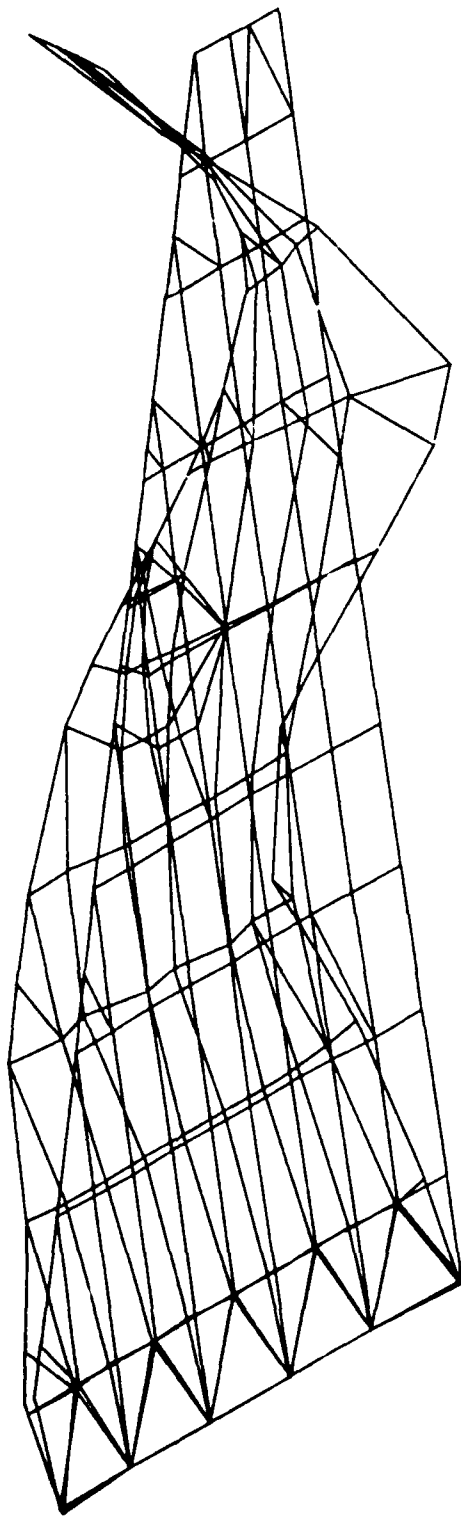
Figure J-17.   2nd Torsional Mode (Model DC-15R)

APPENDIX K

ANALYSIS OF DAMAGE CASE #16

Plot of Wing Displacements at BL 120.0
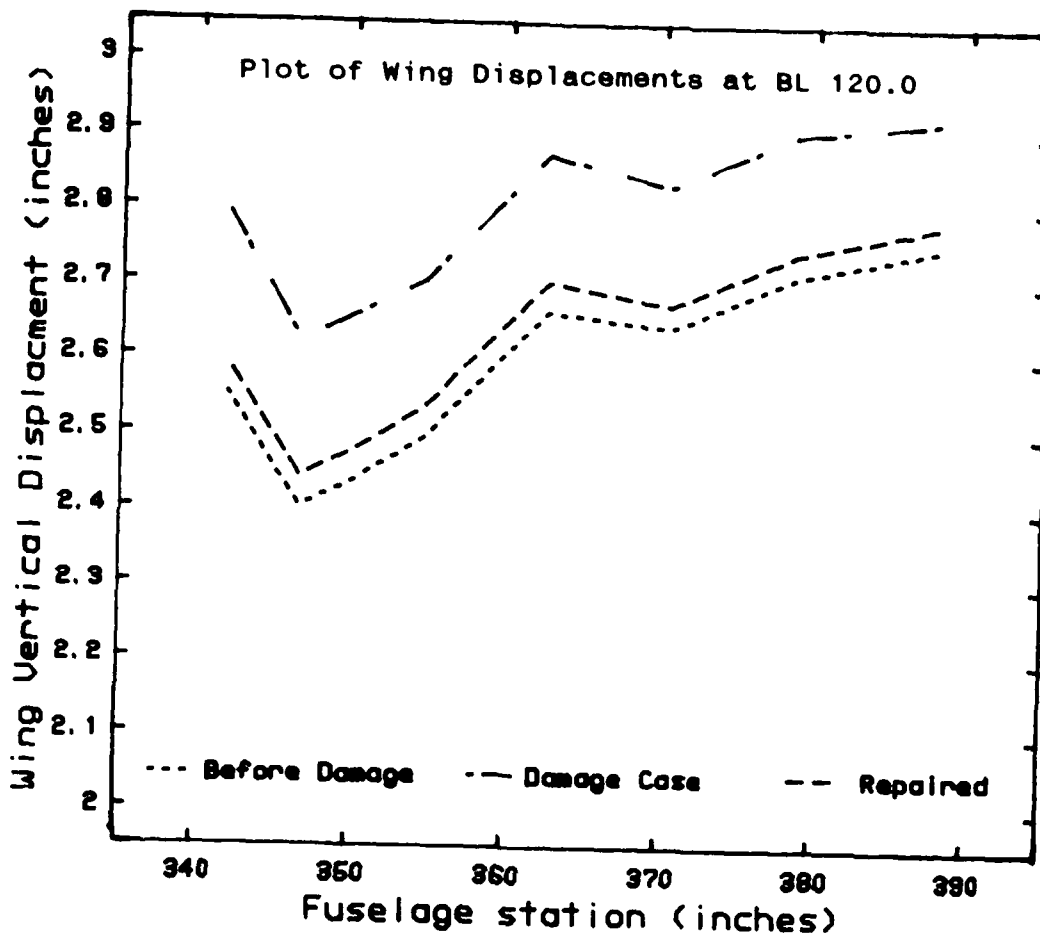
Tabulated Displacements

Fuselage St.	387.9	378.6	370.6	362.6	354.6	349.7	346.6	341.9
Model D-15R	2.75	2.71	2.64	2.66	2.49	2.43	2.40	2.55
Model DC-16	2.92	2.90	2.83	2.87	2.70	2.65	2.62	2.79
Model DC-16R	2.78	2.74	2.67	2.70	2.53	2.47	2.44	2.59

Comparison of Residual Strength

	Av Disp	% Change	Torsion mode	% Change
Model D-15R	2.58		48.12	
Model DC-16	2.79	-8.1	46.13	-4.1
Model DC-16R	2.62	+6.6	48.13	+4.1

Figure K-1.   Summary of Damage Case #16 Results
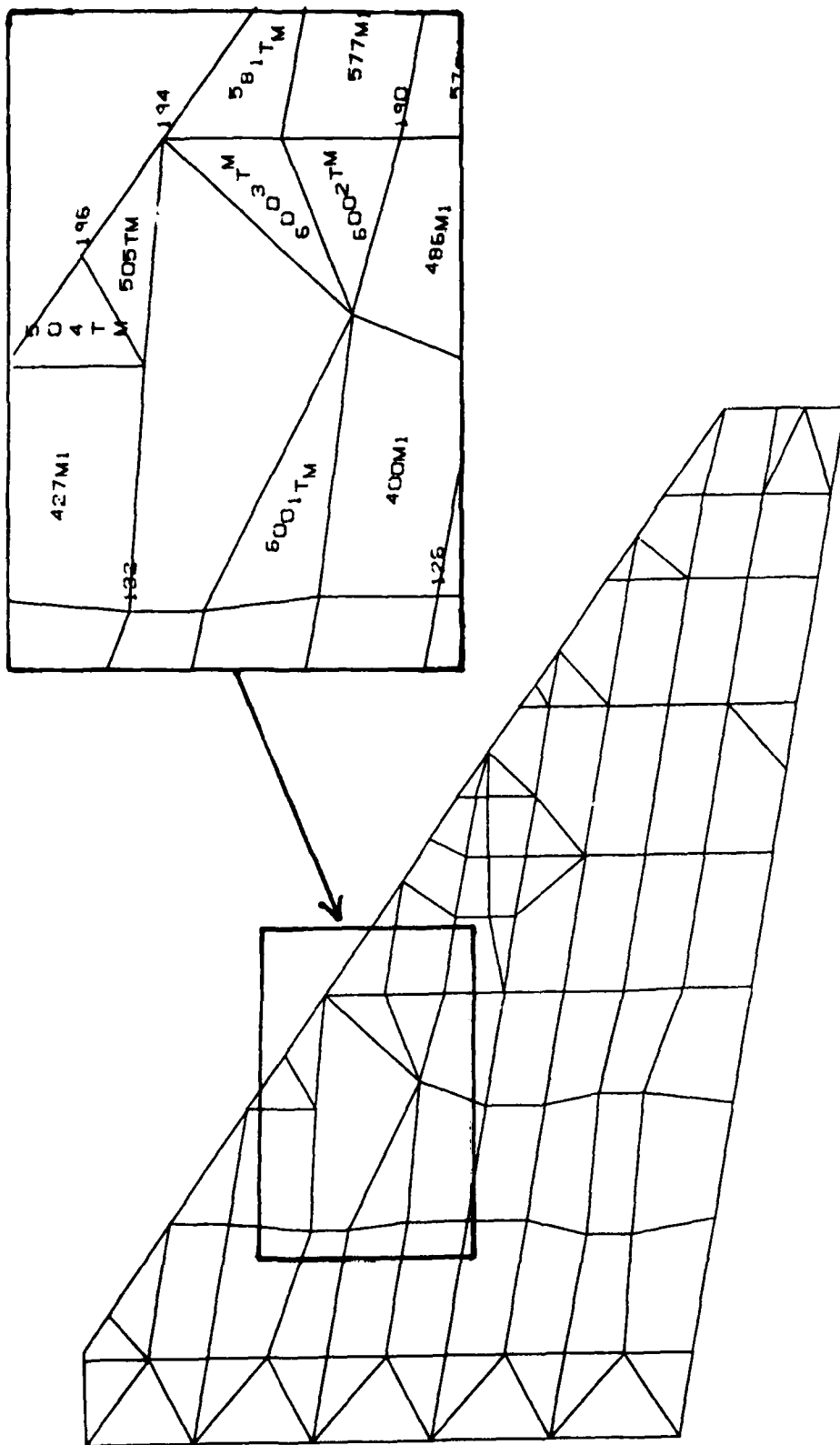
K-2
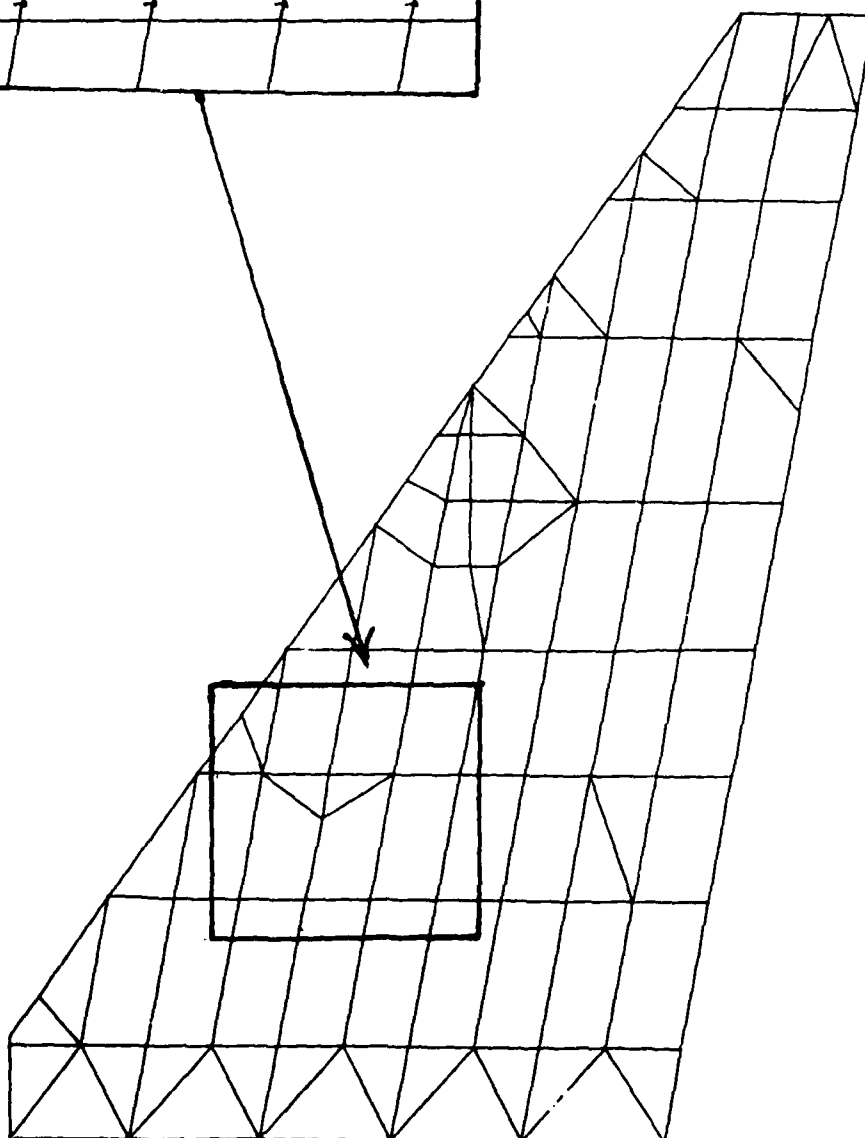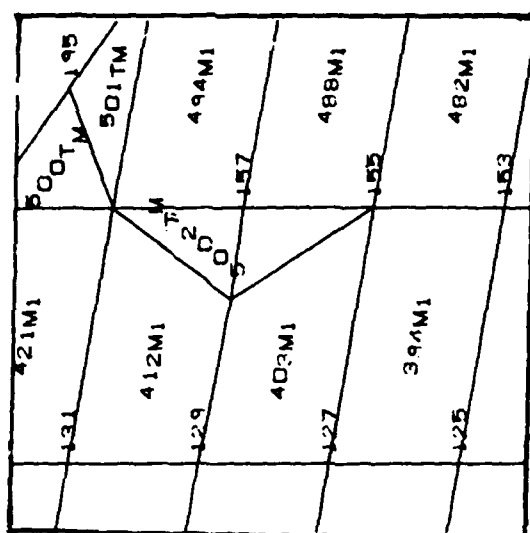
Figure K-2. Upper Wing Surface (Model DC-16)
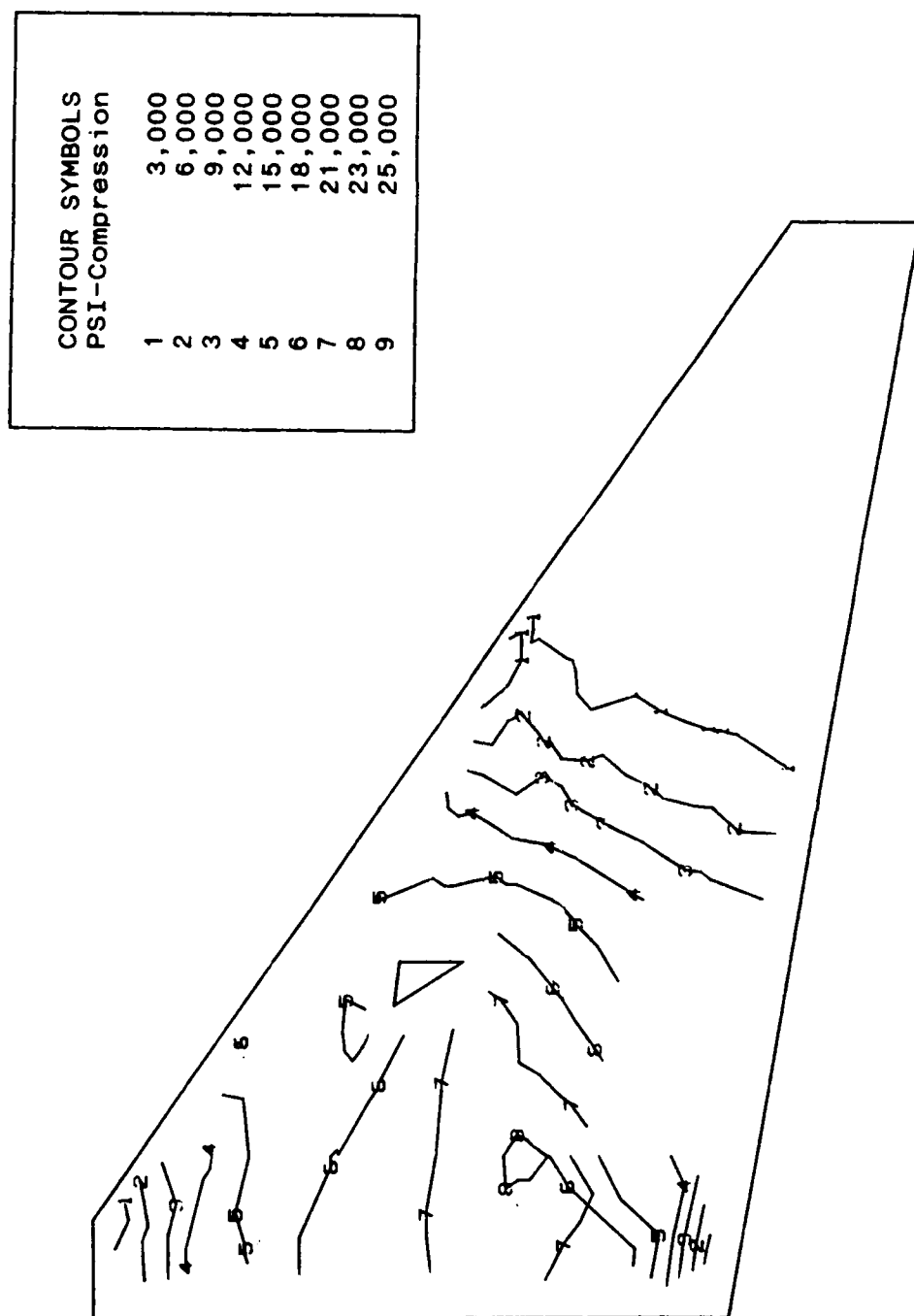
Figure K-3. Lower Wing Surface (Model DC-16)

CONTOUR SYMBOLS
PSI-Compression

1	3,000
2	6,000
3	9,000
4	12,000
5	15,000
6	18,000
7	21,000
8	23,000
9	25,000

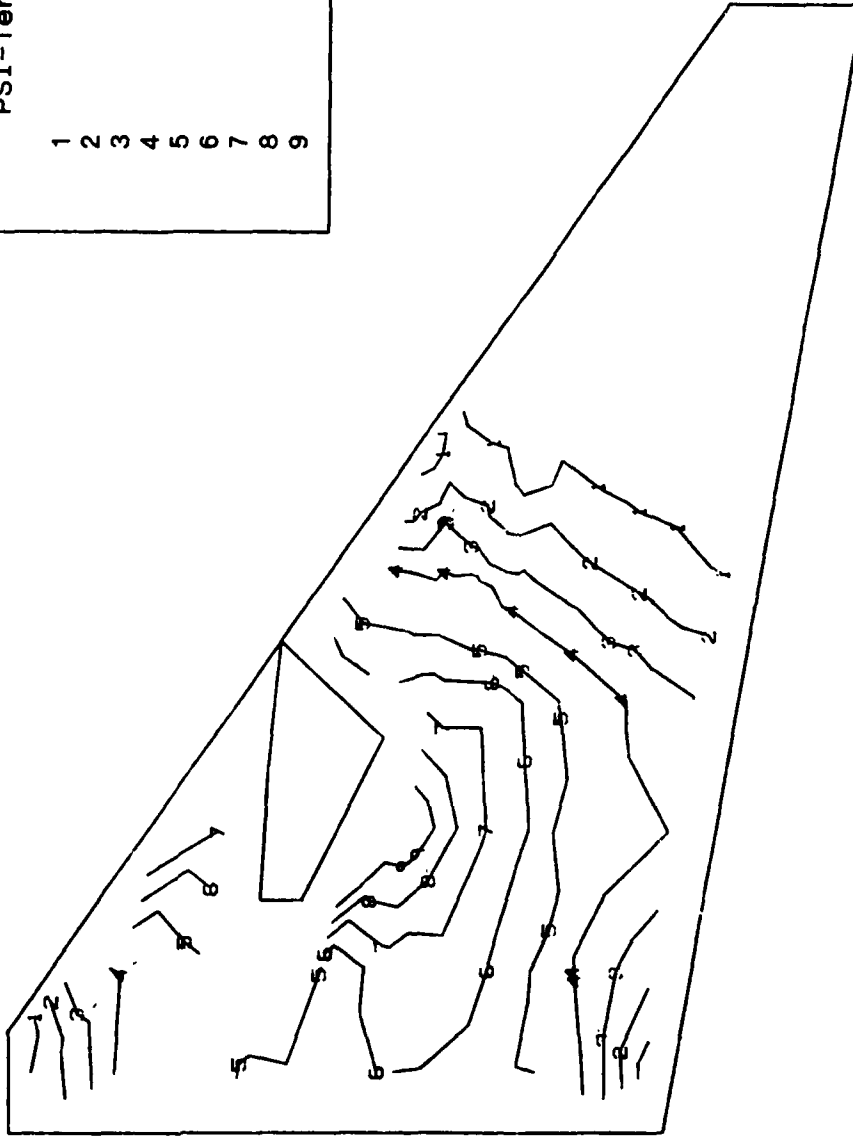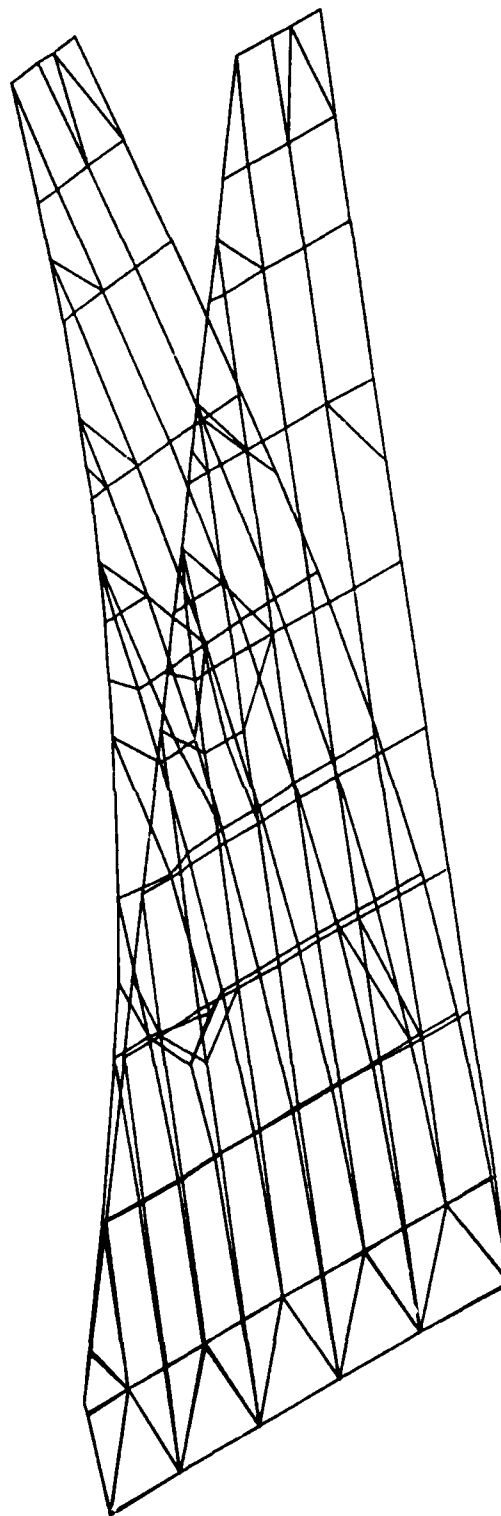Figure K-4. Stress Contours on Upper Wing Surface (Model DC-16)

CONTOUR SYMBOLS
PSI-Tension

1	3,000
2	6,000
3	9,000
4	12,000
5	15,000
6	17,000
7	19,000
8	21,000
9	23,000

Figure K-5.   Stress Contours on Lower Wing Surface (Model DC-16)
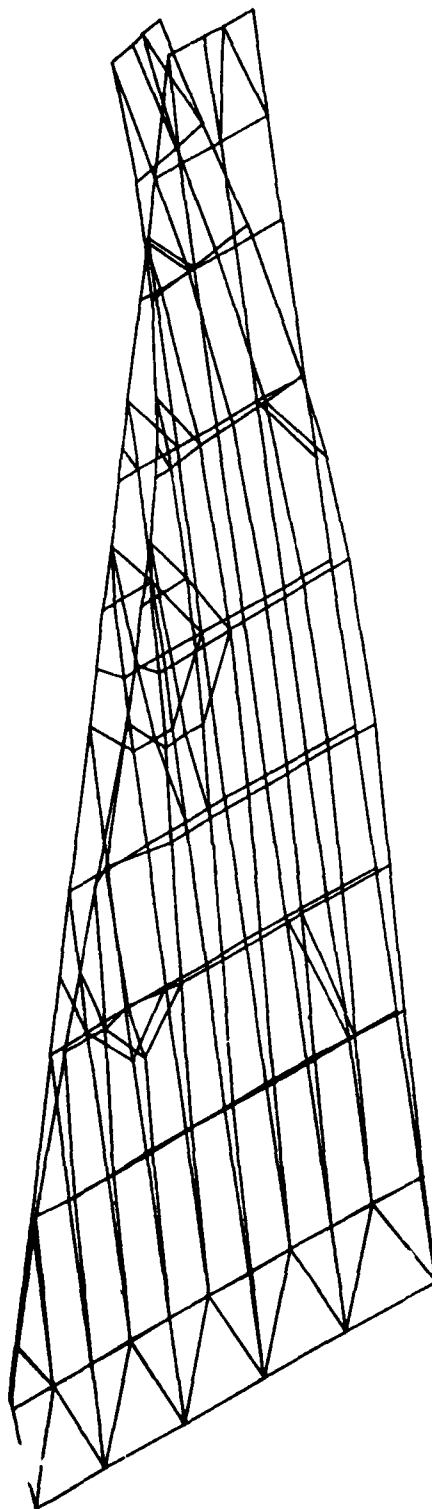
Symmetric Normal Modes for F-16 Wing Model DC-16

Givens Method   Mode 1   Frequency = 10.89 Hertz

Figure K-6.   1st Wing Bending Mode (Model DC-16)

Symmetric Normal Modes for F-16 Wing Model DC-16

Givens Method   Mode 2   Frequency = 36.20 Hertz

Figure K-7.   2nd Wing Bending Mode (Model DC-16)

Symmetric Normal Modes for F-16 Wing Model DC-16
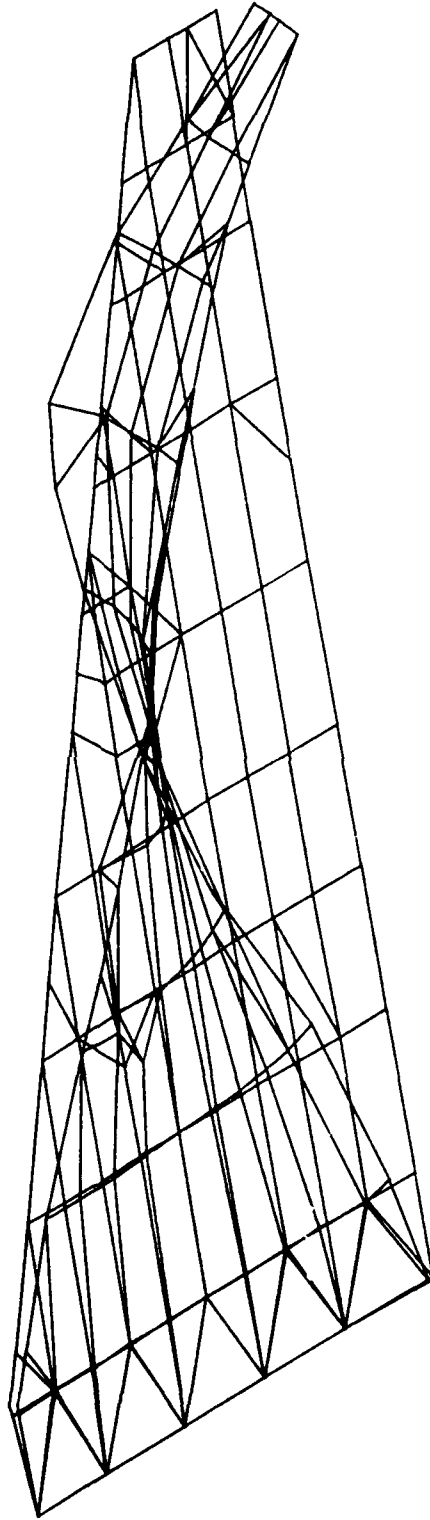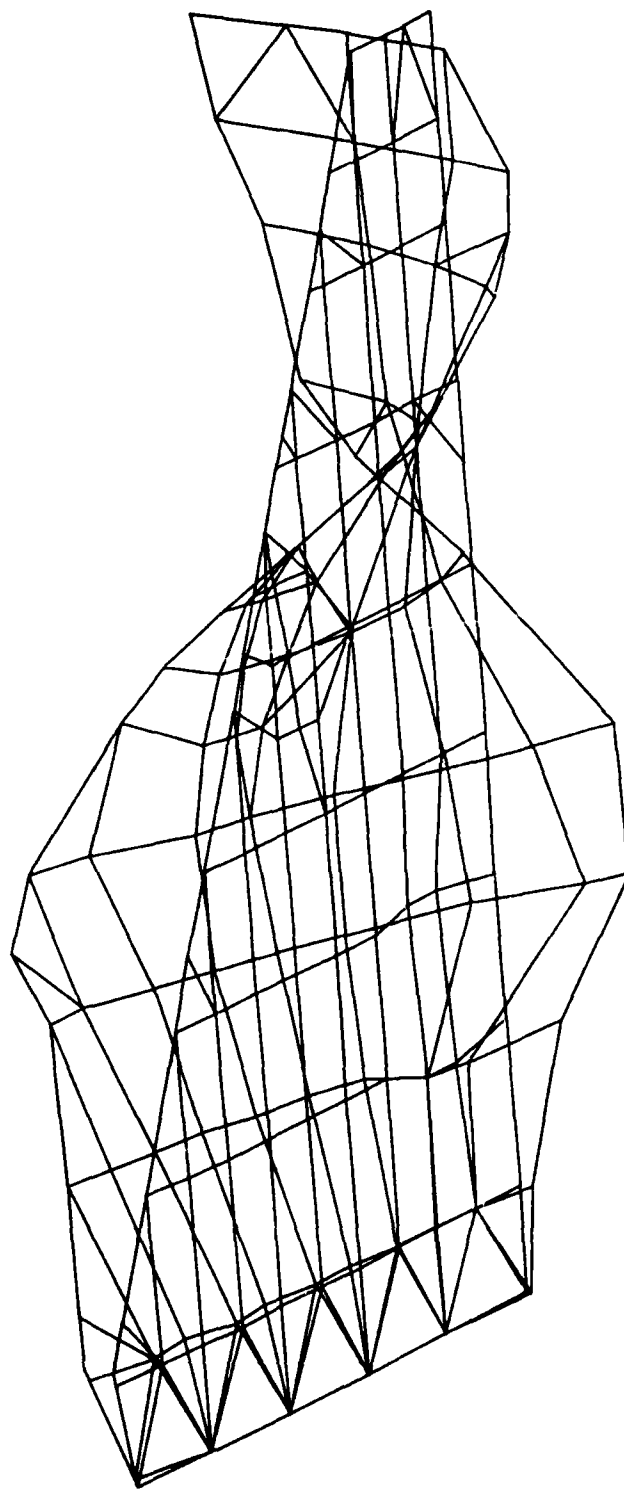
Givens Method   Mode 3   Frequency = 46.13 Hertz

Figure K-8. 1st Torsional Mode (Model DC-16)

Symmetric Normal Modes for F-16 Wing Model DC-16

Givens Method   Mode 4   Frequency = 76.37 Hertz
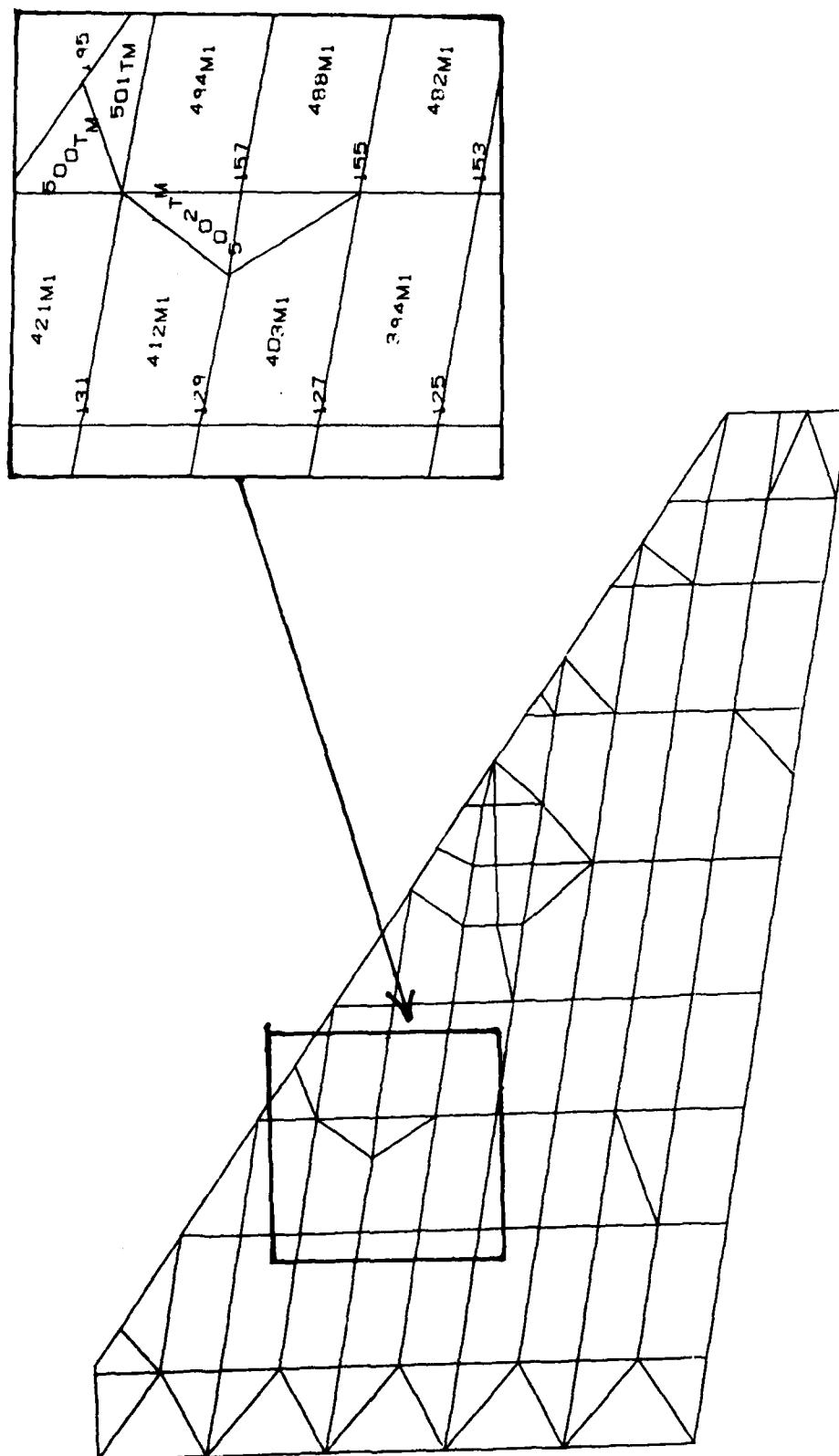
Figure K-9.   2nd Torsional Mode (Model DC-16)
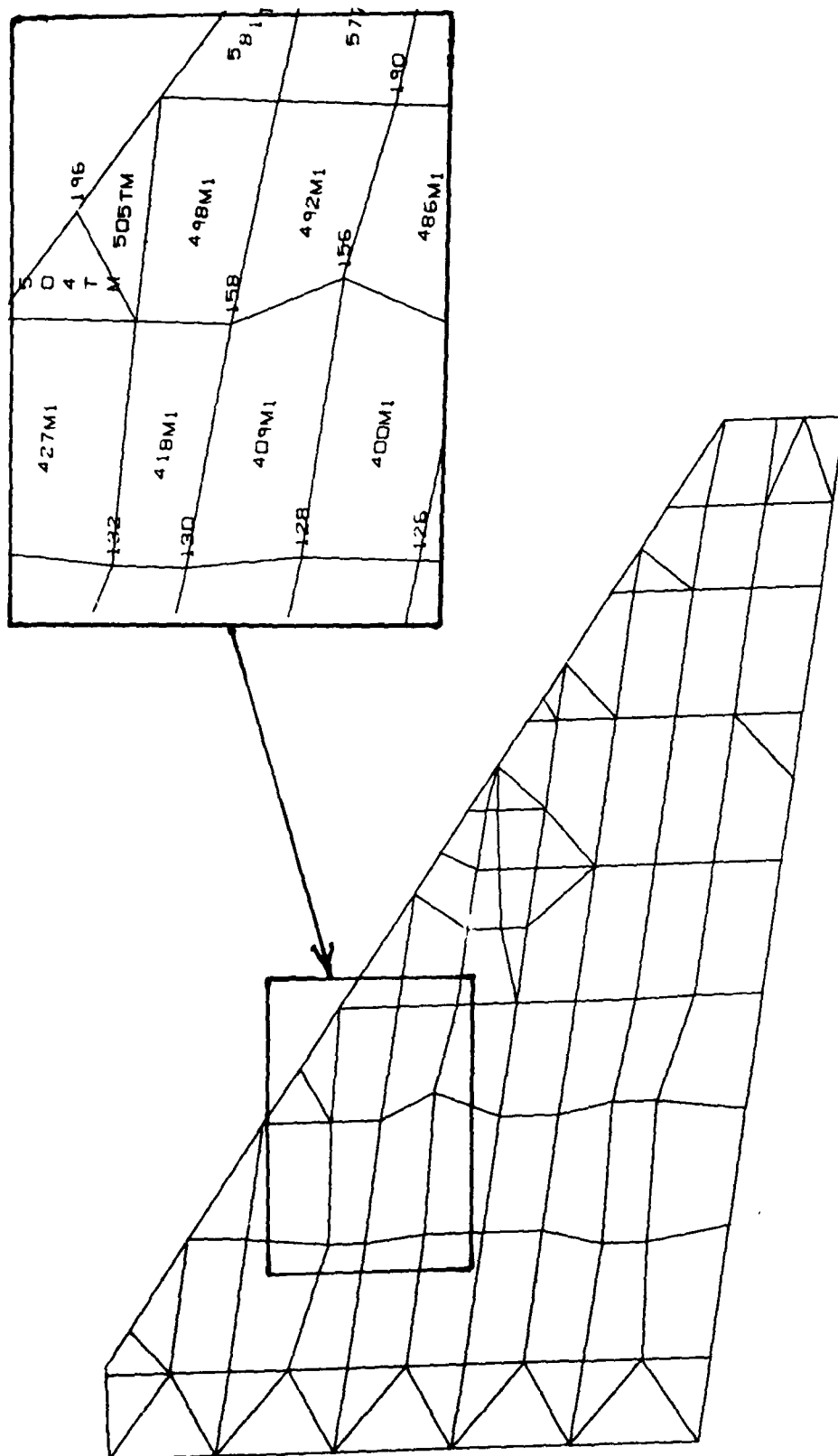
Figure K-10. Upper Wing Surface (Model DC-16R)

Figure K-11. Lower Wing Surface (Model DC-16R)

CONTOUR SYMBOLS
PSI-Compression

1	3,000
2	6,000
3	9,000
4	12,000
5	15,000
6	18,000
7	21,000
8	23,000
9	25,000

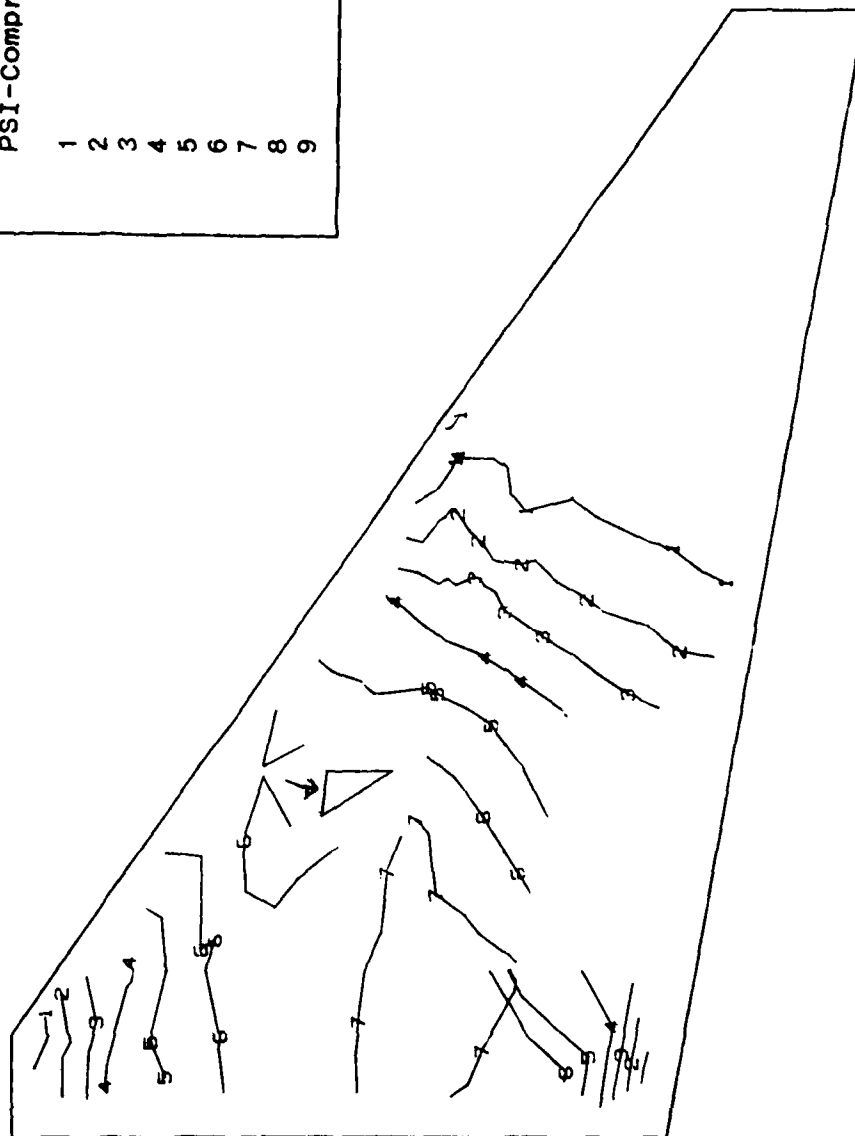Figure K-12. Stress Contours on Upper Wing Surface (Model DC-16R)

K-13

CONTOUR SYMBOLS
PSI-Tension

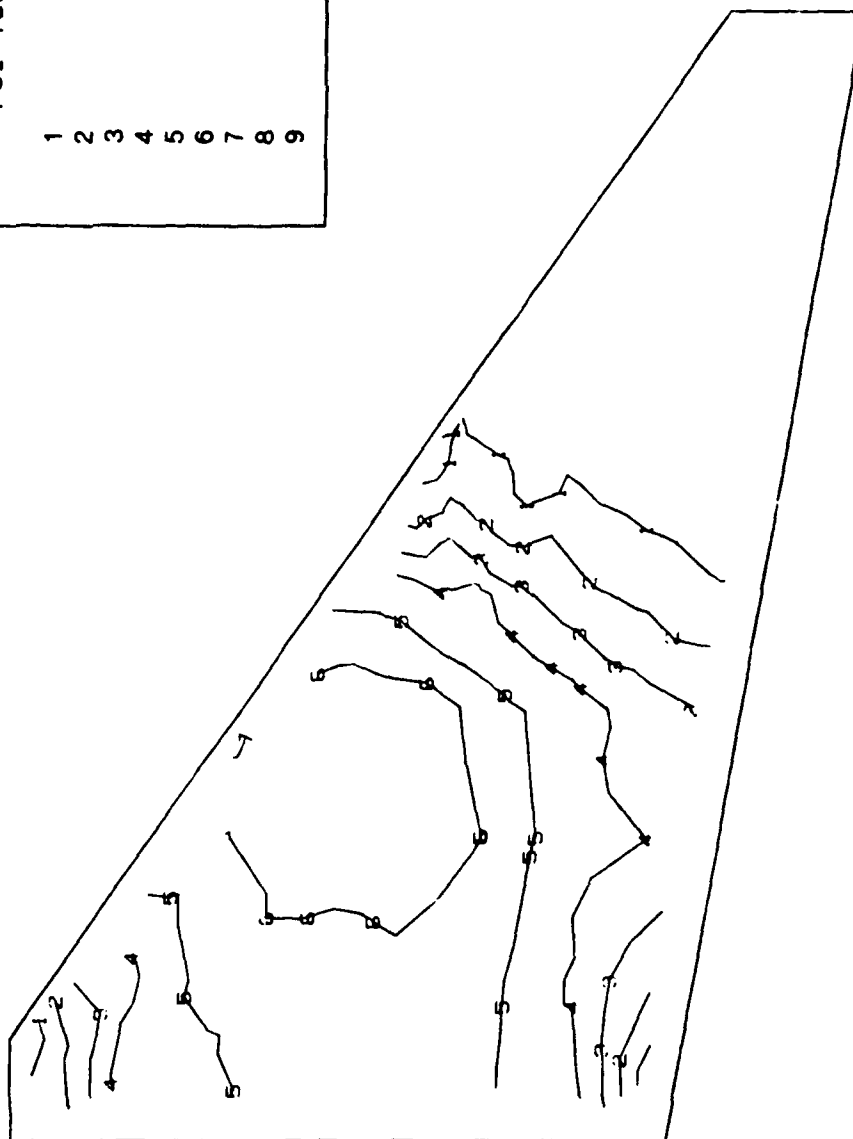| 1	3,000
2	6,000
3	9,000
4	12,000
5	15,000
6	17,000
7	19,000
8	21,000
9	23,000

Figure K-13.   Stress Contours on Lower Wing Surface (Model DC-16R)

Symmetric Normal Modes for F-16 Wing Model DC-16R

Givens Method   Mode 1   Frequency = 10.93 Hertz
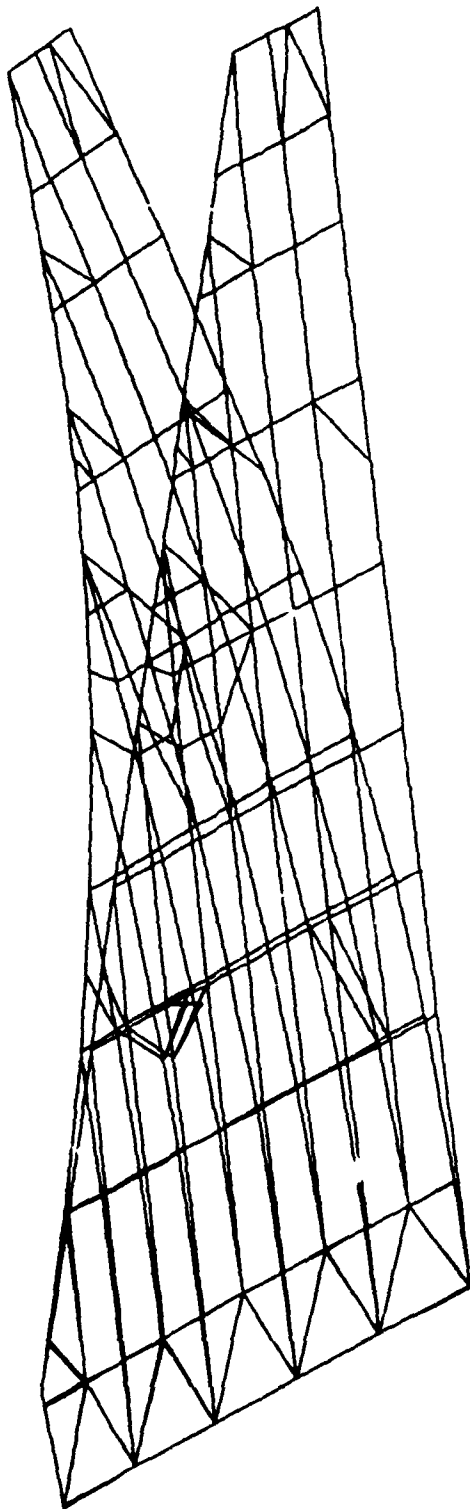
Figure K-14.   1st Wing Bending Mode (Model DC-16R)

Symmetric Normal Modes for F-16 Wing Model DC-16R

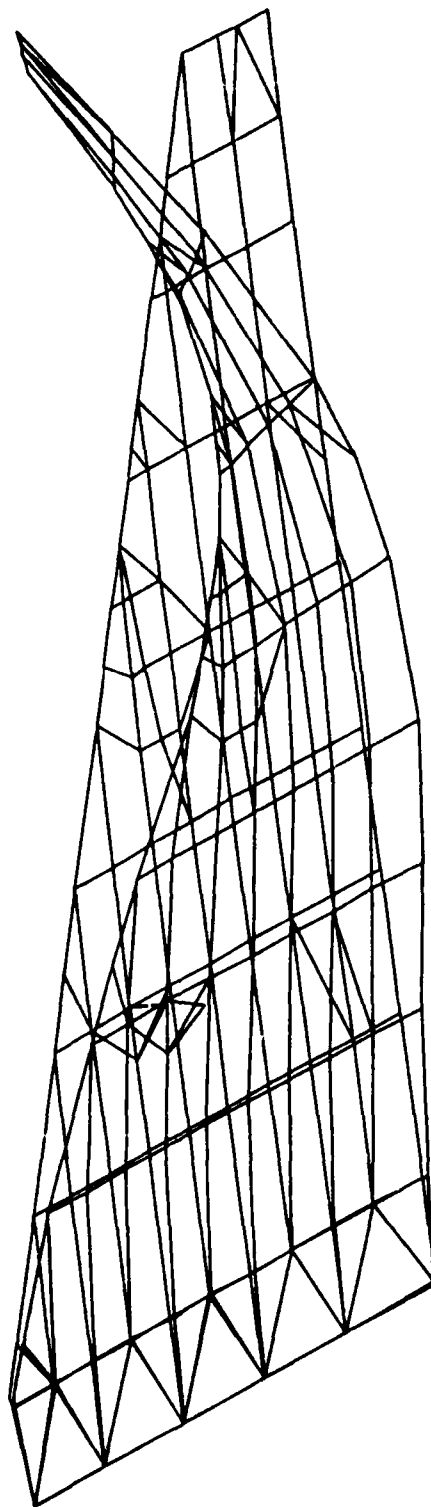Givens Method   Mode 2   Frequency = 37.50 Hertz

Figure K-15.   2nd Wing Bending Mode (Model DC-16R)

Symmetric Normal Modes for F-16 Wing Model DC-16R
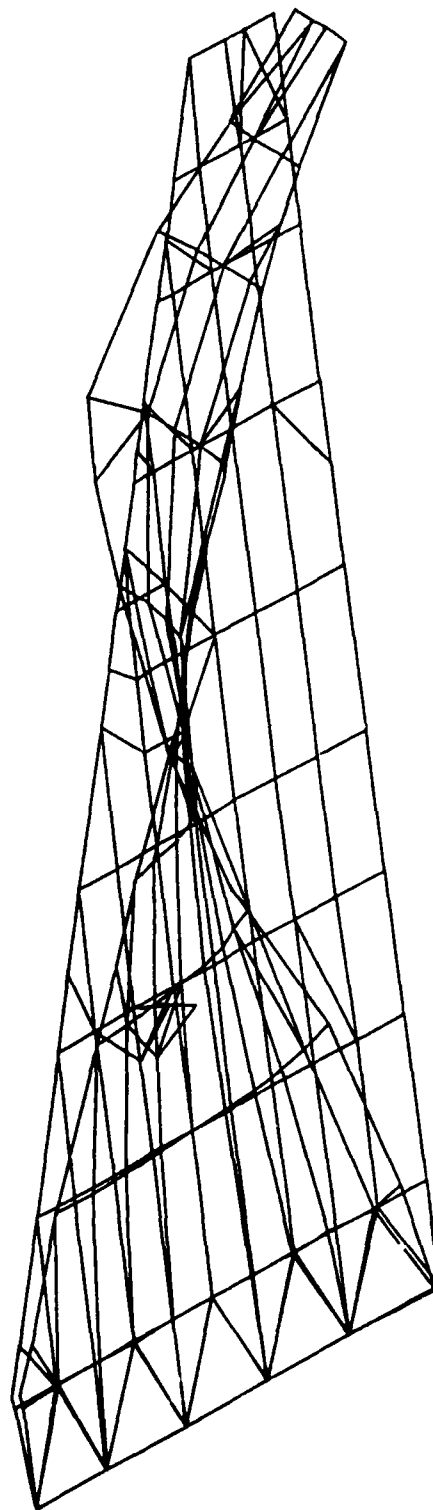
Givens Method   Mode 3   Frequency = 48.13 Hertz

Figure K-16. 1st Torsional Mode (Model DC-16R)

K-17

Symmetric Normal Modes for F-16 Wing Model DC-16R
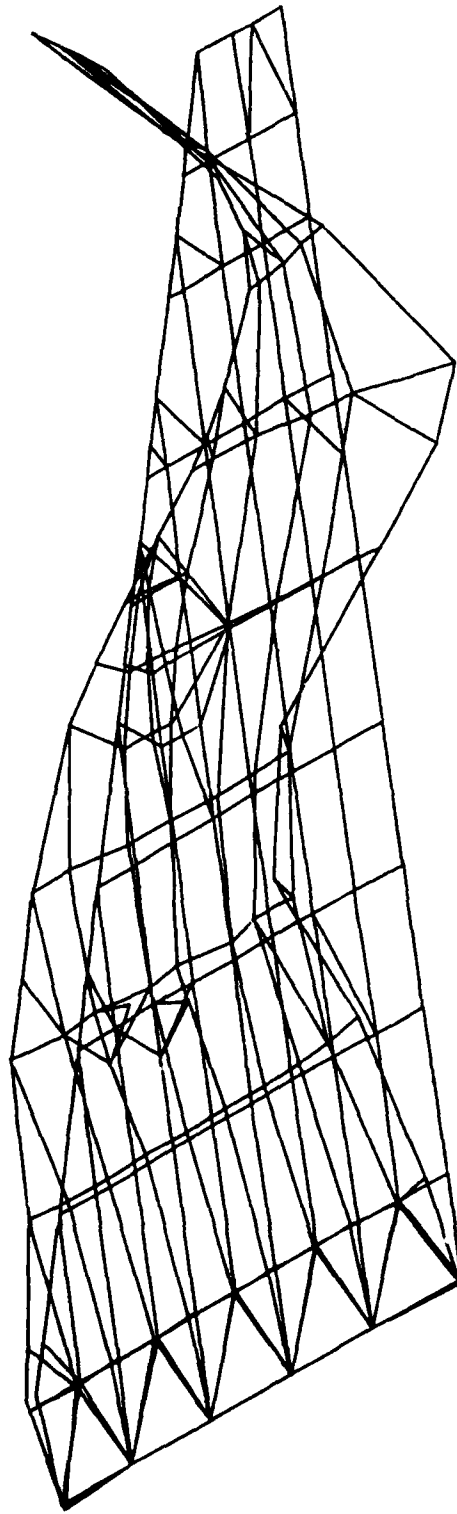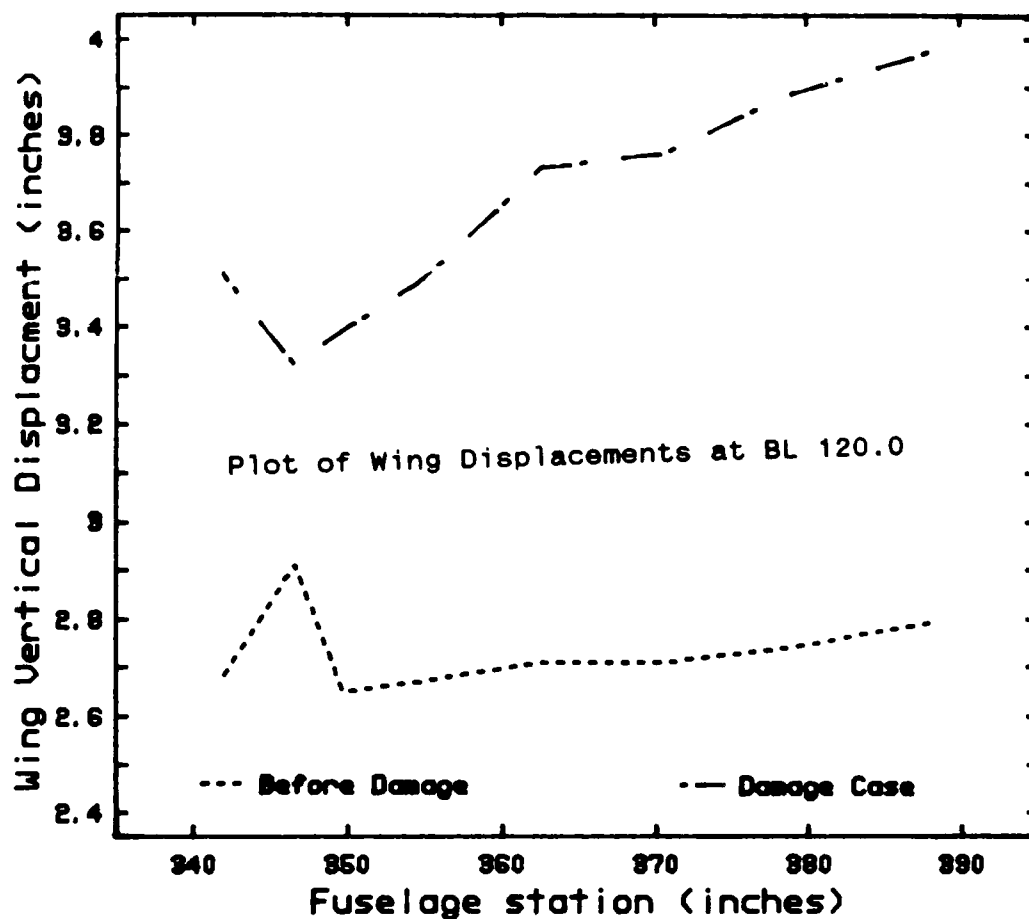
Givens Method   Mode 4   Frequency = 78.37 Hertz

Figure K-17. 2nd Torsional Mode (Model DC-16R)

APPENDIX L

ANALYSIS OF DAMAGE CASE #17

Plot of Wing Displacements at BL 120.0

Tabulated Displacements

Fuselage St.	387.9	378.6	370.6	362.6	354.6	349.7	346.6	341.9
Model D-16R	2.78	2.74	2.67	2.70	2.53	2.47	2.44	2.59
Model DC-17	3.97	3.88	3.76	3.73	3.49	3.39	3.32	3.51

Comparison of Residual Strength

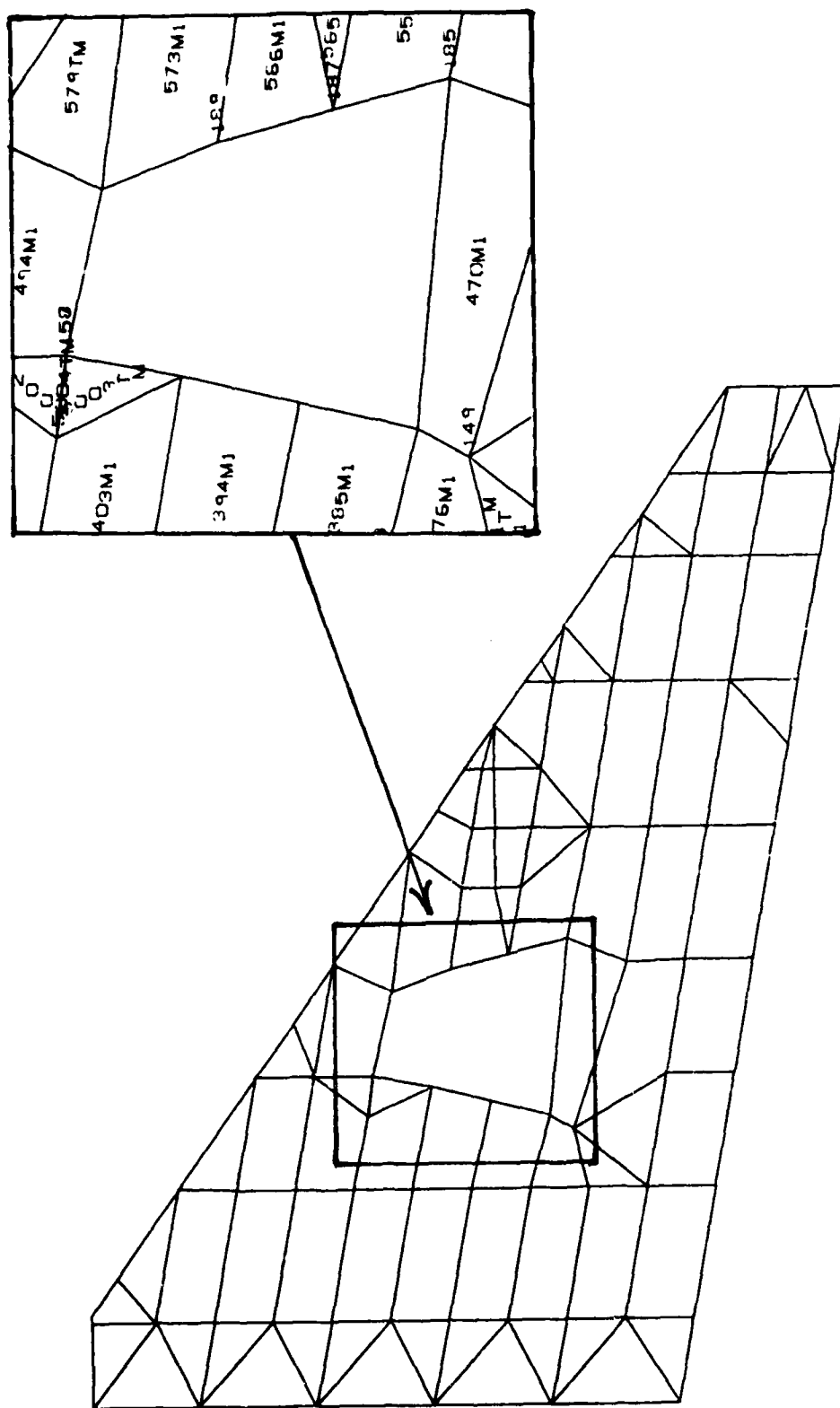|	Av Disp	% Change	Torsion mode	% Change
Model D-16R	2.62		48.13	
Model DC-17	3.79	-44.7	46.13	-4.1

Figure L-1.   Summary of Damage Case #17 Results

L-2

Figure L-2. Upper Wing Surface (Model DC-17)

Figure L-3. Lower Wing Surface (Model DC-17)

CONTOUR SYMBOLS
PSI-Compression

1   3,000
2   6,000
3   9,000
4   12,000
5   15,000
6   18,000
7   21,000
8   23,000
9   25,000

Figure L-4. Stress Contours on Upper Wing Surface (Model DC-17)

CONTOUR SYMBOLS
PSI-Tension

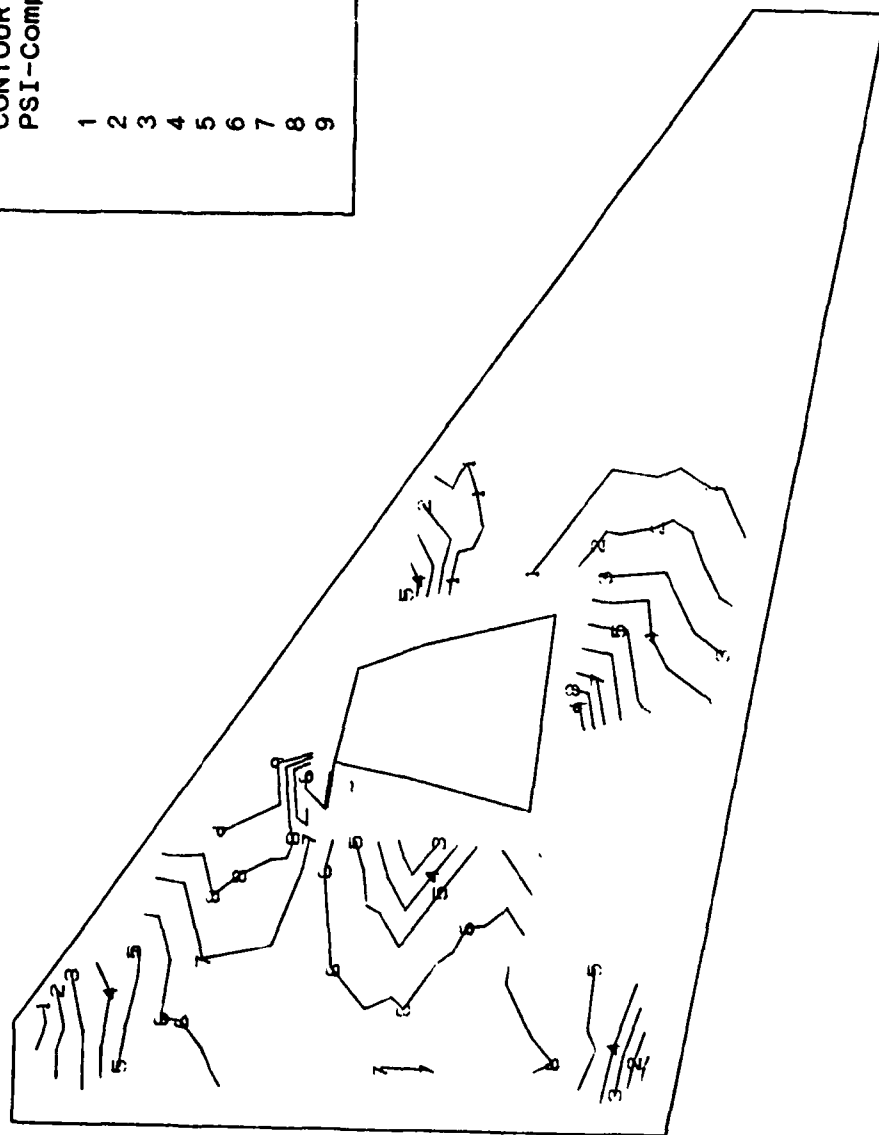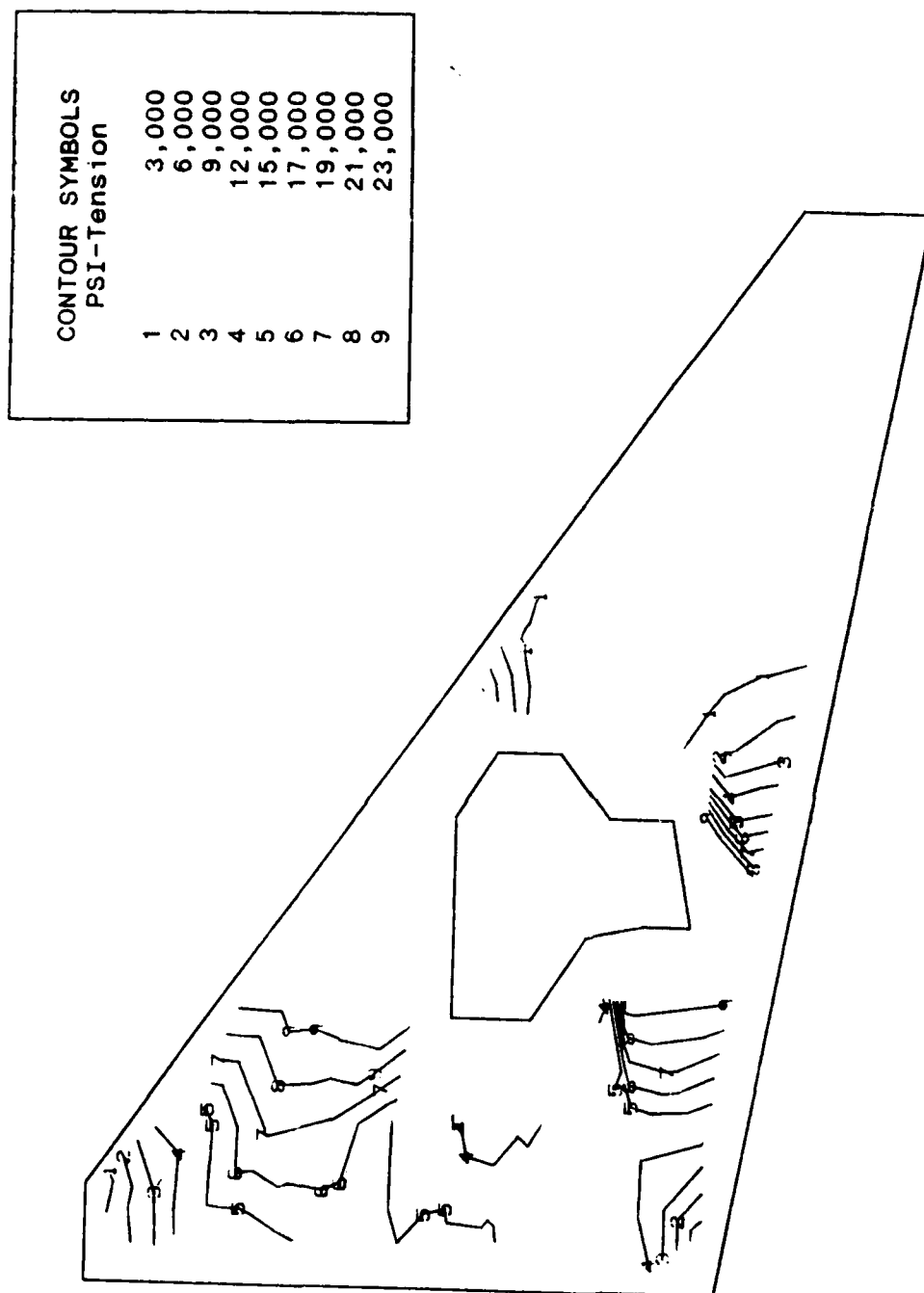|	
1	3,000
2	6,000
3	9,000
4	12,000
5	15,000
6	17,000
7	19,000
8	21,000
9	23,000

Figure L-5. Stress Contours on Lower Wing Surface (Model DC-17)

Symmetric Normal Modes for F-16 Wing Model DC-17

Givens Method   Mode 1   Frequency = 8.96 Hertz
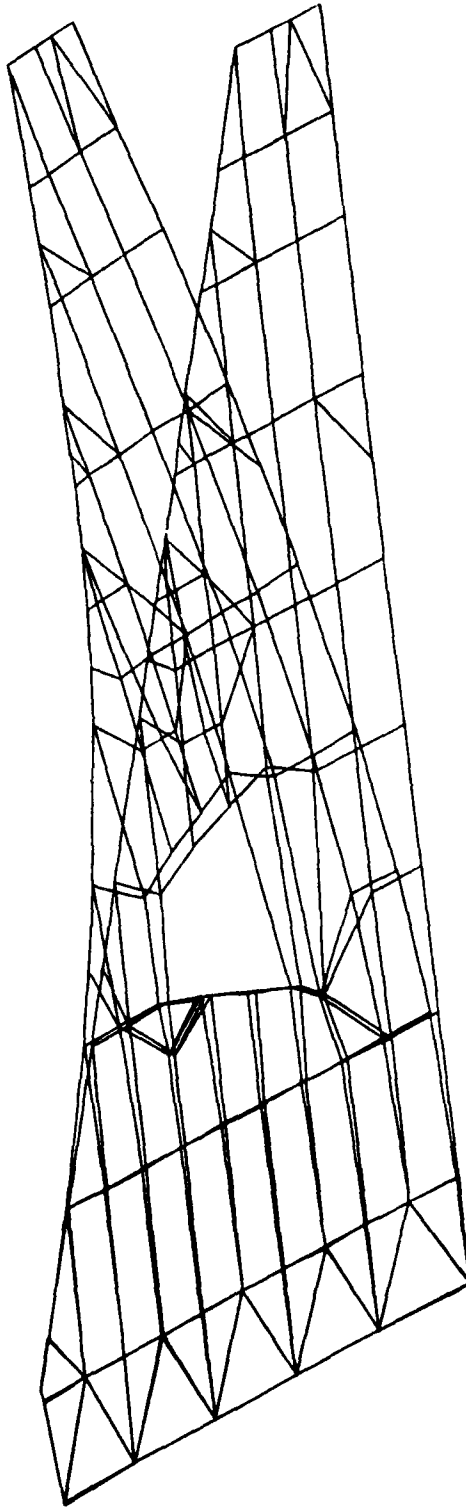
Figure L-6.   1st Wing Bending Mode (Model DC-17)

Symmetric Normal Modes for F-16 Wing Model DC-17

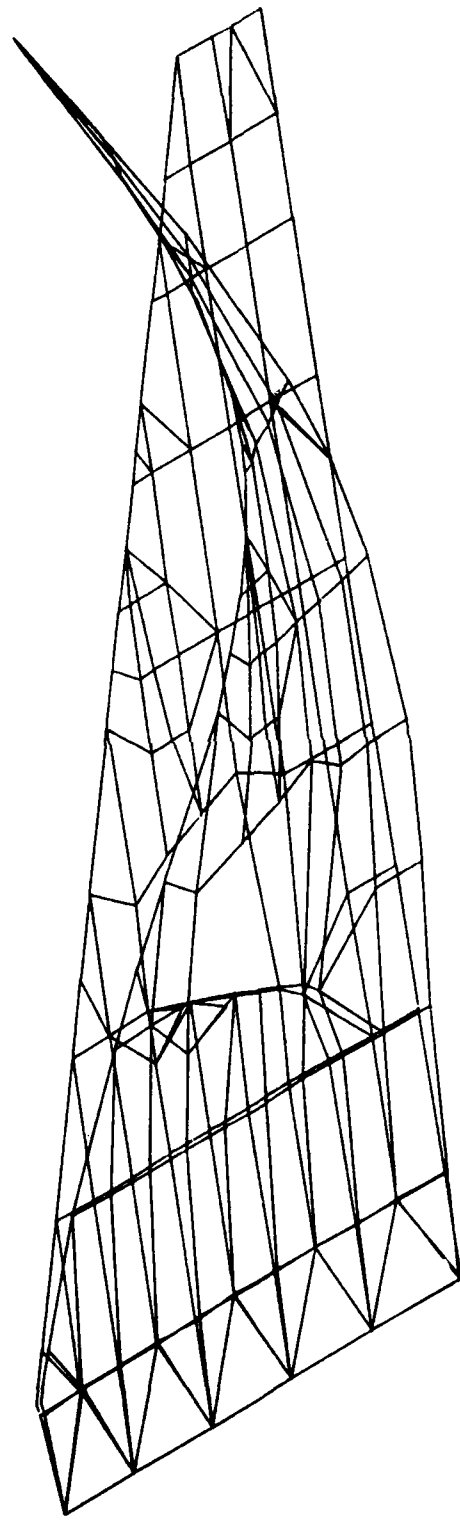Givens Method   Mode 2   Frequency = 36.21 Hertz

Figure L-7.   2nd Wing Bending Mode (Model DC-17)

Symmetric Normal Modes for F-16 Wing Model DC-17

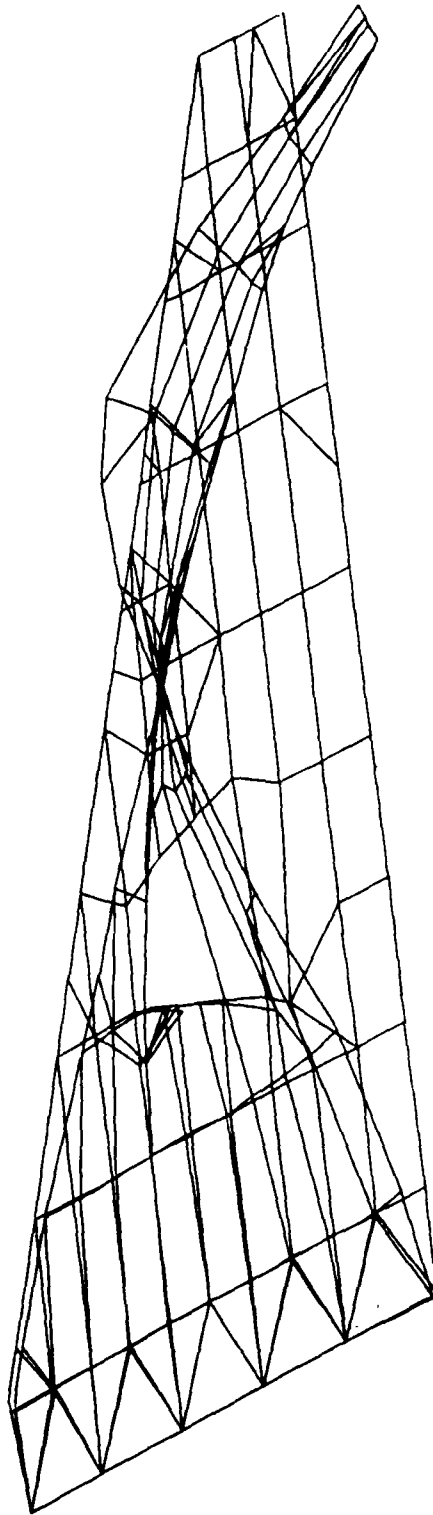Givens Method   Mode 3   Frequency = 46.64 Hertz

Figure L-8.   1st Torsional Mode (Model DC-17)

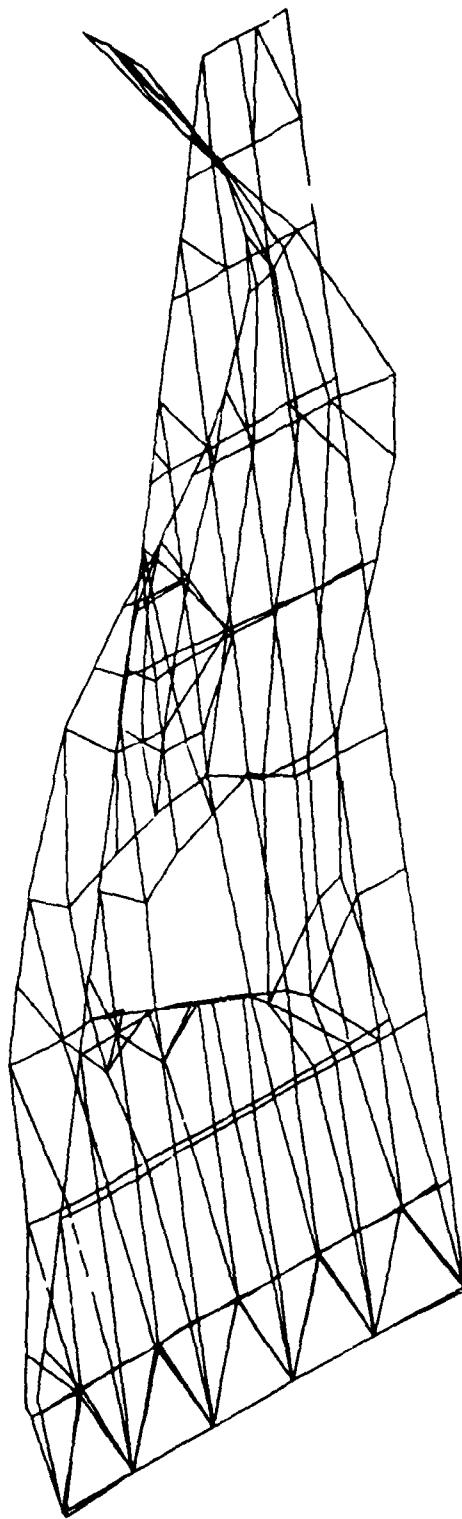Symmetric Normal Modes for F-16 Wing Model DC-17

Givens Method   Mode 4   Frequency = 75.70 Hertz

Figure L-9.   2nd Torsional Mode (Model DC-17)